MECHANICAL PERFORMANCE, INTRACELLULAR CA^{2+} HANDLING AND VENTRICULAR REPOLARISATION IN ISOLATED HEARTS FROM RABBITS WITH HEART FAILURE

A thesis submitted in fulfilment of the degree of

Doctor of Philosophy

to

University of Glasgow

Faculty of Medicine

by

Ghulam André Ng

M.B.Ch.B., M.R.C.P.

Department of Medical Cardiology, Glasgow Royal Infirmary

&

Institute of Biomedical and Life Sciences, University of Glasgow

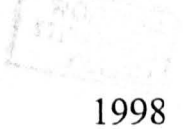

1998

Abstract

In this thesis, a rabbit coronary artery ligation model was used to study the cardiac mechanical performance, Ca^{2+} handling and ventricular activation / repolarisation in heart failure. Significant cardiac dilatation and contractile dysfunction were demonstrated *in vivo* on echocardiography 7 weeks after the initial myocardial infarct resulting from the coronary artery ligation procedure. In addition, liver, lung and heart weights were increased indicating significant organ congestion, cardiac remodelling and hypertrophy as seen in the human clinical syndrome of heart failure. Impaired mechanical performance was also demonstrated *in vitro* in the isolated failing hearts both in the working heart configuration and during Langendorff perfusion, with significant systolic and diastolic dysfunction. The Frank-Starling relationship was attenuated in the failing hearts and there was also a blunted slow response to step increase in pre-load, which may partly explain the findings of the Frank-Starling relationship in the failing hearts. Epicardial Ca^{2+} transients measured from the isolated failing hearts were found to have a prolonged time course. Impaired relaxation was shown to be associated with the prolonged Ca^{2+} transient durations in the failing hearts and there was an increased variation of Ca^{2+} transient durations over the left ventricular epicardial surface in the failing hearts. Monophasic Action Potentials (MAPs) measured from the left ventricular epicardial surface of failing hearts also had a prolonged time course and there was also an increased variation of MAP durations. The prolonged Ca^{2+} transient durations appeared to be associated with prolonged MAP durations in the failing hearts. Finally, delayed ventricular activation with impaired intraventricular conduction was demonstrated in the failing hearts, which may be an additional contributory factor in the mechanical dysfunction in heart failure.

CONTENTS

List of figures

List of tables

Acknowledgements

There are a number of people to whom I owe a great debt of gratitude and without whose help and support I could not have completed this thesis. I would like to express my warmest thanks to:-

The British Heart Foundation for financial support.

Professor Stuart Cobbe for the opportunity of carrying out this work and for his encouragement, guidance and advice throughout the study.

Professor Godfrey Smith for opening me up to the world of science, for his patience and tolerance of my ignorance and sometimes wild ideas; and for being a friend all the time.

Dr Francis Burton for allowing me to share the laboratory equipment and his rig despite not being able to clean everything up to perfection at the end of every experiment and for his help with most of my computer problems.

Drs David Miller, Niall MacFarlane, John McCarron and Marie McIntosh for helpful discussion and stimulating debates.

Dr Martin Hicks for giving me a kick-start with the working heart apparatus and for filling in the purchase forms for the "few" glasswares I have broken.

Diane Smillie, Michael Dunne and Graham Deuchar for their surgical help with the rabbit model and Douglas Robertson and Catherine Brown for their expert help with the care of the animals.

My parents for their much-valued labour in my upbringing, for a decent education and unfailing love and support.

And, to Carmen who has lighted up my life with her charm, kind love and understanding.

Declaration

Coronary artery ligation and sham operations on the rabbits were carried out by technical staff (Mrs Diane Smillie, Mr Michael Dunne and Mr Graham Deuchar) at the Department of Medical Cardiology, Glasgow Royal Infirmary under the supervision of Dr Martin Hicks. All of the experimental work contained within this thesis and echocardiography on the rabbits were undertaken by me. The material has not been submitted previously for any other degree. Some of the results presented have been published during the period of study, details of which are given below.

Publications

Ng GA, Hicks MN, Cobbe SM, Smith GL. Slow changes in cardiac inotropy and output associated with step changes in pre-load in isolated working rabbit hearts. J Mol Cell Cardiol 1995; 27(6): A392.

Ng GA, Hicks MN, Cobbe SM, Smith GL. Slow changes in cardiac inotropy and output associated with step changes in pre-load in isolated working rabbit hearts. J Phys 1995; 487P: 142-143.

Ng GA, Cobbe SM, Smith GL. Abnormal calcium transients in isolated rabbit hearts with left ventricular dysfunction. J Mol Cell Cardiol 1996; 28(6): A143.

Ng GA, Cobbe SM, Smith GL. Abnormal intracellular calcium transients in isolated working rabbit hearts with left ventricular dysfunction. Eur Heart J 1996; 17: 476.

Ng GA, Cobbe SM, Smith GL. Abnormal intracellular calcium transients in isolated rabbit hearts with left ventricular dysfunction. J Mol Cell Cardiol 1996; 28(7): A229.

Ng GA, Cobbe SM, Smith GL. Prolongation and dispersion of calcium transients and monophasic action potentials in isolated hearts from rabbits with heart failure. PACE 1997; 20(4 II): 1175.

Ng GA, Cobbe SM, Smith GL. Abnormal mechanical function, calcium handling and repolarisation in isolated hearts from rabbits with heart failure. Heart 1997; 77(S1): 28.

Ng GA, Cobbe SM, Smith GL. Asynchronous ventricular activation contributes towards the contractile dysfunction in heart failure. Eur Heart J 1997; 18:510.

Ng GA, Cobbe SM, Smith GL. Non-uniform prolongation of intracellular Ca^{2+} transients recorded from the epicardial surface of isolated hearts from rabbits with heart failure. Cardiovas Res 1998; 37(2): 489-502.

Abbreviations

AB	Aortic banding
AM ester	Acetoxymethyl ester
AT	Activation time
AV	Aortic valve
CAD	Coronary artery disease
CaD	Ca^{2+} transient duration
CAL	Coronary artery ligation
CM	Cardiomyopathy
C.O.	Cardiac output
Conc	Concentration
Cyclic AMP	Cyclic adenosine monophosphate
DAD	Delayed afterdepolarisation
DCM	Dilated cardiomyopathy
DHP	Dihydropyridine
$+ dP.dt^{-1}_{(max)}$	Maximum rate of pressure rise
$- dP.dt^{-1}_{(max)}$	Maximum rate of pressure decay
EAD	Early afterdepolarisation
ECG	Electrocardiogram
EDP	End-diastolic pressure
EDD	End-diastolic dimension
EF	Ejection fraction
ESD	End-systolic dimension

HF	Heart failure
ICE	Intra-coronary embolisation
IVCT	Isovolumic contraction time
IVRT	Isovolumic relaxation time
LAD	Left atrial dimension
LV	Left ventricular
LVEDD	Left ventricular end-diastolic dimension
MAP	Monophasic action potential
MAPD	Monophasic action potential duration
Memb	Membrane preparations
Mitochon	Mitochondrial
mRNA	Messenger RNA
MV	Mitral valve
MVD	Mitral valve disease
Myo	Myocytes
NYHA	New York Heart Association
PapM	Papillary muscles
PCR	Polymerase chain reaction
RV	Right ventricular
SHR	Spontaneously hypertensive rat
SR	Sarcoplasmic reticulum
SysP	Peak left ventricular systolic pressure
Trab	Trabeculae
V + P overload	Volume and pressure overload

CHAPTER 1

HEART FAILURE - AN OVERVIEW

Congestive heart failure is a common clinical problem with significant morbidity and mortality. Despite its frequent occurrence, the condition has been difficult to define. Heart failure is not a diagnosis *per se*, but rather a clinical syndrome with a multitude of symptoms and signs resulting from haemodynamic disturbances in the circulatory system. Braunwald (1992) described heart failure as "the pathophysiological state in which an abnormality of cardiac function is responsible for failure of the heart to pump blood at a rate commensurate with the requirements of the metabolising tissue or can do so only from an elevated filling pressure". To truly interpret and apply this definition, one has to know the metabolic requirements of the perfused tissues. Although the definition helps one understand the pathophysiology of heart failure, it is of less use in the clinical setting. Packer (1988) offered an alternative definition which focuses more on the clinical consequences of heart failure: "Congestive heart failure represents a complex clinical syndrome characterised by abnormalities of left ventricular function and neurohormonal regulation which are accompanied by effort intolerance, fluid retention, and reduced longevity". Since "abnormal cardiac function" was mentioned in both definitions, one has to understand the normal "function" of the heart in order to study the condition of heart failure.

Cardiac "function"

The term "cardiac function" implies a certain degree of autonomy on the heart's part as an organ to govern its own business and to fulfil its duty or purpose. A series of questions would emerge if one wishes to study abnormal cardiac "function":- What is the normal "function" of the heart? How can cardiac "function" be measured? What is the gold standard for measuring cardiac "function"? Can cardiac "function" really be measured?

Normal function of the heart

It has been a long-accepted fact that the heart acts as a pump to circulate blood within the body. However, there was some controversy when William Harvey first compared the heart's action to a pump and his views were not widely accepted in the 17th century. In his notes for the Lumleian lecture of April 17, 1616, long before his definitive publication *De Motu Cordis*, he remarked: " ..... the movement of the blood is constantly in a circle, and is brought about by the beat of the heart. It is a question, therefore, whether this is for the sake of nourishment or of heat, the blood ..... being in turn warmed by the heart" (Franklin, 1933). Further prominent investigators on the circulation and the heart like Carl Ludwig and Adolph Fick later developed the concepts of blood pressure and blood flow within the circulation and consolidated Harvey's original suggestion of the heart's function as a pump. The heart generates pressure and also generates flow of the blood around the circulatory system. Which is the primary product of the two? If indeed one is the more important, then measurement of that parameter will give a direct assessment as to how well or poorly the heart is "functioning". However, the answer is not that simple as the heart can generate enormous pressure and yet no flow if its outlet has been blocked or if there is a high after-load which will decrease flow. The parameters of pressure and flow are probably interdependent and are not simply governed by the "function" of the heart but also by the rest of the circulatory system to which the heart is connected.

Blood can only flow in the vasculature when pumped by the heart. Once the heart stops pumping, blood flow in the circulation slows down, pressure in the whole system drops until everything is at a standstill. In simple physical terms, the heart is providing the hydraulic energy required to sustain circulation and that is probably an appropriate simple description of the "function" of the heart. Considering the Law of Conservation of Energy,

the heart can be viewed as an energy-converter transforming chemical energy into hydraulic energy. It is this energy that provides the pressure and the flow in the system. The product of the 2 parameters (pressure x flow) gives the amount of energy provided by the heart per unit time, i.e. power. The heart is thus essentially a power generator from which pressure and flow in the circulatory system originate.

Measuring cardiac 'function'

Considering the heart as a power generator from which pressure and flow in the circulatory system originate, what is the best way to assess the heart's "function"? Some workers advocate the use of cardiac power output (Tan, 1987), estimating the amount of energy provided by the heart over time. This is a logical estimate of the *overall* cardiac "function" as the heart appears to be a power generator. In order to calculate the power output of the heart, measurements of perfusion pressure and cardiac output have to be made. The value obtained at rest is probably of little clinical value as suboptimal cardiac "function" may masquerade as being normal at rest as the metabolic demands on the heart are low and hence the power output is not expected to be high. An abnormal heart will not be capable of generating the same degree of power output in response to inotropic stimulation such as exercise. Cardiac reserve is the difference between the power output achieved by the heart during maximal stimulation and that at rest and is probably a more meaningful description of the "function" of the heart. However, these measurements of power output and cardiac reserve are indirect and involve a certain degree of intervention which may not be widely applicable in the clinical setting.

Many other measurements are used to assess cardiac "function" clinically and are at best approximations and surrogates of the true capability of the heart as a pump. Various terms are used in the description and assessment of cardiac "function". I personally prefer the term

"cardiac performance", which simply describes what the heart does - to perform as a pump. The term "ventricular function" is used widely and loosely but its description involves measurements of pressure, volume and / or dimensions which are interdependent variables. "Contractility" is another term frequently used to describe the heart's pumping "function" but it actually represents the intrinsic property of the cardiac myocyte reflecting the level of activation and cross-bridge kinetics independent of the effects of load. The performance of the heart can be described at various levels:- (a) *myocardial* level, at which contractility is a proper description; (b) at the *pump* level, various parameters are used to describe so-called "ventricular function"; and (c) *output* level, at which the integrated cardiac output will reflect the heart's "function" in the light of its loading conditions. Thus, one has to be careful and clear when describing and measuring the pumping capability of the heart.

Measurements of cardiac "function" used clinically include:-

1) Cardiac output / index - cardiac output is the volume of blood ejected by the heart per unit time and represents blood flow generated by the heart and cardiac index is the cardiac output corrected for body mass.

2) End-diastolic and peak systolic pressure - these are parameters of intraventricular pressure used to estimate pump "function".

3) Ejection fraction - the fractional change in volume of the heart during systole which can be measured with imaging techniques like angiography or echocardiography.

4) Fractional shortening and velocity of shortening - these are calculated from segment length measurements made usually with echocardiography. Fractional shortening is the fractional change in linear dimension and velocity of shortening is the change in length or linear dimension per unit time.

5) End-systolic pressure-volume relationship - the peak left ventricular pressure in an isovolumetrically contracting heart increases as diastolic pressure increases giving a straight line in the physiological range which is described as the end-systolic pressure-volume relationship (ESPVR). The upper left corner of pressure-volume loops of variably loaded beats in the ejecting heart fall close to the isovolumetric ESPVR. The slope of this line, termed end-systolic elastance, describe the contractility or myocardial contractile state of the heart.

6) Maximum rate of ventricular pressure rise [$dP.dt^{-1}_{(max)}$] - an isovolumetric phase index which reflects the contractility of the heart.

These indices or measurements describe different aspects of the pumping capability of the heart and there is probably not one that can describe the *overall* pumping performance of the heart. In the clinical setting, some of these measurements provide information that can be obtained quickly and used to make management decisions. A more detailed use of these pieces of information will require caution and understanding as to what aspect of cardiac performance they address.

What is heart failure?

If a simple definition of the "function" of the heart is to provide hydraulic energy to the circulation, a simple definition of heart failure would be "the heart failing to 'function' as it should". It is usually caused by an intrinsic defect in myocardial contraction, with primary *myocardial* failure leading to the ultimate syndrome. However, the syndrome can also occur in patients with apparently normal myocardial "function" with sudden changes in other components of the circulation which cause the heart to "fail" and one may wish to distinguish such cases as *circulatory* rather than *myocardial* failure.

Clinical causes of heart failure

A decreased pump efficiency of the heart can be the result of many pathological conditions including:- (a) myocardial disease, (b) arrhythmias, (c) valve disease, (d) pericardial disease, and (e) congenital heart disease.

The commonest cause of myocardial failure in the Western world is *coronary artery disease* (Teerlink *et al.* 1991). This is usually the result of coronary thrombosis with myocardial infarction leading to a reduction in the total number of functioning myocytes; and regional wall motion abnormality in the infarcted area can lead to further deterioration in pump efficiency as a result of poor co-ordination in contraction. More recent concepts of myocardial "stunning" (Braunwald and Kloner, 1982) and "hibernation" (Rahimtoola, 1989) state that regional contraction can be abnormal in the absence of the total arterial occlusion. *Cardiomyopathy* encompasses a group of conditions where there is a primary myocardial abnormality in the absence of other cardiac disease. Traditionally, there are 3 types:- Dilated, Hypertrophic and Restrictive. Although the initial definition of these conditions was based on the fact that they were idiopathic and the causes were unknown, recent researchers have identified risk factors and links between the cardiomyopathies and their underlying causes of which there are many, including genetic disorders, immunological mechanisms, alcohol, haemochromatosis, etc. Another cause of myocardial failure is chronic *hypertension* which when untreated can lead to pressure overload of the heart and subsequent decompensation and is itself a risk factor for coronary artery disease. Rarer causes of myocardial failure include *drugs* and *infection.*

Other pathological conditions like arrhythmias, valvular, pericardial and congenital heart diseases cause decreased cardiac pump efficiency as a result of haemodynamic disturbances with subsequent chronic volume and / or pressure overload of the heart.

Pathophysiology of heart failure

The ultimate syndrome of heart failure is arrived at through a cascade of changes in the heart and other organs and systems in the body (Poole-Wilson, 1993). Increased wall stress appears to be the first stimulus to initiate pathophysiological changes in the heart itself. Pressure overload as a result of outflow obstruction or increased after-load leads to myocardial hypertrophy which is commonly described as concentric where there is a predominant increase in myocyte width. There is an increase in mass : volume ratio with no chamber dilatation (unless there is decompensation). Volume overload, on the other hand, leads to what is termed eccentric hypertrophy in which there is chamber dilatation accompanying hypertrophy. Myocyte slippage and reorientation are believed to be mechanisms accompanying an increase in cell length which lead to an enlarged equilibrium volume (LeJemtel and Sonnenblick, 1993) with little change in the mass : volume ratio of the chamber. Hypertrophy tends to normalise wall stress across the myocardium (Wong and Rautaharju, 1968) and the response has been shown to be the result of genetic reprogramming to adapt to increased haemodynamic demands or to compensate for the impaired contractile performance of the pump (Chien *et al.* 1991). Recent evidence suggests that the hypertrophic response may be mediated via different signalling pathways. Angiotensin II has been implicated in mediating myocardial hypertrophy (Dzau, 1993) with predominantly an increase in myocyte width as a result of parallel addition of sarcomeres. A number of other growth factors, like α-adrenergic agonists and endothelin-1, are also believed to mediate myocardial hypertrophy in a similar way as angiotensin II through G-protein coupled receptors (Hefti *et al.* 1997). Recent work (Wollert *et al.* 1996) identified a cytokine, cardiotrophin-1, which can mediate a specific form of cardiac myocyte

hypertrophy characterised by an increase in cell length (with addition of sarcomeres in series) but no significant change in cell width.

Despite the fact that hypertrophy is a well-recognised pathophysiological finding in failing hearts, little is understood of the cellular or molecular events that lead from the adaptive phase to the decompensated stage. Myocyte cell loss is believed to play an important role as it has been documented in both humans and animals during the normal process of ageing, following long-term pressure or volume overload and in idiopathic dilated cardiomyopathy (Anversa *et al.* 1996). The general belief has been that it is the result of cell necrosis, until recently when studies have demonstrated that apoptosis is a significant form of myocyte death in the heart. Apoptosis can be viewed as a programmed suicide of cells which is an energy-requiring process with distinct morphological, biochemical and molecular changes; and is frequently referred to as programmed cell death. It has been shown in animal hearts to occur in ischaemia-reperfusion injury, myocardial infarction, rapid ventricular pacing, pressure overload and in spontaneously hypertensive rats (Colucci, 1996). Mechanical stretch has been implicated in the process (Cheng *et al.* 1995) although other factors may also be responsible. Recently, apoptosis has also been shown to occur in myocytes isolated from patients with end-stage heart failure (Narula *et al.* 1996). In addition to myocyte loss, intrinsic biochemical changes to surviving myocytes with resulting mechanical dysfunction (and defects in excitation-contraction coupling which will be discussed below) contribute towards the gradual deterioration of contractile performance of the heart. There are also changes in the failing heart in the non-contractile components with fibrosis, collagen replacement and changes in cytoskeleton resulting in progression to heart failure (Scheuermann, 1993; Wagoner and Walsh, 1996).

Epidemiology of heart failure

How common is heart failure and why is it important to tackle the problem? Congestive heart failure has been described as a "major public health problem" (Garg *et al.* 1993) and as increasing in "epidemic proportions" (Massie and Shah, 1996). This is no exaggeration. Chronic heart failure is the only common cardiovascular condition that is increasing in incidence and prevalence. Despite an overall decline in age-adjusted cardiovascular disease mortality in industrialised countries over the last few decades (Sytkowski *et al.* 1990), heart failure continues to present a significant and intensifying health care problem with large human and economic costs.

Although reliable epidemiological data are scarce due to the lack of consensus on diagnostic criteria, surveys indicate that heart failure afflicts 1 - 2 % of the population in Europe and the USA (Ho *et al.* 1993b; Cowie *et al.* 1997) with an estimated 15 million patients with heart failure worldwide (Eriksson, 1995). This prevalence is dependent on age, increasing sharply to nearly 10 % above age 80 (Massie and Shah, 1996). Incidence of heart failure also increases with age; with 1 to 5 cases per 1000 population per annum in the general population and 40 cases per 1000 population per annum in those aged over 75 years. With an estimated increase of 30 % in the number of elderly people over the next 10 years, it is no exaggeration that heart failure is increasing in epidemic proportions.

Patients with heart failure are often symptomatic with fatigue, lethargy and breathlessness and their quality of life is adversely affected. Regular outpatient consultation is required as well as hospitalisation which is often prolonged and recurrent. About 120,000 people require hospitalisation for heart failure each year in Scotland (McMurray *et al.* 1993a) which is equivalent to 0.2 % of the population. It follows that the economic cost of managing heart failure is high. McMurray *et al.* (1993b) estimated the direct cost to the

National Health Service (NHS) to be £360 million per year, equivalent to about 1.2 % of the total NHS expenditure.

Prognosis of heart failure

Apart from being a costly and growing public health problem with significant morbidity, congestive heart failure is also a lethal condition with poor prognosis. In the original report of the first population-based study - the Framingham study, 62 % of men and 42 % of women died within 5 years after the development of heart failure (McKee *et al.* 1971). A more recent report (Ho *et al.* 1993a) with the 40-year follow-up data on the Framingham cohort confirmed the trend and showed that only 25 % of men and 38 % women were alive at 5 years once heart failure had developed. The median survival was only 1.7 years in men and 3.2 in women which reflects a mortality rate 6 to 7 times that of the general population of the same age. Other hospital-based studies (Franciosa *et al.* 1983) and pharmacological trials in heart failure (Cohn *et al.* 1986; Swedberg, 1987; The SOLVD investigators, 1991), which involved highly selected groups of patients, also showed similar results with marked reduction in life expectancy at all ages.

Mortality from heart failure increases with clinical severity of the condition as assessed by functional class according to the New York Heart Association (NYHA) criteria. In the SOLVD study (The SOLVD investigators, 1991), mortality for patients (given placebo) with NYHA class IV heart failure was 64% over a mean follow-up of 41.4 months, compared with 51%, 35% and 30% for those with class III, II and I disease respectively. The same investigators also showed that resting left ventricular ejection fraction is a powerful predictor of prognosis in heart failure.

Mode of death in heart failure

Not only do patients with heart failure die as a result of haemodynamic deterioration leading to what has been called pump failure deaths, but many also die suddenly. In the Framingham study, sudden death occurred in 25 % of men and 13 % of women with heart failure (Kannel and Belanger, 1991). This rate was reported to be 5 times the rate for the general population. Although the abrupt onset of symptoms and death within 1 hour is defined as sudden cardiac death, the mode of death is frequently difficult to determine. This problem with classifying heart failure death is highlighted in a recent article by Narang *et al.* (1996). In this review of heart failure studies, it was found that documentation of mode of death was less than adequate. In those studies where sudden and pump failure deaths were defined, between 30 and 40 % of deaths were sudden. It was found that pump failure deaths were more common in studies with a lower mean ejection fraction whilst modes of death other than sudden or pump failure were commoner in studies with higher mean ejection fraction.

In a population of patients with advanced (NYHA class III or IV) heart failure hospitalised for cardiac transplantation evaluation and adjustment of anti-failure treatment, Luu *et al.* (1989) showed that there were various causes or mechanisms behind sudden death in patients with heart failure. A later report and update on their data by Stevenson *et al.* (1993) stated that ventricular tachycardia or fibrillation was the cardiac rhythm at the time of cardiac arrest in 52 % of cases whilst bradyarrhythmias or electromechanical dissociation was the rhythm in the remainder. Although no clear precipitating factors could be found in many of these sudden deaths, a variety of potential causes were identified in 14 arrests (48 %) including acute coronary occlusion, pulmonary embolism, Torsade de Pointes caused by hypokalaemia or drugs that prolong the QT interval, and hyperkalaemia. Despite being a

small series of hospitalised patients, this study helped to highlight the diversity in the mechanisms behind sudden death in heart failure. However, the relative frequency of different mechanisms of sudden death in patients with heart failure outside the hospital is still unknown.

Although ventricular arrhythmias are common in patients with heart failure and are potential causes of sudden death in these patients, Packer (1992) questioned the direct association between ventricular arrhythmias and sudden death in heart failure. His reasons were that (a) complex ventricular arrhythmias on ambulatory monitoring in heart failure patients predicted total cardiac mortality but not sudden death (Califf *et al.* 1982); and (b) Stevenson *et al.* (1988) found that the ability to induce ventricular tachycardia or fibrillation in patients with ventricular dysfunction did not reliably predict sudden death. Packer (1992) suggested that complex ventricular arrhythmias may be a nonspecific manifestation of a poorly functioning left ventricle rather than a specific arrhythmogenic substrate. Other workers (Chakko and Gheorghiade, 1985; Podrid *et al.* 1992) also raised another counter-argument against the link between ventricular arrhythmias and sudden death in heart failure in that antiarrhythmic drugs have not been convincingly shown to be effective for preventing sudden death and in some cases may be proarrhythmic and increases the incidence of sudden death (CAST Investigators, 1989). A recent report from the investigators of the GESICA trial, which was a large multi-centre study involving more than 500 patients with heart failure (Doval *et al.* 1996), showed that nonsustained ventricular tachycardia was an independent marker for increased overall mortality rate and sudden death and the relative risk was 2.8 for sudden death if such arrhythmias were present. These results suggest that the failing heart is indeed electrophysiologically

abnormal and is prone to arrhythmias. Ventricular arrhythmias may well be a surrogate for ventricular dysfunction but many of these arrhythmias can lead to sudden cardiac death.

Ventricular arrhythmias in heart failure

As mentioned above, ventricular arrhythmias are extremely common in patients with heart failure. Complex ventricular premature beats are observed in 80 - 90 % of cases (Chakko and Gheorghiade, 1985; Francis, 1986; Podrid *et al.* 1992) and non-sustained ventricular tachycardia is also highly prevalent (50 - 80 %). The pathogenesis of arrhythmias in heart failure is not fully understood but there are many possible causes (Pye and Cobbe, 1992; Aronson and Ming, 1993). They can be grouped into the usual arrhythmogenic mechanisms which include re-entry, enhanced automaticity and triggered activity. The latter 2 mechanisms give rise to abnormal impulse generation whilst re-entry is an expression of abnormal impulse propagation (Josephson, 1993). Abnormal impulse generation may be the result of either enhanced phase 4 automaticity of normal or abnormal cells or can be triggered leading to early or delayed afterdepolarisations (EADs and DADs). There are 3 well-recognised prerequisites for re-entry:- (a) at least 2 distinct pathways that join proximally and distally to form a closed circuit, (b) unidirectional block in one of the pathways, and (c) slow conduction down the unblocked pathway allowing the blocked pathway to recover excitability. The pathways involved in re-entry may be anatomically distinct or can be functionally different giving rise to the "leading circle" phenomenon suggested by Allessie and co-workers (1977). Re-entry can also occur with a combination of anatomical and functional abnormalities resulting in anisotropy where conduction is faster in one direction in the myocardium than in another.

Coronary artery disease is the major cause of heart failure in the Western world and the majority of patients have had myocardial infarction which gives rise to scar tissue. Dead

and surviving myocardium overlap at the border zone of the infarct giving rise to ideal conditions for re-entrant arrhythmias. Ventricular arrhythmias due to re-entry around the border zone have been demonstrated in both animals and humans (Wit *et al.* 1982; De Bakker *et al.* 1988). Re-entry may also occur in regions remote from the infarcted tissue. In the chronically infarcted heart, remodelling with hypertrophy and interstitial fibrosis (Assayag *et al.* 1997) occurs which leads to cellular uncoupling and the remodelled myocardium is prone to arrhythmias (Qiu *et al.* 1996). The expression of gap junction proteins (connexins) has also been shown to be abnormal in the remodelled myocardium with a reduction in gap junction density and altered isoform expression (Peters *et al.* 1993). Slow conduction and dispersion of refractoriness (Ramdat-Misier *et al.* 1995) in these regions can cause re-entry (Pogwizd *et al.* 1992). Re-entrant tachycardias have also been demonstrated in patients with non-ischaemic cardiomyopathy (Kottkamp *et al.* 1995).

As mentioned above, a fixed anatomical circuit is not mandatory for re-entry. In the failing heart, anomalous intrinsic properties of the myocardium can give rise to the favourable environment for re-entry to take place. One such phenomenon is *dispersion of repolarisation or refractoriness*, which will be discussed in greater detail below. In essence, the difference in recovery of excitability in neighbouring myocardial tissues / cells creates the perfect condition for re-entry. Another phenomenon is *mechano-electric* or *contraction-excitation feedback* (Lab, 1982; Taggart *et al.* 1992a) where mechanical changes result in altered cardiac electrophysiology. Sudden death frequently follows haemodynamic decompensation in patients with heart failure. Several investigators have shown in animals that acute ventricular dilatation in the normal heart shortens refractoriness or action potential duration (Reiter *et al.* 1988; Coulshed and Cowan, 1991; Halperin *et al.* 1993), increases the incidence of arrhythmias (Franz *et al.* 1989; Franz *et al.* 1992; Jalal *et al.*

1992) and dispersion of refractoriness is also increased (Reiter *et al.* 1988). These changes were also observed with sustained load in the whole heart (Zabel *et al.* 1996). Similar changes were demonstrated in humans with shortening of monophasic action potential (MAP) duration during transient aortic occlusion (Taggart *et al.* 1992b). The arrhythmogenic tendency of ventricular dilatation has been shown in models of heart failure (Wang *et al.* 1994; Pye and Cobbe, 1996) and was enhanced in the presence of hypokalaemia (Reiter *et al.* 1993; Evans *et al.* 1995). These electrophysiological changes are believed to be mediated via stretch-activated channels (Hansen *et al.* 1991; Lerman, 1996) but their significance in the pathophysiology of arrhythmias remains to be elucidated.

Electrophysiological abnormalities in the failing myocardium

Apart from structural remodelling, it has also been shown that failing myocardium undergoes electrical remodelling with intrinsic changes that promote arrhythmia initiation and propagation (Aronson and Ming, 1993; Hart, 1994). One consistent finding in studies on the failing myocardium was that the action potential is prolonged and repolarisation delayed (Rossner and Sachs, 1978; Beuckelmann *et al.* 1993; Ming *et al.* 1994; Kaab *et al.* 1996; Qiu *et al.* 1996; Rozanski *et al.* 1997) (see Table 1.1). This is also true in hypertrophied, non-failing tissues and myocytes (Ryder *et al.* 1993; Jauch *et al.* 1994; Hicks *et al.* 1995; Rials *et al.* 1995; McIntosh *et al.* 1998). Intuitively, from a clinical point of view, one would think that this should be anti-arrhythmic since prolongation of refractoriness is the main action of class Ia and III anti-arrhythmic drugs (Roden, 1996). According to the wavelength theory of re-entry (Rensma *et al.* 1988), the likelihood of re-entry is inversely related to the product of the conduction velocity and refractory period of the tissue involved. Prolongation of refractoriness lengthens the path of the re-entrant wave and makes it less likely to sustain a tachycardia. However, in the failing myocardium, the

prolonged action potential has a prominent plateau phase which is known to be labile (Tomaselli *et al.* 1994). It is a time of high membrane resistance during which small changes in current can lead to large changes in membrane potential either way. It is during this labile prolonged repolarisation phase that EADs are likely to be provoked.

What causes the action potential prolongation in failing myocardium? There is reasonable evidence to suggest against L-type Ca^{2+} current being a contributing cause. The majority of workers failed to demonstrate any change (Beuckelmann *et al.* 1991; Mewes and Ravens, 1994; Kaab *et al.* 1996; Qiu *et al.* 1996; Rozanski *et al.* 1997) whilst some demonstrated a decreased L-type Ca^{2+} current in failing myocytes (Rossner, 1991; Hatem *et al.* 1994; Ming *et al.* 1994). Several repolarisation currents involved with K^+ conductance, including the inward rectifier (I_{K1}) and transient outward (I_{to1}) currents, have been found to be depressed in heart failure both in humans (Beuckelmann *et al.* 1993; Näbauer *et al.* 1993) and in animals (Kaab *et al.* 1996; Qiu *et al.* 1996; Thuringer *et al.* 1996; Rozanski *et al.* 1997). These have been suggested to be the main cause for the action potential prolongation in heart failure. The Na^+ / Ca^{2+} exchanger current has also been found to be abnormal in heart failure (Hatem *et al.* 1994; Zhang *et al.* 1996) but the results were not consistent. Changes in this current can have dynamic effects on the repolarisation phase of the action potential and it has been shown to be able to produce EADs (Szabo *et al.* 1994). This may be especially important in heart failure with altered intracellular [Ca^{2+}] and / or [Na^+] as a result of altered excitation-contraction coupling, which will be discussed later. Data on other potassium currents in heart failure are lacking but a decrease in the delayed rectifier current (I_K) has been shown in a feline model of cardiac hypertrophy (Kleiman and Houser, 1989). Alterations of the delayed rectifier current or the relative contribution of its 2 components (I_{Kr} and I_{Ks}) may be involved in the action potential prolongation and / or electrical

instability in the failing myocyte. Recent evidence (Beuckelmann *et al.* 1995; Cerbai *et al.* 1997) also suggests that a hyperpolarisation activated current, I_f, is expressed in myocytes isolated from patients with heart failure which can be potentially arrhythmogenic.

To summarise, there is general consensus in the literature that the main electrophysiological abnormality in heart failure is a prolonged action potential with delayed repolarisation. Changes have been demonstrated in the properties of various ion channels. It would appear that a decreased activity in some repolarising currents is the main mechanism underlying delayed repolarisation and that changes in other currents may contribute towards the electrical instability and arrhythmogenicity in heart failure.

Table 1.1 Electrophysiological changes in heart failure.

Effect	First author	Year	Species	Aetiology	Prep
			Action Potential Duration		
↑	Rossner	1978	Hamster	CM	PapM
↑	Beuckelmann	1993	Human	DCM / CAD	Myo
↑	Ming	1994	Guinea-pig	AB / HF	Myo
↑	Qin	1996	Rat	Post-infarct	Myo
↑	Kaab	1996	Dog	Pacing	Myo
↑	Rozanski	1997	Rabbit	Pacing	Myo
			L-type Ca^{2+} current		
↓	Rossner	1991	Hamster	CM	Myo
↔	Beuckelmann	1991	Human	DCM / CAD	Myo
↔	Mewes	1994	Human	DCM / CAD	Myo
↓	Hatem	1994	Hamster	CM	Myo
↓	Ming	1994	Guinea-pig	AB / HF	Myo
↔	Qin	1996	Rat	Post-infarct	Myo
↔	Kaab	1996	Dog	Pacing	Myo
↔	Rozanski	1997	Rabbit	Pacing	Myo
			Na^{+}-Ca^{2+} exchanger current		
↑	Hatem	1994	Hamster	CM	Myo
↓	Zhang	1996	Dog	Post-infarct	Myo
			Inward rectifier current (I_{K1})		
↓	Beuckelmann	1993	Human	DCM / CAD	Myo
↓	Thuringer	1996	Hamster	CM	Myo
↓	Kaab	1996	Dog	Pacing	Myo
↔	Rozanski	1997	Rabbit	Pacing	Myo
			Transient outward current (I_{to1})		
↓	Beuckelmann	1993	Human	DCM / CAD	Myo
↓	Thuringer	1996	Hamster	CM	Myo
↓	Qin	1996	Rat	Post-infarct	Myo
↓	Kaab	1996	Dog	Pacing	Myo
↓	Rozanski	1997	Rabbit	Pacing	Myo

"Extra-cardiac" triggers for arrhythmias in heart failure

Many extrinsic factors have been found to contribute to the arrhythmogenic tendency in the failing heart. Irrespective of the aetiology, chronic heart failure is accompanied by high sympathetic tone and abnormalities of baroreceptor responsiveness (Cohn *et al.* 1984; Ferguson *et al.* 1984). Sympathetic stimulation increases susceptibility to ventricular fibrillation during ischaemia, promotes afterdepolarisations and triggered activity, and alters ventricular conduction and refractoriness (Schwartz *et al.* 1992). Heart rate variability, a clinical parameter used as a surrogate for autonomic function, is abnormal in patients with previous myocardial infarction (Kleiger *et al.* 1987; La Rovere *et al.* 1998), resuscitated cardiac arrest (Dougherty and Burr, 1992) and heart failure (Casolo *et al.* 1989; Kienzle *et al.* 1992); and has been shown to be a strong prognostic marker.

Patients with heart failure are subject to electrolyte disturbances due to treatment with diuretics and angiotensin converting enzyme (ACE) inhibitors (Packer and Lee, 1986). Potassium and magnesium depletion has been shown to provoke triggered activity with delayed afterdepolarisations and automaticity in failing myocardium (Vermeulen *et al.* 1994).

The renin-angiotensin system is known to be activated in heart failure. Although less well studied, this is believed to enhance arrhythmogenesis by producing electrolyte shifts and altered haemodynamics (Podrid *et al.* 1992). There is some evidence in the ACE inhibitor trials (Cohn *et al.* 1991; Pfeffer *et al.* 1992) that inhibition of the renin-angiotensin system reduces the risk of sudden death in patients with heart failure.

Dispersion of repolarisation and heart failure

As mentioned above, dispersion of repolarisation or refractoriness creates a favourable environment for re-entrant arrhythmias to be initiated and sustained. It is not a new concept at all but has only recently received attention in the pathophysiology of arrhythmogenesis in heart failure and been found to be of prognostic significance.

Non-uniform recovery of excitability

In 1964, Han and Moe (1963) demonstrated that non-uniform recovery of excitability exists in ventricular muscle. They discovered that dispersion of recovery was increased by conditions that predispose to ventricular fibrillation, e.g. sympathetic stimulation and cardiac glycoside toxicity; and that the dispersion was associated with lowered ventricular fibrillation threshold. In the 1970s, Allessie *et al.* (1976; 1977) showed in rabbit atrial muscle that non-uniform recovery of excitability makes re-entrant arrhythmias favourable and that a fixed anatomical circuit is not required. Elegant experiments by Kuo *et al.* (1983b) on mongrel dogs demonstrated the initiation of re-entrant ventricular arrhythmias with a critical level of dispersion of MAP duration.

"Physiological" dispersion

However, nonuniformity is not an exclusively pathological phenomenon. A physiological role is recognised for the modulation of cardiac performance (Brutsaert, 1987). Electrical, mechanical, spatial and temporal non-uniformity exist in the normal heart. Studies have shown heterogeneity in the action potential duration of myocytes from different regions of the ventricular myocardium (Cohen *et al.* 1976; Watanabe *et al.* 1983), with longer action potentials in sub-endocardial cells than in sub-epicardial cells and action potentials from the base being longer than from the apical region. Action potentials recorded *in vivo* and *in*

vitro from the ventricular sub-epicardium of several animal species demonstrate a prominent notch between phases 1 and 2, leading to a distinct "spike and dome" morphology which is absent in the sub-endocardium (Antzelevitch *et al.* 1991). The differences in action potential duration and morphology between sub-epicardial and sub-endocardial ventricular myocytes have been shown to be due to regional variations in the transient outward current (I_{to}) which is much more prominent in the sub-epicardial than in the sub-endocardial cells (Litovsky and Antzelevitch, 1988; Fedida and Giles, 1991; Liu *et al.* 1993; Näbauer *et al.* 1996). Regional variations in other K^+ currents have also been implicated in contributing towards the regional differences in action potential configuration (Furukawa *et al.* 1992).

QT dispersion

Regional variation in ventricular repolarisation has been shown in the whole heart by the demonstration of dispersion of MAP durations recorded from different regions of the ventricle (Kuo *et al.* 1983a; Zabel *et al.* 1995). In the study by Zabel *et al.* (1995), an isolated rabbit heart preparation was used where MAP and 12-lead volume-conducted electrocardiogram (ECG) recordings were made. It was found that dispersion of MAP durations correlated well with QT dispersion on the 12-lead ECG, which was calculated as the difference between the longest QT interval and the shortest QT interval measured. These results supported the previously proposed clinical use of QT dispersion as a simple non-invasive measurement of dispersion of repolarisation (Day *et al.* 1990). Since increased dispersion of repolarisation has been widely acknowledged to signify a considerable arrhythmogenic risk (Han and Moe, 1963; Kuo *et al.* 1983b), many workers sought to validate QT dispersion as a predictor of arrhythmias in different patient groups (Day *et al.* 1990; Priori *et al.* 1994; Pye *et al.* 1994; Higham *et al.* 1995) and demonstrated its potential

value. However, there are technical limitations (Statters *et al.* 1994) in the measurement of QT dispersion as it is not always possible to confidently define the end of the T wave and the ECG may not be of sufficiently good quality to allow QT interval measurements in all 12 leads. Other studies also failed to show the predictive value of QT dispersion in certain patients (Davey *et al.* 1994; Surawicz, 1996) thus casting doubt on its prognostic significance.

Long QT syndrome and heart failure

The long QT syndromes are a group of clinical conditions where a long QT interval is noted on the 12-lead ECG (James, 1996) together with a high incidence of ventricular arrhythmias, especially in the form of Torsade de Pointes polymorphic ventricular tachycardia. It may be acquired, especially with the use of drugs which prolong repolarisation; or it can be congenital, which can be associated with some phenotypic abnormalities e.g. deafness. Recent research has shown that the congenital long QT syndromes are associated with various genetic defects leading to abnormalities in the Na^+ and K^+ channel activity (Roden *et al.* 1996). The hallmarks of long QT syndrome are a prolonged QT interval on ECG signifying delayed repolarisation and an increased QT dispersion which suggests increased dispersion of repolarisation. QT dispersion has been shown consistently in this group of patients to be a marker of arrhythmogenic tendency and to be of prognostic value (Day *et al.* 1990; Hii *et al.* 1992; Priori *et al.* 1994). As mentioned above, repolarisation is delayed in heart failure (Beuckelmann *et al.* 1993). Recent studies (Barr *et al.* 1994; Fu *et al.* 1997) in patients with heart failure also showed that there was a strong association between an increased QT dispersion and sudden cardiac death (presumed to be arrhythmic in origin) thus suggesting that QT dispersion is indeed of prognostic significance. Other invasive studies also showed an increased dispersion of repolarisation or

refractoriness in patients with dilated cardiomyopathy (Dinerman *et al.* 1997) and with remodelled myocardium from previous myocardial infarction (Vassallo *et al.* 1988; Ramdat-Misier *et al.* 1995). The results of these studies suggest a parallel between the electrophysiological abnormalities in the long QT syndromes and in heart failure, namely prolongation of repolarisation and its increased dispersion. One may postulate that the well-recognised arrhythmogenic mechanism in long QT syndrome, with triggered activity causing Torsade de Pointes arrhythmia, may well be an important phenomenon in the arrhythmogenesis in heart failure.

Ca^{2+} and arrhythmias

The transient rise of intracellular [Ca^{2+}] initiated by the action potential underlies the mechanism of excitation-contraction coupling in cardiac muscle. Spontaneous oscillations of intracellular [Ca^{2+}] have been shown in cardiomyocytes (Orchard *et al.* 1983) especially when the cells are Ca^{2+}-overloaded, e.g. with inhibition of the Na^+ / K^+ pump by cardiac glycosides or enhancement of Ca^{2+} influx by catecholamines. The oscillations are believed to be mediated via Ca^{2+}-induced Ca^{2+} release from the sarcoplasmic reticulum (Fabiato and Fabiato, 1975) and have been implicated in the production of aftercontractions following the normal contraction. The elevated intracellular [Ca^{2+}] also produces a transient inward current (I_{ti}) (Berlin *et al.* 1989) which is thought to be able to generate arrhythmias. The I_{ti} current is thought to consist of an inward Na^+ / Ca^{2+} exchange current along with a Ca^{2+}-activated chloride current and / or a Ca^{2+}-activated cationic current (Laflamme and Becker, 1996). Elevated intracellular [Ca^{2+}] has also been shown to be related to the genesis of EADs and DADs in single cells (Deferrari *et al.* 1995) and to the initiation of arrhythmia in an isolated multicellular myocyte model of arrhythmia (Thandroyen *et al.* 1991). It has also been shown that elevated intracellular [Ca^{2+}] can increase electrical heterogeneity in the

myocardium and promote re-entrant activity (Didiego and Antzelevitch, 1994). In the whole heart, Ca^{2+}-overload with elevated intracellular [Ca^{2+}] has been shown to facilitate the induction of ventricular fibrillation (Merillat *et al.* 1990; Billman *et al.* 1991; Kihara and Morgan, 1991). Experiments by Merillat *et al.* (1990) using Ca^{2+}-channel blockers suggested that increases in slow channel Ca^{2+} flux were important in the initiation and maintenance of ventricular fibrillation. Kihara *et al.* (1991) demonstrated an important role Ca^{2+} oscillations played as a trigger for ventricular fibrillation, by measuring intracellular [Ca^{2+}] with the bioluminescent dye, aequorin; and the oscillations were found to be augmented after transition to ventricular fibrillation suggesting a role in the maintenance of the arrhythmia.

Many pathological states are associated with Ca^{2+}-overload and have a high incidence of arrhythmias. Myocardial ischaemia is known to cause significant changes in the intra- and extra-cellular ionic environment with electrophysiological changes which are associated with a high incidence of arrhythmias (Cascio *et al.* 1995). Ischaemia causes changes in intracellular [Ca^{2+}] (Lee *et al.* 1988; Allen *et al.* 1989) and these changes may be non-uniform in different regions of the heart (Figueredo *et al.* 1993). It has also been known for some time that arrhythmias occur not only during ischaemia but also upon reperfusion (Tennant and Wiggers, 1935). Changes in intracellular [Ca^{2+}] have also been shown to be associated with reperfusion-induced ventricular tachycardia and fibrillation (Brooks *et al.* 1995) suggesting again an important role of Ca^{2+} in these arrhythmias. As mentioned above, there is a high incidence of arrhythmias in heart failure. The role of Ca^{2+} in the pathogenesis of arrhythmias in heart failure has not received much attention. This should be pursued as extensive research on Ca^{2+} homeostasis in heart failure has identified abnormalities in various aspects of Ca^{2+} handling which can directly or indirectly affect intracellular [Ca^{2+}].

Excitation-contraction coupling in heart failure

Congestive heart failure is characterised by a reduced pump efficiency of the heart. There is mechanical dysfunction with reduced contractile performance (Hasenfuss *et al.* 1992) and an abnormal relaxation profile (Grossman, 1990). The mechanisms underlying the systolic and diastolic dysfunction are unknown, but changes have been noted in the extracellular matrix and in the structure and function of the myocyte (Scheuermann, 1993; Davies *et al.* 1996). Recent studies have focused on excitation-contraction coupling in heart failure and have demonstrated defects in many of the processes involved (reviewed by Figueredo and Camacho, 1995; Gwathmey and Ingwall, 1995).

Normal excitation-contraction coupling

Normal excitation-contraction coupling (Bers, 1991) in the ventricular myocyte begins with depolarisation of the cell membrane leading to the opening of voltage-gated Na^+ and Ca^{2+} channels (Lederer *et al.* 1990). The L-type Ca^{2+} channel contains a high-affinity receptor for 1,4-dihydropyridine ligands and the ligands can act as antagonists or agonists of the channel. Opening of the L-type Ca^{2+} channel leads to Ca^{2+} influx which occurs during the plateau of the action potential. This Ca^{2+} current, which is partially responsible for maintaining the action potential plateau, triggers Ca^{2+} release via the ryanodine receptors from the sarcoplasmic reticulum (SR). This process is believed to be the result of Ca^{2+}-induced Ca^{2+} release (Fabiato, 1983). The increase in cytosolic $[Ca^{2+}]$ initiates contraction by binding to the contractile proteins resulting in cross-bridge cycling. Relaxation occurs when Ca^{2+} is removed from the cytosol by (a) Ca^{2+} reuptake into the SR and (b) extrusion from the cell (mainly via the Na^+ / Ca^{2+} exchanger). The rise and fall in intracellular $[Ca^{2+}]$ with each cardiac cycle is commonly known as the Ca^{2+} transient.

The reuptake of Ca^{2+} into the SR is mediated by the SR Ca^{2+} ATPase (or SR Ca^{2+} pump) which is a Ca^{2+} transport protein (named SERCA2) concentrated in the longitudinal component of the SR. Phospholamban is a regulator protein that binds to and inhibits Ca^{2+} transport by the SR Ca^{2+}-ATPase. Phosphorylation of phospholamban (via cyclic AMP - dependent protein kinase, Ca^{2+} calmodulin - dependent protein kinase or Ca^{2+} phospholipid - dependent protein kinase at distinct sites) removes the inhibition on the SR Ca^{2+} ATPase and facilitates Ca^{2+} reuptake (Sasaki *et al.* 1992). After uptake by the SR pump, Ca^{2+} is bound to calsequestrin (primarily located in the junctional SR), which is the major Ca^{2+}-binding protein in cardiac muscle.

During relaxation, the fall in intracellular [Ca^{2+}] is brought about mainly by SR reuptake but, in addition, some Ca^{2+} is extruded from the cell. This is mainly via the sarcolemmal Na^+ / Ca^{2+} exchanger which is responsible for 20 - 30 % of the decrease in intracellular [Ca^{2+}] during the decay phase of the Ca^{2+} transient. The Na^+ / Ca^{2+} exchanger is a counterion transporter on which 3 Na^+ are exchanged for each Ca^{2+}. There is also a sarcolemmal Ca^{2+} ATPase which also helps Ca^{2+} extrusion during diastole but its contribution is minimal. During steady state, the amount of Ca^{2+} entering the myocyte via the L-type Ca^{2+} channel with each beat should be equal to that extruded from the cell during diastole and the amount of Ca^{2+} released via the SR ryanodine receptors to the cytosol should equate the amount removed by the SR Ca^{2+} pump.

Abnormalities of excitation-contraction coupling in heart failure

Over the last decade or so, investigators have identified defects in various processes involved in excitation-contraction coupling in heart failure (Figueredo and Camacho, 1995; Gwathmey and Ingwall, 1995). These studies have been performed both in tissues from human subjects with heart failure and also in various animal models of heart failure. Since

hypertrophy is a prominent feature in the failing heart (Parmley, 1989), many studies have involved animal models of hypertrophy to try and understand the pathophysiology of heart failure. There are many well-established genetic models of hypertrophy and animals with hypertrophy and no heart failure tend to be easier to handle with a lower mortality (Smith and Nuttall, 1985; Elsner and Riegger, 1995). Although there are some similar findings in studies on hypertrophy and heart failure, many differences exist and as a result, more questions have been raised than answered. Some of these discrepancies may be explained by species difference but it must be emphasised that results obtained from different models may only be relevant to the individual model. It has been discussed above that there may be different signalling pathways for specific kinds of hypertrophy. The stimulus used to achieve hypertrophy, rather than simply the presence of hypertrophy itself, must have an important role to play in the results generated by the particular model. It is also difficult to find one single animal model of heart failure (or hypertrophy for that matter) that fully mimics the human scenario. One good example is the conflicting results obtained from various models of hypertrophy and heart failure on the L-type Ca^{2+} current density (Hart, 1994). In the review by Hart (1994), 3 of the 16 studies discussed showed significant reductions in Ca^{2+} current density, 2 showed reductions of 50 % while 2 models showed a significant increase with the remaining 9 studies showing no significant change. Therefore, one has to be careful in handling data obtained from studies on heart failure and hypertrophy especially when they come from different models, species and / or preparations. It is an over-simplification to extrapolate results obtained from models of pure hypertrophy (without decompensation) to draw conclusions about the situation in heart failure. The review below summarises the abnormalities in the processes involved in

excitation-contraction coupling identified in tissues from patients with or animal models of heart failure but not from hypertrophy alone.

The intracellular Ca^{2+} transient in heart failure

Most studies on excitation-contraction coupling in heart failure have demonstrated significant mechanical abnormality in the failing myocardium (Hasenfuss *et al.* 1992; Mulieri *et al.* 1992; Davies *et al.* 1995). There is usually reduced peak tension, reduced maximum rate of tension rise and a prolonged relaxation phase. Ca^{2+} handling was the first target of investigation to elucidate the cause for the abnormal force production. Several investigators have studied Ca^{2+} transients in failing myocardium to establish the relationship between Ca^{2+} homeostasis and the abnormal mechanical profile (Table 1.2).

Gwathmey *et al.* (1987) were the first to show that intracellular Ca^{2+} transients recorded in ventricular trabeculae from patients with heart failure were abnormal. Using aequorin, the Ca^{2+}-sensitive light signal showed 2 distinct components in the myopathic muscle. The Ca^{2+} transient in failing myocardium was prolonged and was associated with delayed relaxation. Although the distinct components were not reported by other investigators, Ca^{2+} transients obtained from failing myocardium or myocytes were consistently abnormal in animals (Bing *et al.* 1991; Siri *et al.* 1991; Wikman-Coffelt *et al.* 1991a; Perreault *et al.* 1992; Capasso *et al.* 1993) and in humans (Beuckelmann *et al.* 1992; Vahl *et al.* 1994) verifying that Ca^{2+} handling is indeed abnormal in the failing heart. Some discrepancies exist, however, in the results obtained from different animal models and in human tissue. The majority of the evidence supports a prolonged time course of the Ca^{2+} transient (Gwathmey *et al.* 1990; Beuckelmann *et al.* 1992; Perreault *et al.* 1992; Capasso *et al.* 1993; Vahl *et al.* 1994). Beuckelmann *et al.* (1992) were the first to report this finding in isolated myocytes from patients with heart failure. They also showed that the peak amplitude of the Ca^{2+}

transients was decreased whilst the resting [Ca^{2+}] was raised in the failing myocytes suggesting that the failing myocardium has a low systolic [Ca^{2+}] but a high diastolic [Ca^{2+}], a feature which was also shown by other workers (Wikman-Coffelt *et al.* 1991a; Capasso *et al.* 1993). In contrast, several groups have reported no change in the amplitude of the Ca^{2+} transient in failing myocardium at low (0.3 to 1 Hz) stimulation rates (Gwathmey *et al.* 1990; Perreault *et al.* 1992; Brooks *et al.* 1994; Vahl *et al.* 1994). Brooks *et al.* (1994) found that there was a significant decrease in peak systolic [Ca^{2+}] when the stimulation rate was increased above 2.0 Hz in failing rat hearts and a similar rate-dependent alteration in Ca^{2+} transient amplitude has also been reported by Pieske *et al.* (1995) in failing human myocardium. Vahl *et al.* (1994) found that the Ca^{2+} transients recorded from human failing myocardium were similar to controls under isometric conditions but when the muscle preparations were allowed to shorten with step-wise after-load reduction, the amplitude of the Ca^{2+} transient was increased, time to peak delayed and diastolic decay prolonged in failing myocardium. These discrepancies may be due to methodological factors or limitations but suggest that stimulation frequency and muscle shortening may differentially affect Ca^{2+} handling in heart failure.

Table 1.2 Changes in the intracellular Ca^{2+} transient in heart failure.

(Peak = peak amplitude, TTP = time to peak, RT = relaxation time, Dias = diastolic level)

First author	Year	Ca^{2+} transient				Species	Aetiology	Prep
		Peak	TTP	RT	Dias			
Gwathmey	1987			↑		Human	DCM/CAD	LV/RV trab
Gwathmey	1990	↔		↑	↑	Human	DCM/CAD	LV PapM
Bing	1991		↑		↓	Rat	SHR	LV PapM
Siri	1991	↓	↔	↔	↔	Guinea pig	AB	LV Myo
Wikman-Coffelt	1991	↓			↑	Hamster	CM	Heart
Perreault	1992	↔	↑	↑	↔	Dog	Pacing	LV/RV trab
Beuckelmann	1992	↓		↑	↑	Human	DCM/CAD	Myo
Capasso	1993	↓	↑	↑	↑	Rat	Ischaemia	LV/RV Myo
Brooks	1994	↔/↓				Rat	SHR	Heart
Vahl	1994	↔/↑	↔/↑	↑		Human	DCM	LV strips

L-type Ca^{2+} channels in heart failure

As mentioned above, the majority of workers failed to demonstrate any functional abnormality in the L-type Ca^{2+} channels with no change in the Ca^{2+} current (Beuckelmann *et al.* 1991; Mewes and Ravens, 1994; Kaab *et al.* 1996; Qiu *et al.* 1996; Rozanski *et al.* 1997) whilst some demonstrated a decreased current in failing myocytes (Rossner, 1991; Hatem *et al.* 1994; Ming *et al.* 1994). The picture becomes more confusing when the abundance of the Ca^{2+} channel was investigated by examining the expression of the dihydropyridine (DHP) receptor and the number of DHP binding sites (see Table 1.3). Early studies on the cardiomyopathic hamster, using specific Ca^{2+} channel photoaffinity ligands, indicated an increase in DHP binding sites especially in the early stages (3 - 4 months old) of cardiomyopathy (Finkel *et al.* 1986; Wagner *et al.* 1986; Finkel *et al.* 1987; Kobayashi *et al.* 1987; Kuo *et al.* 1987). This suggested an increase in Ca^{2+} channels which was presumed to cause Ca^{2+} overload - believed to be behind the pathogenesis of the condition. Finkel (1987) found that these differences disappeared by 10 months, indicating a relative decrease over time with the pathological process. However, subsequent studies failed to show any difference in this animal model (Howlett and Gordon, 1987; Bazan *et al.* 1991) and the study by Bazan *et al.* (1991) even showed a small decrease at 8 to 9 months. In humans, DHP binding studies by Rasmussen (1990) showed no difference in idiopathic dilated cardiomyopathy. Takahashi *et al.* (1992a) found that the level of mRNA encoding the DHP receptor was decreased in myocardium from patients with heart failure as was the number of DHP binding sites. These discrepancies may be due to species difference or to the difference in the pathogenesis of the disease process or the progression of the disease with time. There are also suggestions that different DHP binding sites (high or low affinity) were being examined in the individual studies (Bazan *et al.* 1991).

Taking all the data as a whole, it seems that there should be an adequate Ca^{2+} trigger in the failing ventricular myocardium as the bulk of the evidence suggests against gross abnormality in the Ca^{2+} current. Defects in other processes have to be sought to explain the abnormal Ca^{2+} handling and force production in heart failure.

Table 1.3 Changes in L-type Ca^{2+} channels in heart failure.

Effect	First author	Year	Species	Aetiology	Prep
			m-RNA level for DHP receptors		
↓	Takahashi	1992	Human	DCM / CAD	RNA
			DHP binding		
↑	Finkel	1986	Hamster	CM	Memb
↑	Wagner	1986	Hamster	CM	Memb
↑ / ↔	Finkel	1987	Hamster	CM	Memb
↑	Kuo	1987	Hamster	CM	Memb
↑	Kobayashi	1987	Hamster	CM	Memb
↔	Howlett	1987	Hamster	CM	Memb
↔	Rasmussen	1990	Human	DCM	Memb
↔ / ↓	Bazan	1990	Hamster	CM	Memb
↓	Takahashi	1992	Human	DCM / CAD	Memb

SR Ca^{2+}-release (Ryanodine) channels in heart failure

The first study on mRNA coding of Ca^{2+}-release channels in patients with heart failure by Brillantes *et al.* (1992) showed that the expression was decreased in ischaemic cardiomyopathy whilst there was a non-significant increase in idiopathic dilated cardiomyopathy. Subsequent studies showed decreased expression in patients with heart failure of various aetiology (Arai *et al.* 1993; Go *et al.* 1995). This was, however, not matched by a decrease in the amount of protein, with the study by Meyer *et al.* (1995) showing no change in the level of the Ca^{2+}-release channel (see Table 1.4).

Ryanodine binding studies produced an even more confusing picture. Two studies on the cardiomyopathic hamster (Finkel *et al.* 1992; Sapp and Howlett, 1994) showed an increase in radioligand binding capacity with no change in affinity suggesting an increase in ryanodine binding sites. Lachnit *et al.* (Lachnit *et al.* 1994) did not confirm these results but, rather, showed a decrease in ryanodine binding site density associated with a decreased mRNA level for the channel in the myopathic hamster. Studies on the dog with dilated cardiomyopathy or pacing-induced heart failure also showed a decrease in ryanodine binding sites (Cory *et al.* 1993; Vatner *et al.* 1994) whilst two studies on other models of heart failure (rabbit and rat) showed no change (Bouanani *et al.* 1994; Gomez *et al.* 1997). Despite the conflicting data described, it would seem that the majority of the evidence is suggesting a downregulation of the Ca^{2+}-release channel in heart failure. This is supported by functional studies (D'Agnolo *et al.* 1992; Cory *et al.* 1993) which showed a decreased activity of the Ca^{2+}-release channel. The decreased expression, amount and / or activity of the SR Ca^{2+}-release channel may explain the decreased peak amplitude of the Ca^{2+} transient (or systolic $[Ca^{2+}]$) in heart failure as the Ca^{2+} trigger appears to be adequate. The radioligand binding studies by Lachnit *et al.* (1994) and Vatner *et al.* (1994) showed no

difference in DHP receptor density but that there was a decrease in ryanodine receptor density. This altered ryanodine to DHP receptor ratio may play an important role in the abnormal excitation-contraction coupling in heart failure with a direct effect on the Ca^{2+}-amplification (Ca^{2+}-induced Ca^{2+} release) process. A recent study (Gomez *et al.* 1997) also showed that the effectiveness of the trigger Ca^{2+} to evoke Ca^{2+} release may also be impaired in heart failure as a result of altered micro-architecture in the arrangement between L-type Ca^{2+} channels and SR Ca^{2+}-release channels. In this study, Gomez *et al.* (1997) showed a reduced amplitude of the Ca^{2+} transient in a hypertension-induced heart failure model of the rat. There was no change in Ca^{2+} current density or SR Ca^{2+}-release channels as measured by ryanodine binding. However, the ability of Ca^{2+} influx to trigger SR Ca^{2+}-release was significantly impaired with a reduced probability of evoking Ca^{2+} sparks (fundamental SR Ca^{2+}-release events). The authors concluded that, in the absence of changes in the L-type Ca^{2+} channels or SR Ca^{2+}-release channels, the defect was in the architectural arrangement between the two, as it was believed that SR Ca^{2+}-release is very sensitive to the geometric arrangement of the 2 groups of channels.

Table 1.4 Changes in SR Ca^{2+}-release (Ryanodine) channels in heart failure.

Effect	First author	Year	Species	Aetiology	Prep
			m-RNA level		
↓	Brillantes	1992	Human	CAD	RNA
↔	Brillantes	1992	Human	DCM	RNA
↓	Arai	1993	Human	DCM / CAD	RNA
↓	Go	1995	Human	DCM / CAD	RNA
			Protein level		
↔	Meyer	1995	Human	DCM	LV homogenate
			Ryanodine binding		
↑	Finkel	1992	Hamster	CM	Membrane
↓	Cory	1993	Dog	DCM / pacing	Membrane
↔	Bouanani	1994	Rabbit	V + P overload	Membrane
↑	Sapp	1994	Hamster	CM	Membrane
↓	Lachnit	1994	Hamster	CM	Membrane
↓	Vatner	1994	Dog	Pacing	Membrane
↔	Gomez	1997	Rat	Hypertension	SR vesicles
			Activity		
↓	Cory	1993	Dog	DCM / pacing	Membrane
			Gating mechanism		
↓	D'Agnolo	1992	Human	DCM	Skinned fibres

SR Ca^{2+}-ATPase in heart failure

As mentioned above, prolonged diastolic Ca^{2+} decay was found to be a consistent feature in studies of intracellular Ca^{2+} transients in heart failure. Much attention has been focused upon Ca^{2+}-reuptake by the SR (Table 1.5). Studies on the expression of SR Ca^{2+}-ATPase have uniformly demonstrated depressed mRNA levels in failing myocardium (Mercadier *et al.* 1990; Feldman *et al.* 1991; Kuo *et al.* 1992; Takahashi *et al.* 1992b; Arai *et al.* 1993; Studer *et al.* 1994; Schwinger *et al.* 1995; Linck *et al.* 1996). There is, however, debate as to the level of SERCA IIa protein in heart failure with some groups showing a decrease (Hasenfuss *et al.* 1994; Studer *et al.* 1994; Kiss *et al.* 1995; Meyer *et al.* 1995; Gupta *et al.* 1997) that was not confirmed by others (Movsesian *et al.* 1994; Schwinger *et al.* 1995; Linck *et al.* 1996). This may be the result of differences in the preparation of tissues studied or variation in the underlying aetiology and in control tissues. The discrepancy in the results of protein level studies contrast with the agreement in the finding of a decreased mRNA level in heart failure, leading some authors to suggest that the regulation of protein levels may be independent of the encoding mRNA levels (Schwinger *et al.* 1995; Linck *et al.* 1996).

The majority of functional studies on the SR Ca^{2+} pump examining Ca^{2+} uptake have shown a decreased SR Ca^{2+}-ATPase activity in heart failure (Limas *et al.* 1987; Whitmer *et al.* 1988; Kuo *et al.* 1992; Cory *et al.* 1993; Bouanani *et al.* 1994; Kiss *et al.* 1995; Gupta *et al.* 1997). Movesesian *et al.* (1989) did not find a difference in left ventricular vesicle preparations from patients with dilated cardiomyopathy. Schwinger *et al.* (1995) found a decreased Ca^{2+} uptake activity in crude membrane preparations but no difference in vesicle preparations. The difference in the results between membrane preparations and vesicle preparations may be the direct effect of the isolation procedure, with changes in the

preparation during the gradient centrifugation process affecting subsequent Ca^{2+}-uptake activity. Denvir *et al.* (1995; 1996) examined SR Ca^{2+}-loading ability using caffeine-induced contractures in saponin-skinned trabeculae from patients with heart failure (Denvir *et al.* 1995) and in a rabbit coronary artery ligation model (Denvir *et al.* 1996). It was found that SR Ca^{2+}-loading ability decreased with increasing severity of heart failure in human subjects whilst it was shown to be enhanced in the rabbit model. This rather anomalous result in the rabbit heart failure model may be due to a reduced SR Ca^{2+} leak in the failing myocardium (with an increased net accumulation of Ca^{2+} despite a possibly reduced uptake), increased total volume of SR or to changes specific to the rabbit model (Denvir *et al.* 1996).

Taking all the results as a whole, the expression of SR Ca^{2+}-ATPase is decreased in heart failure. This is translated into decreased function with reduced Ca^{2+}-uptake activity demonstrated in the majority of studies, although there is still debate as to the level of the SR Ca^{2+} pump protein. These findings correspond with the prolonged decay phase of intracellular Ca^{2+} transients measured in the failing myocardium.

Table 1.5 Changes in SR Ca^{2+}-ATPase in heart failure.

Effect	First author	Year	Species	Aetiology	Prep
			m-RNA levels		
↓	Mercadier	1990	Human	DCM / CAD	RNA
↓	Feldman	1991	Human	DCM	RNA - PCR
↓	Takahashi	1992	Human	DCM / CAD	RNA
↓	Kuo	1992	Hamster	CM	RNA
↓	Arai	1993	Human	DCM / CAD	RNA
↓	Studer	1994	Human	DCM / CAD	RNA
↓	Schwinger	1995	Human	DCM	RNA
↓	Linck	1996	Human	DCM / CAD	RNA
			Protein levels		
↓	Hasenfuss	1994	Human	DCM / CAD	LV homogenate
↔	Movsesian	1994	Human	DCM	LV vesicles
↓	Studer	1994	Human	DCM / CAD	LV homogenate
↓	Meyer	1995	Human	DCM	LV homogenate
↓	Kiss	1995	Guinea-pig	AB / HF	LV homogenate
↔	Schwinger	1995	Human	DCM	vesicles / membrane
↔	Linck	1996	Human	DCM / CAD	LV homogenate
↓	Gupta	1997	Dog	ICE	LV vesicles
			Activity		
↓	Limas	1987	Human	DCM	RV Biopsy
↓	Whitmer	1988	Hamster	CM	Homogenate
↔	Movsesian	1989	Human	DCM	LV vesicles
↓	Kuo	1992	Hamster	CM	SR membranes
↓	Cory	1993	Dog	DCM / pacing	SR membranes
↓	Bouanani	1994	Rabbit	V + P overload	LV homogenate
↓	Kiss	1995	Guinea-pig	AB / HF	LV homogenate
↓	Schwinger	1995	Human	DCM	membrane
↔	Schwinger	1995	Human	DCM	vesicles
↓	Denvir	1995	Human	DCM / CAD	RV skinned trab
↑	Denvir	1996	Rabbit	CAL	LV/RV skinned trab
↓	Gupta	1997	Dog	ICE	LV vesicles

Phospholamban in heart failure

Studies on the expression of phospholamban in human heart failure have been consistent in showing a decreased mRNA level (Feldman *et al.* 1991; Arai *et al.* 1993; Schwinger *et al.* 1995; Linck *et al.* 1996) (Table 1.6). However, the results of the level of phospholamban protein in heart failure were less congruous with some groups reporting a decrease in protein level (Kiss *et al.* 1995; Meyer *et al.* 1995; Hasenfuss *et al.* 1996) and others showing no difference between failing myocardium and control tissue (Bohm *et al.* 1994; Movsesian *et al.* 1994; Schwinger *et al.* 1995; Linck *et al.* 1996).

Phospholamban is a regulatory protein that normally inhibits SR Ca^{2+}-ATPase. Decreased expression and or level of phospholamban would remove the inhibition on the SR Ca^{2+} pump and improve Ca^{2+} reuptake by the SR. This could be seen as a compensatory mechanism for the reduced SR Ca^{2+}-ATPase activity in heart failure. In the study by Kiss *et al.* (1995), there was reduction in both SR Ca^{2+}-ATPase (by 15% compared to controls) and phospholamban levels (by 35% compared to controls). Even with the relatively greater reduction of phospholamban level than SR Ca^{2+} pump, Ca^{2+} uptake rate by the SR was still reduced. However, Movesesian *et al.* (1990) showed that phospholamban-mediated stimulation of SR Ca^{2+} uptake was unchanged in patients with idiopathic dilated cardiomyopathy. Phosphorylation of phospholamban normally removes its inhibition on the SR Ca^{2+}-ATPase. Bohm *et al.* (1994) found no change in cyclic AMP - dependent phosphorylation of phospholamban whilst others demonstrated a decrease (Bartel *et al.* 1996; Schmidt *et al.* 1996). Basal cyclic AMP content was found to be reduced by Bohm *et al.* (1994) which would agree with the well-recognised fact that adrenergic effects are blunted in the failing heart as a result of β_1-adrenoceptor down-regulation. This may help explain the finding of reduced cyclic AMP - dependent phosphorylation in heart failure but

does not exclude the possibility of phosphorylation via other protein kinase systems (Currie and Smith, 1996). One study (Rouetbenzineb *et al.* 1996) showed a decrease in protein kinase C activity and expression of Ca^{2+}-dependent protein kinase C isoforms in a rabbit model of heart failure whilst another report (Kirchhefer *et al.* 1997) suggested an increase in Ca^{2+} / calmodulin - dependent protein kinase activity in human heart failure. Either of these kinase systems may affect the phosphorylation of phospholamban and hence SR Ca^{2+}-ATPase activity. These results bring further confusion as to the functional significance of phospholamban in the abnormal Ca^{2+} handling and pathogenesis in heart failure.

Table 1.6 Changes in phospholamban in heart failure.

Effect	First author	Year	Species	Aetiology	Prep
			m-RNA levels		
↓	Feldman	1991	Human	DCM	RNA - PCR
↓	Arai	1993	Human	DCM /CAD	RNA
↓	Schwinger	1995	Human	DCM	RNA
↓	Linck	1996	Human	DCM / CAD	RNA
			Protein levels		
↔	Movsesian	1994	Human	DCM	LV vesicles
↔	Bohm	1994	Human	DCM / CAD	Homogenate
↓	Meyer	1995	Human	DCM	LV homogenate
↓	Kiss	1995	Guinea-pig	AB / HF	LV homogenate
↔	Schwinger	1995	Human	DCM	vesicles/membrane
↔	Linck	1996	Human	DCM / CAD	LV homogenate
↓	Hasenfuss	1996	Human	DCM / CAD	LV homogenate
			Activity		
↔	Movsesian	1990	Human	DCM	LV vesicles
			Phosphorylation		
↔	Bohm	1994	Human	DCM / CAD	Homogenate
↓	Bartel	1996	Human	DCM / CAD	Homogenate

Na^+ / Ca^{2+} exchanger in heart failure

Studies on the expression, protein level and activity of the Na^+ / Ca^{2+} exchanger suggest an upregulation in the trans-sarcolemmal counterion transporter in human heart failure (Table 1.7). Studer *et al.* (1994) and Flesch *et al.* (1996) both showed increased mRNA and protein levels of the Na^+ / Ca^{2+} exchanger in failing human myocardium. Reinecke *et al.* (1996) also showed an increase in the exchanger protein level and, in addition, the activity of the exchanger as measured by Na^+ gradient-induced Ca^{2+} transport was also increased. This is thought to be a compensatory mechanism for the reduced activity of the SR Ca^{2+}-ATPase in the failing myocardium but is also thought to play a potentially arrhythmogenic role in generating inward currents with Na^+ influx. However, there are also reports on animal models of hypertrophy (Naqvi and MacLeod, 1994) that the exchanger activity may also be reduced in hypertrophied cardiomyocytes. As mentioned in the section *"Electrophysiological abnormalities in the failing myocardium"*, studies on the Na^+ / Ca^{2+} exchanger current have shown abnormal activity in heart failure but it has been shown to be both increased (Hatem *et al.* 1994) and decreased (Zhang *et al.* 1996) in different animal models of heart failure. Despite the rather conflicting results from animal models, human studies provide compelling data that the Na^+ / Ca^{2+} exchanger is upregulated in heart failure and it may play an important role in the altered Ca^{2+} homeostasis in heart failure.

Table 1.7 Changes in Na^+ / Ca^{2+} exchanger in heart failure.

Effect	First author	Year	Species	Aetiology	Prep
			m-RNA levels		
↑	Studer	1994	Human	DCM / CAD	RNA
↑	Flesch	1996	Human	DCM / CAD	RNA
			Protein levels		
↑	Studer	1994	Human	DCM / CAD	LV membranes
↑	Flesch	1996	Human	DCM / CAD	Homogenate
↑	Reinecke	1996	Human	DCM / CAD	LV membranes
			Activity		
↑	Reinecke	1996	Human	DCM / CAD	LV membranes

SR Ca^{2+} storage in heart failure

There is consistent information that both the expression (Takahashi *et al.* 1992a; Arai *et al.* 1993) and level (Movsesian *et al.* 1994; Meyer *et al.* 1995) of the SR Ca^{2+} binding protein calsequestrin are unchanged in human heart failure (Table 1.8). The amount of another Ca^{2+} binding protein found in the SR, calreticulin was also found to be unchanged in human heart failure (Meyer *et al.* 1995) indicating that there is no major abnormality in SR Ca^{2+} storage in heart failure.

Myofilament abnormalities in heart failure

The majority of studies examining Ca^{2+} sensitivity of skinned myocardial fibres (Wankerl *et al.* 1990; D'Agnolo *et al.* 1992; Hajjar and Gwathmey, 1992; Denvir *et al.* 1995; Denvir *et al.* 1996) showed no significant change in heart failure (Table 1.9). There are some studies suggesting an increase in Ca^{2+} sensitivity in the failing myocardium (Schwinger *et al.* 1994; Wolff *et al.* 1995). The lack of evidence that myofilament Ca^{2+} sensitivity is reduced in heart failure suggests that this is not the mechanism behind the systolic impairment in the failing heart. Despite the fact that myofibrillar content and myofibrillar Mg-ATPase activity appear to be reduced in the failing heart (Pagani *et al.* 1988; Hasenfuss *et al.* 1992), the major disturbance in systolic force production appears to lie in the Ca^{2+} control mechanisms rather than the contractile units *per se* in heart failure.

Table 1.8 Calsequestrin in heart failure.

Effect	First author	Year	Species	Aetiology	Prep
			m-RNA levels		
↔	Takahashi	1992	Human	DCM / CAD	RNA
↔	Arai	1993	Human	DCM / CAD	RNA
			Protein levels		
↔	Movsesian	1994	Human	DCM	LV vesicles
↔	Meyer	1995	Human	DCM	LV homogenate

Table 1.9 Myofilament Ca^{2+} sensitivity in heart failure.

Effect	First author	Year	Species	Aetiology	Prep
↔	Wankeri	1990	Human	DCM / CAD / MVD	skinned fibres
↔	Hajjar	1992	Human	DCM	skinned fibres
↔	D'Agnolo	1992	Human	DCM	skinned fibres
↑	Schwinger	1994	Human	DCM	skinned fibres
↔	Denvir	1995	Human	DCM / CAD	skinned fibres
↑	Wolff	1995	Dog	Pacing	skinned myocytes
↔	Denvir	1995	Rabbits	CAL	skinned fibres

There is no doubt that excitation-contraction coupling is abnormal in the failing heart. Changes in the various processes involved may be directly or indirectly related to the systolic and diastolic dysfunction seen in the remodelled failing myocardium. Ca^{2+} handling is abnormal and depressed SR function appears to be the major defect in the abnormal excitation-contraction coupling process. Investigations are already underway focusing on the SR as the potential target for gene therapy (Luo *et al.* 1996; Hajjar *et al.* 1997) with a view to correcting the contractile abnormality in heart failure. Disappointing results from clinical trials on positive inotropic agents (e.g. phosphodiesterase inhibitors), which increased morbidity and mortality in patients with heart failure despite haemodynamic benefits (Packer *et al.* 1991), serve to provide a cautionary note. Even in drugs that have been shown to be of prognostic benefit in heart failure, like angiotensin converting enzyme inhibitors (Swedberg, 1987; The SOLVD investigators, 1991) and third-generation β-blockers (e.g. carvedilol) (Bristow *et al.* 1996; Packer *et al.* 1996), their therapeutic effects are not full understood particularly at the tissue level. Clearly, much work has still to be done to investigate the relationship between the various abnormal processes involved in the pathogenesis and progression of heart failure.

CHAPTER 2

THESIS AIMS & LAYOUT

Aims of study

As discussed in Chapter 1, congestive heart failure is a common and growing problem with high morbidity and mortality. Despite the vast amount of research work over the years, there are still many gaps in our knowledge about much of the pathophysiology behind the clinical syndrome. Many animal and human studies yielded different results. This may be partly explained by species difference but in some cases, the animal models of heart failure are not representative of the human situation. The main aim of this study is to examine heart failure using an animal model which is clinically relevant and to study such changes in the isolated heart under conditions as close to those *in vivo* as possible. A rabbit coronary artery ligation model was used which had been developed and characterised by Pye *et al.* (1996) at the Department of Medical Cardiology, Glasgow Royal Infirmary. Rabbits were allowed to develop heart failure over time after coronary artery ligation. This process is similar to the scenario in the commonest cause of human heart failure in the Western world in which failure occurs months or years after myocardial infarction. The degree of cardiac dysfunction was assessed *in vivo* by echocardiography. *In vitro* mechanical dysfunction was studied in greater detail in the isolated heart using Langendorff perfusion and the working heart configuration. Ca^{2+} handling in heart failure was examined by developing a technique that allowed the measurement of changes of $[Ca^{2+}]$ with the cardiac cycle (i.e. Ca^{2+} transients) from different regions in Langendorff-perfused whole hearts. Electrical events of activation and repolarisation were studied in the same regions from where the Ca^{2+} transients were sampled. With these measurements, the mechanical, Ca^{2+}-handling and electrical properties of hearts from rabbits with heart failure were studied and correlated using the same clinically relevant model.

Thesis layout

Chapter 3 outlines all the methods involved in the experimental work described in this thesis. These include:-

a) the coronary artery ligation procedure to produce myocardial infarction and subsequent heart failure in the rabbit.

b) echocardiography to assess *in vivo* cardiac dysfunction.

c) the working heart configuration for studying mechanical performance of the isolated heart.

d) measurements of $[Ca^{2+}]$ from the epicardial surface of Langendorff-perfused hearts.

e) measurements of Monophasic Action Potentials from the epicardial surface of Langendorff-perfused hearts.

f) assessment of heart failure and cardiac remodelling by organ weights.

Chapter 4 describes the assessment of the degree of cardiac dysfunction and remodelling produced by the coronary artery ligation model in rabbits used for the experimental studies. These include echocardiographic measurements and organ / tissue weight measurements.

Chapters 5 and *6* describe the results of the experiments looking at the mechanical performance of the isolated heart. *Chapter 5* summarises the results of experiments on the working heart configuration in normal stock rabbit hearts. The response of the isolated working heart to load changes and the Frank-Starling mechanism were studied. In *Chapter 6,* the mechanical performance of the failing heart in the working heart configuration was studied as well as the response to load changes. The mechanical performance of the failing heart in the Langendorff mode was also described. The *in vitro* cardiac performance of the failing hearts were correlated with *in vivo* echocardiographic measurements.

Chapters 7 and *8* include the results of $[Ca^{2+}]$ measurements in the isolated Langendorff perfused heart. The novel method of measuring Ca^{2+} transients from different regions of the left ventricular epicardial surface in the isolated beating heart was described and characterised in *Chapter 7*. *Chapter 8* summarises the analysis of the data obtained from failing hearts and controls.

Chapter 9 describes the results of experiments examining ventricular repolarisation in the failing heart by measuring Monophasic Action Potentials (MAPs) over the left ventricular epicardial surface of the isolated beating heart.

Chapter 10 attempts to correlate the changes seen in the failing heart in mechanical performance, Ca^{2+} handling and ventricular repolarisation and discusses their significance in the pathophysiology of the syndrome.

Chapter 11 addresses a separate issue which is the effect of altered conduction on the mechanical performance of the failing heart. Analysis of data on Ca^{2+} transients and MAP signals revealed significant abnormality which may be attributable to abnormal electrical conduction pattern in the failing heart. The potential contribution of such abnormality to the impaired mechanical performance seen in heart failure was investigated and discussed.

Chapter 12 is a synopsis of the thesis summarising the results from all the experimental studies and attempts to relate these results with our current knowledge of the pathophysiology of heart failure.

CHAPTER 3

METHODS

Coronary artery ligation in the rabbit

Background

Many animal models have been used to study heart failure (Smith and Nuttall, 1985; Elsner and Riegger, 1995), with different causes of the final heart failure state. The pathogenesis of heart failure may be specific to the individual models and what happens in the human clinical syndrome may be quite different. If an animal model of heart failure is to be used, it has to reflect the human situation so that the results from such studies can be applied to provide insights into the human condition.

A rabbit coronary artery ligation model of heart failure was used for this study. This model was established and developed in the Department of Cardiology, Glasgow Royal Infirmary by Dr. Maurice Pye and Prof. Stuart Cobbe. Coronary artery disease is by far the commonest cause of heart failure in the Western world with myocardial infarction giving rise to contractile dysfunction and pump failure. The rabbit coronary artery ligation model has been characterised and shown to produce heart failure as a result of left ventricular dysfunction arising from myocardial infarction (Pye *et al.* 1996), thus making it a clinically relevant model. The rabbit has a poorly developed collateral coronary circulation (Maxwell *et al.* 1987), similar to humans and the pig. Ligation of a coronary artery produces a well defined myocardial infarct, which leads to cardiac remodelling in a similar way to that seen in humans. The severity of subsequent contractile dysfunction varies according to the size of the initial infarct and the remodelling process or compensatory mechanisms - this allows a range of cardiac performance to be studied and compared. In addition, processes involved in excitation-contraction coupling including electrophysiology and Ca^{2+} handling are

relatively similar to humans in the rabbit compared to other common laboratory animals like the rat or mouse.

Method

Adult male New Zealand White rabbits (2.5 - 3.0 kg) were premedicated with 0.4 $ml.kg^{-1}$ intramuscular Hypnorm [fentanyl citrate (0.315 $mg.ml^{-1}$) : fluanisone (10 $mg.ml^{-1}$), Janssen Pharmaceuticals]. Anaesthesia was induced with 0.25 - 0.5 $mg.kg^{-1}$ midazolam (Hypnovel, Roche) given via an indwelling cannula in the marginal ear vein. The rabbit was intubated with an uncuffed size 3 - 3.5 endotracheal tube inserted over a soft-tipped wire introducer with the aid of a Wisconsin paediatric straight blade (size 1) laryngoscope. The endotracheal tube was secured by taping to the operating table and was connected to a Harvard small animal ventilator. The rabbit was ventilated with a 1:1 mixture of nitrous oxide and oxygen containing 1 % halothane at a tidal volume of 50 ml and a frequency of 40 min^{-1}. Preoperative antibiotic prophylaxis was given with 1 ml Amfipen (ampicillin 100 $mg.ml^{-1}$, Mycofarm UK Ltd) intramuscularly and the rabbit was placed on a pre-warmed table with body temperature maintained by means of a thermostatically controlled heating mat. The anterior chest wall was shaved and cleaned with Hibidil in isopropyl alcohol.

A left thoracotomy was performed through the 4^{th} intercostal space. The left lung was gently retracted exposing the heart. The pericardium was incised and the heart was lifted up with a tie placed through the ventricular apex to allow easier manipulation. Quinidine hydrochloride 10 $mg.kg^{-1}$ (Sigma Pharmaceuticals) was administered intravenously prior to coronary artery ligation to reduce the incidence of ventricular fibrillation. Coronary circulation in the rabbit is different from that in humans. The left anterior descending artery is short and only supplies a small area of the interventricular septum. The left circumflex coronary artery gives off a marginal branch which supplies the left ventricular apex and

most of the left ventricular free wall. This artery was identified and ligated halfway between the atrioventricular groove and the ventricular apex using 6 / 0 Ethicon suture to produce an ischaemic area of 30 - 40 % of the left ventricle. As there is relatively little collateral circulation in the rabbit, a homogenous apical infarct was produced. Ventricular fibrillation occurred in approximately 30 % of cases, usually 8 to 12 min following occlusion and defibrillation was undertaken with a 5 - 10 J DC shock using small sterilised paddles applied directly on the epicardial surface of the heart.

Once the animal was stable, the left lung, which would normally be collapsed, was re-inflated by occluding the outlet of the ventilator. The chest was then closed in layers using 2 / 0 interrupted catgut sutures for the deep layer bringing the ribs together, 4 / 0 catgut continuous suture for the subcutaneous layer and 2 / 0 Dexon for a continuous subcuticular suture to close the skin. The animal was then given 20 ml of isotonic saline intravenously to replace perioperative fluid losses and allowed to convalesce in a warm clean environment with adequate monitoring for any early signs of distress. Analgesia was given with 0.04 $mg.kg^{-1}$ intramuscular Vetergesic (buprenorphine hydrochloride 0.3 $mg.ml^{-1}$, Reckitt & Colman Products Ltd) immediately after surgery and the next morning. Heart failure was allowed to develop in these rabbits for 8 weeks prior to sacrifice for the experimental studies.

Sham-operated rabbits which underwent thoracotomy, pericardium incision and had the heart manipulated in a similar fashion as ligated animals but without coronary artery ligation were used as controls. Experimental studies were again carried out 8 weeks after the surgical procedure so that the control animals would be of a similar maturity as the ligated animals at the time of sacrifice.

Echocardiography

Background

Echocardiography is a diagnostic technique using high frequency ultrasound (2 to 7 MHz) to assess structural, functional and haemodynamic status of the cardiovascular system. Edler and Hertz (1954) were the first to record movement of cardiac structures with ultrasound in 1954. In 1965, Feigenbaum *et al.* (1965) reported the first ultrasound detection of pericardial effusion and introduced the technique into the clinical practice of cardiology. Echocardiography is now widely used clinically for assessing cardiac chamber sizes, valvular function and ventricular performance. It can be performed in a transthoracic manner which is non-invasive and the heart and its motion during the cardiac cycle can be visualised in real-time. Chronic impairment in ventricular performance can lead to volume overload with dilatation of cardiac chambers which can be seen easily with echocardiography. Left ventricular ejection fraction has been shown to be a reasonable estimate of ventricular performance with clinical and prognostic significance (Nelson *et al.* 1975). Measurements can be made from two-dimensional echocardiography of ventricular volumes from which ejection fraction can be calculated. This has been shown to be reliable in human studies (Stamm *et al.* 1982) and also in dogs (Buda and Zotz, 1986). Pye *et al.* (1996) in the Department of Cardiology, Glasgow Royal Infirmary have shown that echocardiography provides a non-invasive yet powerful means of characterising haemodynamic performance of the heart *in vivo* in the same model of heart failure used in this thesis.

Method

Echocardiography was performed 1 week prior to sacrifice for the experimental studies to assess *in vivo* cardiac performance, using a 5 MHz paediatric probe with a Toshiba sonograph (Sonolayer 100). The rabbit was sedated with 0.3 $mg.kg^{-1}$ Hypnorm and a small area of the anterior chest wall was shaved to allow a satisfactory echo window. The animal was placed in the left lateral position and a parasternal long-axis view was obtained to assess the left atrial dimension (LAD) and left ventricular end-diastolic dimension (LVEDD) in the M-mode (see Figure 3.1). Ejection fraction (EF) was assessed in the short-axis view at a level just below the tips of the mitral valve leaflets. Using the end-diastolic and end-systolic frames captured, the endocardial border was marked and the enclosed area automatically computed (Figure 3.2). EF was calculated as the percentage area reduction with systole.

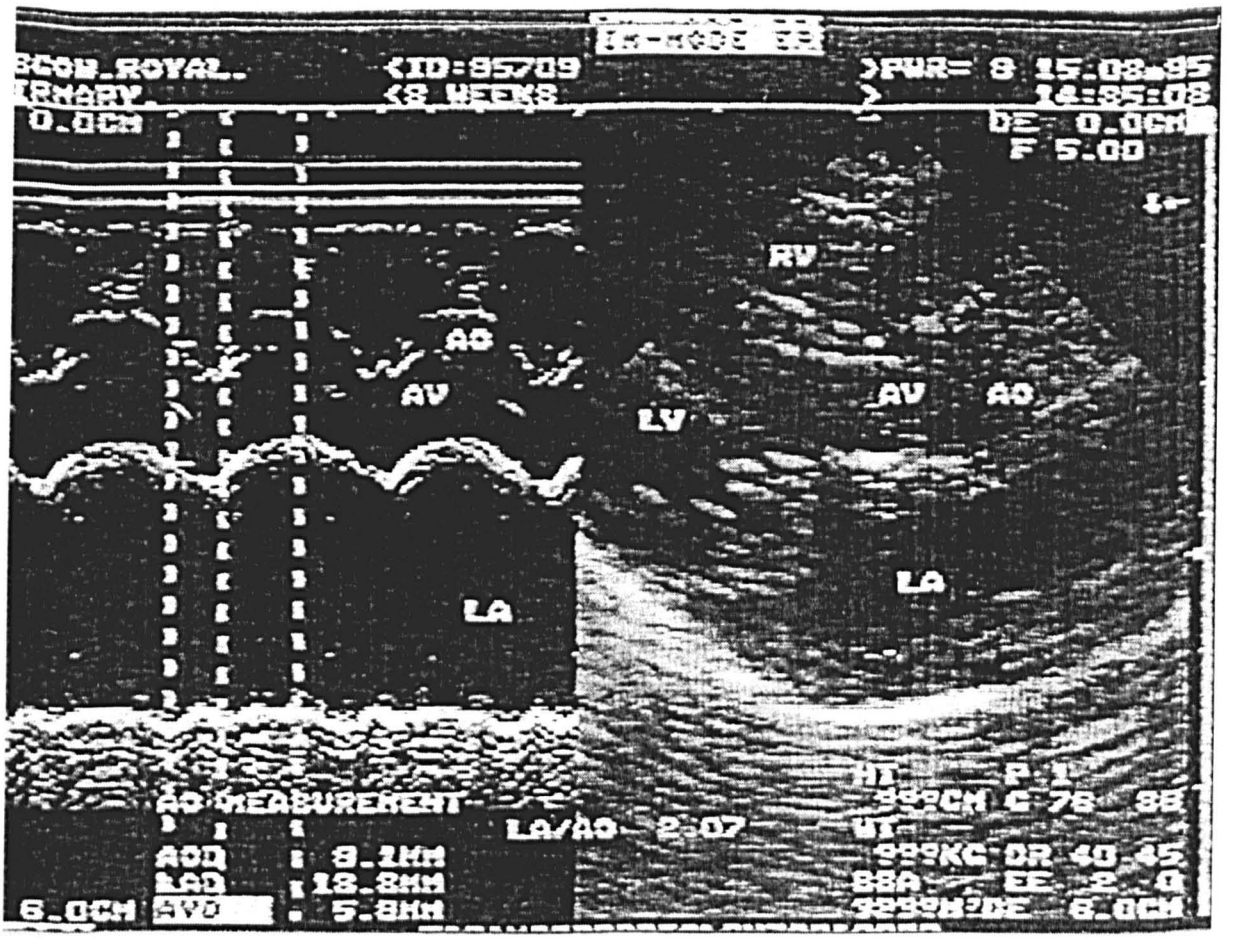

Figure 3.1 Parasternal long-axis view (right panel) on echocardiography in a rabbit with heart failure with M-mode recordings (left panel) at the level of aortic valve (AV) showing measurements for aorta (Ao) and left atrium (LA).

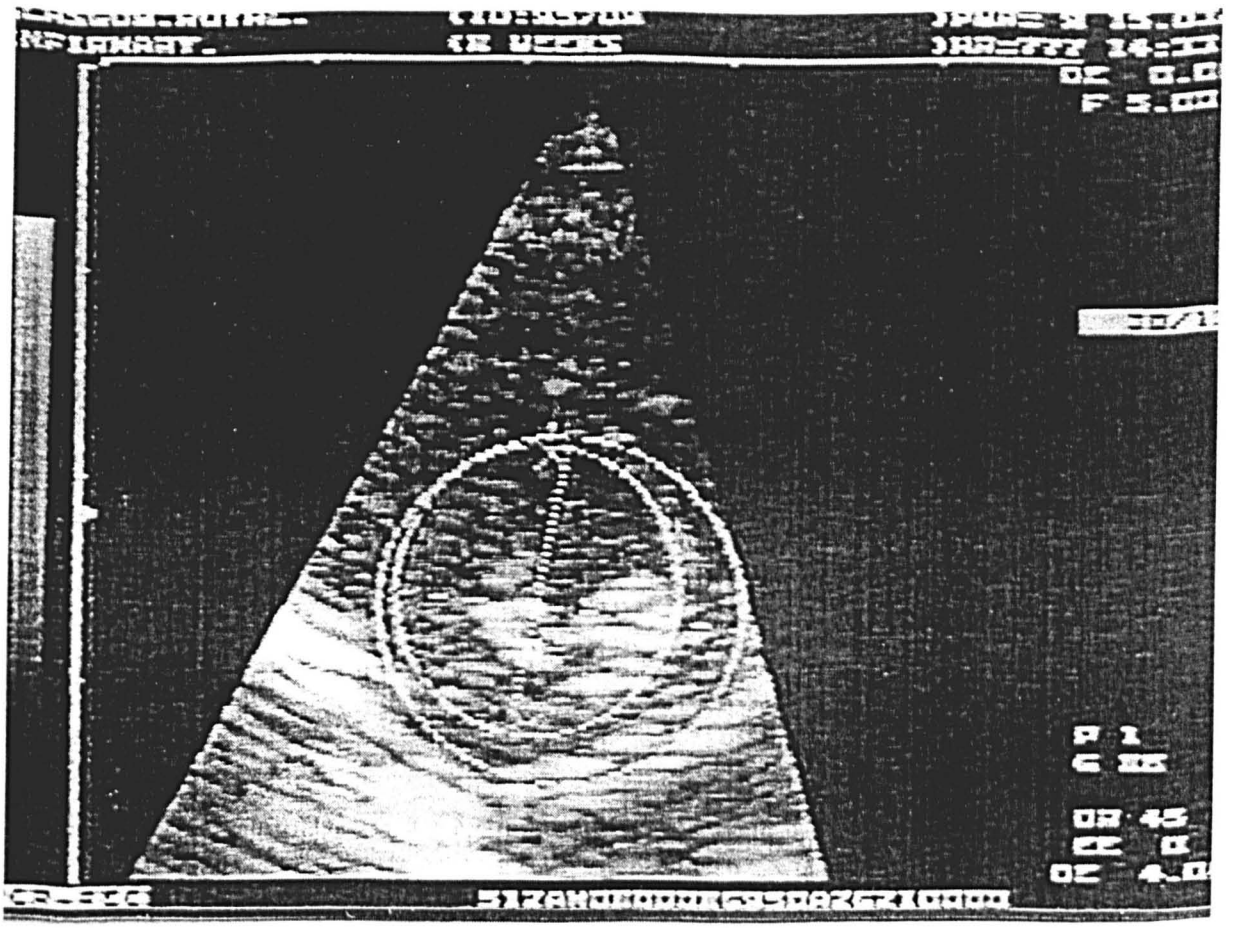

Figure 3.2 **Transverse view on echocardiography in a rabbit with heart failure with endocardial circumference during diastole and systole marked with circles. Ejection fraction is measured as the fractional decrease in area on systole (see text).**

In vitro cardiac performance in isolated ejecting working rabbit hearts

Background

The ejecting working heart configuration was originally described by Neely *et al.* (1966) in which an isolated rat heart preparation was capable of pumping fluid and performing *in vitro* mechanical work. The aorta and left atrial appendage were cannulated and perfusate was introduced into the left atrium and left ventricle through the mitral valve. Left ventricular contraction pumped the perfusate out via the aorta which then perfused the heart via the coronary arteries. Thus, the heart performed work and it was perfused in the same way as *in vivo* in the anterograde direction - as opposed to retrograde aortic perfusion of the non-working heart by the Langendorff technique (Langendorff, 1895).

The working heart preparation allows the contractile behaviour of the heart to be examined under controlled conditions without the influence of *in vivo* haemodynamic changes and autonomic influence. Loading conditions and heart rate can be controlled and the heart can perform work *in vitro* in a similar manner as it does *in vivo*.

Methods

The apparatus originally set up by Dr. Maurice Pye in the Department of Cardiology, Glasgow Royal Infirmary was used initially. It was found that the pre-load arrangement in the original set-up was providing a phasic fluid flow into the heart. Although a steady mean pre-load pressure could be maintained, the phasic nature of the inflow into the heart was undesirable for the measurement of instantaneous haemodynamic changes. The pre-load arrangement was therefore substantially modified to provide a constant pre-load pressure and thus fluid inflow into the heart. The experimental set-up is shown in Figure 3.3.

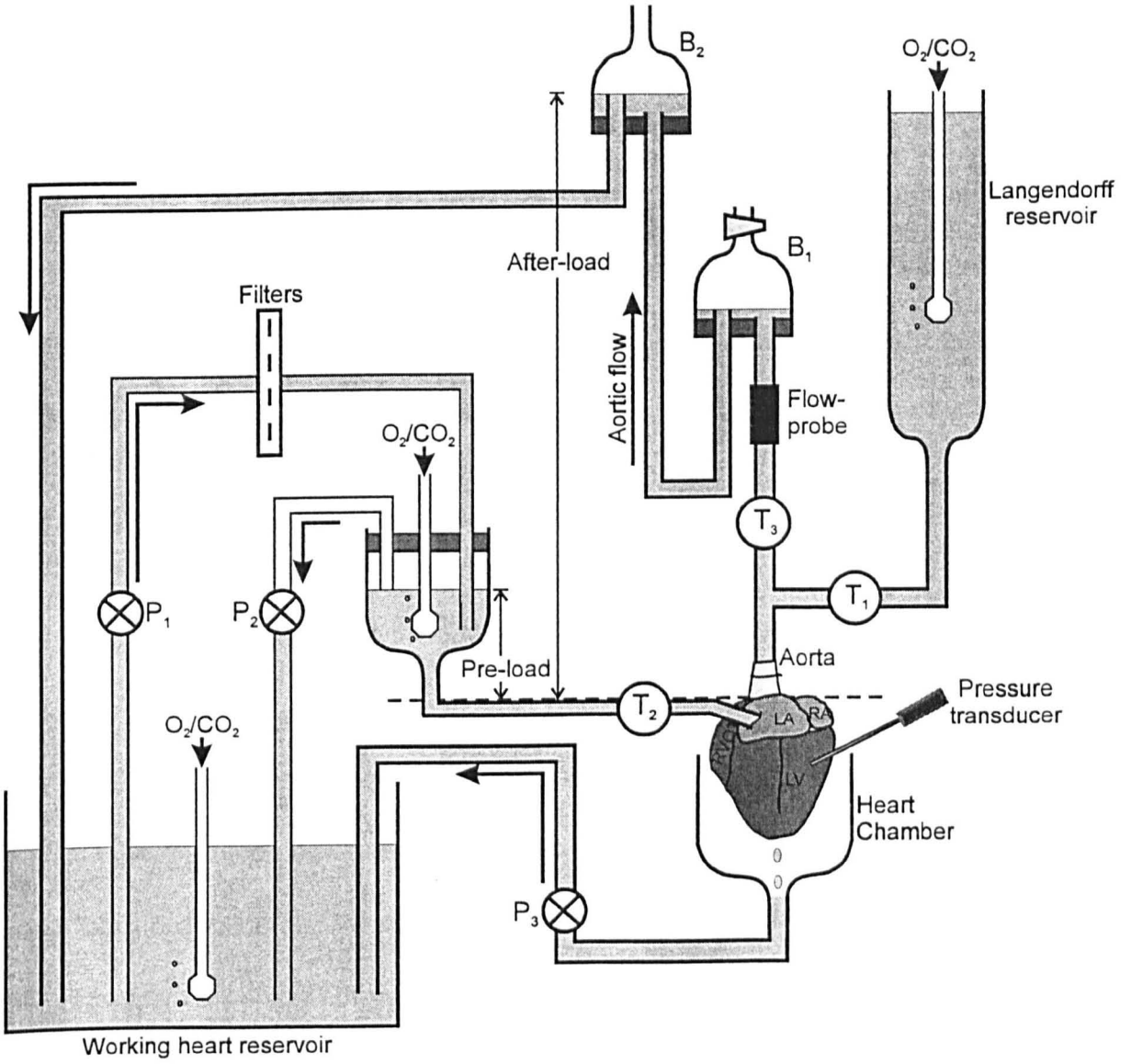

Figure 3.3 Schematic diagram of the *in vitro* Langendorff and working heart apparatus. The representation of an isolated rabbit heart is shown with the right ventricular outflow tract (RVOT), left atrium (LA), right atrium (RA) and left ventricle (LV) detailed. See text for description of the various components of the perfusion apparatus.

Initial preparation and Langendorff perfusion

At the beginning of the experiment the whole perfusion system was primed with modified Tyrode's solution of the following composition (mM): Na 138, K 4.0, Ca 1.8, Mg 1.0, HCO_3 24.0, H_2PO_4 0.4, Cl 121, glucose 11. The pH of the solution was maintained at 7.4 by continuously bubbling with 95 % O_2 / 5 % CO_2 mixture. Water-baths were used both for heating the perfusion solution and for supplying warm water to water-jackets in the glassware to reduce heat loss, thus maintaining a temperature of 37 °C at the heart. Care was taken to ensure that there were no air bubbles in the perfusion apparatus prior to starting the experiment.

Rabbits were sacrificed with an intravenous injection of 0.5 $ml.kg^{-1}$ Euthatal (sodium pentobarbitone 200 $mg.ml^{-1}$, Rhône Mérieux) mixed with 500 IU of heparin. After ensuring that there was absence of corneal and withdrawal reflexes, the abdominal cavity was opened by making a transverse subcostal incision with scissors. The diaphragm was transected and lateral incisions made along both sides of the rib cage. The anterior chest wall was folded back exposing the contents of the mediastinum. The heart was picked up and protected with fingers and incisions were made (a) at the inferior vena cava, (b) at both lung hila, and (c) at the great vessels and superior vena cava. Care was taken to ensure that the left atrium was not lanced or incised and that an adequate length of the ascending aorta was preserved. The isolated heart was then put into a beaker containing modified Tyrode's solution chilled to 4 °C to reduce metabolic rate and inhibit contraction.

The heart was then picked up by the aorta with fine-tipped forceps and slipped onto the aortic cannula of the perfusion apparatus and held in place with a bulldog clip. The cannula was made of stainless steel, grooved about 1 mm from the tip to accommodate ligatures. It was important to ensure free flow of perfusate during the cannulation to prevent air emboli

into the coronary arteries. The aorta was then secured with silk ligatures and the bulldog clip was removed. A small incision was then made at the pulmonary artery which was often occluded with the aortic ligatures. This allowed free flow of the coronary effluent, collected from the coronary sinus into the right heart, when Langendorff perfusion was started with the resumption of cardiac contraction. The time from asystole to reperfusion was usually under 3 min. The height of the fluid level in the Langendorff reservoir was kept at around 70 cm above the level of the aorta by topping up with perfusate.

Working heart configuration

Set-up. Once the heart was being perfused in the Langendorff mode, time could be taken to clean up adherent fatty and fibrous tissue. The heart was rotated to position the atrial cannula next to the left atrium. The atrial cannula was similar to the aortic cannula except that it was angulated for easy attachment of the left atrium. The lumina of the pulmonary veins were located and the surrounding tissues were cut to produce a single hole large enough to receive the atrial cannula. Again free flow of perfusate was ensured during the cannulation to prevent air entry and embolism. The atrial tissue was secured onto the cannula with a bulldog clip and then a silk ligature. The silicone tubing leading to the atrial cannula could be unclamped briefly to allow flow of the perfusate to ensure there was no leakage in the atrium or at the connection with the cannula. Leakage could be easily stopped with a second silk ligature.

Perfusion. After the left atrial cannula had been connected and the heart had stabilised for about 15 min, perfusion was switched from Langendorff mode to working heart mode. This was achieved by switching off / clamping the Langendorff perfusion inlet (T_1) and simultaneously opening / unclamping the left atrial inflow from the pre-load chamber (T_2) and the aortic outflow to the compliance chamber (T_3). Perfusate would enter the heart via

the left atrium and be pumped out from the left ventricle via the aorta - the same way as blood would enter the left heart and be ejected *in vivo*. Coronary perfusion would then occur via anterograde aortic flow as *in vivo* as opposed to via retrograde aortic flow during Langendorff perfusion.

Pre-load chamber. The height of the pre-load chamber can be adjusted. A constant fluid level was maintained by the use of 2 high-speed roller pumps (Watson-Marlow 505S) with one pump (supply pump, P_1) being used to supply the chamber with perfusate and the other (removal pump, P_2) pumping perfusate out via a vertically placed glass tubing connected to the pump via silicone tubing. The rate of the removal pump was set faster than that of the supply pump so that the fluid would be kept at the level of the tip of the vertical glass tubing. A baseline pre-load level of 10 cm above the level of the aorta was found to be the minimal input required to provide a steady output from the ejecting heart. The perfusate in the pre-load chamber was bubbled with 95 % O_2 / 5 % CO_2 mixture to maintain pH of 7.4 and adequate oxygenation.

Compliance chamber. The aortic cannula was connected to a "bubble trap" (B_1) which was used as a compliance chamber. The "bubble trap" was a glass chamber with rubber bung fitted with stainless steel cannulae. It was found that a compliance chamber was necessary to mimic the vascular compliance *in vivo*. Otherwise, the performance of the ejecting heart would deteriorate and heart would become unstable. The compliance provided by the chamber was adjusted by altering the volume of air inside the chamber using a silicone tubing and syringe connected to the top of the bubble trap. In a set of control experiments, it was found that the cardiac output obtained (see later) was positively correlated with the volume of air inside the compliance chamber up to 25 ml after which a plateau was

obtained. All the experiments were therefore performed with the volume of air inside the compliance chamber set at 25 ml.

After-load chamber. The compliance chamber was connected to an analogue calibrated low resistance flow meter for an estimate of the aortic flow. This was then connected to a "bubble trap" (B_2). The fluid column between this second "bubble trap" and the aortic valve provided the hydrostatic pressure the left ventricle had to contract against and hence represented the after-load. This second "bubble trap" therefore acted as the after-load chamber and its height was set at 75 cm above the aorta, representing a pressure of about 55 mmHg. This pressure is regarded as representative of a physiological equivalent to the mean systemic aortic pressure *in vivo*.

Recirculation of perfusate. After the after-load chamber, the perfusate would flow back via silicone tubings to the working heart reservoir inside the heated water bath. The reservoir was also bubbled with 95 % O_2 / 5 % CO_2 mixture to maintain pH and oxygenation. Coronary effluent flowing out of the pulmonary artery was collected in the heart chamber, also water-jacketed to keep the heart warm, and returned to the working heart reservoir via a low-speed pump (P_3). Temperature at the epicardial surface of the heart was monitored with an electronic probe (Libra Medical ET 250 temperature monitor, Berks., England) and maintained at 35 °C. This would give a consistent intracardiac temperature of 37 °C.

The recirculated solution would inevitably contain particulate material after perfusion through the heart. Filters (a prefilter, pore size 70 μm, Millipore ;and a filter, pore size 5.0 μm, Whatman International Ltd, England) were housed in a tight-fitting filter holder placed between the supply pump and the pre-load chamber so that the perfusate would be filtered prior to flowing into the left atrium to prevent micro-embolism of the coronary circulation which may cause myocardial infarction and deterioration of the preparation. Filters were

changed regularly during the course of the experiment and the perfusion fluid was also replaced every hour to ensure adequate glucose concentration.

Pacing. A pair of platinum electrodes (Grass Instruments, USA) were inserted into the right atrial appendage for atrial pacing using an electrical stimulator (Digitimer Ltd. DS2A) driven by a custom-written computer program.

Cardiac performance assessment

Cardiac output. As mentioned above, an analogue calibrated low resistance flow meter, connected between the compliance and after-load chambers, was used to obtain a rough estimate of the mean aortic flow. This measurement was used as a guide to the condition and stability of the preparation. It was found in previous work using a similar apparatus (Pye, 1992) that healthy, stable preparations should be able to produce a consistent aortic flow of above 80 $ml.min^{-1}$. Hearts which produced an aortic flow of less than this value were excluded from the study. Total cardiac output included aortic flow and coronary circulation. Coronary effluent could be collected from the heart chamber over a period of time to estimate the coronary flow. Together with the aortic flow, an estimate of the total cardiac output could be made. Coronary effluent was also collected at various points during the experiments and the samples were sent to the Biochemistry Department at Glasgow Royal Infirmary for assessment of lactate concentration to ensure that there was no significant acidosis resulting from hypoxia or "ischaemia".

Since one of the aims of the study was to examine the instantaneous, beat-to-beat and potentially small changes in haemodynamic parameters in the isolated working heart, a more elaborate method of assessing cardiac output was employed. An ultrasonic probe (Transonic Systems Inc., 3 mm diameter), vertically placed in series between the aortic cannula and the compliance chamber, was used to measure the beat-to-beat variation in flow

in the aortic cannula using crystal doppler technology with the Transonic Systems Inc. (New York) T106 flow-meter.

Intraventricular pressure. Left ventricular pressure was measured with an 18-gauge cannula inserted into the free wall of the left ventricle. The cannula was connected to a stiff wide-bore piece of plastic tubing leading to a Gould Inc. pressure transducer. The signal from the pressure transducer was calibrated using a sphygmomanometer with known pressure prior to each experiment and a "zero" pressure was obtained at the end of each experiment by keeping the cannula at the same level and removing the heart, thus opening the cannula to air.

Cardiac dimensions. Measurements of the left ventricular dimension and the beat-to-beat variations during the cardiac cycle were made using sonomicrometry. This was first described by Rushmer *et al.* (1956) who showed that it was possible to measure cardiac dimensions and changes during contractions accurately, using barium titanate crystals based on the sonar principle. In the current study, a pair of sonomicrometer crystals (Triton Technology Inc., 2 mm diameter) were placed subepicardially along the anteroposterior axis of the left ventricle. The sonomicrometer crystals were half-spherical structures with the convex ultrasonic emission and receiving surface on one side and a flat electrical connection surface on the other. With a needle, a small hole was made in the left ventricular epicardium, halfway between the atrioventricular groove and the left ventricular apex, just next to the left anterior descending artery. The hole was expanded with a pair of fine-tipped forceps to create a small space underneath the epicardium. The first crystal was inserted into this space. In a similar manner, the second crystal was inserted into a space made at the posterior surface of the left ventricle just next to the posterior descending artery, along the anteroposterior axis at the same level as the first crystal. The distance measured between the

crystals (resolution of 0.05 mm) should be the maximal diameter of the epicardial circumference of the left ventricle at that level. The two crystals were connected to 2 sonomicrometry amplifiers connected to a 6-channel mainframe (Triton Technology Inc.) and the beat-to-beat changes in cardiac dimension were measured.

Signal measurement and analysis

The signals recorded from the ultrasonic flow probe, pressure transducer and sonomicrometer crystals were displayed continuously on a Gould Inc. (Cleveland, Ohio) 2800S 6-channel chart recorder and stored on video tape using a Medical Systems Corporation PCM 8-channel videocassette recorder adapter. These signals were digitised at 1 kHz with 12-bit precision using the program WCP (Dr. J. Dempster, Strathclyde Electrophysiology Software). Ten successive sweeps (representing a continuous recording of about 5 s) were averaged before the waveforms of the various signals were analysed.

$[Ca^{2+}]$ measurements in Langendorff perfused rabbit hearts

Background

Chemical light has been employed by humans in various ways for a long time (Campbell and Sala-Newby, 1993). It ranges from the practical use of fireflies in torches or lamps to the less practical luminous golf balls. Chemiluminescence is the emission of light as a result of a chemical reaction and bioluminescence is visible light emission from luminous organisms. Such light emission properties from chemical reaction within living cells, tissues and organs, and other biochemical reactions with a similar basis have been applied scientifically to the study of many biological processes and phenomena.

Ca^{2+} is one of the most important intracellular messengers. It carries various messages like nerve cell signal transmission, hormone secretion and immune cell activation. In cardiac cells, Ca^{2+} plays a pivotal role in the process of excitation-contraction coupling and the measurement of fluctuations in cytosolic $[Ca^{2+}]$ is central to the understanding of cardiac contractile function. The evolution of techniques for measuring intracellular ion concentration has allowed the study of intracellular $[Ca^{2+}]$ in cardiac myocytes, muscle preparations and the whole heart. Several methods have been developed to examine Ca^{2+} in its physiological role and in disease states (Bentivegna *et al.* 1991; Cannell and Thomas, 1994):-

1) Dye absorbance - the early optical methods for measuring ion concentration involved the measurement of dye absorbance with metallochromic indicators like murexide, arsenazo or antipyrylazo. The low level of absorbance in small preparations limit its use only in large invertebrate cells or muscle fibres.

2) Bioluminescence - the photoprotein, aequorin, has been used for bioluminescent measurements of intracellular [Ca^{2+}]. Photoproteins are enzymes that catalyse the oxidation of a bound prosthetic group (e.g. coelenterazine) and a photon is given off as a result of the oxidation reaction, with Ca^{2+} regulating the catalytic process. Hence, light is emitted when the photoprotein combines with free, ionised Ca^{2+}. Difficulty in introducing the photoprotein into the cell is one of the main drawbacks of this technique. Aequorin has to be injected into the preparation (Allen and Kurihara, 1980; Kihara *et al.* 1989) and Ca^{2+} transients can only be measured from a localised area of myocardium where the aequorin has been injected. In addition, aequorin has limited sensitivity in the lower range of [Ca^{2+}], making measurement of diastolic [Ca^{2+}] difficult; and a time-dependent consumption of the photoprotein is recognised.

3) Fluorescent indicators - these are relatively new agents which have been developed and used over the last 2 decades for the study of ionic activity. Light is emitted from both fluorescent indicators and bioluminescence probes with the return of an excited state to the ground state when photons are released. The main difference between the two is that external energy is required to excite the electron in the case of fluorescence whilst the energy to excite the electron comes from the chemical reaction in bioluminescence. Fluorescent indicators will be discussed in greater detail below.

4) Nuclear Magnetic Resonance (NMR) spectroscopy - this technique has been used in the study of Ca^{2+} homeostasis especially in the whole heart using the Ca^{2+}-sensitive fluorescent indicator 5,5'-F_2-1,2-bis(o-aminophenoxy)ethane-N,N,N',N',tetraacetic acid (5F-BAPTA). The ^{19}F NMR spectra acquired consist of 2 peaks - one representing the free ligand of 5F-BAPTA and the other representing the Ca^{2+}-bound species. [Ca^{2+}] can be calculated from the areas under the 2 peaks (Marban *et al.* 1990). This technique has the advantage of

allowing the simultaneous measurement of other ions and metabolites (using ^{31}P NMR spectroscopy to obtain values for inorganic phosphate, ATP, phosphocreatine and intracellular pH). However, several cardiac cycles would have to be averaged in order to obtain meaningful NMR spectra. As a result, alterations in Ca^{2+} handling cannot be detected with NMR on a beat-to-beat basis. Only an estimate of the Ca^{2+} transient may be constructed using gated averaging to obtain [Ca^{2+}] measurements at various stages during the cardiac cycle (Marban *et al.* 1990). In addition, significant buffering occurs with the introduction of the indicator causing significant impairment of contractile function with prolongation of both time to peak pressure and rate of relaxation.

Fluorescence

Fluorescence is the emission of light as a result of a three-stage process that occurs in certain molecules (generally polyaromatic hydrocarbons or heterocycles) called fluorophores or fluorescent dyes / indicators (Cannell and Thomas, 1994). The first stage of the fluorescence process involves the supply of a photon by an external source (e.g. an incandescent lamp or laser) to the fluorophore which is excited to a higher-energy "singlet" state. The excited state lasts for a short time (about 1 to 10 nanoseconds) during which the fluorophore undergoes conformational changes and descends the vibrational ladder with the molecule returning to the ground state with the emission of a photon. The emitted photon may be reabsorbed or there may be other molecular interactions like collisional quenching, fluorescence energy transfer and intersystem crossing which may dissipate energy without emitting photons. The number of emitted photons are generally less than the number of absorbed photons and the ratio between them is called the fluorescence quantum yield or quantum efficiency (typically about 0.3 in modern fluorophores). As energy is dissipated on returning from the singlet state to ground state, the energy of the emitted photon is lower,

and hence its wavelength longer, than the excitation photon. The difference in energy or wavelength, called the Stokes shift, is fundamental to the sensitivity of fluorescence techniques as it allows emission photons to be detected against a low background, isolated from excitation photons. Unless the fluorophore is irreversibly destroyed in the excited state (a phenomenon known as photobleaching), the same fluorophore can be repeatedly excited and detected.

Fluorescent Ca^{2+} indicators

As mentioned above, ion-sensitive fluorescent indicators are molecules that emit light on excitation with a given wavelength and the intensity of the emitted light is a function of the amount of ion bound to the molecule. The resulting fluorescence is used as a measure of the free ionic concentration in the medium studied. However, the measured fluorescence depends on a number of factors including (a) concentration of the indicator, (b) extinction coefficient of the indicator, (c) optical pathlength, (d) excitation source intensity and stability, (e) quantum yield of the indicator, (f) fluorescence collection efficiency of the detection system, (g) tissue or cell autofluorescence, and (h) concentration of the ion the indicator is measuring.

Second generation fluorescent Ca^{2+} indicators have made a major contribution to advances in the understanding of the role of Ca^{2+} in cellular regulation since their introduction in 1985. These were developed by Dr Roger Tsien and collaborators (Grynkiewicz *et al.* 1985) and indo-1 and fura-2 are the two most widely used dyes for measuring intracellular [Ca^{2+}]. These indicators combine a stilbene fluorophore with an octacoordinate tetracarboxylate chelating site characteristic of EGTA and BAPTA. These indicators have many advanced features over their predecessor, quin-2:-

a) they offer up to 30-fold brighter fluorescence with much greater quantum yield,

b) there are major changes in wavelength upon Ca^{2+} binding in addition to intensity in the second generation dyes, with spectral shift which will be discussed below,

c) they have slightly lower affinities for Ca^{2+} than quin-2, hence less likely to cause buffering and less likely to be saturated at micromolar levels,

d) the preferred excitation wavelength for quin-2 is 339 nm which is too short and can cause significant autofluorescence and biological side effects whereas the excitation wavelengths required for the newer dyes are slightly longer, and

e) the newer dyes have much greater selectivity for Ca^{2+} over other divalent cations like Mg^{2+} than quin-2.

When compared to the bioluminescent indicator, aequorin, the second generation fluorescent indicators have a higher quantum yield and are more sensitive in the lower (diastolic) range of $[Ca^{2+}]$.

Spectral shifts and ratiometric measurements

In some of the second generation fluorescent dyes, the fluorescence excitation spectrum or the emission spectrum (or both) will shift on binding Ca^{2+}. For indo-1, the *emission* spectrum shifts to shorter wavelengths with increasing $[Ca^{2+}]$ and Ca^{2+}-binding. This means that when excited at a certain wavelength (360 nm), the emitted fluorescence at a shorter wavelength (405 nm) increases with Ca^{2+}-binding whilst that at a longer wavelength (495 nm) decreases. This allows the ion concentration to be estimated from the relative levels of fluorescence measured at 2 different wavelengths. This is known as ratiometric fluorescence measurement. The ratio has the advantage that it is insensitive to factors which proportionally affect both intensities identically such as indicator concentration and to a certain extent, motion artefacts. There are emission or excitation wavelengths in these

ratiometric dyes called isosbestic points, where fluorescence does not change with Ca^{2+} binding. The emission wavelengths (or excitation wavelengths) will have to be chosen on either side of the isosbestic point for ratio measurements in excitation-shifted (or emission-shifted) fluorescent dyes.

Introduction into cells, tissues and organs

For the measurement of intracellular [Ca^{2+}], it is necessary to introduce fluorescent Ca^{2+} indicators into the cells, tissues or organs studied. This is usually carried out by direct injection or by the ester loading technique.

Direct injection

In cellular studies, the fluorescent dyes may be injected into the cell through a microelectrode (Cannell and Thomas, 1994) or loaded through the electrode when the cell-attached patch recording technique is used. The indicators may also be micro-injected using iontophoresis into myocardial cells at different sites of the trabeculae (Backx and ter Keurs, 1993) which then diffuse via gap junctions to give a more uniform distribution for the study of isolated muscle preparations. For the whole heart, injection techniques have been used with the bioluminescent indicator, aequorin (Kihara *et al.* 1989). Intramyocardial injection of the acetoxy-methyl ester form of fluorescent indicators (Mohabir *et al.* 1991) has also been described in the isolated heart but cellular loading of the indicator is by trans-sarcolemmal diffusion of the ester (see below).

Ester loading

A popular technique in loading myocytes with fluorescent Ca^{2+} indicators is by using the acetoxy-methyl (AM) ester form of the indicator (Tsien, 1981). This avoids the potentially disruptive nature of direct injection; and cells (Sipido and Callewaert, 1995) and tissues

(Hanley and Loiselle, 1998) can be easily incubated and the whole heart (Lee *et al.* 1987) perfused with the ester-containing solution for indicator loading. Fluorescent indicators are multiply charged molecules (with carboxyl groups in most) at physiological pH. By esterifying into the AM form, the derivative is not an active indicator but is lipophilic enough to permeate the cell membrane. After entering the cell, intracellular esterases cleave the derivative to release the active indicator. As the indicator will become highly charged again, it will stay inside the cell.

However, loading the fluorescent indicator into the cells, tissues or whole heart is not without its potential problems. There may be (i) unhydrolysed AM ester in the cytosol which is fluorescent but not Ca^{2+}-sensitive, (ii) loading of mitochondria and other organelles, (iii) autofluorescence which may be substantial, (iv) binding to intracellular protein altering the spectral properties and Ca^{2+}-affinity, and (v) loading of non-myocyte component, e.g. vascular endothelium, in the case of muscle preparations and whole heart. All these may affect the interpretation of collected fluorescence as a measure of intracellular $[Ca^{2+}]$ (Bassani *et al.* 1995). These will be discussed in greater detail in Chapter 7.

Calibration and concentration

In order to translate the fluorescence measured into $[Ca^{2+}]$, the signals have to be calibrated against known $[Ca^{2+}]$. For ratiometric dyes, the free $[Ca^{2+}]$ is related to the fluorescence ratio R (Grynkiewicz *et al.* 1985) by the formula:-

$$Free[Ca^{2+}] = K_d \cdot S \cdot \frac{(R - R_{min})}{(R_{max} - R)}$$

where S is a scaling factor given by the fluorescence at the denominator wavelength (495 nm for indo-1) of R at zero $[Ca^{2+}]$ divided by the fluorescence at a saturating $[Ca^{2+}]$ and R_{min} and R_{max} are the ratio at zero and saturating $[Ca^{2+}]$ respectively.

It is obvious the calculation of absolute free [Ca^{2+}] in the cytosol depends on K_d in addition to fluorescence and ratio measured. K_d obtained *in vivo* may be significantly different from that *in vitro* (Bassani *et al.* 1995) and will directly affect the [Ca^{2+}] measured.

Methods

Langendorff perfusion

Rabbits were sacrificed with an intravenous injection of 0.5 $ml.kg^{-1}$ Euthatal (sodium pentobarbitone 200 $mg.ml^{-1}$, Rhône Mérieux) mixed with 500 IU of heparin. The hearts were rapidly excised and perfused in the Langendorff mode with Tyrode's solution of the following composition (mM): Na 115, K 4.7, Ca 1.8, Mg 1.0, HCO_3 25.0, H_2PO_4 0.5, Cl 135, glucose 10, probenecid 0.3. The pH of the solution was maintained at 7.4 by continuously bubbling with 95 % O_2 / 5 % CO_2 mixture. Temperature at the heart was maintained at 37 °C by the use of water-jackets in the glassware connected to a heated water bath. A constant perfusion rate of 50 $ml.min^{-1}$ was maintained using a Gilson Minipuls 3 peristaltic pump. A 6 cm long, 6 F polypropylene catheter (Portex, Kent, England) was inserted at the apex of the left ventricle for draining thebesian venous effluent. Intraventricular pressure was monitored with a fluid-filled latex balloon connected with a 6 F cannula to a pressure transducer (Triton Technology Inc, San Diego, California) and inserted into the left ventricle via the left atrium. The volume of the balloon was adjusted to give zero end-diastolic pressure. Perfusion pressure was monitored with a second pressure transducer in series with the aortic cannula. Pairs of platinum electrodes (Grass Instruments, USA) were inserted into the right atrial appendage and the posterior aspect of the right ventricular apex for atrial and ventricular pacing respectively. Under control conditions the hearts were paced via the right atrium at a cycle length of 350 ms.

Fluorescence measurement system

Fluorescence from areas of the left ventricular epicardial surface were measured using a custom-built apparatus shown in Figure 3.4. Illumination was provided by a Nikon 75 W Xenon lamp filtered at 360 ± 10 nm (F_1) and focused via a 385 nm long-pass dichroic mirror (D_1) onto a 3 mm-diameter liquid light guide (Ultrafine Technology, UK) in contact with the left ventricular epicardial surface of the isolated heart. Emitted light from the preparation was collected by the same light guide and light with wavelengths greater than 385 nm passed through the dichroic mirror (D_1) and was subsequently split by a second dichroic mirror (D_2). Light with wavelengths greater than 460 nm passed through the second dichroic mirror onto a photomultiplier (Thorn EMI, UK) fitted with an optical band-pass filter centred on 495 ± 20 nm. The remaining light was reflected onto a second photomultiplier with a band-pass filter centred on 405 ± 35 nm. The output of the photomultipliers were passed to an electronic ratio circuit so that an effectively continuous signal of fluorescence intensity ratio (F_{405}/F_{495}) could be obtained. This analogue ratio signal, the fluorescence intensity of the individual wavelengths and the electrical signals representing intraventricular pressure and perfusion pressure were displayed continuously on a Gould TA-11 chart recorder and stored on video tape using a CRC VR-100B digital recorder (Instrutech Corp, USA).

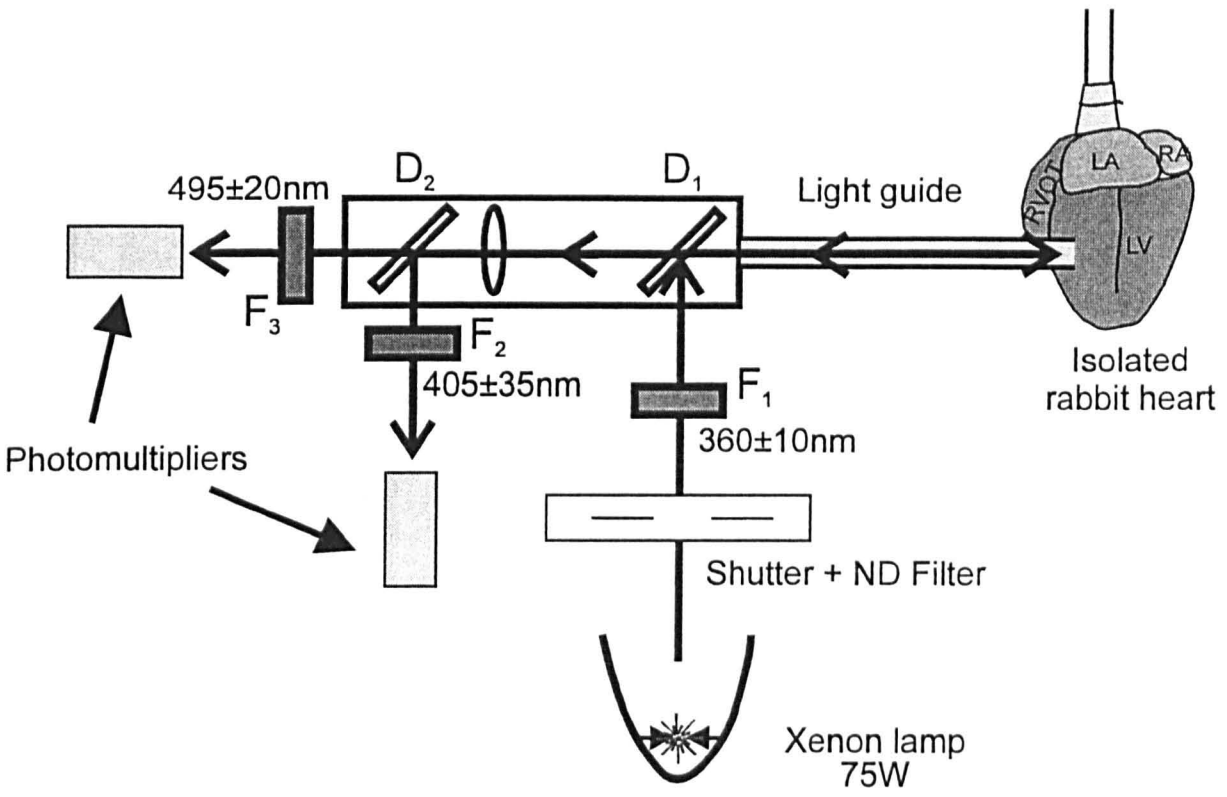

Figure 3.4 Schematic diagram of the optical arrangement used to measure Indo-1 fluorescence from the epicardial surface of the isolated Langendorff perfused rabbit heart. D_1 is a 385 nm long-pass dichroic mirror and D_2 is a 460 nm long-pass dichroic mirror. F_1, F_2 and F_3 are optical filters with peak transmission wavelengths and band-widths as shown on the diagram. The representation of an isolated rabbit heart is shown with the right ventricular outflow tract (RVOT), left atrium (LA), right atrium (RA) and left ventricle (LV) detailed.

Indo-1 loading

Loading solution. Indo-1 AM (Molecular Probes Inc, Ohio) stock solution was initially prepared by dissolving 1 mg of indo-1 AM in 1 ml dimethyl sulphoxide (DMSO) / 25 % (w/v) pluronic acid F-127 solution. This was then added to 100 ml Tyrode's solution with 5 % foetal calf serum to make up a concentration of 10 μM indo-1 AM.

Loading protocol. After an initial equilibration period of 30 min with normal Tyrode's solution, the hearts were perfused with the indo-1 AM containing solution at a rate of 25 $ml.min^{-1}$ at room temperature (25 °C) for a period of 60 min and atrial pacing was slowed to 60 $beats.min^{-1}$. The solution was recirculated but not bubbled with 95 % O_2 / 5 % CO_2 mixture during the loading period. HEPES buffer (0.6 ml of 500 mM stock solution) was added prior to loading to keep the pH of the loading solution at 7.4. The loading of the myocardium with the fluorescence indicator was observed by illuminating the preparation for 10 s at regular intervals, with the light guide being held at the same position throughout the loading procedure. At the end of this period, the hearts were perfused with normal Tyrode's solution for 15 min with the perfusion rate increased back to 50 $ml.min^{-1}$ and temperature back to 37 °C. This ensured that the intracellular indo-1 AM was fully cleaved to the Ca^{2+}-sensitive free acid form and that the indo-1 AM containing solution was washed out of the circulation prior to intracellular Ca^{2+} measurements.

Comments. This loading protocol was arrived at after some initial control experiments and was found to be effective in loading the myocardium of the beating heart with indo-1 giving stable and reasonably long-lived fluorescence signals without significant buffering of the heart as evident from the unaltered intraventricular pressure signal after loading (see later). Initial trial experiments without the use of probenecid showed that fluorescence signals as a result of indo-1 loading were short-lived. After initial indo-1 loading, the signals would

only last for about 1 hr, with deterioration of signal quality with time. This was clearly not desirable as one of the aims of the study was to measure the fluorescence signals at different parts of the beating heart which could be time-consuming. Probenecid is an organic anion transport protein inhibitor (Di Virgilio *et al.* 1990). Indo-1 transport outside the dye-loaded myocyte would be inhibited by probenecid. As in several other studies (Mohabir *et al.* 1991; Turvey and Allen, 1994), 0.3 mM of probenecid was used in these experiments and was shown to produce good-quality fluorescence signals after indo-1 loading which lasted for a considerable amount of time (up to 5 hours) and showed no significant deterioration in quality.

Loading at a slower perfusion rate at a low temperature and heart rate was shown to produce more substantial increase in fluorescence, and hence better indo-1 signals. In the initial trial experiments when indo-1 loading was carried out at 37 °C, oxygenation of the perfusion solution was required. As a result of the detergent nature of the DMSO in the solution, significant amount of froth was produced in the bubbled, recirculated solution which posed a danger of overflow and solution spillage. When loading was subsequently carried out at low temperature, it was found that extra oxygenation was not necessary as the heart was working at a low metabolic rate. No change in the pressure profile of the beating heart was observed with or without bubbling the loading solution with the 95 % O_2 / 5 % CO_2 mixture. Thus, the loading solution was not bubbled and the problem of frothing was solved. However, pH of the loading solution had to be buffered to 7.4 with the use of HEPES as a result. Lactate samples were taken for several control experiments and verified that there was no significant hypoxia / acidosis during the course of the low temperature, low flow perfusion period.

Signal Measurements and Analysis

Indo-1 fluorescence measurements were made at 15 sites over the left ventricular epicardial surface. The locations of the sites were based on anatomical features (see Figure 3.5) with the left anterior descending artery forming the left border and the posterior descending artery forming the right. Measurements were made at each of the 15 sites sequentially. Signal reproducibility was verified by repeated sampling at the initial sites at 30 min intervals. Intraventricular pressure recordings indicated the stability of the preparation during the course of the experiments.

Pressure and fluorescence signals were digitised at 1 kHz with 12-bit precision using the computer program WCP (Dr. J. Dempster, Strathclyde Electrophysiology Software). Using this software, 30 successive sweeps were averaged before measurements were made. Another computer program "Transient Analyser" was written (using Microsoft Visual Basic 4.0 programming language) with the help of Dr. F. L. Burton, University of Glasgow, to analyse the time course and amplitude of the signals. This program allowed the digitised signals to be imported from WCP and the individual transient signals could be analysed in a semi-automated fashion.

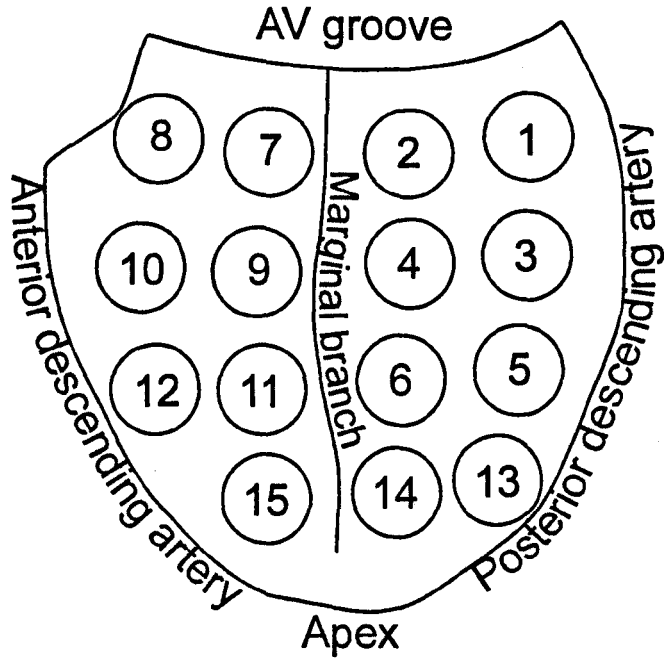

Figure 3.5 **A representation of the left ventricular epicardial surface illustrating the 15 sites used for fluorescence measurements. The anatomical features used as points of reference are shown:- Atrio-ventricular (AV) groove, Anterior descending artery, Posterior descending artery, Marginal branch of the left circumflex artery and Apex.**

Monophasic Action Potential measurements in isolated Langendorff perfused rabbit hearts

Background

The use of glass micropipettes or microelectrodes to make intracellular electrical recordings began with the pioneering work of Ling and Gerard (1949) who measured resting potentials in frog muscle. The technique has seen many improvements over the years and is now widely used to study the electrical properties of living cells, including cardiac myocytes. However, this is not feasible in the beating heart, because of obvious problems with instability and artefact. An alternative was available even before intracellular action potential measurements were made. This is the Monophasic Action Potential (MAP) which is an extracellularly recorded signal that reflects changes in the intracellular action potential (Franz, 1991). Even as early as 1882, Burdon-Sanderson and Page recorded MAPs in the frog heart by placing one electrode on the intact epicardial surface and the other on an injured site. Schultz devised a refined technique in 1931 which gave better and longer-lasting MAPs and later introduced the suction electrode in 1935 which produced MAPs with less damage to the heart, greater simplicity and better quality (Schultz, 1936). The principle of the suction electrode is that the electrode inside the suction tube presses on the myocardium that is drawn into the tube and membranes of the cells in this region are depolarised and made non-excitable. The recording electrode is situated just outside the suction tube and the potential difference between the 2 electrodes reflects changes during the action potential at the recording electrode. There are fundamental differences however between the MAP signal and intracellular action potential:- (a) the MAP signal is not representative of the absolute voltage of resting and action potential amplitude as the

reference potential for the MAP signal is mildly depolarised myocardium and not 0 mV; (b) the upstroke of the MAP signal is slower than the phase 0 upstroke of the intracellular action potential; and (c) the MAP signal represents an averaged record from a collection of cells over an area. Despite the fundamental differences, the MAP signal has been shown to accurately reflect the onset of depolarisation and the entire repolarisation phase of the transmembrane action potential recorded from cells in the same vicinity (Hoffman *et al.* 1959). The main advantage of MAP recording is that it allows recordings from the intact beating heart both *in vitro* and *in vivo* and MAPs have been used extensively in studying the effects on repolarisation of drugs, ischaemia, heart mechanics, etc. in normal and diseased myocardium (Franz *et al.* 1984; Lab, 1991; Yuan *et al.* 1994).

Methods

Monophasic Action Potential recording

Monophasic Action Potential (MAP) was measured using a suction electrode applied to the epicardial surface of the Langendorff perfused heart. The suction electrode was a custom-made bipolar electrode constructed using Silver / Silver Chloride pellets (1 mm diameter), wire and rubber tubing and insulated with silicone rubber gel. Suction was applied using a high-flow water Venturi pump to maintain the electrode on the epicardial surface of the beating heart. The pellet inside the suction catheter would impale the epicardium and partially depolarise the cells at that site whilst the MAP signal could be recorded at the second pellet situated just outside the suction catheter 2 mm away. The signal was amplified by a custom-made high input impedance differential amplifier with a frequency response from DC to 1.25 kHz. A DC offset control was incorporated to compensate for the high electrode DC polarisation appearing on the electrodes. A 20 mV signal was available in the

amplifier for calibration. The MAP signals may contain artefact or be of low amplitude if there was poor contact of the electrode with the heart or if either of the pellets was in contact with fibrous or vascular tissue. The signals were considered unacceptable for analysis if any part of the repolarisation phase fell below baseline or the amplitude of the plateau fell below 15 mV. In these cases, suction was adjusted or the MAP electrode was re-orientated, which usually rectified the problem. The amplified MAP signal was then displayed on a Gould TA-11 chart recorder and stored on video tape using a CRC VR-100B digital recorder (Instrutech Corp, USA) as in the fluorescence signals.

Signal Measurements and Analysis

MAPs were recorded sequentially at the same 15 left ventricular epicardial sites as for the fluorescence signals. The recorded MAP signals were digitised and analysed in a similar manner using the computer programs WCP and Transient Analyser respectively. Since the signal to noise ratio was greater in the MAP signals than fluorescence signals, only 10 successive sweeps of the MAP signals were averaged prior to analysis, representative of a 10 s continuous recording period, as opposed to 30 sweeps in the fluorescence analysis.

Cardiac remodelling and organ congestion

Background

It has been shown in animals (Pfeffer, 1991) and in humans (McKay *et al.* 1986) that there are significant structural changes to the heart after myocardial infarction. This has been termed remodelling (Braunwald and Pfeffer, 1991) which includes significant degree of hypertrophy in an attempt to compensate for contractile dysfunction resulting from the infarction.

In the clinical syndrome of chronic heart failure, organ congestion is one of the well-recognised hallmarks (Katz *et al.* 1960). Contractile dysfunction of a pumping chamber will lead to increased back-pressure in the vasculature and organs proximal to that chamber. Hence, left ventricular failure leads to pulmonary congestion and oedema and right ventricular failure leads to raised systemic venous pressure and hepatic congestion. The commonest cause of right ventricular failure is left ventricular failure when long-standing pulmonary congestion leads to pulmonary hypertension and right ventricular overload.

Methods

An attempt was made to assess the degree of compensatory hypertrophy / remodelling and of organ congestion in this rabbit model of heart failure as a result of left ventricular myocardial infarction. Liver and lungs were excised from the animals at the time of sacrifice, blotted to remove excess blood and their wet weights were measured. After each experiment, the heart was removed carefully from the perfusion apparatus, taking care to preserve the aorta and other structures. The heart was blotted and the wet weight was measured. It was then cut along the atrioventricular groove, separating the atria and great vessels from the ventricles. The right ventricular free wall was carefully dissected away

from the left ventricle and both were dried in an oven heated to 50 °C for 2 weeks after which their dry weights were obtained.

Data presentation and Statistical analysis

All experimental data presented in the subsequent Chapters are expressed as mean ± standard error. Comparison between groups of data was made with Student's t-test (paired when appropriate) unless otherwise stated. Two-tailed p-value of less than 0.05 was considered significant.

CHAPTER 4

HEART FAILURE AS A RESULT OF CORONARY ARTERY LIGATION IN THE RABBIT

Introduction

Fluid retention and organ congestion are well-recognised features in the clinical syndrome of heart failure. Left heart failure results in increased back pressure in the pulmonary vasculature with pulmonary congestion and interstitial oedema (Katz *et al.* 1960). With time and if untreated, this causes right ventricular overload and failure with increased filling pressure in the systemic venous system and hepatic congestion. Activation of the renin-angiotensin system causes further Na^+ and water retention perpetuating the vicious cycle (Parmley, 1989). Wall stress is increased in the heart as a result of the haemodynamic changes and this is believed to be the stimulus for the remodelling process (Braunwald and Pfeffer, 1991) in the myocardium of the failing heart with hypertrophy, fibrosis and other cellular changes (Weber and Brilla, 1991; LeJemtel and Sonnenblick, 1993).

Methods

The degree of cardiac dysfunction and remodelling as a result of coronary artery ligation and its systemic consequences were assessed in the rabbit heart failure model. Echocardiography was performed in all of the rabbits 1 week prior to sacrifice for the experiments. In the working heart experiments, 8 rabbits in the heart failure group were compared with 8 sham-operated animals. For the Ca^{2+} measurement experiments, 17 rabbits with heart failure were studied with 13 controls. MAP measurements were made in some of the hearts used in the Ca^{2+} measurement experiments. Echocardiographic data were available, therefore, in 25 (17 + 8) rabbits in the heart failure group and 21 (13 + 8) sham-operated rabbits.

Heart, liver and lung weights were not measured in all of the experiments but were available in 20 rabbits in the heart failure group and 18 controls.

Results

Cardiac dysfunction and Chamber dilatation

Echocardiographic data showed that significant *in vivo* cardiac dysfunction was produced by the rabbit heart failure model 7 weeks after coronary artery ligation. Ejection fraction was significantly lower in rabbits in the heart failure group and cardiac chambers were significantly enlarged as measured by the left atrial and left ventricular end-diastolic dimensions (see Table 4.1). This shows that cardiac performance in these rabbits was impaired leading to volume overload and ventricular dilatation. Ejection fraction was significantly correlated with left atrial dimension ($r = -0.86$, $p < 0.001$) and left ventricular end-diastolic dimension ($r = -0.77$, $p < 0.001$) (Figure 4.1).

Distension of the left atrium could be the result of increased filling pressure or due to mitral regurgitation as a result of annular dilatation or papillary muscle dysfunction. Post-mortem examination of the heart after the experiments frequently showed infarction of one or both of the papillary muscles attached to the mitral valve as a result of the coronary artery ligation procedure.

Table 4.1 Comparison of echocardiographic parameters and organ and tissue weights between rabbits with heart failure (HF) and controls (Sham).

For body weight and echocardiographic parameters, n = 25 for HF and n = 21 for Sham. For organ and tissue weights, n = 20 for HF and n = 18 for Sham. (LAD = left atrial dimension, LVEDD = left ventricular end-diastolic dimension)

	HF	Sham	p value
Body weight (kg)	3.60 ± 0.05	3.56 ± 0.07	NS
Ejection fraction (%)	42.6 ± 1.3	71.2 ± 1.4	< 0.001
LAD (mm)	15.8 ± 0.3	10.9 ± 0.3	< 0.001
LVEDD (mm)	20.0 ± 0.3	16.8 ± 0.3	< 0.001
Liver wet weight (g)	93.0 ± 2.4	81.0 ± 4.0	< 0.02
Lung wet weight (g)	13.1 ± 0.8	10.9 ± 0.3	< 0.01
Heart wet weight (g)	13.1 ± 0.4	11.3 ± 0.4	< 0.005
LV dry weight (g)	1.40 ± 0.06	1.15 ± 0.04	< 0.002
RV dry weight (g)	0.57 ± 0.05	0.39 ± 0.02	< 0.005

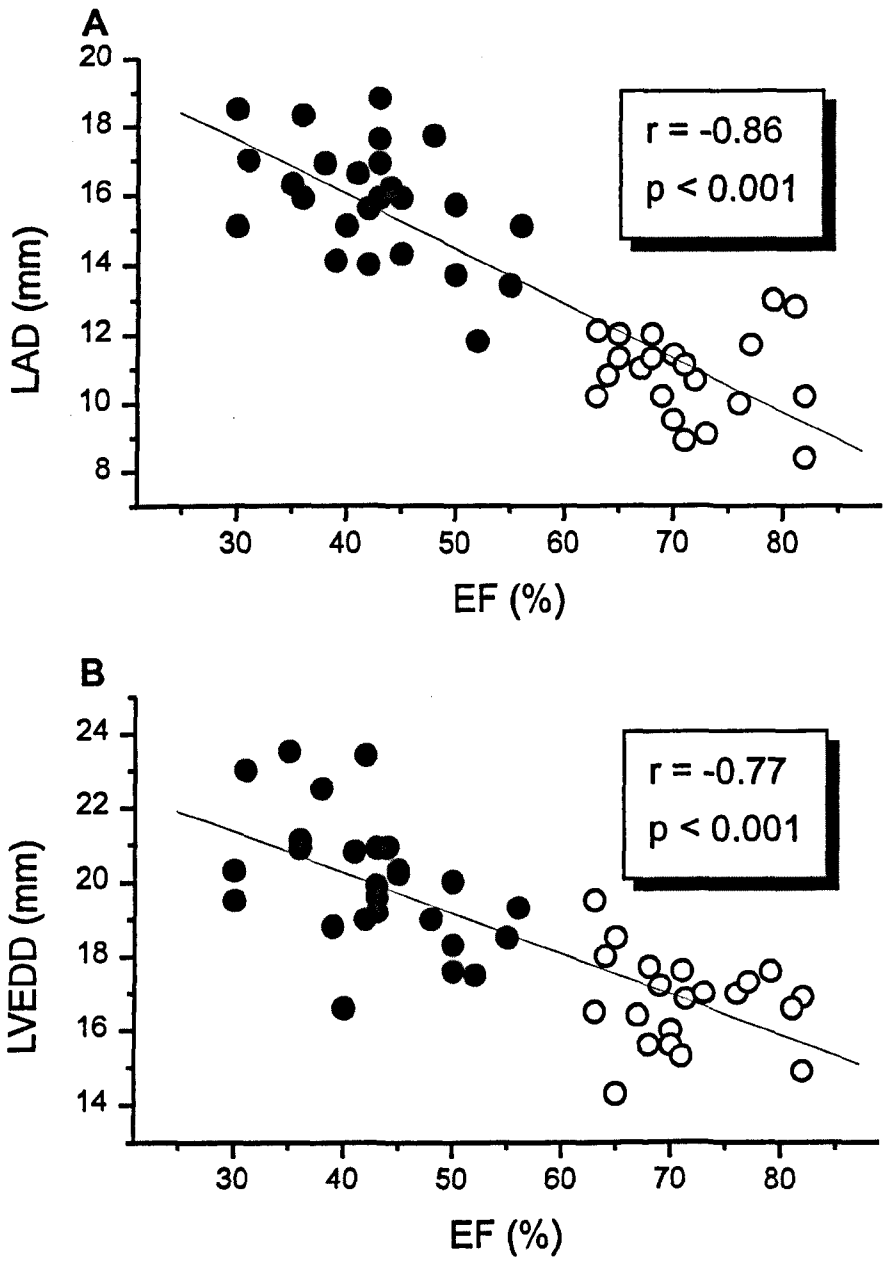

Figure 4.1 **Plots of (A) left atrial dimension (LAD) and (B) left ventricular end-diastolic dimension (LVEDD) against ejection fraction (EF) from sham-operated (○) and heart failure (●) groups. Solid lines represent linear regression of the pairs of parameters with correlation coefficients (r) and significance values (p) shown in the shaded boxes.**

Organ congestion

Liver and lung weights from rabbits in the heart failure group were increased when compared to controls (see Table 4.1). The increased organ weights were associated with the degree of left ventricular dysfunction as assessed by echocardiography (Figure 4.2 A & B) with the lung and liver weights when corrected for body weight being significantly correlated with ejection fraction. This suggests that left ventricular dysfunction in the heart failure group led to increased back-pressure in the lungs and in the liver causing congestion in these organs. The presence of right ventricular hypertrophy was demonstrated by the increased right ventricular dry weight (Table 4.1) in the heart failure group which was also correlated with ejection fraction (Figure 4.2 C). This shows that the left ventricular dysfunction produced by the rabbit coronary artery ligation model gave rise to right heart failure as a result of right ventricular overload which is the common sequence of events seen in human congestive biventricular failure. The link between right ventricular hypertrophy and liver congestion was further demonstrated in Figure 4.2 D in that the right ventricular dry weight and liver weight, both corrected to body weight, were significantly correlated ($r = 0.52$, $p < 0.005$). The distribution of the data suggests that this relationship may not be linear; this may be explained by the occurrence of liver cirrhosis in rabbits in the heart failure group with extreme right ventricular overload. Indeed, some post-mortem liver specimens had shrunken, cirrhotic appearances in addition to the honeycomb appearance associated with congestion.

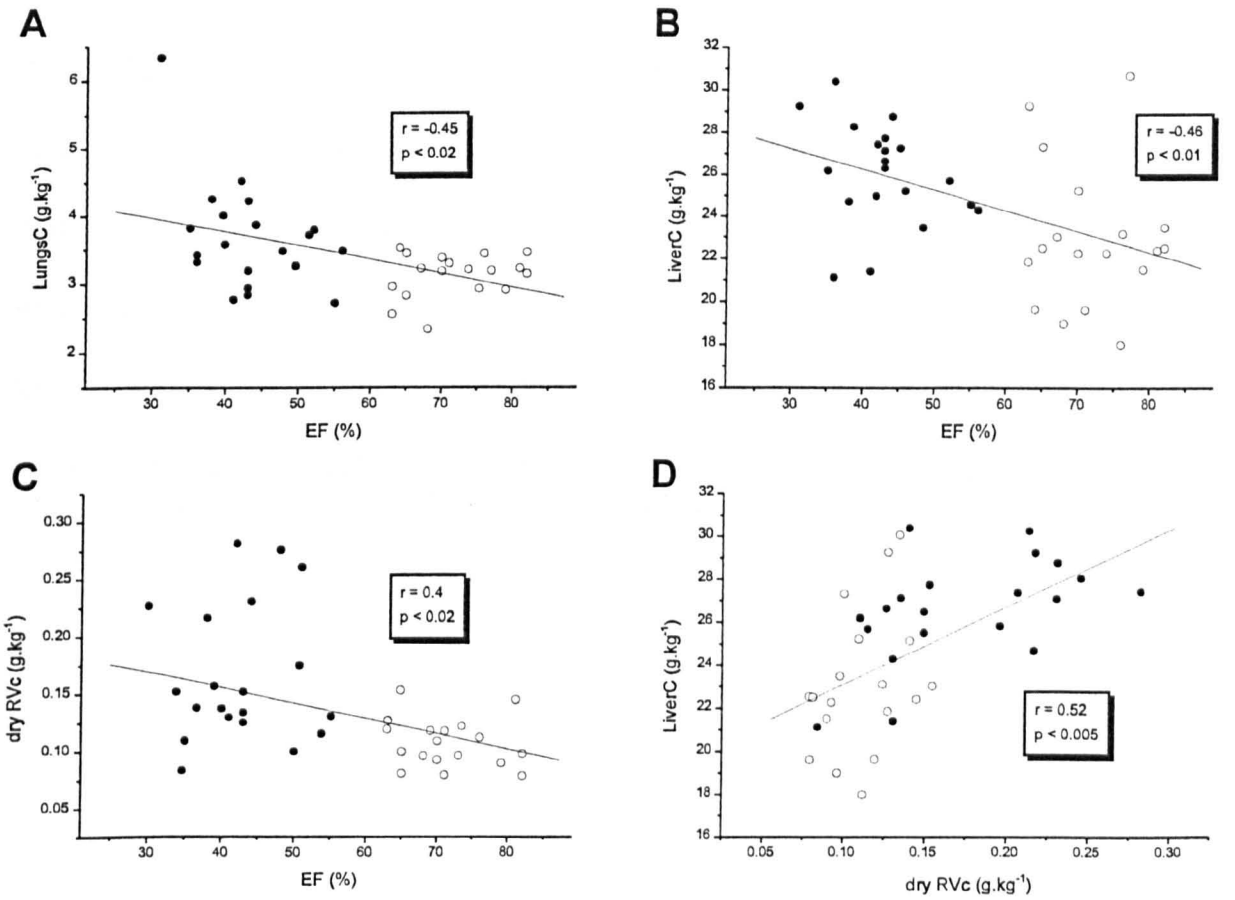

Figure 4.2 **Plots of (A) corrected lung weight (lungsC), (B) corrected liver weight (liverC) and (C) corrected right ventricular dry weight (dry RVc) against *in vivo* ejection fraction (EF) from sham-operated (○) and heart failure (●) groups. Panel D shows the plot of corrected liver weight (liverC) against corrected right ventricular dry weight (dry RVc) from the two groups. Solid lines represent linear regression of the pairs of parameters with correlation coefficients (r) and significance values (p) shown in the shaded boxes.**

Cardiac remodelling

Hearts from rabbits with heart failure had increased left ventricular dry weight when compared to controls (see Table 4.1). There was a significant correlation between the left ventricular dry weight, corrected to body weight, and ejection fraction (Figure 4.3). This shows that significant compensatory hypertrophy occurred in rabbits with heart failure as a result of the left ventricular dysfunction caused by myocardial infarction. Despite a loss of tissue due to the infarct, there was increased left ventricular tissue mass.

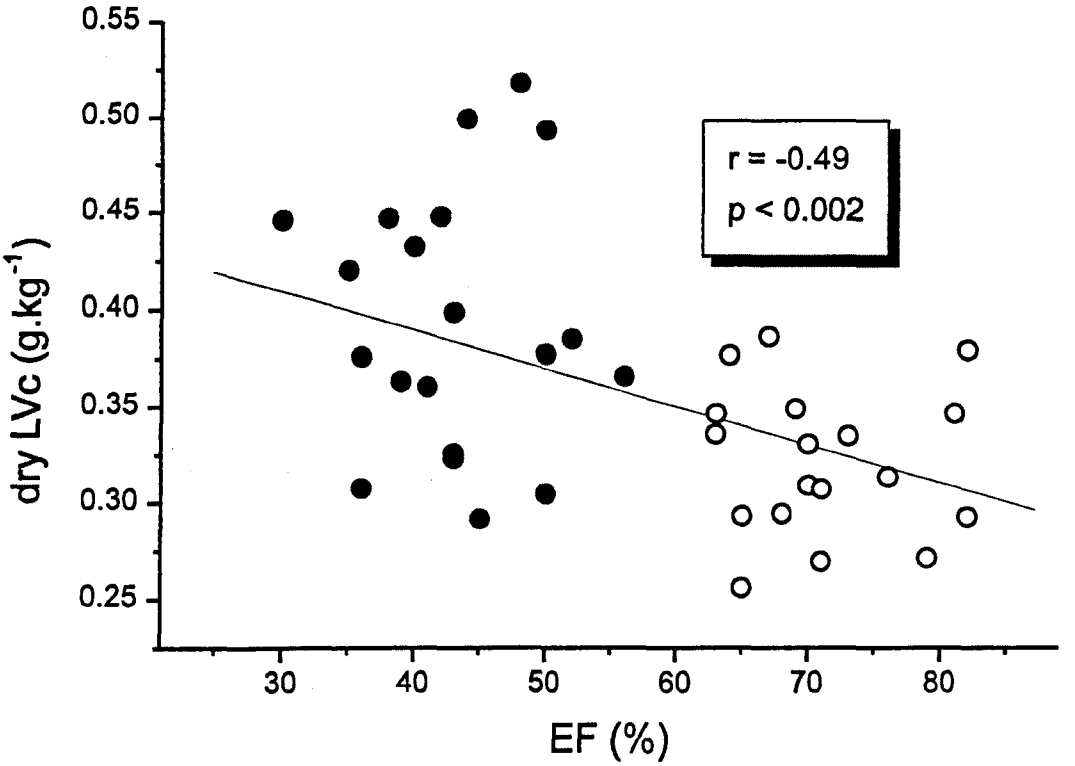

Figure 4.3 **Plot of corrected left ventricular dry weight (dry LVc) against ejection fraction (EF) in sham-operated (○) and heart failure (●) groups. The solid line is a linear regression of the two parameters ($r = -0.49$, $p < 0.002$).**

Discussion

The echocardiographic data and the organ / tissue weight measurements demonstrated that the rabbit coronary artery ligation model of heart failure produced both local and systemic changes which parallel those seen in the human clinical syndrome. In human coronary artery disease, myocardial infarction produces an area of abnormal contraction in the ventricle which leads to increased wall tension. This stimulates a hypertrophic response attempting to compensate for the contractile dysfunction. As a result of the volume overload and increased back pressure from the left ventricle, pulmonary congestion, right ventricular overload and hepatic congestion follow. This is the usual sequence of events seen in patients who develop congestive biventricular failure as a result of left ventricular dysfunction which is commonly caused by myocardial infarction in the Western world. There were similar changes in this rabbit model of heart failure with increased lung weight suggesting significant pulmonary congestion as a result of left ventricular dysfunction and increased liver weight indicating significant hepatic congestion from right heart failure secondary to left heart failure. Changes in the heart were also demonstrated with dilated left heart chambers seen on echocardiography and ventricular hypertrophy measured by the increased left and right ventricular dry weights. This cardiac remodelling process was likely to be caused by increased stress in the ventricle resulting from contractile dysfunction secondary to the myocardial infarct and is distinct from other animal models of hypertrophy used to study heart failure using pressure overload e.g. hypertension or aortic banding. This rabbit coronary artery ligation model is, therefore, a clinically relevant model of heart failure and structural and functional changes seen in these "failing" hearts should reflect the changes seen or expected in the human situation.

CHAPTER 5

CARDIAC PERFORMANCE OF THE ISOLATED EJECTING WORKING RABBIT HEART

Introduction

The relation between muscle length and developed tension in cardiac muscle has been extensively studied and the cellular mechanisms of this length-tension relation were reviewed by Allen and Kentish (1985). It has been known for a long time that cardiac muscle produces more tension when stretched. Otto Frank was the first to extend the knowledge of length-tension relationship in skeletal muscle to cardiac muscle. He showed in his landmark paper (Frank, 1895) that in a frog ventricle contracting isovolumetrically, the developed intraventricular pressure was a function of end-diastolic filling and volume - peak pressure increased with end-diastolic filling up to a certain level beyond which it declined. It took more than a decade before Ernest Starling and his colleagues (Patterson *et al.* 1914) described a similar phenomenon in the warm-blooded mammalian heart which was later called the Law of the Heart. It was shown in the dog heart-lung preparation that cardiac output increased with venous filling pressure when aortic pressure was held constant. The phenomena described by Frank and Starling are distinct but clearly related and describe the length-tension relationship that exists in the heart which has become known as the Frank-Starling relationship. This has been shown to be an important mechanism by which cardiac output is regulated. In addition to heart rate and contractility, the Frank-Starling mechanism plays a significant part in increasing cardiac performance during haemodynamic challenges such as exercise. Although a descending limb of the Frank-Starling relationship has been described, its functional significance is questionable.

Over the last several decades, many investigators have focused on the length-tension relationship in cardiac muscle and have examined the phenomenon in isolated preparations including trabeculae (intact or skinned) and myocytes. The length-tension relationship in cardiac muscle is much steeper than one would expect if it is simply the result of the

physical sliding of myofilaments over the physiological range. It was discovered that activation factors have to play a central role and hence length-dependent activation has been shown to be the important mechanism behind the cardiac length-tension relationship. Parmley and Chuck (1973) were the first to show in papillary muscles that following a sudden increase in length, there was an immediate increase in tension followed by a further slow increase over several minutes. This has been confirmed by other investigators on the isolated muscle preparation (Lakatta and Jewell, 1977). Allen and Kurihara (1982) studied Ca^{2+} transients from cat and rat papillary muscles micro-injected with aequorin. They showed that after an increase in muscle length, the peak amplitude of the Ca^{2+} transient was unchanged whilst there was an immediate increase in tension. This was followed by a slow increase in the peak amplitude of the Ca^{2+} transient which followed the time-course of the slow increase in tension. This suggests that the immediate changes in tension are due to changes in myofilament Ca^{2+} sensitivity as a result of the immediate length change whilst the slow changes are due to changes in Ca^{2+} handling which could be the result of altered Ca^{2+} entry and / or Ca^{2+} release and uptake by the sarcoplasmic reticulum. Kentish *et al.* (1992) showed that the slow changes in tension as a result of length change can be reversed by isoprenaline in isolated rabbit papillary muscles. These results suggest that the slow tension responses to length change may be mediated via cyclic AMP.

The slow response to length change has also been described in single guinea-pig ventricular myocytes (White *et al.* 1995). Its presence in the whole heart has been described by Tucci *et al.* (1984) and Lew (1988) in the dog heart but Noble *et al.* (1994) questioned its role in humans. Tucci *et al.* performed experiments in isolated isovolumetric blood-perfused dog hearts whilst Lew's experiments were performed *in situ* in anaesthetised dogs. Both groups showed a time-dependent increase in contractility in response to myocardial stretch with

increased diastolic filling. Noble *et al.* studied 8 human subjects undergoing left heart catheterisation and used body-tilt to alter ventricular filling and produce stretch (causing a mean increase in left ventricular end-diastolic pressure of 8 mmHg). Some but not all of the patients were paced either at the atrium or the ventricle. The heart rate and haemodynamic and loading conditions of the patients at rest were variable. In addition, patients were given β-blockers to "prevent reflex and heart rate effects". This could affect cyclic AMP levels which could directly affect the slow response. This group did not demonstrate any slow component although there was an estimated 18% immediate increase in stroke volume with the body tilt. All but 2 of the patients had coronary artery disease with 4 patients having impaired left ventricular function with ejection fractions of 40% or less. All these factors may have contributed to the lack of slow response in the study by Noble *et al.*

This Chapter describes experiments using the working heart configuration to assess *in vitro* cardiac performance of the isolated rabbit heart. The relationships between various parameters measured using the working heart configuration were studied. Contractile function of the working heart was studied by altering ventricular filling pressure in order to examine the Frank-Starling relationship. The possibility of time-dependent activation of myocardium subsequent to a step change in pre-load was examined. The contribution of this 'slow response' to the overall Frank-Starling mechanism was studied.

Methods

The performance of the isolated heart in the working heart configuration was studied in 5 normal stock New Zealand White rabbits. No cardiac surgery had been performed in these rabbits. They were healthy and their cardiac function was presumed to be normal. The heart was harvested from the sacrificed animal in a similar way as described in Chapter 3. As opposed to the coronary ligation and sham-operated animals where the pericardium had

been incised during cardiac surgery, the normal stock rabbits had not been operated on and the pericardium was still intact. The pericardium had to be incised and inverted in order that the heart could be "freed" to be mounted onto the working heart apparatus. After the heart had been properly attached and connected to the apparatus, perfusion was switched from Langendorff mode to working heart mode. At a baseline pre-load of 10 cmH_2O (8 mmHg) and after-load of 75 cmH_2O (55 mmHg) and with the heart being paced at a cycle length of 300 ms at the right atrium, a mean aortic flow of 80 $ml.min^{-1}$ or above was ascertained before including in the study as previous work on a similar set-up (Pye, 1992) demonstrated that healthy hearts could produce that level of cardiac output. Intrinsic cycle length of the isolated beating heart in the working heart configuration at 37 °C had been found to be around 330 ms to 350 ms and thus a pacing cycle length of 300 ms was chosen to ensure a constant, atrially paced rhythm during the experiments.

Measurements of cardiac dimension, intraventricular pressure and cardiac output were made as described in Chapter 3. The Frank-Starling relationship was examined by raising the pre-load from 10 to 25 cmH_2O (i.e. 8 to 18 mmHg) in 5 cmH_2O steps with an equilibration period of 15 min after each step increase - the after-load and pacing rate being kept constant. The effect of the step change in pre-load on the various parameters were continually monitored and recorded.

Results

Characteristics of the parameters measured in the isolated, ejecting working heart

Figure 5.1 shows the recordings from a typical experiment with the changes in pressure in the left ventricle, cardiac output as measured by the ultrasonic flow probe and cardiac dimension with time. The tracings represent an average of 10 successive sweeps during a

continuous 5 s recording. The hearts were all paced via the right atrium at a cycle length of 300 ms with a baseline pre-load of 10 cmH_2O (8 mmHg) and a baseline after-load of 75 cmH_2O (55 mmHg). The relationship between the pressure, flow and cardiac dimension tracings allows the various phases of the cardiac cycle to be analysed and the timing of the opening and closing of cardiac valves (mitral and aortic) to be inferred. When intraventricular pressure reached the level of the pre-load, i.e. point 'a' in Figure 5.1, the pressure rose sharply. This represented the closure of the mitral valve and the beginning of isovolumic contraction. Cardiac dimension stayed relatively constant during this period. When the intraventricular pressure exceeded the after-load (point 'b'), the aortic valve opened and positive flow could be detected in the ultrasonic flow probe. Cardiac dimension started to decrease during this ejection phase. Intraventricular pressure decreased when fluid was ejected from the heart whilst aortic flow continued. When intraventricular pressure fell below after-load (point 'c'), the aortic valve closed and isovolumic relaxation began. Intraventricular pressure fell sharply until it was lower than pre-load (point 'd') when mitral valve opened again and ventricular filling resumed with another cardiac cycle. The interval between points 'c' and 'd' represents the isovolumic relaxation time. However, cardiac dimension according to the sonomicrometer crystals was not constant during this period. As the crystals were place on the subepicardial surface of the left ventricle, the slight increase in cardiac dimension recorded during the isovolumic relaxation phase could represent an increase in ventricular wall thickness whilst the intraventricular volume might have stayed the same. Aortic flow measured with the flow probe showed a sinusoidal pattern during the cardiac cycle. This will be discussed below.

The profile of the left ventricular pressure tracings from the 5 normal stock hearts and the timing of the various phases of the cardiac cycle are summarised in Table 5.1 under baseline pre-load and after-load conditions.

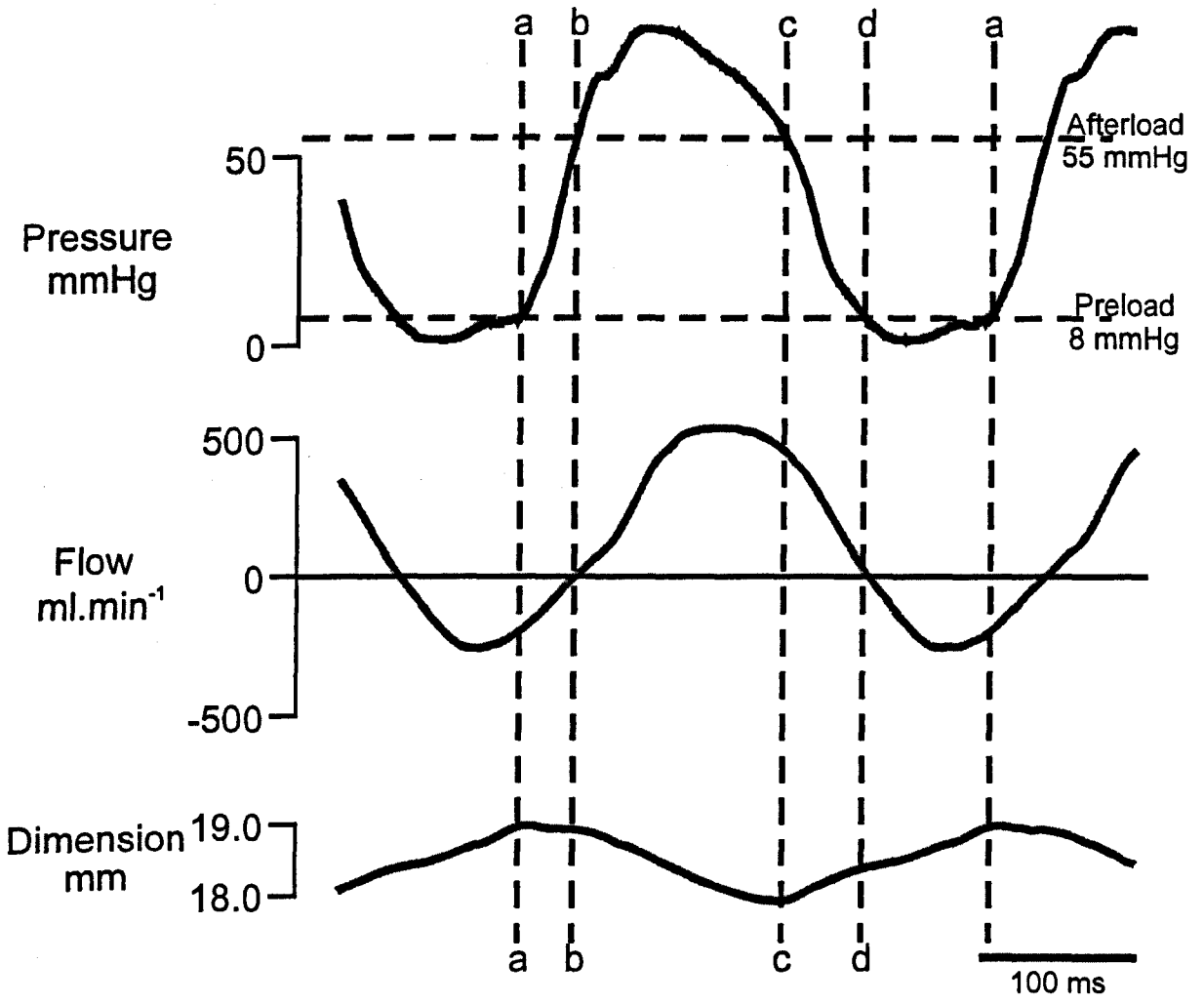

Figure 5.1 Representative tracings of left ventricular pressure (Pressure), aortic flow (Flow) as measured with the ultrasonic flow probe and cardiac dimension (Dimension) as measured with sonomicrometer crystals in the isolated working heart, paced via the right atrium at 300 ms cycle length. Recordings were made at a baseline pre-load level of 10 cmH_2O (8 mmHg) and after-load level of 75 cmH_2O (55 mmHg) both marked with horizontal broken lines. Vertical broken lines represent the timing of (a) the beginning of systole, (b) aortic valve opening , (c) aortic valve closure and (d) mitral valve opening. Isovolumic contraction phase is represented by the interval (a - b), ejection phase by interval (b - c), isovolumic relaxation phase by (c - d) and ventricular filling phase by (d - a).

Table 5.1 Different phases of the cardiac cycle in 5 normal isolated rabbit hearts in the working heart configuration under baseline conditions.

Measurements were made at a pre-load 10 cmH_2O (8 mmHg) and after-load of 75 cmH_2O (55 mmHg) with right atrial pacing at a cycle length of 300 ms. (IVCT = isovolumic contraction time, $dP.dt^{-1}_{(max)}$ = maximum rate of change of pressure, AV = aortic valve, MV = mitral valve, IVRT = isovolumic relaxation time)

	Normal hearts (n = 5)
Isovolumic Contraction Phase	
IVCT (ms)	30.9 ± 1.3
+ $dP.dt^{-1}_{(max)}$ ($mmHg.ms^{-1}$)	2.34 ± 0.12
Ejection Phase	
Ejection time (ms)	150.4 ± 1.3
+ $dP.dt^{-1}_{(max)}$ ($mmHg.ms^{-1}$)	1.75 ± 0.10
- $dP.dt^{-1}_{(max)}$ ($mmHg.ms^{-1}$)	1.65 ± 0.03
Isovolumic Relaxation Phase	
AV closure time (ms)	178.1 ± 3.5
MV opening time (ms)	223.2 ± 4.8
IVRT (ms)	45.1 ± 2.9
- $dP.dt^{-1}_{(max)}$ ($mmHg.ms^{-1}$)	1.67 ± 0.02

Characterisation of cardiac output measured with the ultrasonic flow probe

Aortic flow, as measured with the ultrasonic probe showed a sinusoidal pattern which is different from what one would expect *in vivo*. The flow probe was vertically placed and connected in series to the aortic cannula. Cardiac output from the ejecting heart was recorded as positive flow during the ejection phase. When the aortic valve closed, flow in the aorta should decrease to zero until the next ejection phase when the aortic valve opened again. However, a negative flow was recorded in this working heart set-up. It could be due to (a) coronary arterial flow, (b) back-flow into the left ventricle due to aortic regurgitation, or both. In a few initial experiments where the aortic cannula was connected too close to the aortic valve causing aortic regurgitation, there was progressive dilatation of the left ventricle and deterioration of the preparation. The sinusoidal pattern with negative aortic flow was observed in all of the experiments where the hearts were stable and with no progressive dilatation of the left ventricle. Back-flow into the left ventricle was thought not to be the cause of the negative flow although the presence of minor aortic regurgitation could not be ruled out. A more probable explanation for the negative flow would be flow into the coronary arteries.

Correlation between ultrasonic flow probe recordings with aortic flow and coronary effluent

In order to investigate the components of the recordings from the ultrasonic flow probe, aortic flow and coronary effluent were collected over 30 s, during low and normal flow in 5 experiments and correlated with the flow probe signals. The digitised flow probe signals were exported into a Microsoft Excel spreadsheet and mathematically integrated to give a positive and negative flow over 30 s. Figure 5.2 summarises the relationship between the

recorded and measured flow components. The Transonic Systems T106 flow-meter gives an instantaneous electronic mean in addition to the phasic flow signals. The electronic mean was found to correlate well with the mean flow calculated from the digitised signals (positive minus negative flow) ($r = 0.99$, $p < 0.001$, Figure 5.2 A). This calculated mean flow was found to correlate well with the aortic flow collected ($r = 0.998$, $p < 0.001$, Figure 5.2 B). It was found that the positive flow correlated well with the total amount of effluent collected over time (aortic flow plus coronary effluent) ($r = 0.99$, $p < 0.002$, Figure 5.2 C). There was also an association between the negative flow and the amount of coronary effluent collected over time ($r = 0.93$, $p < 0.05$, Figure 5.2 D).

The Pearson correlation coefficients between the pairs of variables suggested strong associations between them and the regression coefficients were close to unity suggesting that the individual variable within the pairs varied to the same extent in parallel with one another. These data showed that:- (a) the positive flow recorded by the flow probe represented the total cardiac output from the ejecting working heart; (b) the electronic mean flow produced by the Transonic flow-meter reflected the calculated mean flow which represented the proportion of the total cardiac output flowing through the working heart apparatus into the compliance and after-load chambers, measured as aortic flow by the analogue flow meter; and (c) the negative flow measured by the flow probe reflected the proportion of cardiac output flowing into the coronary arteries after the ejection phase and was close to the amount of coronary effluent collected - although coronary flow during systole could not be accurately measured, this was likely to be small as there was little difference between the coronary effluent collected and the negative flow.

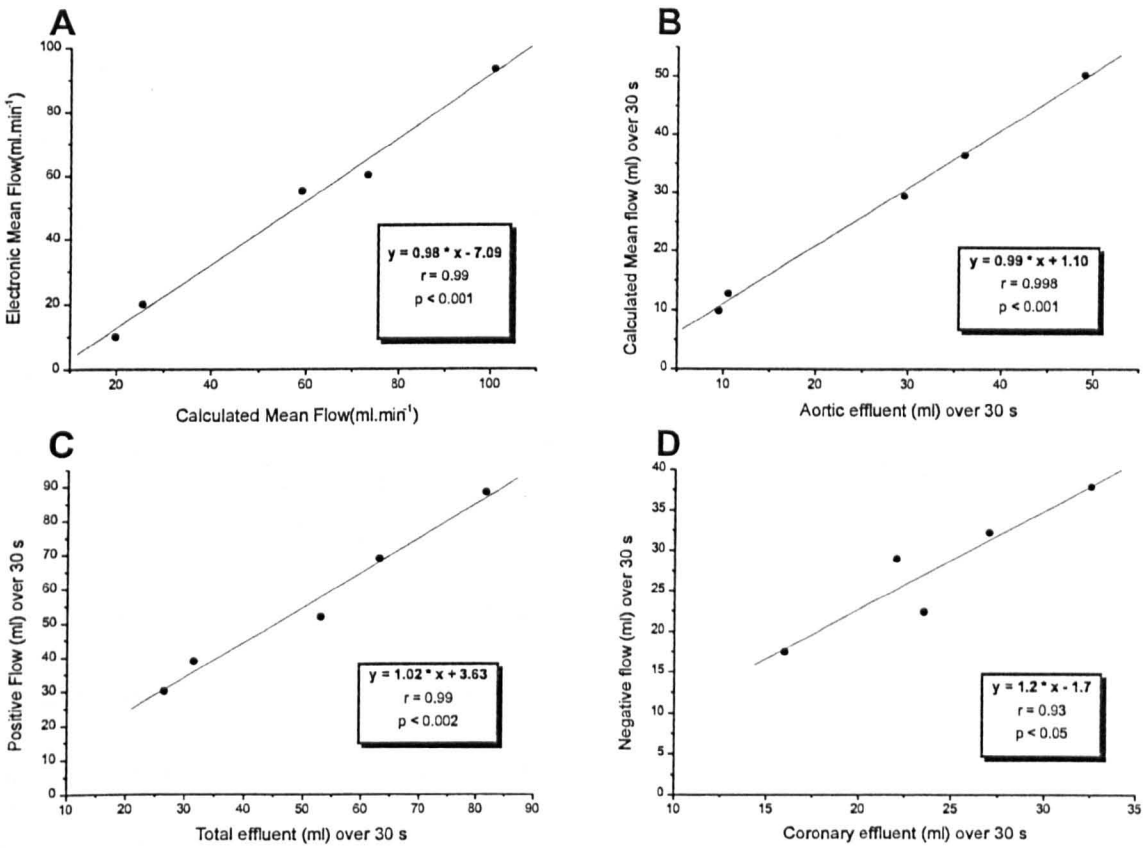

Figure 5.2 **Correlation between flow signals recorded by the ultrasonic flow probe and measured flow in the working heart configuration in 5 experiments during low and high flow conditions. Panel A shows a plot of the electronic mean flow signal from the Transonic flow meter against the mean flow calculated by subtracting the negative flow from positive flow. Panel B shows a plot of the calculated mean flow against aortic flow collected over 30 s. Panel C shows a plot of the positive flow recorded by the flow probe against amount of aortic flow plus coronary effluent collected over 30 s. Panel D shows a plot of the negative flow recorded by the flow probe against the amount of coronary effluent collected over 30 s. Lines represent linear regression of the 2 parameters with the equation (shown in bold type), correlation coefficients (r) and significance levels (p) shown in the shadowed boxes.**

Slow response to step increase in pre-load

The effects of a step increase in pre-load, from a baseline level of 10 cmH_2O (8 mmHg) to 15 cmH_2O (11 mmHg) above the level of the aorta, on the haemodynamic parameters over time were observed. Hearts were paced at a cycle length of 300 ms via the right atrium. Steady state was obtained prior to the load change and the effect of the change was observed with continuous recording of the parameters until a new steady state was reached. The results of a typical experiment are shown in Figure 5.3. The step increase in pre-load produced an immediate increase in left ventricular peak systolic pressure and aortic flow which was quickly followed by a decrease in the two parameters (phase I). These reached a minimal value before increasing slowly to a steady state over time (phase II). The results of the changes in the various haemodynamic parameters over time in the 5 normal hearts as a result of the step change in pre-load are summarised in Table 5.2. When pre-load was increased from 10 to 15 cmH_2O (i.e. 8 to 11 mmHg) above the level of the aorta, left ventricular peak systolic pressure rose initially to 107 ± 3 % whilst the cardiac output increased to 115 ± 5 %, followed by a fall in the 2 parameters to 102 ± 3 % and 110 ± 7 % respectively over 1.5 ± 0.2 min. There was also an immediate increase in both end-diastolic (to 101.8 ± 0.8 %) and end-systolic dimensions (to 100.9 ± 0.3 %) followed by a further rise in both parameters during this initial phase. End-diastolic pressure rose initially to 155 ± 13 % reaching 156 ± 12 % at the end of phase I. These results suggested that the increase in pre-load caused an increase in left ventricular inotropy as measured by the immediate changes in intraventricular pressure and cardiac output. The gradual fall in peak systolic pressure and cardiac output during phase I was accompanied by a gradual increase in systolic dimension and, to a lesser extent, diastolic dimension. Over the next 5.6 ± 0.4 min (phase II), left ventricular systolic pressure recovered to 105 ± 3 % and cardiac output to

113 ± 6 % but these changes were not associated with any significant change in left ventricular end-diastolic dimension which remained at 101.9 ± 0.7 %. Both left ventricular systolic pressure and cardiac output at the end of stage II were significantly different from those at the end of stage I ($p < 0.01$ and 0.02 respectively). These changes during phase II suggested that there was a slow increase in inotropy. This slow response to a step change in pre-load is better demonstrated in Figure 5.4 which was modified from Figure 5.3 with the peak systolic pressure and end-systolic dimension amplified to show the slow increase in inotropy with time. There was an average increase in peak systolic pressure of 2.9 ± 0.6 mmHg and cardiac output of 5.3 ± 2.4 $ml.min^{-1}$ during phase II. The data are graphically represented in Figure 5.5.

There was no significant change in the coronary flow as measured by the negative flow in the ultrasonic flow probe over time after the step increase in pre-load. The mean coronary flow was 68.1 ± 1.7 $ml.min^{-1}$ at a pre-load of 10cmH_2O (8 mmHg) and 68.0 ± 1.7 $ml.min^{-1}$ at the end of phase II (p = NS). This suggests that coronary flow was not altered by a change in cardiac output as a result of change in pre-load. Previous work on this working heart set-up by Dr. Maurice Pye (1992) had suggested that the coronary arteries in the isolated heart were maximally vasodilated under these conditions. Coronary flow was thus not critically dependent on coronary vascular tone. Since coronary flow occurred predominantly during diastole and after-load was maintained at a constant level of 75 cmH_2O (55 mmHg) above the level of the aorta, coronary flow would be constant and would not be altered by changes in cardiac output as a result of changes in pre-load. The absence of change in coronary flow with an increase in pre-load further verified that the changes observed in systolic pressure and cardiac output were truly due to an increase in inotropy and not due to a change in coronary flow. Increase in coronary flow could cause an

increase in cardiac output and systolic pressure as a result of the garden-hose effect. The results showed that the slow response was not due to such an effect.

With the coronary flow staying constant throughout the time course after the increase in pre-load, the changes in mean aortic flow reflected changes in the total cardiac output. As mentioned earlier, since the electronic mean produced by the Transonic flow-meter correlated well with the mean aortic flow, this was monitored over time and used to reflect changes in total cardiac output after step increases in pre-load in the following experiments examining the Frank-Starling relationship.

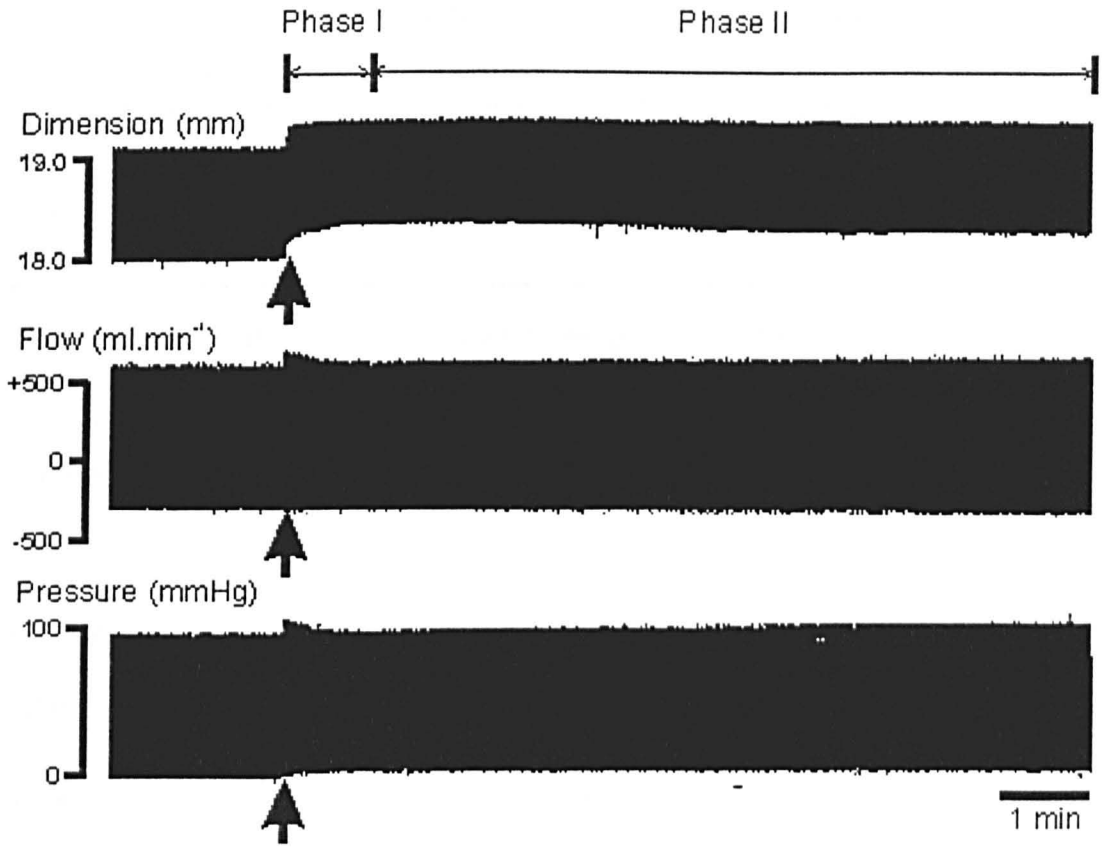

Figure 5.3 Effect of step change in pre-load on cardiac dimension (Dimension), cardiac output (Flow) and intraventricular pressure (Pressure) over time in the isolated ejecting working heart. Arrows show the point when pre-load was increased from a level of 10 cmH_2O (8 mmHg) to 15 cmH_2O (11 mmHg). Phases I and II are shown as marked (see text).

Table 5.2 Response of haemodynamic parameters to step increase in pre-load in 5 normal rabbit hearts in the working heart configuration.

After-load was kept at 75 cmH_2O (55 mmHg) with right atrial pacing at a cycle length of 300 ms. Changes in the individual parameters are shown as percentage (%) relative to the baseline value at 10 cmH_2O. (C.O. = cardiac output, SysP = peak left ventricular systolic pressure, EDD = end-diastolic dimension, ESD = end-systolic dimension, LVEDP = left ventricular end-diastolic pressure)

	Preload 10 cmH_2O	Immediate change 10 to 15 cmH_2O	End of phase I	End of phase II
C.O. ($ml.min^{-1}$)	202 ± 8	230 ± 6	221 ± 8	226 ± 6
(%)		115 ± 5	110 ± 7	113 ± 6
SysP (mmHg)	93 ± 5	100 ± 6	94 ± 6	97 ± 6
(%)		107 ± 3	102 ± 3	105 ± 3
EDD (mm)	18.8 ± 1.0	19.1 ± 1.0	19.2 ± 1.0	19.2 ± 1.0
(%)		101.8 ± 0.8	101.9 ± 0.8	101.9 ± 0.7
ESD (mm)	17.9 ± 0.9	18.0 ± 0.9	18.2 ± 0.9	18.2 ± 0.9
(%)		100.9 ± 0.3	101.8 ± 0.6	101.7 ± 0.6
LVEDP (mmHg)	5.7 ± 1.7	10.2 ± 1.6	10.5 ± 2.1	9.5 ± 1.6
(%)		155 ± 13	156 ± 12	147 ± 13

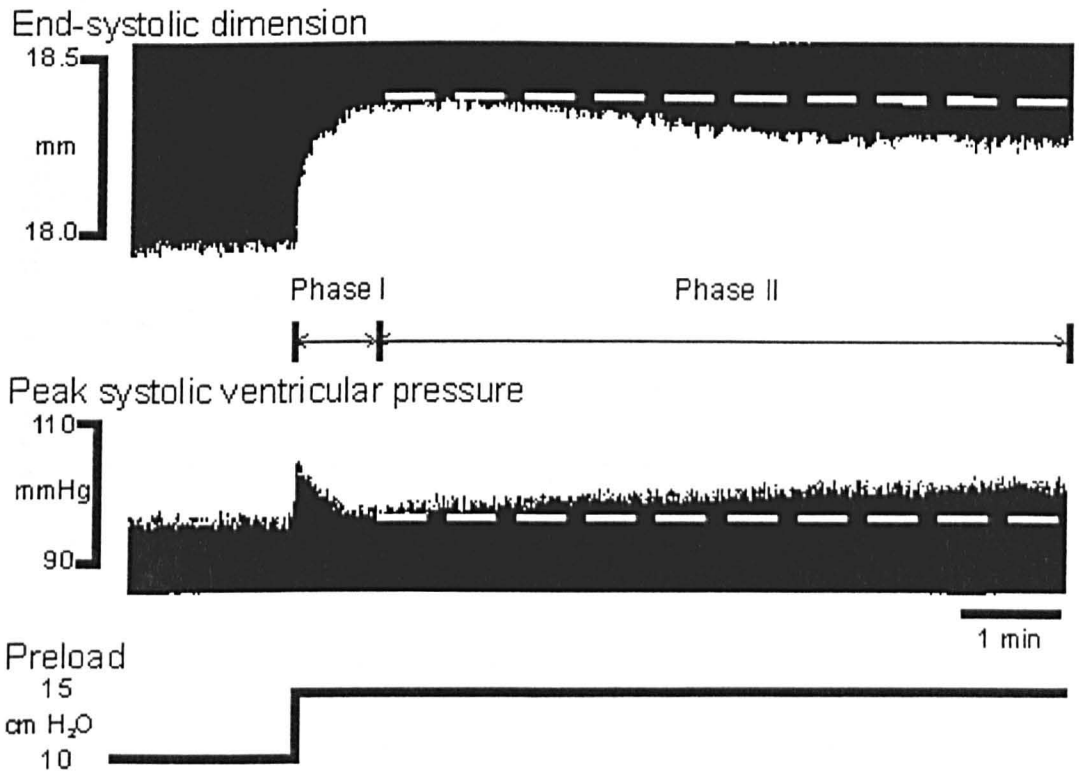

Figure 5.4 Modification of Figure 5.3 showing the effect of step change in pre-load on end-systolic dimension and peak systolic pressure over time in the isolated ejecting working heart. Broken white lines are drawn at the level of both parameters after equilibration during phase I (see text), further illustrating the slow response during phase II (see text) with an increase in peak systolic pressure and decrease in end-systolic dimension with time.

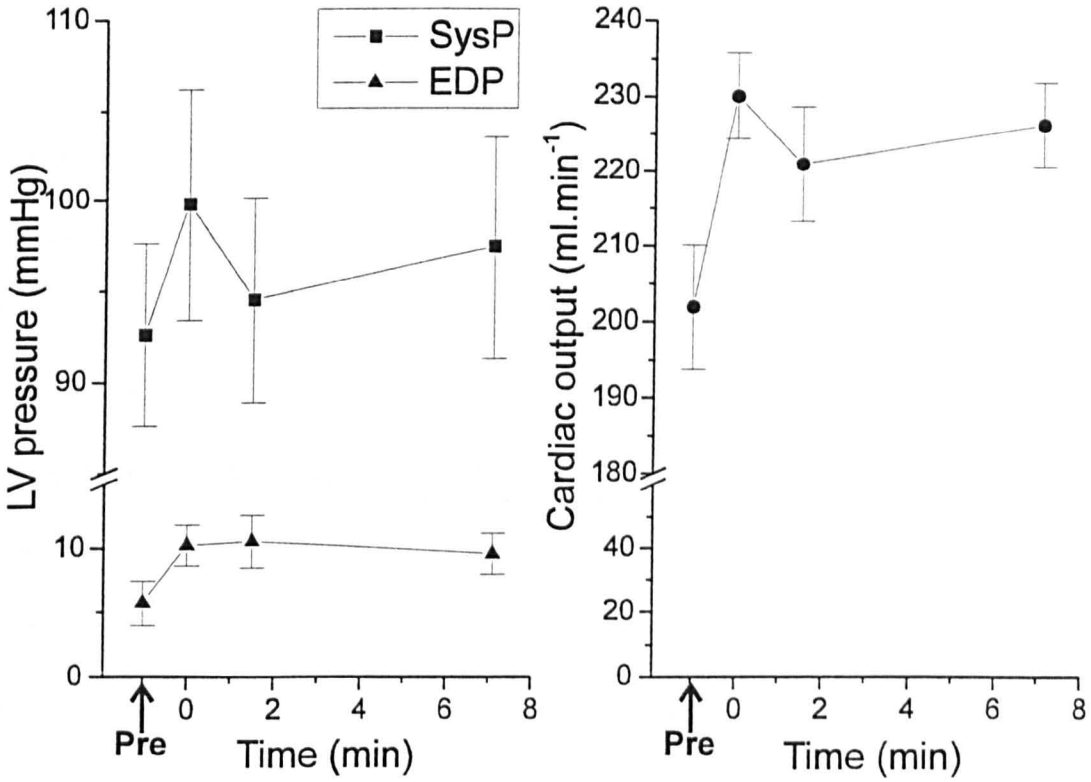

Figure 5.5 Graphical representation of the changes in left ventricular systolic pressure (SysP), end-diastolic pressure (EDP) and cardiac output in response to a step increase in pre-load from 10 cmH_2O (8 mmHg) [marked "Pre" with arrow] to 15 cmH_2O (11 mmHg) over time in 5 normal stock rabbit hearts in the working heart configuration.

Frank-Starling mechanism

The inotropic response of the 5 normal hearts on the working heart configuration was further studied by examining the form of the Frank-Starling relationship. The parameters were measured at steady state after a 15 min equilibration period at each pre-load level and the results are summarised in Table 5.3 and in Figure 5.6. There was an increase in peak left ventricular systolic pressure and aortic flow on increasing the pre-load from 10 to 15 cmH_2O (i.e. 8 to 11 mmHg) and then from 15 to 20 cmH_2O (i.e. 11 to 15 mmHg) with appropriate increases in left ventricular end-diastolic pressure, as would be expected by the Frank-Starling relationship. The increase in end-diastolic pressure in each of the 2 increases in pre-load was about 4 mmHg (equivalent to 5.4 cmH_2O) which was close to the 5 cmH_2O step change. However, on increasing pre-load from 20 to 25 cmH_2O (i.e. 15 to 18 mmHg), there was a much smaller increase in end-diastolic pressure (about 2 mmHg) and there was a decrease in systolic pressure and aortic flow instead. Lactate levels were collected from the coronary effluent at the end of each load-change for all the experiments but did not show any increase at high pre-loads, suggesting against the possibility that the decrease in systolic pressure and aortic flow was due to hypoxia. This apparent descending limb of the Frank-Starling curve may be due to the limitations of this working heart set-up, which will be considered in detail below in the *Discussion* section.

Table 5.3 Frank-Starling relationship in 5 isolated normal rabbit hearts in the working heart configuration.

After-load was kept at 75 cmH_2O (55 mmHg) with right atrial pacing at a cycle length of 300 ms. (Flow = aortic flow, SysP = peak left ventricular systolic pressure, LVEDP = left ventricular end-diastolic pressure)

	Preload (cmH_2O)			
	10	15	20	25
Flow ($ml.min^{-1}$)	107 ± 14	133 ± 11	138 ± 12	133 ± 17
SysP (mmHg)	93 ± 5	97 ± 6	99 ± 6	97 ± 8
LVEDP (mmHg)	5.7 ± 1.7	9.5 ± 1.6	12.9 ± 1.1	14.7 ± 0.4

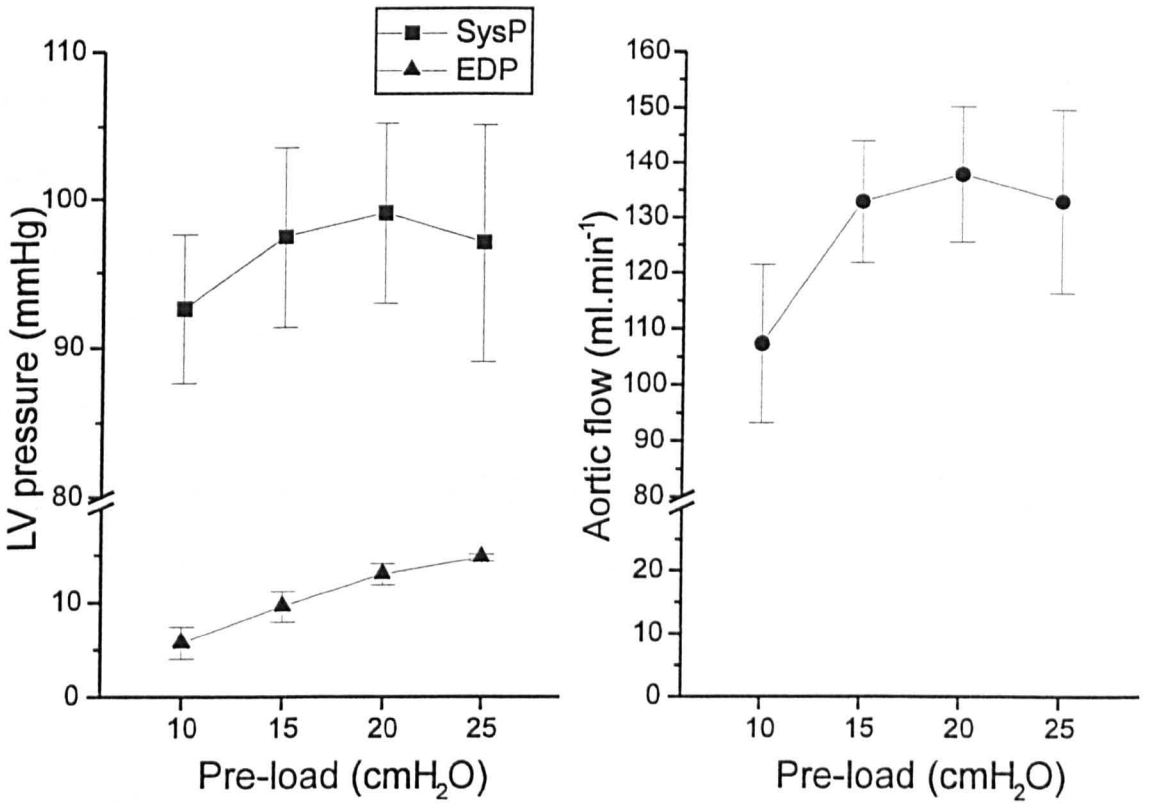

Figure 5.6 Graphical representation of the Frank-Starling relationship in 5 normal stock rabbit hearts in the working heart configuration with changes in left ventricular systolic pressure (SysP), end-diastolic pressure (EDP) and aortic flow in response to increases in pre-load from 10 cmH_2O (8 mmHg) to 25 cmH_2O (18 mmHg) in 5 cmH_2O steps.

Discussion

The working heart configuration allowed the mechanical performance of the heart to be studied *in vitro* with the isolated heart functioning in a similar way as it would do *in vivo*. The loading conditions could be controlled and the heart could be studied without the influence of biological factors like autonomic nervous system and hormonal influence which may be difficult to control *in vivo*. Changes in left ventricular pressure, cardiac output and cardiac dimensions during the cardiac cycle could be measured.

It was shown that a slow response to a step increase in pre-load was present in normal rabbit hearts. The increase in pre-load from 10 to 15 cmH_2O (i.e. 8 to 11 mmHg) produced a rise in left ventricular end-diastolic pressure from 5.7 to 9.5 mmHg which is within a physiological range. Although the magnitude of slow response was small (about 2 % increase in systolic pressure and cardiac output), the effect was evident and significant. The step increase in pre-load produced an increase in end-diastolic left ventricular dimension of about 2 % as opposed to an 8 to 10 % length change used in studies on papillary muscle strips which produced a much larger slow response (Parmley and Chuck, 1973; Lakatta and Jewell, 1977; Allen and Kurihara, 1982).

An ascending limb of the Frank-Starling curve was produced by step increases in pre-load in the normal hearts showing the normal inotropic response to increased end-diastolic pressure / volume. At a high pre-load level (25 cmH_2O), an apparent descending limb was observed. This might have been a real effect or an artefact due to the working heart set-up. The pericardium had been removed from the isolated hearts prior to mounting onto the working heart apparatus and the apparent descending limb is unlikely to be due to inadequate ventricular filling as a result of pericardial constriction. A mean left ventricular end-diastolic pressure of 14.7 mmHg at 25 cmH_2O (18 mmHg) pre-load, which is not

particularly high, suggested against a true descending limb. As mentioned above, this level of end-diastolic pressure was lower than would be expected for the level of pre-load. It was quite often observed in these experiments that at high pre-load levels, the left atrium of the working heart was significantly dilated or "ballooned". With the hearts being paced at a constant cycle length which was relatively fast, it would appear that left ventricular filling might not have been complete at high pre-load levels. This would cause left atrial dilatation and a left ventricular end-diastolic pressure which was lower than would be expected from the level of pre-load. The decrease in systolic pressure and aortic flow at high pre-load level is more difficult to explain. One possibility may be that the metabolic demands at high pre-load and hence high workload outweighed the supply to the ejecting working heart. Oxygenation and coronary flow in the set-up could have been insufficient for the working heart at high pre-load levels. However, lactate levels measured from the coronary effluent collected at each pre-load change for all 5 experiments did not show any significant increase even at high pre-load levels. This suggested against the possibility that ischaemia or hypoxia was the cause for the apparent descending limb. Another possibility may be that at high pre-load levels, the hearts were dilated to the extent that mitral regurgitation occurred as a result of stretch of the valve annulus. This would cause part of the cardiac output to be pumped back into the left atrium during systole, causing left atrial dilatation (which was observed at high pre-load levels) and decrease in left ventricular systolic pressure and aortic flow.

CHAPTER 6

CARDIAC PERFORMANCE OF HEARTS ISOLATED FROM RABBITS WITH HEART FAILURE

Introduction

Increased heart size, elevated ventricular filling pressure and low cardiac output have been well-recognised hallmarks of the syndrome of heart failure for a long time. Hope (1832) was the first to put forward the concept of "backward failure" in which the overworked ventricle hypertrophies and then dilates. With the development of technology to measure ventricular pressures, it was found that end-diastolic pressure was raised in the failing heart chamber (Wiggers, 1952) and an elevated ventricular end-diastolic pressure was taken to signify the presence of heart failure (Braunwald and Ross, 1963). Mackenzie (1913), however, proposed the theory of "forward failure" and stated that the impairment of the blood supply from a failing heart was the main feature in heart failure. With the Law of the heart (Starling, 1918) came the awareness of the length-tension relationship or pressure-volume relationship in the heart. Experiments by Spann *et al.* (1972) showed that contractile performance was depressed in failing cat ventricles with decreased peak developed tension and velocity of contraction under the same loading conditions as normal hearts. The main haemodynamic sequelae in the syndrome of heart failure were regarded to be the result of systolic dysfunction in the pump leading to poor cardiac output and raised filling pressure. More recently, Grossman *et al.* (1979) introduced the concept of diastolic dysfunction in heart failure. It was shown that in many patients with heart failure, the rate of ventricular relaxation was significantly decreased in failing hearts with decreased rate of ventricular pressure decline. Left ventricular diastolic distensibility or compliance was also decreased in failing hearts. This would fit with the pathophysiological observation that there was significant hypertrophy in the chronically overloaded failing heart. Hypertrophy in the heart itself would cause impaired relaxation and chamber stiffness. Additional factors involved in the structural remodelling and biochemical changes in the myocardium would contribute to

the abnormal diastolic function of the failing heart. Some patients may have symptoms of heart failure in the absence of abnormal systolic function (Dougherty *et al.* 1984) as a result of diastolic dysfunction. This has been termed diastolic heart failure and the importance of differentiating systolic from diastolic heart failure has been emphasised as the approach to therapy is different (Goldsmith and Dick, 1993). However, the majority of patients with chronic heart failure have systolic dysfunction with reduced pump efficiency, and diastolic dysfunction can also be demonstrated in many of them.

As mentioned in Chapter 1, the depressed contractile performance of the failing heart is attributable to many factors ranging from intrinsic myocyte abnormality to geometrical inefficiency due to structural remodelling (Figueredo and Camacho, 1995; Wagoner and Walsh, 1996). Some of the mechanisms by which a normal heart can improve performance have been found to be impaired in the failing heart. Down regulation of β-adrenoceptors, as a result of chronic sympathetic over-activity, leads to blunted catecholamine responsiveness in the failing heart (Bristow *et al.* 1982). The ability of the myocardium or myocyte to improve contraction with stimulation rate via the force-frequency relationship (the Bowditch effect) is also impaired (Mulieri *et al.* 1992; Davies *et al.* 1995). There is, however, debate as to whether the Frank-Starling relationship is intact in the failing heart. Schwinger *et al.* (1994) reported that there was no increase in the force of contraction in skinned-fibre preparations of left ventricular papillary muscle strips from human failing hearts when stretched to 150 % of the resting length and Ca^{2+} sensitivity of the skinned fibres was insensitive to stretching. On the other hand, Holubarsch *et al.* (1996) examined the Frank-Starling mechanism in excised human whole left ventricles, isolated left ventricular muscle strips and skinned fibre preparations and found that it was well-preserved in failing hearts but diastolic compliance was reduced. In chronic heart failure,

left ventricular dilatation and hypertrophy occur leading to a shift of the pressure-volume curve to the right and upwards (LeJemtel and Sonnenblick, 1993). The equilibrium volume is increased and chamber compliance is reduced. These may alter the Frank-Starling relationship in failing hearts but the mechanism may not be completely absent. As discussed in Chapter 5, there are slow changes following an immediate increase in inotropy in response to a step increase in pre-load or muscle length in the whole heart or myocardial tissue. This has not been investigated in the failing heart or failing myocardial tissue and its relevance in the Frank-Starling relationship in heart failure is unknown.

In this Chapter, mechanical performance of the isolated heart from rabbits with heart failure was examined. Firstly, performance in the working heart configuration was studied in similar ways to those described in Chapter 5 for normal stock hearts. Secondly, the *in vitro* performance of these hearts in the working heart configuration was correlated with *in vivo* echocardiographic measurements. Thirdly, the performance of isolated hearts in the Langendorff mode, which was used for experiments on Ca^{2+} transient and Monophasic Action Potential measurements described in subsequent Chapters, was studied and correlated with *in vivo* measurements.

Methods

Cardiac performance of failing hearts in working heart configuration

The mechanical performance of the hearts from rabbits with heart failure was studied *in vitro* using the working heart configuration. The hearts (n = 8) were isolated from rabbits 8 weeks after the initial coronary artery ligation procedure as described in Chapter 3. Sham-operated animals (n = 8) were used as controls. The hearts were studied on the working heart set-up, paced at a cycle length of 300 ms via the right atrium. After-load was kept at a

level of 75 cmH_2O (55 mmHg) above the level of the aorta. Baseline parameters at a pre-load level of 10 cmH_2O (8 mmHg) of the failing hearts and controls were compared. Changes during the different phases of the cardiac cycle were also analysed and compared. The effect of a step increase in pre-load from 10 to 15 cmH_2O (i.e. 8 to 11 mmHg) was observed in the 2 groups to investigate the slow response as mentioned in Chapter 5. The Frank-Starling relationship in the heart failure group was also compared with that in controls by increasing the level of pre-load from 10 to 25 cmH_2O (i.e. 8 to 18 mmHg) in 5 cmH_2O steps.

At the end of the working heart experiments, a modified Tyrode's solution containing 10 mM K^+ was used for perfusion in the Langendorff mode to inhibit cardiac contraction. The heart was relaxed and a latex balloon was inserted via the left atrium into the left ventricle to measure passive compliance. The latex balloon was connected via a 6F cannula to a water-filled syringe and a pressure transducer. Incremental 0.5 ml boluses of water were injected into the balloon whilst monitoring the pressure inside the balloon which represented the intraventricular pressure. The volume of the balloon used was about 5 ml when fully filled (but not stretched). This volume was chosen so that it was greater than the maximum expanded volume of the left ventricle in either group of hearts; there would be no tension generated by the balloon itself with the volume increments and the pressure measured would reflect intraventricular pressure alone. These results were used to describe the static pressure-volume relationship of the left ventricle.

Correlation between *in vitro* working heart performance and *in vivo* echocardiographic measurements in heart failure

In vivo cardiac performance was assessed in all the experimental animals 1 week prior to sacrifice as described in Chapters 3 and 4. Ejection fraction (EF) as measured on

echocardiography was used as an indicator of systolic function *in vivo* and this was correlated with *in vitro* parameters of contractile performance, namely left ventricular systolic pressure and cardiac output in both experimental groups under baseline working heart conditions (pre-load of 10 cmH_2O [8 mmHg] and after-load of 75 cmH_2O [55 mmHg]) at 37 °C with right atrial pacing at 300 ms cycle length.

Cardiac performance of Langendorff perfused hearts from rabbits with heart failure and correlation with *in vivo* measurements

Subsequent Chapters will describe experiments measuring Ca^{2+} transients and Monophasic Action Potentials (MAPs) in isolated rabbit hearts from both the heart failure and sham-operated groups. In these experiments, the isolated hearts were perfused in the Langendorff mode and a latex balloon was inserted into the left ventricle to monitor intraventricular pressure. Water was injected into the balloon to alter the volume thereby adjusting the end-diastolic pressure to zero at the beginning of the experiments. This would standardise the loading conditions in both experimental groups and allow the comparison and analysis of *in vitro* cardiac performance. The pressure profiles of 17 hearts from the heart failure group and 13 from the sham-operated group were analysed during right atrial pacing at 350 ms. This was then correlated with *in vivo* cardiac performance as measured by the ejection fraction on echocardiography. With Langendorff perfusion, it was found that the intrinsic cycle length of the beating heart was longer (and heart rate slower) than in the working heart configuration (380 to 400 ms vs. 330 to 350 ms - see *"Methods"* section in Chapter 5). The slightly slower pacing rate with a cycle length of 350 ms (i.e. about 170 $beats.min^{-1}$) was still close to the physiological heart rate of the rabbit (around 180 to 200 $beats.min^{-1}$ *in vivo*) and still ensured a constant, paced rhythm during the experiments but allowed the time

course of the Ca^{2+} transients and MAP signals to be better analysed with greater resolution (see subsequent Chapters).

Results

Cardiac performance of failing hearts in working heart configuration

Baseline haemodynamic parameters in heart failure

The results of the baseline haemodynamic parameters measured on the working heart set-up in hearts from the heart failure group and controls are summarised in Table 6.1. At a baseline pre-load of 10 cmH_2O, left ventricular end-diastolic pressure was significantly higher (15.7 ± 1.0 vs. 10.4 ± 1.7 mmHg, $p < 0.02$) and left ventricular systolic pressure (87.1 ± 2.8 vs. 96.4 ± 2.8 mmHg, $p < 0.05$) and total cardiac output (175 ± 10 vs. 212 ± 7 mmHg, $p < 0.05$) significantly lower in the heart failure group when compared to controls. There was no significant difference in coronary flow, as measured by the negative flow in the ultrasonic flow probe, between the two groups (75 ± 3 vs. 75 ± 3 $ml.min^{-1}$, p = NS). This suggested that the coronary vascular tone was not significantly different on the working heart set-up in the 2 groups and that the difference observed in the haemodynamic parameters could not be explained by a difference in coronary arterial perfusion.

Cardiac dimensions measured with the sonomicrometer crystals during diastole and systole were increased in the heart failure group when compared to controls (Table 6.1), in agreement with the echocardiographic findings *in vivo* and the tissue weights as mentioned in Chapter 4.

Table 6.1 Comparison of baseline haemodynamic parameters measured in the isolated ejecting working heart between rabbits with heart failure (HF) and controls (Sham).

Measurements were made at a pre-load 10 cmH_2O (8 mmHg) and after-load of 75 cmH_2O (55 mmHg) with right atrial pacing at a cycle length of 300 ms. (LVEDP = left ventricular end-diastolic pressure, SysP = left ventricular peak systolic pressure, C.O. = total cardiac output, EDD = end-diastolic dimension, ESD = end-systolic dimension)

	HF (n = 8)	Sham (n = 8)	p value
LVEDP (mmHg)	15.7 ± 1.0	10.4 ± 1.7	< 0.02
SysP (mmHg)	87.1 ± 2.8	96.4 ± 2.8	< 0.05
C.O. ($ml.min^{-1}$)	175 ± 10	212 ± 7	< 0.05
Coronary flow ($ml.min^{-1}$)	75 ± 3	75 ± 3	NS
EDD (mm)	22.0 ± 0.9	19.3 ± 1.0	< 0.05
ESD (mm)	20.6 ± 0.8	18.1 ± 1.0	< 0.05

Baseline haemodynamic parameters in sham-operated group and normal stock hearts

Most of the baseline haemodynamic parameters measured in the 8 hearts from the sham-operated group at a pre-load of 10 cmH_2O (8 mmHg) and after-load of 75 cmH_2O (55 mmHg) with right atrial pacing at 300 ms were comparable to those measured in the 5 normal stock hearts described in Chapter 5 (Table 6.1 and Table 5.2). The peak left ventricular systolic pressure, cardiac output, end-diastolic dimension and end-systolic dimension were similar ($p = NS$). However, the left ventricular end-diastolic pressure was significantly higher in the sham-operated group when compared to normal stock hearts (10.4 ± 1.7 vs. 5.7 ± 1.7 mmHg, $p < 0.05$).

Changes during the phases of the cardiac cycle

The difference between the heart failure group and sham-operated group was also analysed by examining the changes during the different phases of the cardiac cycle. The intraventricular pressure signals were averaged in the 8 hearts in each group and compared. The 2 averaged traces are shown in Figure 6.1. It is evident that the mean left ventricular peak systolic pressure was lower and the mean left ventricular end-diastolic pressure higher in failing hearts than in controls. The data on the different phases of the cardiac cycle are summarised in Table 6.2. The parameters obtained from the 8 sham-operated hearts were comparable to those from the 5 stock rabbit hearts described in Chapter 5 (cf. Table 5.1).

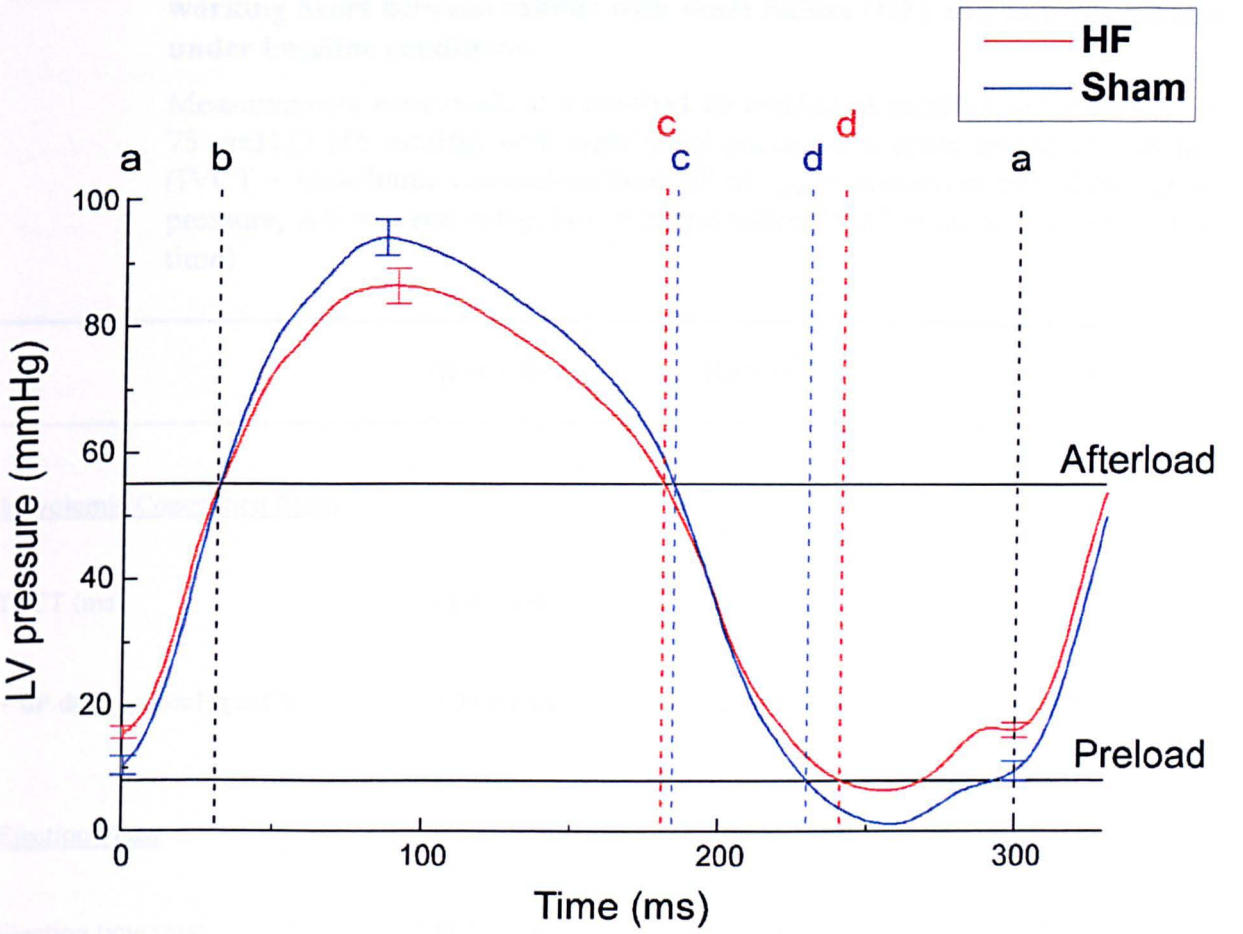

Figure 6.1 Averaged tracings of left ventricular pressure in 8 hearts from the heart failure group (HF - red solid line) and 8 control hearts (Sham - blue solid line) in the working heart configuration, paced via the right atrium at 300 ms cycle length, at a baseline pre-load level of 10 cmH_2O (8 mmHg) and after-load level of 75 cmH_2O (55 mmHg) - both marked with horizontal solid lines. Vertical broken lines represent the timing of (a) the beginning of systole, (b) aortic valve opening , (c) aortic valve closure and (d) mitral valve opening. Isovolumic contraction phase is represented by the interval (a - b), ejection phase by interval (b - c), isovolumic relaxation phase by (c - d) and ventricular filling phase by (d - a).

Table 6.2 Comparison of different phases of the cardiac cycle in the isolated ejecting working heart between rabbits with heart failure (HF) and controls (Sham) under baseline conditions.

Measurements were made at a pre-load 10 cmH_2O (8 mmHg) and after-load of 75 cmH_2O (55 mmHg) with right atrial pacing at a cycle length of 300 ms. (IVCT = isovolumic contraction time, $dP.dt^{-1}_{(max)}$ = maximum rate of change of pressure, AV = aortic valve, MV = mitral valve, IVRT = isovolumic relaxation time)

	HF (n = 8)	Sham (n = 8)	p value
Isovolumic Contraction Phase			
IVCT (ms)	31.6 ± 1.6	31.3 ± 2.3	NS
$+ dP.dt^{-1}_{(max)}$ ($mmHg.ms^{-1}$)	1.99 ± 0.10	2.34 ± 0.14	< 0.05
Ejection Phase			
Ejection time (ms)	148.7 ± 5.9	153.7 ± 4.2	NS
$+ dP.dt^{-1}_{(max)}$ ($mmHg.ms^{-1}$)	1.40 ± 0.10	2.09 ± 0.13	< 0.002
$- dP.dt^{-1}_{(max)}$ ($mmHg.ms^{-1}$)	1.43 ± 0.08	1.70 ± 0.06	< 0.02
Isovolumic Relaxation Phase			
AV closure time (ms)	180.2 ± 4.8	185.0 ± 3.0	NS
MV opening time (ms)	241.0 ± 7.9	228.4 ± 3.5	NS
IVRT (ms)	60.7 ± 3.8	43.3 ± 1.2	< 0.001
$- dP.dt^{-1}_{(max)}$ ($mmHg.ms^{-1}$)	1.44 ± 0.08	1.70 ± 0.06	< 0.02

Isovolumic contraction phase

After ventricular filling, the sharp rise in left ventricular pressure marks the beginning of the isovolumic contraction phase. This phase ends with the opening of the aortic valve when intraventricular pressure exceeds the after-load. The working heart experiments were carried out under a constant after-load of 75 cmH_2O (55 mmHg). The isovolumic contraction phase was the time for the intraventricular pressure to reach that level after its initial sharp rise. When this phase was analysed in the 2 experimental groups, it was found that there was no difference in the time taken to reach an after-load of 55 mmHg. The isovolumic contraction time was 31.6 ± 1.6 ms in the heart failure group and 31.3 ± 2.3 ms in controls (p = NS). However, during this phase the maximum rate of pressure rise was decreased in the heart failure group when compared to controls (1.99 ± 0.10 vs. 2.34 ± 0.14 $mmHg.ms^{-1}$, $p < 0.05$).

Ejection phase

When the left ventricular pressure exceeded the after-load of 55mmHg, the aortic valve opened and the ejection phase began. The maximum rate of pressure rise during this ejection phase was decreased in the heart failure group (1.40 ± 0.10 vs. 2.09 ± 0.13 $mmHg.ms^{-1}$, $p < 0.002$), reaching a lower peak systolic pressure than the control group as mentioned above. This, together with the abnormality during isovolumic contraction, suggested significant abnormal mechanical function of the failing hearts during systole.

The maximum rate of pressure decline during the ejection phase was also decreased in the heart failure group when compared to controls (1.43 ± 0.08 vs. 1.70 ± 0.06 $mmHg.ms^{-1}$, $p < 0.02$). When the left ventricular pressure dropped below the after-load level of 55 mmHg, the aortic valve closed and this marked the end of the ejection phase. The total duration of the ejection phase was slightly shorter in the heart failure group (148.7 ± 5.9 vs. 153.7 ± 4.2

ms) but this did not reach statistical significance as the time of aortic valve closure was only slightly earlier in the heart failure group when compared to controls (180.2 ± 4.8 vs. 185.0 ± 2.0 ms from the beginning of systole); this difference being again non-significant.

Isovolumic relaxation phase

The interval between aortic valve closure and mitral valve opening during the cardiac cycle is termed the isovolumic relaxation phase. In the working heart set-up, it was the time taken for the left ventricular pressure to fall from the after-load level of 55 mmHg (when the aortic valve closed) to the pre-load load of 8 mmHg (when the mitral valve opened). As mentioned above, the time of aortic valve closure was only slightly earlier in the heart failure group than controls. The time of mitral valve opening was slightly later in the heart failure group (241.0 ± 7.9 vs. 228.4 ± 3.5 ms from the beginning of systole) although this difference did not reach statistical significance. The interval between those two timings, i.e. the isovolumic relaxation time, was significant longer in the heart failure group when compared to controls (60.7 ± 3.8 vs. 43.3 ± 1.2 ms, $p < 0.001$) (see Figure 6.2). In addition, the maximum rate of pressure decay during this phase was significant lower in the heart failure group (1.44 ± 0.08 vs. 1.70 ± 0.06 $mmHg.ms^{-1}$, $p < 0.02$). This suggested that there was significant diastolic abnormality in the failing hearts.

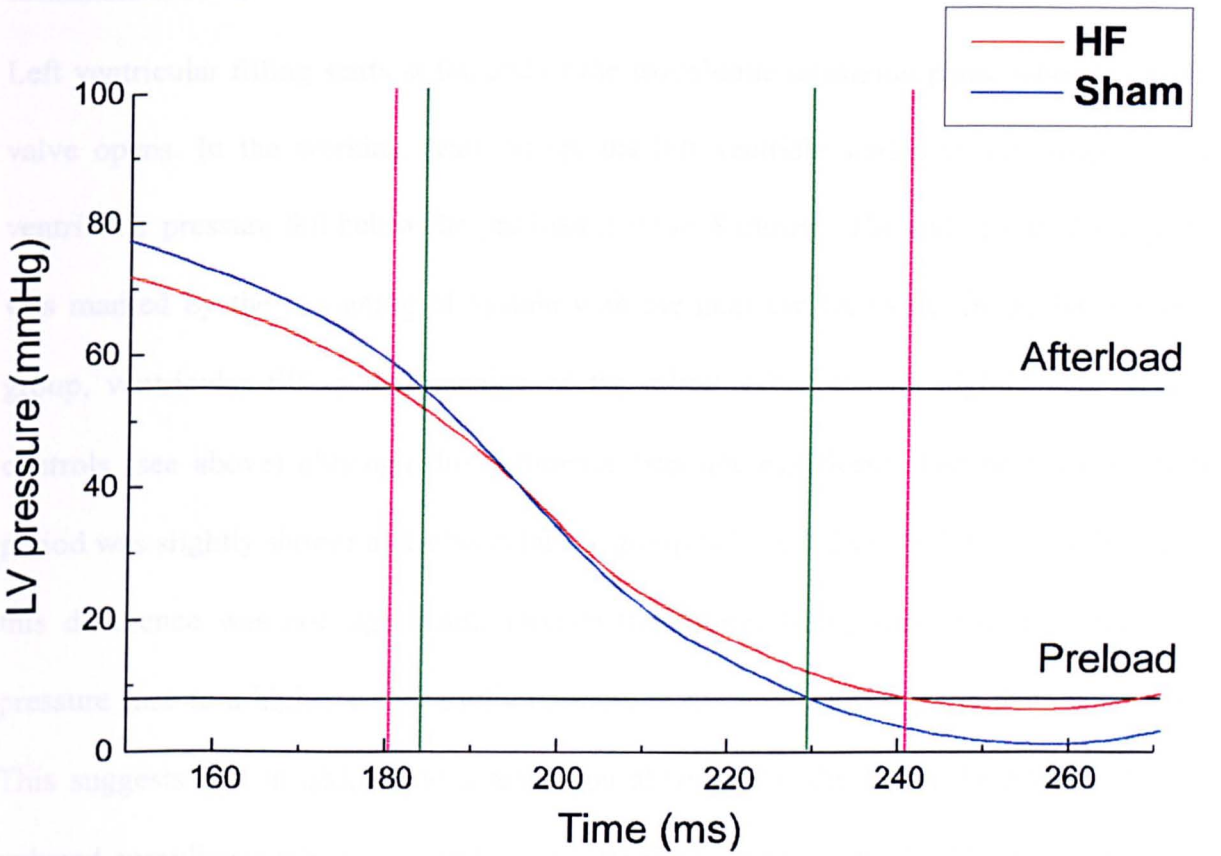

Figure 6.2 Modification of Figure 6.1 with the period during diastole expanded to show the isovolumic relaxation time in the heart failure (HF) group (interval marked by magenta lines) and in the control (Sham) group (interval marked by green lines).

Ventricular filling

Left ventricular filling starts at the end of the isovolumic relaxation phase when the mitral valve opens. In the working heart set-up, the left ventricle started to fill when the left ventricular pressure fell below the pre-load level of 8 mmHg. The end of the filling phase was marked by the beginning of systole with the next cardiac cycle. In the heart failure group, ventricular filling, i.e. opening of the mitral valve, started slightly later than in controls (see above) although this difference was not significant. The ventricular filling period was slightly shorter in the heart failure group (67.2 ± 5.2 vs. 75.2 ± 3.7 ms) but again this difference was not significant. Despite the shorter filling time, the left ventricular pressure rose to a higher end-diastolic pressure in the heart failure group than in controls. This suggests that in addition to a relaxation abnormality, the failing hearts may have a reduced compliance which impaired ventricular filling during diastole. This possibility was investigated as described below.

Passive compliance in the isolated heart

The pressure-volume relationship in the K^+-arrested heart was studied with a latex balloon. When 0.5 ml boluses of water were injected into the balloon, there was a point (V_0) where pressure started to rise in an exponential manner. The pressure-volume data could be fitted to an exponential function with the equation: Pressure = A * (Volume) ^{k} where A and k are constants and Volume represents the volume above V_0. The mean values of A and k for the 8 hearts in the heart failure group and 5 hearts in the control group are shown in Table 6.3. Sample data from one experiment from each group and the representative exponential curves for the mean values in both groups are shown in Figure 6.3. This showed that for a same level of pressure rise, there was a smaller increase in volume in the heart failure group

than in the sham-operated group indicating that failing hearts had a reduced compliance or increased stiffness when compared to controls.

Table 6.3 Comparison of left ventricular passive compliance between 8 failing hearts (HF) and 5 controls (Sham).

Passive compliance was described by the Pressure - Volume relationship, Pressure = A * (Volume) ^{k} (see text).

	HF (n = 8)	Sham (n = 5)	p value
A	22.2 ± 4.0	2.1 ± 0.3	< 0.005
k	1.3 ± 0.1	2.5 ± 0.3	< 0.002

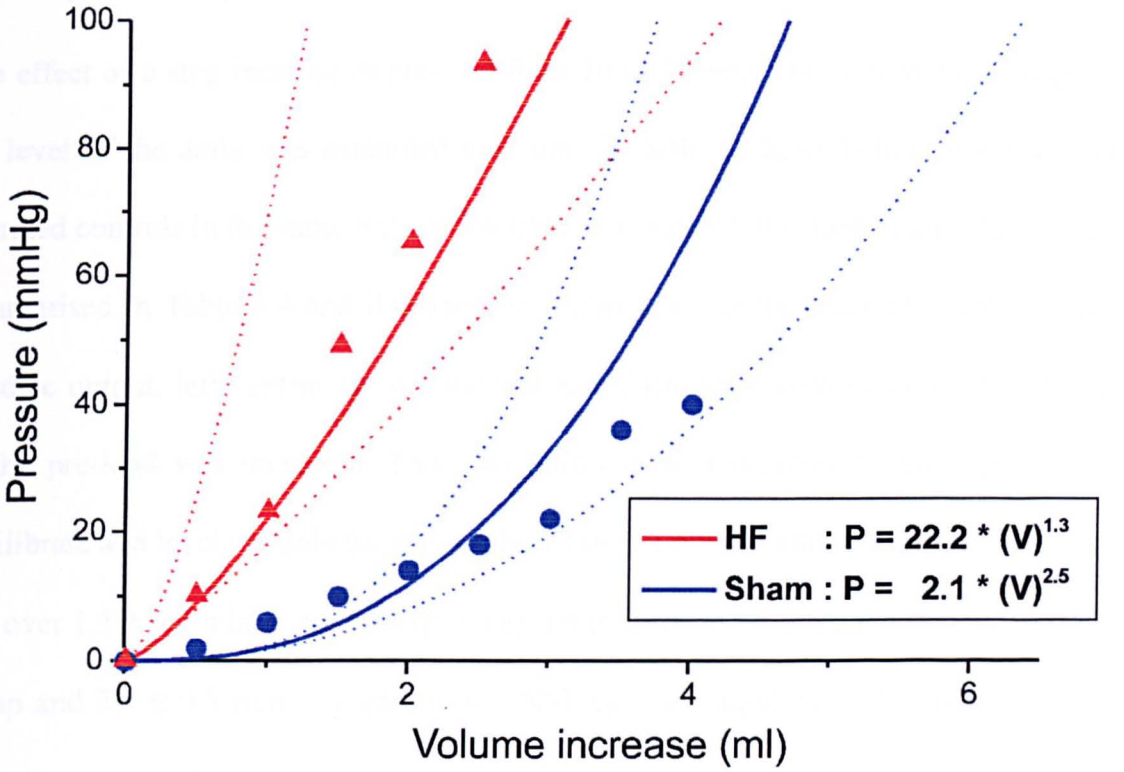

Figure 6.3 Comparison of passive compliance in K^+ arrested hearts as measured by the pressure - volume relationship (see text) between the heart failure group (shown in red, n = 8) and controls (shown in blue, n = 5). Dotted lines represent standard errors. Sample data from one failing heart (▲) and one control (●) are shown.

Slow response to step increase in pre-load

The effect of a step increase in pre-load from 10 to 15 cmH_2O (i.e. 8 to 11 mmHg) above the level of the aorta was examined over time in both the heart failure group and sham-operated controls in the same way as described in Chapter 5 for stock hearts. The results are summarised in Table 6.4 and illustrated in Figure 6.4. All the haemodynamic parameters (cardiac output, left ventricular systolic and end-diastolic pressure) increased immediately as the pre-load was increased. This was followed by a decrease in these parameters to equilibrate at a level towards the end of phase I over 1.6 ± 0.3 min in the heart failure group and over 1.5 ± 0.2 min in controls (p = NS). Over the next 5.7 ± 0.5 min in the heart failure group and 5.6 ± 0.3 min in controls (p = NS), cardiac output and left ventricular systolic pressure increased over time to reach a steady state at the end of phase II. The left ventricular end-diastolic pressure stayed at the same level over the course of phase II in the heart failure group but decreased over time in controls.

Coronary flow in the heart failure group at the end of phase II was 74 ± 3 $ml.min^{-1}$ as compared to 75 ± 3 $ml.min^{-1}$ prior to the step increase (p = NS). Similarly, there was again no significant difference in coronary flow as a result of the pre-load increase in the control group (74 ± 4 $ml.min^{-1}$ after the load change as compared to 75 ± 3 $ml.min^{-1}$ before, p = NS).

The end-diastolic and end-systolic dimensions in both groups followed a similar pattern of change over time in response to the step increase in pre-load as the stock hearts described in Chapter 5. There was an initial increase in both parameters immediately following the pre-load increase. End-diastolic dimension stayed the same throughout phase I and II in both experimental groups. There was a further increase in end-systolic dimensions in both groups during the course of phase I followed by a small decrease over the course of phase II.

There was an increase in left ventricular pressure by 3.5 ± 0.7 mmHg ($p < 0.02$) and cardiac output by 5.0 ± 0.9 $ml.min^{-1}$ ($p < 0.005$) during phase II in the sham-operated hearts with these 2 parameters at the end of stage II being significantly different from those at the end of stage I. These changes were similar to those observed in normal stock hearts and represent slow increase in inotropy. In the heart failure group, there was a mean change in left ventricular pressure of 0.4 ± 0.2 mmHg and that in cardiac output of 1.3 ± 0.7 $ml.min^{-1}$ during phase II. These values at the end of stage II were not significantly different from those at the end of stage I and suggest that the slow increase in inotropy was either small or non-existent. The slow increases in left ventricular pressure and cardiac output observed in sham-operated controls were significantly different from the change in the 2 parameters in failing hearts during phase II ($p < 0.05$ and $p < 0.01$ respectively).

Table 6.4 Response of haemodynamic parameters to step increase in pre-load in 8 hearts in the heart failure group (HF) and 8 controls (Sham) in the working heart configuration.

After-load was kept at 75 cmH_2O (55 mmHg) with right atrial pacing at a cycle length of 300 ms. (C.O. = cardiac output, SysP = peak left ventricular systolic pressure, EDD = end-diastolic dimension, ESD = end-systolic dimension, LVEDP = left ventricular end-diastolic pressure)

	Pre-load 10 cmH_2O	Immediate change 10 to 15 cmH_2O	End of phase I	End of phase II
C.O. ($ml.min^{-1}$)				
HF	175 ± 10	183 ± 10	171 ± 10	172 ± 10
Sham	212 ± 7	227 ± 6	211 ± 6	215 ± 6
SysP (mmHg)				
HF	87 ± 5	90 ± 6	85 ± 6	86 ± 6
Sham	96 ± 3	103 ± 3	95 ± 3	98 ± 2
EDD (mm)				
HF	22.0 ± 0.9	22.1 ± 1.0	22.1 ± 1.0	22.1 ± 1.0
Sham	19.3 ± 1.0	19.5 ± 1.0	19.5 ± 1.0	19.5 ± 1.0
ESD (mm)				
HF	20.6 ± 0.8	20.7 ± 0.8	20.8 ± 0.8	20.7 ± 0.8
Sham	18.1 ± 1.0	18.2 ± 1.0	18.4 ± 1.0	18.3 ± 1.0
LVEDP (mmHg)				
HF	15.7 ± 1.0	19.3 ± 0.9	18.8 ± 1.0	18.8 ± 1.0
Sham	10.4 ± 1.7	14.6 ± 2.1	14.1 ± 1.9	13.8 ± 2.0

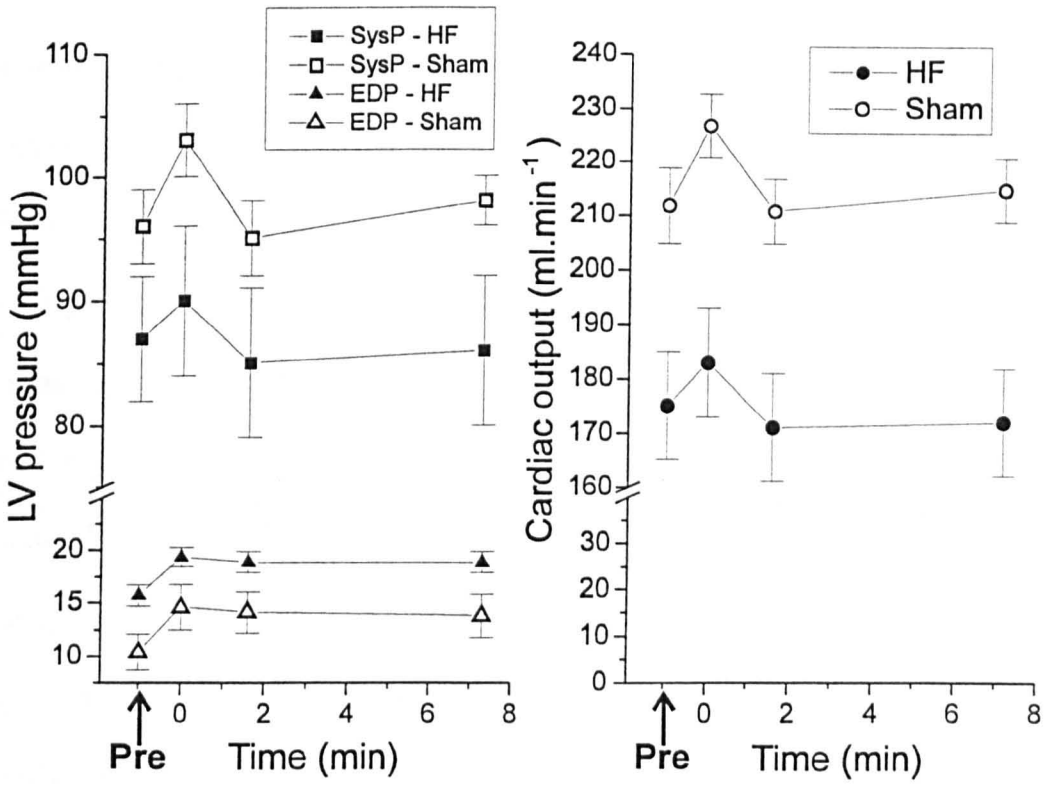

Figure 6.4 Graphical representation of the changes in left ventricular systolic pressure (SysP), end-diastolic pressure (EDP) and cardiac output in response to a step increase in pre-load from 10 cmH_2O (8 mmHg) [marked "Pre" with arrow] to 15 cmH_2O (11 mmHg) over time in 8 hearts from the heart failure group (data in closed symbols) and 8 from the sham-operated group (data in open symbols) in the working heart configuration.

Frank-Starling relationship

The inotropic response of the isolated working hearts in the heart failure group and controls were examined further by studying the Frank-Starling relationship on increasing the pre-load from 10 cmH_2O (8 mmHg) to 25 cmH_2O (18 mmHg) above the level of the aorta in 5 cmH_2O steps. The results are summarised in Table 6.5 and illustrated in Figure 6.5.

In the sham-operated group, all 8 isolated working hearts were stable when the pre-load was increased from 10 through to 20 cmH_2O (i.e. 8 to 15 mmHg). Significant periods of arrhythmia developed in 2 experiments in the sham-operated group when the pre-load was increased from 20 to 25 cmH_2O (i.e. 15 to 18 mmHg) when the hearts became unstable and the experiments had to be terminated. Thus data were available for all 8 control hearts up to 20 cmH_2O (15 mmHg) and for 6 at a pre-load of 25 cmH_2O (18 mmHg). In the heart failure group, the 8 hearts were stable when the pre-load was increased from 10 to 15 cmH_2O. Two of the 8 became unstable when the pre-load was increased from 15 to 20 cmH_2O (i.e. 11 to 15 mmHg) and another 2 of the remaining 6 developing ventricular fibrillation when the pre-load was increased to 25 cmH_2O (18 mmHg). Thus data were available for all 8 failing hearts at pre-load 10 and 15 cmH_2O (i.e. 8 and 11 mmHg), 6 of the 8 at pre-load 20 cmH_2O (15 mmHg) and 4 at 25 cmH_2O (18 mmHg). Lactate levels of the coronary effluent were checked at the various pre-load levels in 2 hearts in the heart failure group and 3 in the control group which showed no significant change with the pre-load increase.

End-diastolic pressure in both experimental groups increased with increased pre-load with the pressure being higher in the heart failure group at all pre-load levels. As observed in normal stock hearts on the working heart configuration mentioned in Chapter 5, the increase in end-diastolic pressure did not follow a linear relationship with the increase in pre-load especially at high pre-load levels. This was observed in both experimental groups. Left

ventricular systolic pressure and aortic flow increased when the pre-load was raised from 10 to 15 cmH_2O (i.e. 8 to 11 mmHg) and from 15 to 20 cmH_2O (i.e. 11 to 15 mmHg) in the sham-operated group indicating a positive inotropic response to pre-load increase as described by an ascending limb of the Frank-Starling relationship. This was not observed in the heart failure group. At the equivalent levels of pre-load increase, both haemodynamic parameters remained the same suggesting a flattened Frank-Starling curve at these pre-load levels. When the pre-load was raised from 20 to 25 cmH_2O, the left ventricular systolic pressure and aortic flow decreased in both experimental groups.

Table 6.5 Frank-Starling relationship in isolated hearts from the heart failure group (HF, n = 8) and controls (Sham, n = 8) in the working heart configuration.

After-load was kept at 75 cmH_2O (55 mmHg) with right atrial pacing at a cycle length of 300 ms. (Flow = aortic flow, SysP = peak left ventricular systolic pressure, LVEDP = left ventricular end-diastolic pressure)

	Pre-load (cmH_2O)			
	10	15	20	25
Flow ($ml.min^{-1}$)				
HF	89 ± 7	87 ± 6	87 ± 6	72 ± 1
Sham	128 ± 9	138 ± 9	139 ± 10	120 ± 5
SysP (mmHg)				
HF	87 ± 5	86 ± 6	87 ± 3	83 ± 3
Sham	96 ± 3	98 ± 2	99 ± 2	92 ± 2
LVEDP (mmHg)				
HF	15.7 ± 1.0	18.8 ± 1.0	20.1 ± 1.0	21.0 ± 1.0
Sham	10.4 ± 1.7	13.8 ± 2.0	15.9 ± 1.6	16.7 ± 1.7

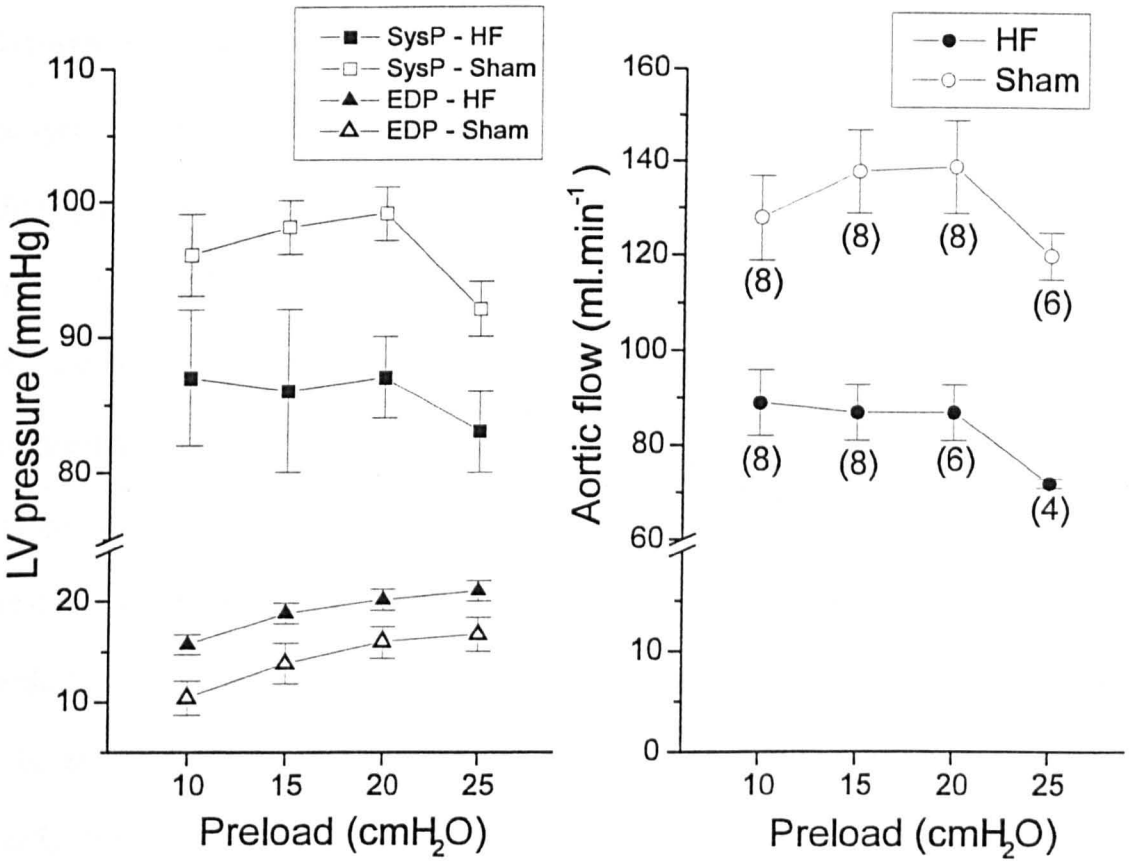

Figure 6.5 Graphical representation of the Frank-Starling relationship in 8 hearts from the heart failure group (data in closed symbols) and 8 from the sham-operated group (data in open symbols) in the working heart configuration with changes in left ventricular systolic pressure (SysP), end-diastolic pressure (EDP) and aortic flow in response to increases in pre-load from 10 cmH_2O (8 mmHg) to 25 cmH_2O (18 mmHg) in 5 cmH_2O steps. Numbers in brackets shown on the right hand panel for changes in aortic flow represent the number of hearts within each group from which data was available at each pre-load level where a steady stable state was achieved.

Correlation between *in vitro* working heart performance and *in vivo* echocardiographic measurements in heart failure

The ejection fraction (EF) measured on echocardiography in the 8 rabbits from the heart failure group was significantly lower than that measured in the 8 sham-operated controls (46 ± 3 % vs. 67 ± 1 %, $p < 0.001$). This shows that there was significant contractile dysfunction demonstrated *in vivo* in the heart failure group. Cardiac performance measurements *in vitro* in the working heart configuration were consistent with the *in vivo* findings. Under baseline working heart conditions (pre-load of 10 cmH_2O [8 mmHg] and after-load of 75 cmH_2O [55 mmHg]) at 37 °C with right atrial pacing at 300 ms cycle length, both left ventricular systolic pressure and cardiac output were significantly lower in the heart failure group than in controls (Table 6.1). Figure 6.6 shows that there was a significant correlation between *in vivo* ejection fraction and these 2 *in vitro* parameters ($r = 0.50$, $p < 0.05$ for left ventricular systolic pressure and $r = 0.62$, $p < 0.02$ for cardiac output).

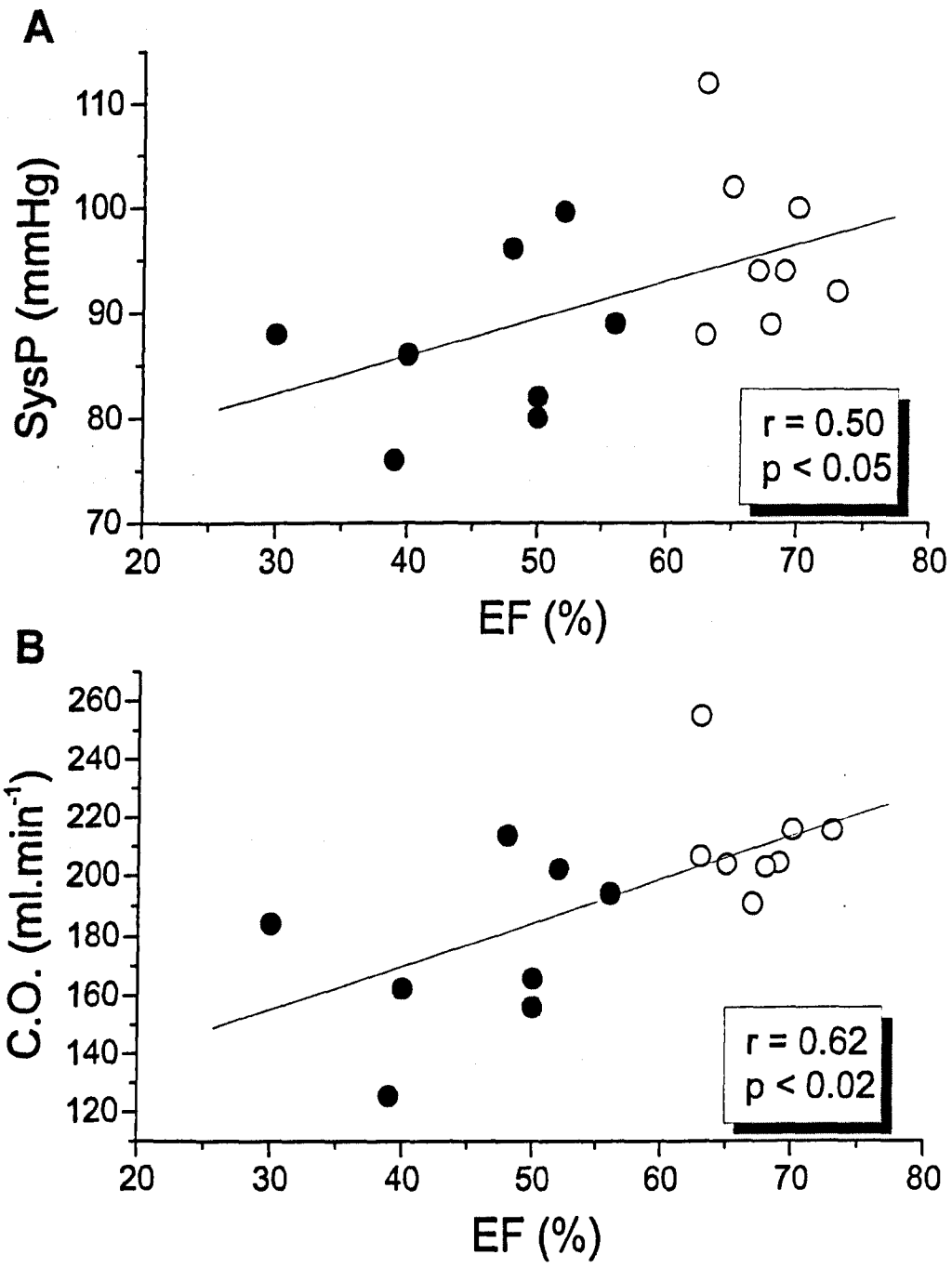

Figure 6.6 **Plot of (A) peak systolic left ventricular pressure (SysP) and (B) cardiac output (C.O.) measured *in vitro* in isolated working hearts under baseline loading conditions against *in vivo* ejection fraction (EF) from sham-operated (○) and heart failure (●) groups. The solid lines represent linear regression of the pairs of parameters with the correlation coefficients (r) and significance values (p) shown in the shaded boxes.**

Cardiac performance of Langendorff perfused hearts from rabbits with heart failure and correlation with *in vivo* measurements

The left ventricular pressure profiles of 17 Langendorff perfused hearts from the heart failure group and 13 from the sham-operated group as measured with the intraventricular balloon, adjusted to give zero end-diastolic pressure, were analysed during right atrial pacing at 350 ms and the data are summarised in Table 6.6. The peak left ventricular systolic pressure was significantly lower in the heart failure group when compared to controls (26.2 ± 3.7 mmHg vs. 49.0 ± 2.6 mmHg, $p < 0.001$). Both the maximum rate of pressure rise and the maximum rate of pressure decay were slower in failing hearts. These data again showed that there was significant systolic and diastolic dysfunction in the failing hearts demonstrated in the Langendorff perfusion mode as in the working heart configuration mentioned in previous sections. *In vivo* cardiac performance was also impaired in the failing hearts when compared to controls as shown by the significantly lower ejection fraction (41.3 ± 1.4 % vs. 73.8 ± 1.9 %, $p < 0.001$). When the *in vitro* and *in vivo* parameters were considered together, it was shown that left ventricular peak systolic pressure was significantly correlated with ejection fraction ($r = 0.73$, $p < 0.001$, see Figure 6.7).

Table 6.6 Comparison of in vitro and *in vivo* cardiac performance parameters measured in the isolated Langendorff perfused heart between rabbits with heart failure (HF) and controls (Sham).

In vitro measurements were made during right atrial pacing at 350 ms cycle length. (SysP = left ventricular peak systolic pressure, $dP.dt^{-1}_{(max)}$ = maximum rate of pressure change, EF = ejection fraction)

	HF (n = 17)	Sham (n = 13)	p value
SysP (mmHg)	26.2 ± 3.7	49.0 ± 2.6	< 0.001
$+ dP.dt^{-1}_{(max)}$ ($mmHg.ms^{-1}$)	0.50 ± 0.05	0.96 ± 0.07	< 0.001
$- dP.dt^{-1}_{(max)}$ ($mmHg.ms^{-1}$)	0.32 ± 0.04	0.66 ± 0.05	< 0.001
EF (%)	41.3 ± 1.4	73.8 ± 1.9	< 0.001

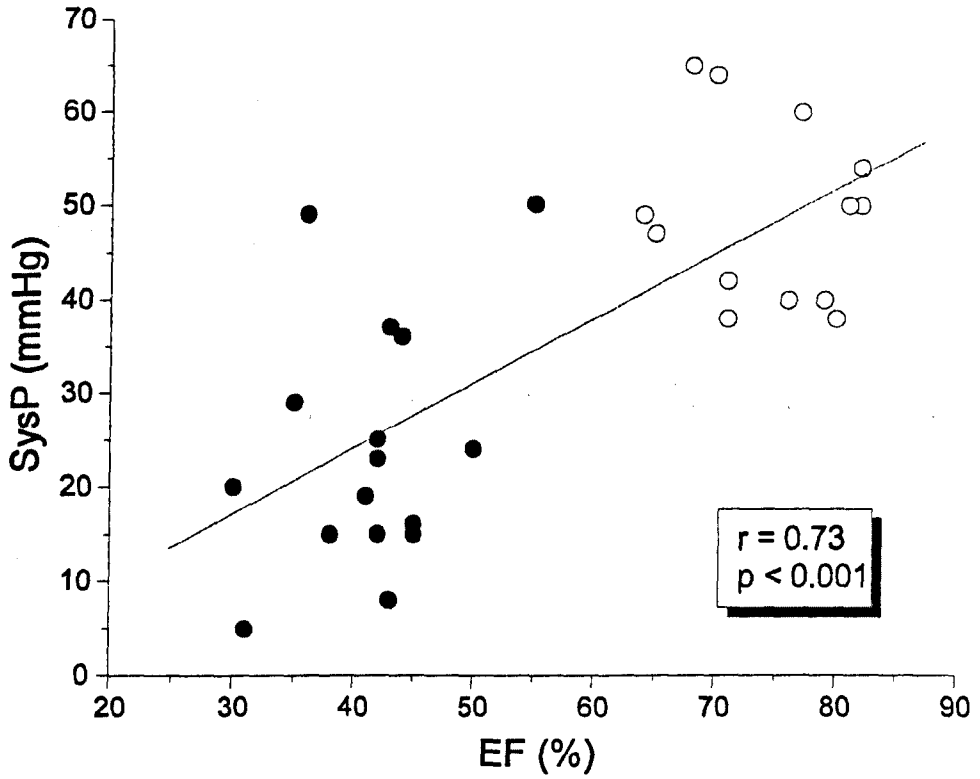

Figure 6.7 Plot of peak systolic left ventricular pressure (SysP) measured *in vitro* in isolated Langendorff perfused hearts against in vivo ejection fraction (EF) from sham-operated (○) and heart failure (●) groups. The solid line is a linear regression of the two parameters with the correlation coefficient (r) and significance value (p) shown in the shaded box.

Discussion

Significant mechanical dysfunction was demonstrated *in vitro* in the heart failure group under baseline working heart conditions. Left ventricular end-diastolic pressure was increased and peak systolic pressure and cardiac output were decreased when compared to controls. These are similar to changes seen in human heart failure. Coronary flow was not different between the heart failure group and controls suggesting that the abnormality in baseline haemodynamic parameters in the failing hearts cannot be due to a difference in coronary vascular tone.

The baseline haemodynamic parameters in the sham-operated group were comparable to those measured in normal stock hearts described in Chapter 5 apart from a higher left ventricular end-diastolic pressure in the sham-operated group. The sham-operated group had undergone thoracic surgery with a tie applied to the left ventricular apex, the pericardium opened and with the heart manipulated in the same way as the heart failure group apart from the coronary artery ligation procedure. This was done so that the changes seen in the heart failure group when compared to the sham-operated controls would only be subsequent to the effect of coronary artery ligation and the production of the myocardial infarct. The higher left ventricular end-diastolic pressure in the sham-operated group when compared to the normal stock hearts may be due to the effect of the thoracic surgery described or it could be due to a difference in age as the experiments were carried out 8 weeks after thoracic surgery in the sham-operated group (to be comparable with the 8 weeks in the coronary artery ligation group to develop heart failure) whilst those in the normal stock rabbits were carried out very close to their arrival from the suppliers. Nevertheless, comparison of the haemodynamic parameters between the heart failure and sham-operated groups showed that there was significant mechanical dysfunction in the failing hearts.

Further scrutiny of the left ventricular pressure demonstrated that the mechanical dysfunction in the heart failure group was evident at the various phases of the cardiac cycle and that there was significant systolic and diastolic dysfunction. The rate of pressure rise was slower during the isovolumic contraction phase and ejection phase when compared to controls. Rate of pressure decline was slower during the ejection phase and the isovolumic relaxation phase. Isovolumic relaxation time, which is used clinically as a measure of diastolic function, was significantly prolonged in the heart failure group.

Left ventricular diastolic compliance is determined by the level of operating pressure and the diastolic pressure-volume relation (Gaasch *et al.* 1976). The relation is curvilinear and chamber stiffness (or its reciprocal, chamber compliance) is described by this relation which is best fitted with a power law function (Mirsky, 1984). When the pressure-volume relationship was studied with a latex balloon in the K^+-arrested hearts, it was shown that the passive compliance was decreased in the failing hearts. The increased stiffness in the failing hearts would significantly impair ventricular filling during diastole. This could be the result of myocardial and non-myocardial changes. Compensatory hypertrophy of the surviving myocardium in response to increased wall stress as a result of the myocardial infarct would lead to a reduced compliance (Francis and Chu, 1994). Changes in the extracellular matrix with fibrosis would further reduce the compliance of the failing heart.

A slow response to a step increase in pre-load from 10 to 15 cmH_2O (i.e. 8 to 11 mmHg) was observed in sham-operated hearts similar to that described in Chapter 5 for normal stock hearts. There was a slow increase in cardiac output and left ventricular systolic pressure with time during phase II with the end-diastolic dimension remaining constant and the left ventricular end-diastolic pressure decreasing during that phase. These changes are consistent with a slow increase in inotropy in response to the initial increase in pre-load.

This step increase in pre-load from 10 to 15 cmH_2O (i.e. 8 to 11 mmHg) caused a similar rise in left ventricular end-diastolic pressure (about 3 mmHg) in the heart failure group as that in sham-operated hearts but produced a much smaller increase in cardiac output and left ventricular systolic pressure over time during phase II. The step increase in pre-load actually produced a small decrease in these parameters in the heart failure group at 15 cmH_2O (11 mmHg) when compared to a pre-load of 10 cmH_2O (8 mmHg). This suggests that despite an apparently adequate stimulus with the step increase in pre-load producing a corresponding increase in left ventricular end-diastolic pressure, there was a much attenuated slow response in the failing hearts.

When the Frank-Starling relationship was studied in the 2 experimental groups, it was shown that the inotropic response to pre-load increase was much attenuated in the failing hearts. The peak systolic pressure and aortic flow increased in the control group following an ascending limb of the Frank-Starling curve up to a pre-load of 20 cmH_2O (15 mmHg) whilst these parameters remained relatively constant (or with a small decrease) in the heart failure group. When pre-load was increased from 20 to 25 cmH_2O (i.e. 15 to 18 mmHg), both parameters decreased in both experimental groups similar to the response of normal stock hearts on the working heart configuration described in Chapter 5. As discussed in Chapter 5, this may be due to the relatively fast pacing rate leading to incomplete left ventricular filling during diastole, left atrial compliance with left atrial "ballooning" or it may be due to mitral regurgitation as a result of annular dilatation. The similar response in the sham-operated and heart failure groups at the high pre-load level suggested that the blunted Frank-Starling curve observed in failing hearts at a lower pre-load was not due to the fact that the failing hearts were dilated or were working at a higher end-diastolic pressure implying that they were working at a different part of the same Frank-Starling

curve as the sham-operated hearts. Rather, the results suggested that the failing hearts and the control hearts were functioning on different Frank-Starling curves due to intrinsic differences in their mechanical performance.

The results on the working heart configuration suggested that the hearts isolated from rabbits with heart failure produced by the coronary artery ligation model had significantly impaired mechanical performance with systolic and diastolic dysfunction. Passive compliance was reduced in the failing hearts and the Frank-Starling relationship was attenuated, which may be caused by the lack of a slow response to step increase in pre-load. The cellular basis for the slow response is not well understood. It has been suggested that the slow response may be mediated via cyclic AMP (Kentish *et al.* 1992). Down-regulation of β-adrenoceptors is a well-recognised feature in human heart failure (Bristow *et al.* 1982) and preliminary data from a rabbit coronary artery ligation model (Maurice *et al.* 1997) have shown decreased β-adrenoceptor density in failing rabbit hearts. One may speculate that the attenuated slow response observed in the failing hearts in the current study may be associated with changes in β-adrenoceptor activity which can directly affect cyclic AMP activity.

In vitro measurements in the Langendorff perfused hearts also showed significant systolic and diastolic dysfunction in the heart failure group. There was significant correlation between *in vivo* measurements of cardiac performance by echocardiography and *in vitro* parameters in the working heart configuration and with Langendorff perfusion. These studies suggest that the *in vitro* contractile behaviour of the isolated failing heart reflects *in vivo* contractile dysfunction in heart failure.

CHAPTER 7

$[CA^{2+}]$ MEASUREMENTS IN THE ISOLATED LANGENDORFF PERFUSED RABBIT HEART

Introduction

Different methods have been developed in measuring intracellular [Ca^{2+}] in the whole heart including the use of bioluminescent dyes, fluorescent indicators and Nuclear Magnetic Resonance (NMR) spectroscopy (Bentivegna *et al.* 1991). The use of the bioluminsecent dye, aequorin involves injection into a region of the myocardium and hence Ca^{2+} transients can only be obtained from one localised area (Kihara *et al.* 1989). NMR spectroscopy has the problem of significant buffering and not being able to detect alterations in Ca^{2+} handling on a beat-to-beat basis (Marban *et al.* 1990). Fluorescent indicators have the advantage of ester-loading via perfusion which means that [Ca^{2+}] can theoretically be measured from myocardium anywhere in the heart. The ability of fluorescent indicators to measure intracellular [Ca^{2+}] depends on its binding with free Ca^{2+} in the cytosol. Compared to the earlier indicators, the second generation dyes have lower affinity and higher quantum yield, thus requiring lower concentration of the indicators. Ca^{2+}-buffering is not a major problem and contractile function is not adversely affected. However, loading the preparations using the AM ester of the indicator is not without its problems (Table 7.1):-

(a) *unhydrolysed AM ester.* After getting into the cytosol, the AM ester may not be completely cleaved to give the Ca^{2+}-sensitive indicator. The ester is fluorescent, although not Ca^{2+}-sensitive. The presence of unhydrolysed AM ester means that part of the fluorescence collected is not due to Ca^{2+}. $MnCl_2$ quenches fluorescence due to the hydrolysed Ca^{2+}-sensitive indicator alone. By perfusing the indicator-loaded heart with $MnCl_2$ solution, Brandes *et al.* (1993b) reported that levels of unhydrolysed AM ester was negligible whilst others (Lee *et al.* 1988; Field *et al.* 1994) showed a small but significant (11 - 30 %) proportion of the fluorescence was not quenched, indicating presence of unhydrolysed AM ester. This discrepancy may be caused by different loading methods or

different concentration of indicator used. In the study by Lee *et al.* (1988), Mn^{2+}-quench studies were also performed in tissue homogenates which showed that the majority of the unhydrolysed indo-1/AM ester was associated with organelles especially mitochondria.

(b) *mitochondrial loading.* Once inside the cell, the indicator may go into organelles either unhydrolysed, giving Ca^{2+}-insensitive fluorescence or hydrolysed, giving Ca^{2+}-sensitive fluorescence that is unrelated to cytosolic [Ca^{2+}]. In the study by Lee *et al.* (1988), tissue homogenisation was used, with Mn^{2+}-quenching, to identify areas of localisation of the indicator within the cell. It was shown that 72.2 % of the total Ca^{2+}-specific fluorescence was in the cytosol, 3.6 % was in mitochondria, 3.4 % in microsomal fraction and 20.8 % in the nuclear portion. This contrasts with the findings by Field *et al.* (1994) where localisation of Fura-2 in the mitochondria was found to account for 43.9 % of the fluorescence measured from the surface of Fura-2 loaded rat hearts. Using calculations of cytosolic [Ca^{2+}] based on mitochondrial free [Ca^{2+}] (Miyata *et al.* 1991), Brandes *et al.* (1993b) inferred that mitochondrial loading of indo-1 is not a major factor. It would appear that the majority of evidence suggests that most of the Ca^{2+}-sensitive indicator is contained within the cytoplasm whilst the Ca^{2+}-insensitive AM ester is localised in intracellular organelles with the whole heart ester perfusion technique.

Table 7.1 Potential artefacts in [Ca^{2+}] measurements in the whole heart using fluorescent indicators.

Proportions of measured fluorescence that are not due to Ca^{2+}-sensitive indicator in the cytosol are shown as percentages. (Mitochon = mitochondrial)

First author	Year	Indicator	Loading Conc	Species	Unhydro-lysed AM	Mitochon hydrolysed	Endothelial
Lee	1988	Indo-1	2.5 μM	Rabbit	30 %	3.6 %	-
Lorell	1990	Indo-1	5 μM	Rabbit	-	-	portion
Brandes	1993	Indo-1	5 μM	Rat	negligible	probably low	< 18 %
Field	1994	Fura-2	3 μM	Rat	11.2 %	43.9 %	33.6 % max

(c) *Endothelial loading.* A non-myocyte contribution to the overall fluorescence can arise from the loading of fluorescent indicator into vascular endothelial cells. Bradykinin increases endothelial cell [Ca^{2+}] which triggers the release of autacoids including endothelium-derived relaxing factor and prostacyclins that promote vasodilation of underlying vascular smooth muscle. Luckhoff (1986) showed that fluorescence obtained from indo-1 loaded endothelial cells increased with the application of bradykinin. Lorell *et al.* (1990) showed the same effect when indo-1 loaded rabbit hearts were perfused with 10 μM bradykinin together with a slight fall in coronary perfusion pressure consistent with mild coronary vasodilation. This led the authors to conclude that a component of Ca^{2+}-sensitive fluorescence in the indo-1 loaded hearts is contributed by endothelial cells. Brandes *et al.* (1993b) and Field *et al.* (1994) later attempted to quantify this endothelial contribution to the overall fluorescence in rat hearts loaded with indo-1 and fura-2 respectively. There was a maximal increase of 18 % in the indo-1 fluorescence ratio with 10 μM bradykinin in the study by Brandes *et al.*, with a difference of 60 nM in the estimated systolic [Ca^{2+}] but no change in diastolic [Ca^{2+}] with and without correcting for endothelial cell loading - leading the authors to suggest that the endothelial loading may be neglected. On the other hand, Field *et al.* used 3 μM bradykinin and found that the maximal endothelial fura-2 fluorescence ratio constituted about 34 % of the maximal myocardial fura-2 ratio. Despite the potential contribution of Ca^{2+}-sensitive endothelial fluorescence to the overall myocardial fluorescence, it was shown that bradykinin did not have any effect on the time-course of the Ca^{2+} transients (Lorell *et al.* 1990; Field *et al.* 1994) as the endothelial fluorescence did not vary on a beat-to-beat basis.

The above-mentioned limitations in loading the whole heart with the fluorescent indicator in the AM ester form preclude direct translation of the measured fluorescence ratio into

myocardial cytosolic [Ca^{2+}]. Another factor which contributes to the measured fluorescence but is not related to myocardial [Ca^{2+}] is tissue autofluorescence. Fralix *et al.* (1990) have shown that this "background" fluorescence is mainly due to the reduced pyridine nucleotide, NAD(P)H and the fluorescence increases during hypoxia. All these factors will have to be taken into account and their contribution subtracted from the measured fluorescence before quantifying the myocardial [Ca^{2+}] (Brandes *et al.* 1993a). However, quantification of myocardial cytosolic [Ca^{2+}] from measured fluorescence is not easy, as there are limitations with calibration techniques and problems with determining the K_d *in vivo* (Brandes *et al.* 1993b; Bassani *et al.* 1995). Different methods have been used to determine diastolic and systolic [Ca^{2+}] in various physiological preparations but a wide range of values have been obtained (Mohabir *et al.* 1991; Wikman-Coffelt *et al.* 1991b; Brandes *et al.* 1993a; Bassani *et al.* 1995).

In addition to the above-mentioned considerations, measuring [Ca^{2+}] in the whole heart using fluorescent indicators is also difficult because of movement of the beating heart. This may cause motion artefacts in the fluorescence signals obtained and give rise to erroneous estimation of [Ca^{2+}]. The use of ratiometric dyes is an advantage, as opposed to fluorescent indicators in which the emission or excitation spectra do not shift. Motion artefacts should affect both of the emission or excitation wavelengths and the effects would be cancelled out in the ratio. It has been shown that the effect of motion artefacts on the fluorescence ratio is indeed small in indo-1 perfused hearts (Brandes *et al.* 1992; Brandes *et al.* 1993a).

This Chapter describes the use of the system developed to measure intracellular [Ca^{2+}] from the epicardial surface of isolated rabbit hearts using a single-core light guide with the fluorescent indicator indo-1. The loading technique and fluorescence measurements are characterised in both hearts from rabbits with heart failure and controls.

Methods

[Ca^{2+}] measurements were made in isolated hearts from sham-operated rabbits and from the heart failure group using indo-1. The loading procedure and the fluorescence measurement system have been described in Chapter 3. After harvesting from the sacrificed animal, the heart was perfused in a constant flow Langendorff mode. It was then perfused with indo-1 AM to load the myocardium with the Ca^{2+}-sensitive dye. Fluorescence was measured with a single-core liquid light guide used both to transmit the incident excitation light to and collect the emitted fluorescence from the left ventricular epicardial surface of the beating heart.

Indo-1 loading characteristics

The characteristics of the indo-1 loading procedure was studied in the 17 hearts from the heart failure group and 13 sham-operated controls with the light guide held at the same position (site 1, Figure 3.5) throughout the loading procedure. Fluorescence (F) was collected at wavelengths of 405 nm and 495 nm and the ratio of the fluorescence at both wavelengths (F_{405} / F_{495}) was also measured. The initial background fluorescence was measured and the increase in fluorescence due to indo-1 loading was observed by intermittently illuminating the preparation for 10 s at regular intervals during the 1 hr loading period.

Measurement of intracellular Ca^{2+} transient

After the loading procedure, the heart was perfused with normal Tyrode's solution and paced via the right atrium at a cycle length of 350 ms with the temperature being maintained at 37 °C. Fluorescence signals collected from the left ventricular epicardial surface were analysed. As mentioned in the *"Methods"* section in Chapter 6, a pacing cycle

length of 350 ms was chosen for the [Ca^{2+}] and Monophasic Action Potential measurement experiments in the Langendorff perfused hearts as opposed to 300 ms in the working heart experiments as the intrinsic heart rate of the isolated heart during Langendorff perfusion was found to be slower than in the working heart configuration. The slightly slower pacing rate with a cycle length of 350 ms (i.e. about 170 beats.min^{-1}) was still close to the physiological heart rate of the rabbit (around 180 to 200 beats.min^{-1} *in vivo*) and still ensured a constant, paced rhythm during the experiments but allowed the time course of the Ca^{2+} transients and MAP signals to be better analysed with greater resolution (see later).

Measuring fluorescence from the left ventricular epicardial surface of the beating heart with a single-core light guide was a novel technique. It was important that the character of the signals obtained be examined and that any potential artefacts be excluded so that the fluorescence signals and the ratio obtained truly reflected changes in the intracellular [Ca^{2+}] - the Ca^{2+} transient - in the region measured in the beating heart. A number of control experiments were therefore carried out for that purpose.

Depth of myocardium sampled with the single-core light guide

It is known that action potential duration is longer in sub-endocardial than sub-epicardial myocytes (Fedida and Giles, 1991). This may have a direct effect on the Ca^{2+} transient duration in sub-endocardial and sub-epicardial myocytes. Data on such difference are scarce in the rabbit but Figueredo *et al.* (1993) reported that such difference exists in the rat. If the Ca^{2+} transients from sub-endocardial myocytes were also sampled with the single-core light guide whilst recording from the left ventricular epicardial surface, this may lead to an average Ca^{2+} transient composed of characteristics of both sub-epicardial and sub-endocardial myocytes. The Ca^{2+} transient would vary in duration depending on the number

of myocytes sampled of each kind. The effect of depth of myocardium sampled with the single-core light guide on the Ca^{2+} transient signal was investigated in two ways:-

Endocardial freezing

The possibility that Ca^{2+} signals from sub-endocardial myocytes were also recorded by the single-core light guide from the epicardial surface was examined by freezing the inside of 3 normal stock hearts using a technique described by Allessie *et al.* (1989). A small glass test tube was inserted in the left ventricle of the isolated, Langendorff perfused, indo-1 loaded heart via the left atrium. The size of the glass test tube allowed firm contact with the endocardial surface of the beating heart. Liquid nitrogen was poured into the test tube via a silicone tubing connected to a funnel. The heart was continuously perfused with warm Tyrode's solution with overflow via the coronary effluent over the left ventricular epicardial surface to protect the sub-epicardial layer from damage. Fluorescence signal was obtained from the same left ventricular epicardial site during the freezing and the time course of the Ca^{2+} transient was analysed.

Varying excitation light intensity

Another way of examining the effect of depth of myocardium sampled with the single-core light guide on the Ca^{2+} transient signal was to reduce the intensity of the excitation light. With the light guide being kept on the same left ventricular epicardial site to record the Ca^{2+} transient signal, the effect of reducing the light intensity by a factor of 10 or 100 using neutral density filters was examined in 3 normal stock hearts.

Effect of altered intraventricular conduction

Fluorescence was recorded from the left ventricular epicardial surface using a light guide of 3 mm diameter. Therefore, the signal represents the average Ca^{2+} transient from cells within

an area of approximately 7 mm^2. If the activation of the myocytes within this region were not completely synchronous, the time course of the average Ca^{2+} transient may be affected by altered patterns of excitation of the myocardium. The time course of the average Ca^{2+} transient measured with the light guide may be abnormal even though the Ca^{2+} transient at the individual myocytes in the sampled region may be normal. This probability was investigated by comparing the time course of the Ca^{2+} transient obtained during atrial pacing with that obtained at the same site during direct ventricular pacing. The direct stimulation of the ventricle will generate a different excitation pattern with delay in ventricular activation when compared to atrial pacing which uses the His-Purkinje system (Rosenqvist *et al.* 1996). At the same pacing cycle length of 350 ms, the fluorescence signal obtained at one site was recorded when pacing was switched from the right atrium to the right ventricle in 8 hearts from the sham-operated group and 8 from the heart failure group.

Endothelial contribution to indo-1 fluorescence signals

Studies in isolated hearts using fluorescence dyes with acetoxymethyl ester loading via coronary perfusion (Lorell *et al.* 1990; Brandes *et al.* 1993b; Field *et al.* 1994) suggested that a substantial proportion of the fluorescence signal was due to loading of vascular endothelial cells. Bradykinin increases endothelial $[Ca^{2+}]_i$ which triggers the relaxation of vascular smooth muscle causing vasodilatation. The possibility that this vascular endothelial component of the fluorescence signal may affect the time course of the Ca^{2+} transient was examined by perfusing the heart with Tyrode's solution containing 10 μM bradykinin whilst recording the fluorescence signal from the left ventricular epicardial surface in 3 normal stock rabbit hearts.

Results

Indo-1 loading characteristics

The characteristics of the indo-1 loading procedure were examined in the 17 hearts in the heart failure group and the 13 sham-operated controls. Figure 7.1 shows the time course of the rise in fluorescence at 405 nm (F_{405}) and 495 nm (F_{495}) above background level together with the F_{405}/F_{495} signal in a typical experiment. Fluorescence started to rise around 1.5 to 2 min after perfusion with the indo-1 AM containing solution, which was the time taken for the solution to arrive at the heart. The rise in fluorescence routinely reached a plateau after about 45 min with the ratio signal reaching a steady state at the same time. Typically, indo-1 loading increased the F_{405} by 1.37 ± 0.05 times background level while an increase of 3.08 ± 0.24 times background level was seen at F_{495}. Phasic changes in the F_{405}/F_{495} ratio were discernible after 10 min loading and the signal to noise ratio improved as loading progressed. There was no change in the amplitude or slowing of the time course of the intraventricular pressure during the loading period indicating that there was no significant buffering of intracellular Ca^{2+} by indo-1.

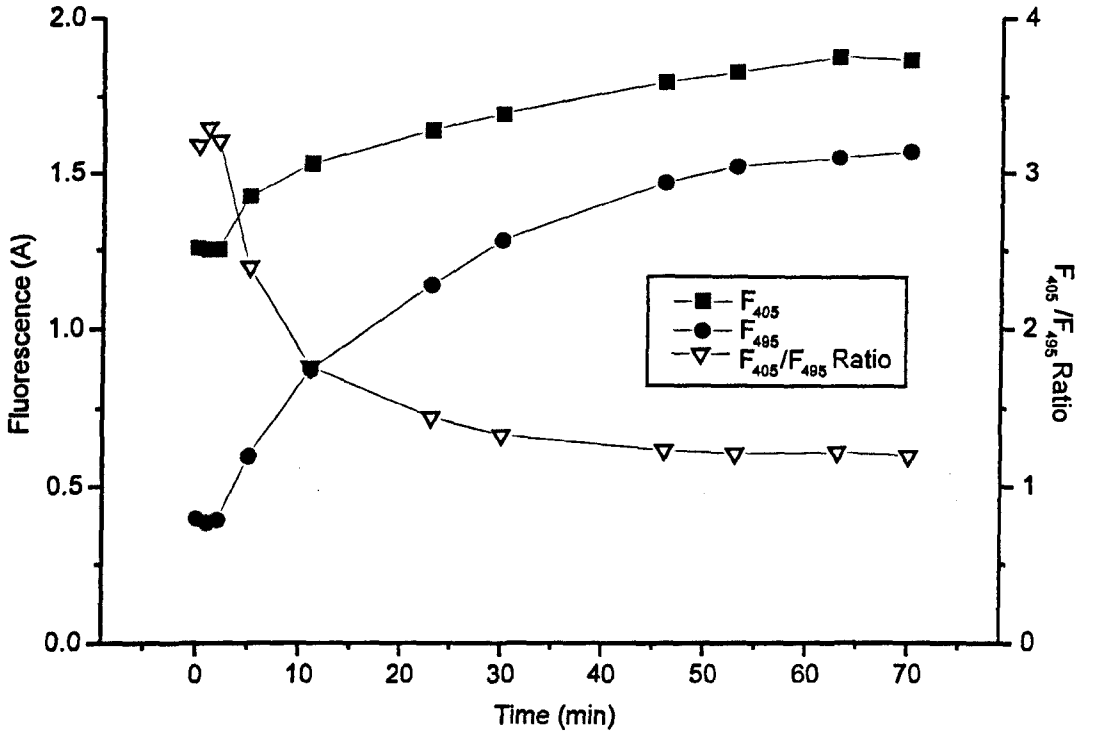

Figure 7.1 **Measurements of fluorescence at 405 nm (F_{405} - ■) and 495 nm (F_{495} - ●) expressed in terms of photomultiplier current (A) measured at one epicardial site during the perfusion of an isolated rabbit heart with Tyrode's solution containing 10 μM Indo-1 AM. Total fluorescence ratio (F_{405}/F_{495} Ratio - ▽) is also shown on the same plot (right-hand side scale).**

The fluorescence due to indo-1 loading alone could be obtained at site 1 by subtracting the background fluorescence for each wavelength to generate results illustrated in Figure 7.2. The time courses of the rise in F_{405} and F_{495} were fitted to an exponential curve and the time to half maximal fluorescence noted for individual wavelengths. As illustrated in Figure 7.2, an exponential time course describes the increase in fluorescence satisfactorily, with approximately the same half-time for each wavelength. This analysis allowed the loading characteristics of failing and sham hearts to be compared. These results are summarised in Table 7.2 and show that background fluorescence at site 1 and the extent of loading with indo-1 were similar in the 2 groups. The values for the half-times indicate that indo-1 loading occurred with a slightly faster time course in the control group when compared to failing hearts, but this difference did not reach statistical significance.

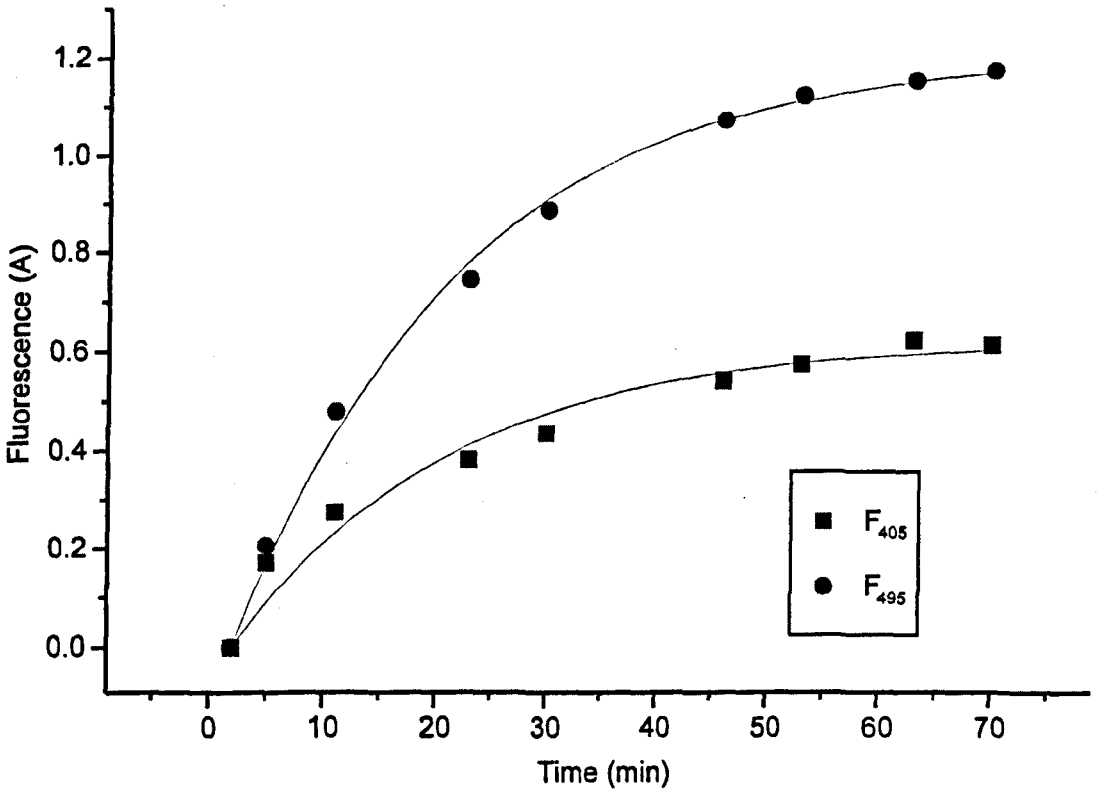

Figure 7.2 Indo-1 fluorescence expressed as photomultiplier current (A) at 405 nm (■) and 495 nm (●) obtained by subtraction of background fluorescence. Solid lines describe the best fit curves to the points using the equation $F = A * (1 - e^{-t/k})$. For fluorescence at 405 nm, A = 0.62 and k = 19.6 min; for fluorescence at 495 nm, A = 1.22 and k = 20.4 min.

Table 7.2 Comparison of Indo-1 loading characteristics between failing (HF) and control (Sham) hearts.

	Background Fluorescence (A)		Increase in Fluorescence (A)		Half-time of loading (min)	
	405 nm	495nm	405nm	495nm	405nm	495nm
HF (n = 17)	1.32 ± 0.05	0.39 ± 0.02	0.48 ± 0.09	0.77 ± 0.11	19.9 ± 2.4	16.6 ± 1.3
Sham (n = 13)	1.31 ± 0.03	0.35 ± 0.01	0.46 ± 0.08	0.74 ± 0.13	13.1± 2.4	13.1 ± 1.0
p value	NS	NS	NS	NS	0.08	0.09

Measurement of intracellular Ca^{2+} transient

Figure 7.3 illustrates the individual fluorescence signals (F_{405} and F_{495}) measured from site 1 on the surface of the left ventricle and the simultaneously recorded isovolumic pressure record in a typical experiment. The fluorescence records prior to loading with indo-1 showed no phasic changes and the fluorescence ratio was constant with a value of approximately 4. These recordings illustrate that this particular optical arrangement did not generate significant movement artefact in the fluorescence signal from the contracting myocardium below the light guide. After the loading procedure, the fluorescence of the epicardial surface had increased significantly at both wavelengths and as indicated in Fig 7.3 A, phasic signals were evident at both 405 nm and 495 nm. The value of the fluorescence ratio was now approximately 2, due to the relatively greater increase in fluorescence at 495 nm. In addition to this, the signal contained a significant phasic component as shown on an expanded scale in Figure 7.3 B. The fluorescence ratio increased rapidly to a peak and fell gradually to steady level and represents the time course of the changes of intracellular [Ca^{2+}] within the myocardium at site 1.

Conventionally, the fluorescence ratio is calculated after the subtraction of background fluorescence, and the values of maximum and minimum fluorescence ratio represent the systolic and diastolic intracellular [Ca^{2+}] respectively. However, in this study the subtraction of background fluorescence for all 15 sites was not feasible for two reasons:- (a) Precise background fluorescence measurements would have to be made at the 15 sites, either prior to indo-1 loading or after quenching the Ca^{2+}-sensitive signal at the end of the experiment. Due to the optical system used in these experiments, the magnitude of background fluorescence was approximately the same as that of the indo-1 fluorescence. Imprecise positioning of the light guide would generate errors in the estimation of

background fluorescence leading to large errors in the estimation of the indo-1 fluorescence ratio values. This was confirmed by preliminary measurements of indo-1 fluorescence ratio which showed large variations in value when comparing a number of sites over the epicardial surface of one heart or the same site over a number of individual hearts within one experimental group. (b) As shown in Figure 7.3 A, fluorescence signals at 405 nm and 495 nm consisted of small variations of photomultiplier current on top of substantial baseline values. Background subtraction at 15 sites would have to be performed off-line on digitised data. The resolution of the A / D converter (12 bit) limits the precision of the measurements of small signals on top of a large base line value and therefore substantially degrades the computed ratio signal. For these two reasons, the fluorescence ratio measurements quoted in this study represent the ratio of the total fluorescence signals provided by an analogue divider circuit. These measurements preclude comparisons of diastolic and systolic [Ca^{2+}] values across the epicardial surface. However, the time course of the transient changes in signal can be used to examine the duration of the intracellular [Ca^{2+}] signal. To illustrate the similarities in the time course of the two fluorescence ratio signals, the calculated indo-1 fluorescence ratio is plotted (as individual points) superimposed on the continuous analogue signal of total fluorescence ratio in Figure 7.3 B. It is clear that both fluorescence ratio values, although different in magnitude, have similar time courses.

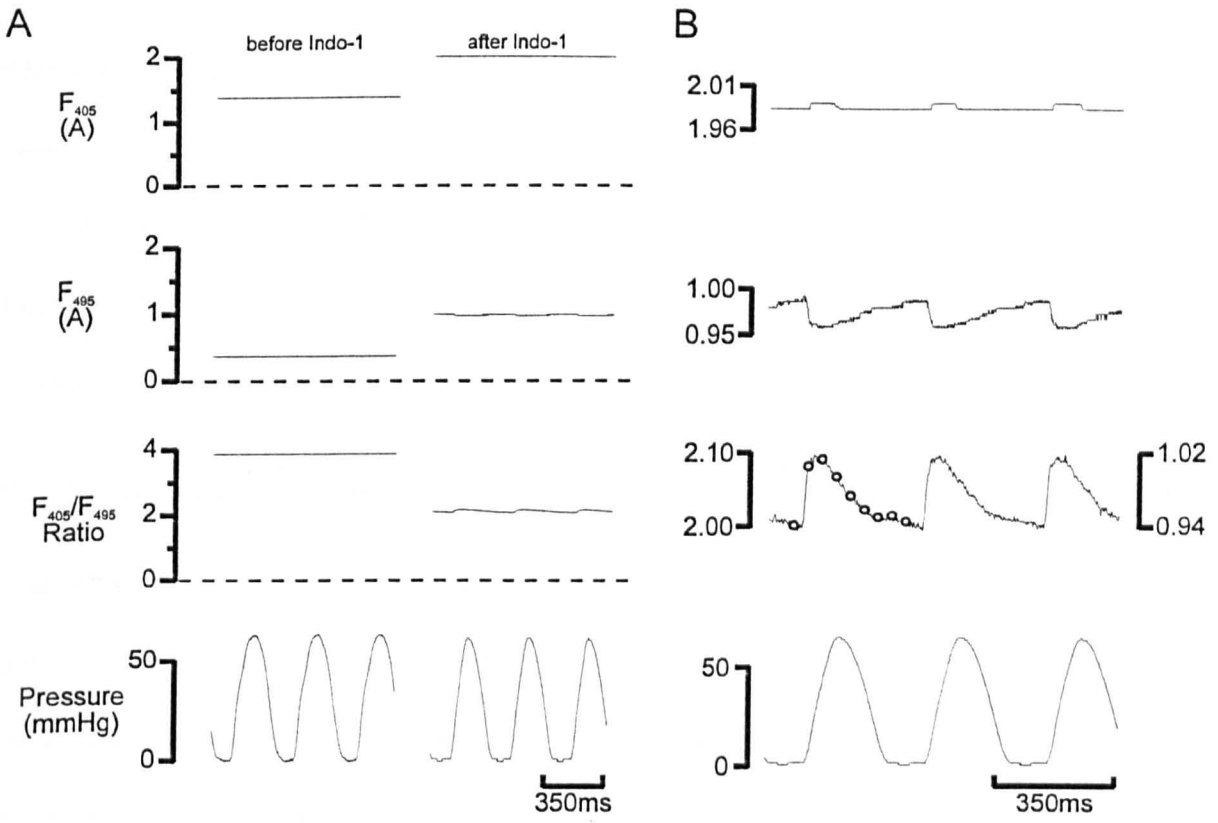

Figure 7.3 Panel A, records of fluorescence at 405 nm (F_{405}), 495 nm (F_{495}), fluorescence ratio (F_{405}/F_{495}) and left ventricular isovolumic pressure (Pressure) from an isolated Langendorff perfused rabbit heart at 37 $^{-}$C, paced via the right atrium at a cycle length of 350 ms. Records are shown before and after Indo-1 loading procedure. Each trace is an average of 30 recordings. Panel B shows sections of the above traces after Indo-1 loading on an expanded vertical and horizontal scale. The individual points (○) superimposed on the F_{405}/F_{495} Ratio record are the calculated Indo-1 fluorescence ratio values (right-hand side axis, see text).

Measurement of Ca^{2+} transient duration

The Ca^{2+} transients described here and in subsequent Chapters were averaged over 30 sweeps (equivalent of about 30 s recording) prior to analysis. The time course of the Ca^{2+} transient described in this Chapter was measured from the beginning of the upstroke of the transient to the point of 50 % decay of the signal. This was taken as the duration of the Ca^{2+} transient at the left ventricular epicardial site measured.

Depth of myocardium sampled with the single-core light guide

The depth of myocardium sampled with the single-core light guide was estimated in 3 normal stock rabbit hearts by destroying the endocardial and intramural layers of the beating, indo-1 loaded hearts with liquid nitrogen. After this procedure, only a 0.5 - 0.7 mm thick epicardial layer remained viable, as judged by the colour change in the myocardium when the left ventricle was opened and examined after the experiment. The Ca^{2+} transient signal obtained at the same left ventricular epicardial site showed no change in the amplitude or time course before and after the freezing procedure (results not shown). This suggests that the epicardial Ca^{2+} transients were recorded from a layer not more than 0.7 mm deep.

Another method was used to investigate the effect of depth of myocardium sampled by the single-core light guide on the indo-1 fluorescence signals in 3 normal stock rabbit hearts. Figure 7.4 shows the effects on fluorescence signals when the light intensity of the ultraviolet light source was reduced by a factor of 10 and 100 with neutral density filters (ND 1.0 and ND 2.0 respectively). When the light intensity of the excitation light was reduced using ND 1.0 filter, the emitted fluorescence collected at 405 nm and at 495 nm decreased. There was a greater decrease in F_{405} than in F_{495} leading to a fall in the F_{405} / F_{495}

ratio. A decrease in the amplitude of the Ca^{2+} transient was also observed in the ratio signal with no obvious change in the left ventricular pressure tracing. In addition, there was an increase in the noise to signal ratio. When the excitation light intensity was reduced using ND 2.0 filter, similar changes were observed:- (a) F_{405} and F_{495} were reduced, (b) F_{405} / F_{495} ratio decreased, (c) amplitude of the Ca^{2+} transient was smaller, (d) signal to noise ratio declined but (e) no change in the left ventricular pressure signal was observed. The time course of the Ca^{2+} transients at the different excitation light intensities were analysed and no difference was observed. Figure 7.5 shows the Ca^{2+} transient signals obtained at the 3 different excitation light intensities. When the normalised signals were superimposed, it was evident that there was no significant difference in the time course of the Ca^{2+} transients obtained at the different excitation light intensities.

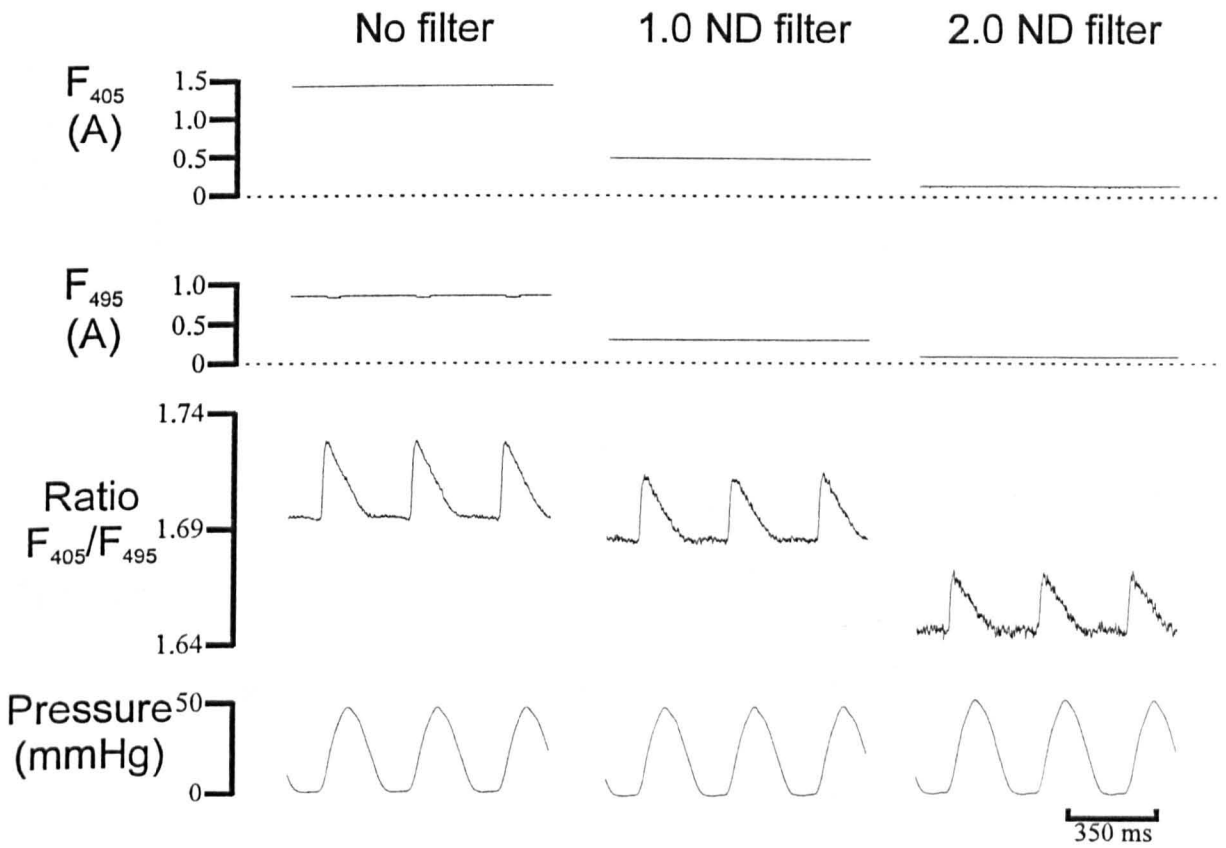

Figure 7.4 **Records of fluorescence at 405 nm (F_{405}), 495 nm (F_{495}), and fluorescence ratio (F_{405}/F_{495}) recorded at one epicardial site and left ventricular isovolumic pressure (Pressure) from an isolated Langendorff perfused rabbit heart at 37 ¯C, paced via the right atrium at a cycle length of 350 ms. Traces shown were recorded at the same epicardial site either with no neutral density filter, an ND 1.0 filter or an ND 2.0 filter in front of the excitation source.**

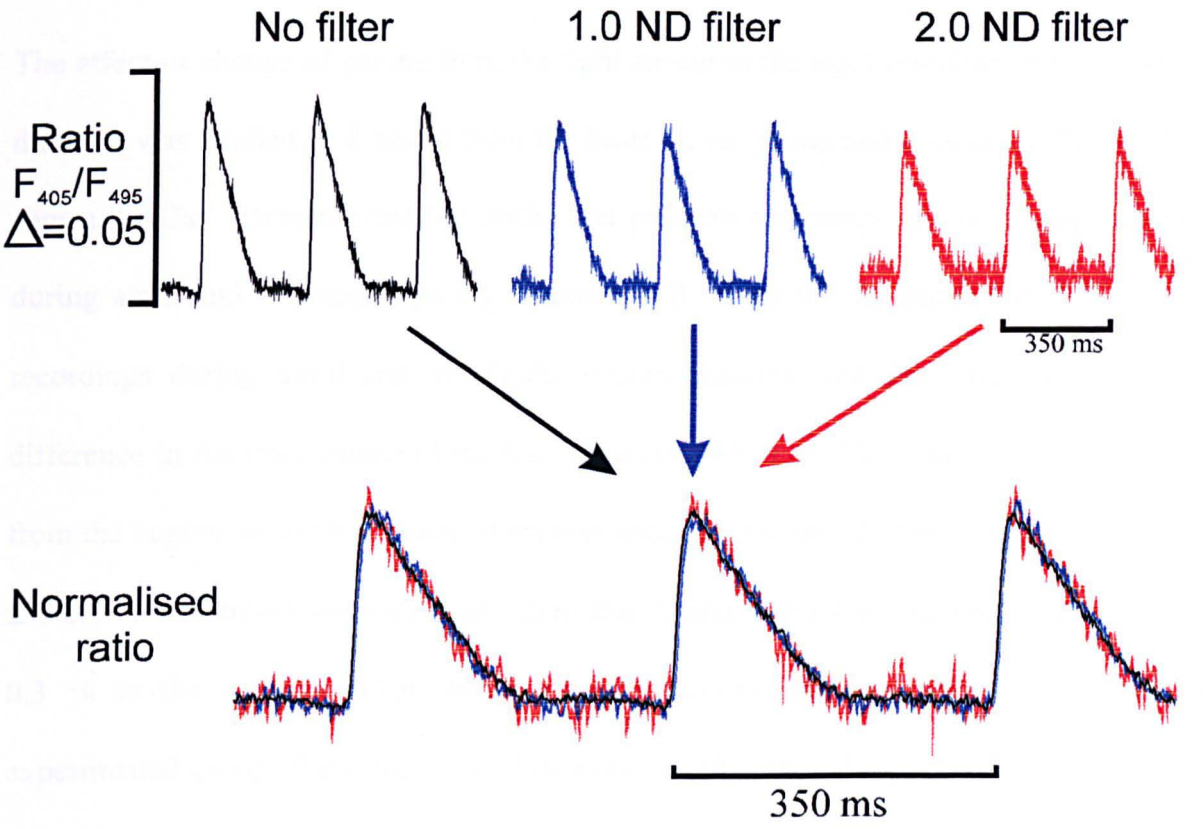

Figure 7.5 Records of fluorescence ratio (F_{405}/F_{495}) at one epicardial site from an isolated Langendorff perfused rabbit heart at 37 °C, paced via the right atrium at a cycle length of 350 ms, with different excitation light intensities - no neutral density filter, an ND 1.0 filter (data shown in blue) or an ND 2.0 filter (data shown in red) in front of the excitation source as in Figure 7.4. The Ca^{2+} transient signals obtained at the different excitation light intensities are aligned at the baseline in the upper panel and are normalised and superimposed at the bottom panel.

Effect of altered intraventricular conduction

The effect of change of pacing from the right atrium to the right ventricle on Ca^{2+} transient duration was studied in 8 hearts from the heart failure group and 8 controls. Figure 7.6 A shows the Ca^{2+} transients and left ventricular pressure recordings in a sham-operated heart during atrial and ventricular pacing. Figure 7.6 B shows the superimposed Ca^{2+} transient recordings during atrial and ventricular pacing showing that there was no significant difference in the time course of the Ca^{2+} transient. When the Ca^{2+} transient duration (time from the beginning to 50 % decay of the transient) was measured, there was a change of 0.9 ± 0.6 % on changing from atrial to ventricular pacing in the heart failure group and 0.7 ± 0.3 % in the controls. This change was not statistically significant in either of the experimental group. There was a small decrease in left ventricular peak systolic pressure on ventricular pacing. This would be discussed in greater detail in Chapter 11.

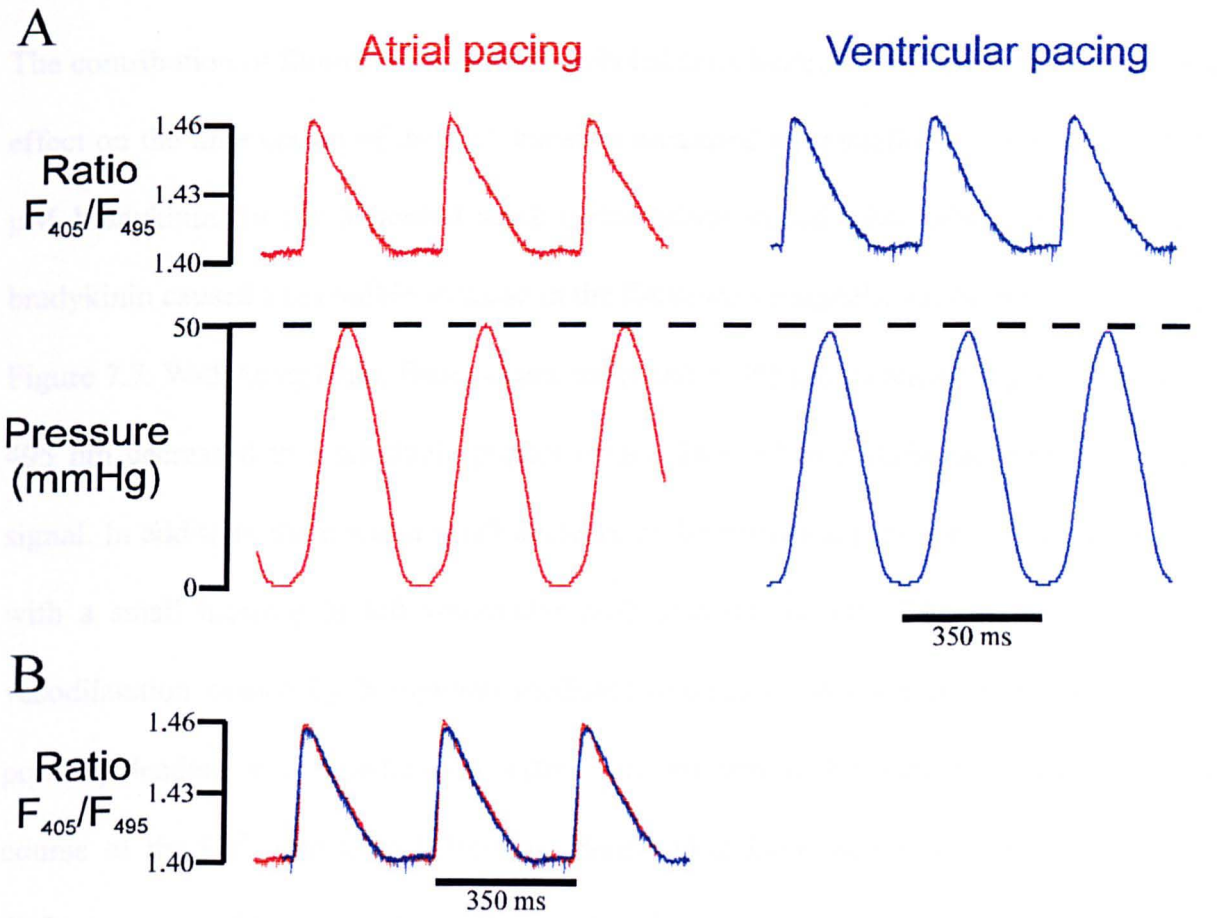

Figure 7.6 **Panel A shows fluorescence ratio records (F_{405}/F_{495}) recorded from one epicardial site and isovolumic left ventricular pressure (Pressure) in an isolated Langendorff perfused rabbit heart at 37 °C paced at a cycle length of 350 ms via electrodes either on the right atrium (data shown in red) or on the right ventricle (data shown in blue). The horizontal broken line shows the level of peak left ventricular systolic pressure during atrial pacing. Panel B shows the fluorescence ratio records superimposed.**

Endothelial contribution to indo-1 fluorescence signals

The contribution of fluorescence from endothelial cells loaded with indo-1 and the potential effect on the time course of the Ca^{2+} transient measured were studied by perfusion with 10 μM bradykinin. In the 3 normal stock rabbit hearts loaded with indo-1, perfusion with bradykinin caused a reversible increase in the fluorescence signals. An example is shown in Figure 7.7. With bradykinin, fluorescence measured at 405 nm increased slightly and that at 495 nm decreased to a relatively greater extent. This led to a slight increase in the ratio signal. In addition, there was a small decrease in the perfusion pressure signal (not shown) with a small increase in left ventricular peak systolic pressure. This is consistent with vasodilatation caused by bradykinin mediated through an increase in endothelial [Ca^{2+}], possibly leading to a "garden-hose effect" on left ventricular pressure. When the time course of the Ca^{2+} transients before and during bradykinin perfusion were analysed, no difference was observed. This is illustrated in Figure 7.7 B showing the superimposed, normalised signals.

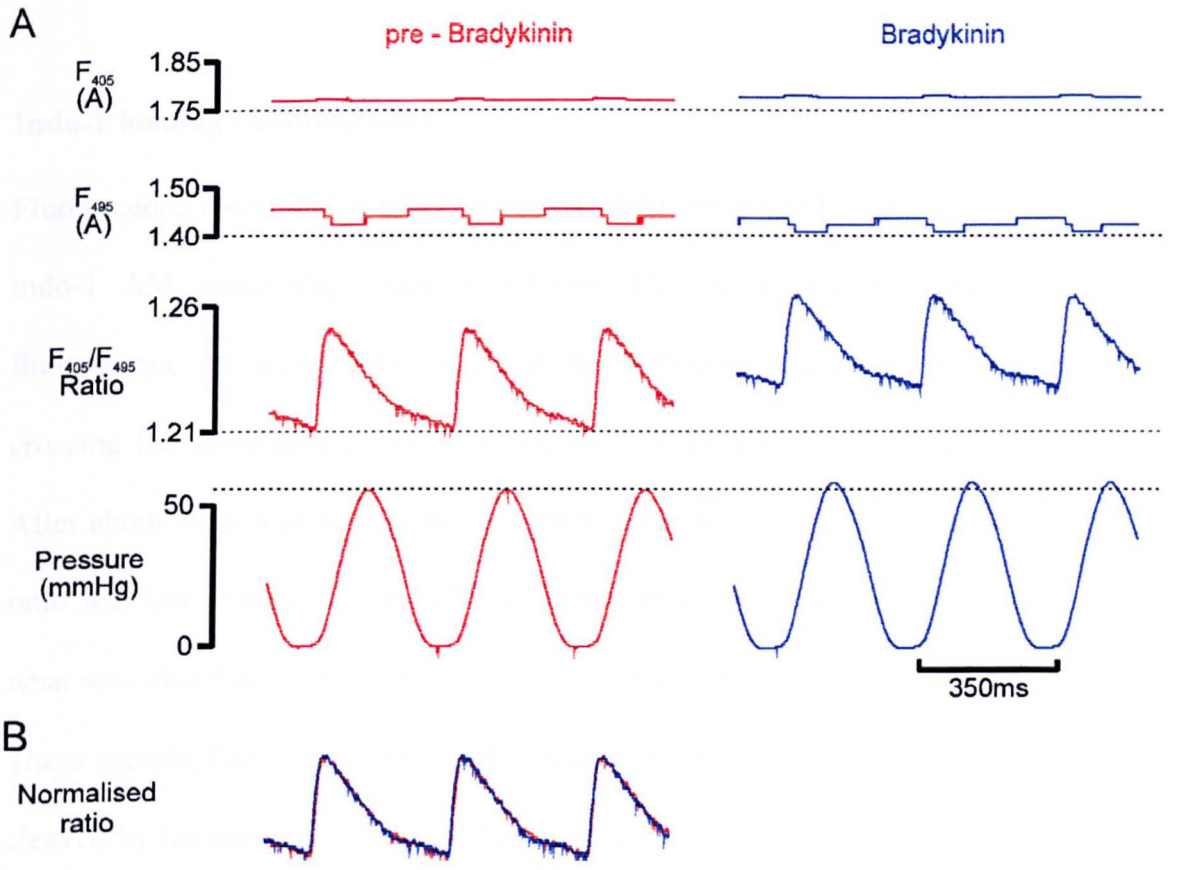

Figure 7.7 **Panel A shows fluorescence at 405 nm (F_{405}), 495 nm (F_{495}), and fluorescence ratio (F_{405}/F_{495}) recorded from one epicardial site and left ventricular isovolumic pressure (Pressure) of an isolated Langendorff perfused rabbit heart at 37 °C paced at a cycle length of 350 ms via the right atrium, before (shown in red) and during (shown in blue) perfusion with 10 μM bradykinin. Panel B shows the normalised fluorescence ratio records superimposed.**

Discussion

Indo-1 loading characteristics

Fluorescence monitored at site 1 increased while the isolated hearts were perfused with the indo-1 AM containing Tyrode's solution. The initial rise was probably due to the fluorescence of indo-1 AM, firstly in the perfusate in the coronary vasculature, then crossing the sarcolemma into the myocytes with progressive build-up inside the cytosol. After about 10 min perfusion, phasic signals were discernible. Although the signal to noise ratio was low in these first signals, the characteristics followed what one would expect and what was observed after full loading to be representative of the intracellular Ca^{2+} transient. These signals, therefore, represented signals from the Ca^{2+}-sensitive indo-1 which had been cleaved by intracellular esterases. The increase in fluorescence at both 405 nm and 495 nm followed an exponential time course and reached a plateau at around 45 min. By that time of loading, an equilibrium had been reached between the perfusate in the coronary vasculature and the cytosol. Subsequent Ca^{2+} transient measurements were made after a 15 min washout period with normal Tyrode's solution. There was no obvious decrease in the measured fluorescence after washout suggesting that at the end of the loading period, the fluorescence measured with the light guide was exclusively from intracellular indo-1. The absence of any changes in the amplitude and time course of intraventricular pressure during the loading procedure suggested that significant Ca^{2+}-buffering by indo-1 was not a feature of this loading.

With the indo-1 loading procedure described here using the single-core light guide, there was an increase in fluorescence intensity at both wavelengths by a factor of 1.4 to 3.1. This is in contrast to other studies using bifurcated light guides for measuring intracellular [Ca^{2+}]

in intact hearts using indo-1 where a much higher (up to 20-fold) increase in fluorescence intensity above original tissue autofluorescence was observed (Lee *et al.* 1987; Lorell *et al.* 1990; Mohabir *et al.* 1991). One explanation may be that the background fluorescence measured with the optical arrangement described here using a single light guide was higher than in other studies leading to a lower relative increase in fluorescence intensity with indo-1 loading. A number of preliminary experiments (n = 3) were performed using a bifurcated liquid light guide in a modified set-up using the same indo-1 loading protocol. This showed a much lower background fluorescence and a 10-15 fold increase in fluorescence intensity with indo-1 loading. Although the reason for this difference in background fluorescence obtained with the two methods is unknown, results of these experiments would suggest that the contribution of epicardial fluorescence to the background fluorescence was less using a bifurcated light guide. Despite a higher background fluorescence using a single light guide, measurements could be made in a smaller, more discrete area of myocardium and signals were less prone to movement artefacts than signals recorded using a bifurcated light guide. These features are of particular importance in the experiments described in subsequent Chapters for the measurement of fluorescence signals from multiple sites over the epicardial surface of the left ventricle.

Comparison of indo-1 loading between failing hearts and controls

Background fluorescence at both wavelengths prior to indo-1 loading were similar in both the control and heart failure groups. Fralix *et al.* (1990) showed that the majority of this tissue autofluorescence is due to intracellular metabolite, NAD(P)H. This would suggest that there was no significant difference in the resting metabolic state at the myocardium sampled with the light guide between failing hearts and controls.

The indo-1 loading characteristics were similar in the failing hearts and controls with both groups achieving the same level of fluorescence increase above background. However, the half-time in fluorescence increase in the failing hearts was slightly longer (although not statistically significant) suggesting a lower esterase activity in these hearts when compared to controls.

Measurement of intracellular Ca^{2+} transient

After indo-1 loading, the analogue ratio of the total fluorescence at 405 and 495 nm revealed phasic changes with the time course and features characteristic of the intracellular Ca^{2+} signal. While the peak systolic and diastolic values of this signal do not simply reflect systolic and diastolic [Ca^{2+}], the time course of the fluorescence change reflects the time course of intracellular [Ca^{2+}] change. This assertion was verified by calculating the indo-1 fluorescence ratio change (after background subtraction) at site 1 which followed the time course of the analogue ratio accurately. This shows that the time course of the total fluorescence ratio change is not sensitive to the level of the background fluorescence.

However, the amplitude of the calculated indo-1 fluorescence ratio was much less than expected on the basis of the indo-1 spectrum published by Grynkiewicz *et al.* (1985). There are a number of possible reasons for this:- (a) The dichroic mirror (385 nm long-pass) will reduce the fluorescence collected by the 405 nm photomultiplier. (b) The indo-1 spectrum may be shifted significantly within the myocyte (Hove-Madsen and Bers, 1992; Brandes *et al.* 1993a). (c) Several studies have shown that there is a non-cytosolic component to the Ca^{2+}-sensitive fluorescence due to loading of dye into organelles such as mitochondria and sarcoplasmic reticulum (Lee *et al.* 1988; Brandes *et al.* 1993b; Field *et al.* 1994). Miyata *et al.* (1991) showed that fluorescence from indo-1 located in mitochondria did not affect the beat-to-beat variation of the total fluorescence signal. (d) There may be a component of

unhydrolysed indo-1 AM in the signal but there is debate about the importance of its contribution to the total fluorescence (Lee *et al.* 1988; Brandes *et al.* 1993b). (e) Lorell *et al.* (1990) suggested that a substantial proportion of the fluorescence signal was due to indo-1 loading of vascular endothelial cells but this was shown not to affect the time course of the ratio signal which is consistent with the controls experiments performed in this study with bradykinin.

All the above-mentioned factors may affect the intensity of the fluorescence signals at the individual wavelengths and make the quantitation of cytosolic [Ca^{2+}] in intact hearts difficult. Different techniques (Mohabir *et al.* 1991; Wikman-Coffelt *et al.* 1991b; Brandes *et al.* 1993a) have been used which yielded different normal ranges for systolic and diastolic [Ca^{2+}]. Calibration measurements of the intracellular [Ca^{2+}] were not made in view of the potential limitations. Since it was planned to sample 15 sites over the left ventricular epicardial surface, measurement of background fluorescence prior to indo-1 loading at the exact 15 positions would be required for the quantitation of [Ca^{2+}] at all sites. The main objective was to examine the time course of the Ca^{2+} transients from different sites over the left ventricular epicardial surface rather than the absolute value of [Ca^{2+}] at each site. The factors described above which affect the intensity of the fluorescence signals and hinder the quantitation of [Ca^{2+}] have been shown not to affect the time course of the ratio signal.

There are other factors which may potentially influence the time course of the recorded fluorescence signal and these were considered in this study and are discussed below:-

(a) Conduction delay over epicardial surface. The absence of difference between the time course of Ca^{2+} transients on atrial and ventricular pacing showed that conduction delay over the epicardial surface studied with the light guide would not account for any change in Ca^{2+} transient duration.

(b) Depth of tissue sampled with light guide. Previous studies suggested that fluorescence was typically detected from within the first millimeter of the epicardium (Stewart, 1985; Turvey and Allen, 1994). Attempts were made to examine this in two ways in this study:- (i) The left ventricle of Langendorff perfused hearts were progressively frozen from the endocardial surface towards the epicardium while monitoring the epicardial Ca^{2+} transient. These measurements suggested that the majority of the signal was recorded from within 0.7 mm of the epicardial surface. (ii) As described in Figure 7.5, there was no change in the time course of the Ca^{2+} transient when the intensity of the excited light was reduced by 10- and 100-fold. Since decreasing the intensity of excitation light will lead to reduction in the layer of tissue illuminated, this procedure examines Ca^{2+} transients from differing thickness of myocardium. Despite the fact that the time course of the ratio signal was unchanged, there was a difference in the degree to which the emitted fluorescence collected at the 2 wavelengths was decreased, when the excitation light intensity was reduced. This suggests that thickness of myocardial tissue and hence the distance travelled by the emitted light may affect the intensity of individual emission wavelengths differently. This may due to different tissue absorbance of the 2 wavelengths. Nevertheless, the time course of the ratio signal appeared to be insensitive to this optical difference.

(c) Movement artefacts. The application of the 3 mm-diameter light guide to the surface of the beating heart appeared not to incur significant movement artefact in either background or indo-1 fluorescence signals. Moreover, the use of the ratio of fluorescence at the two emission wavelengths would cancel out any potential artefact (Brandes *et al.* 1992; Brandes *et al.* 1993a).

CHAPTER 8

LEFT VENTRICULAR EPICARDIAL CA^{2+} TRANSIENTS IN HEART FAILURE

Introduction

Ca^{2+} plays a central role in the excitation-contraction process in cardiac muscle. Since the development of fluorescence techniques in measuring intracellular [Ca^{2+}], researchers have been applying these to investigate the possibility that the abnormal contractile function in heart failure may be related to defects in the Ca^{2+}-handling processes. Gwathmey *et al.* (1987) used the bioluminescent indicator, aequorin, and showed that Ca^{2+} transients were prolonged in ventricular trabeculae isolated from patients with heart failure. It was also shown that Ca^{2+} transients were prolonged in myocytes from patients with heart failure later by Beuckelmann *et al.* (1992) using fura-2. However, the measurements were made at abnormally low stimulus rates (and temperatures) in these studies. In the study by Gwathmey *et al.*, the trabeculae were paced at 3 s intervals at 30 °C whilst the myocytes in the study by Beuckelmann *et al.* were paced at 0.5 Hz at 35 °C. It is difficult to extrapolate from these results to predict the behaviour of the intracellular [Ca^{2+}] and its impact on mechanical function under more physiological conditions.

Regional differences in Ca^{2+} handling in the heart have not received much attention although one early study (Saari and Johnson, 1980) reported differences in the Ca^{2+} content and uptake rate for different segments from normal rabbit hearts. A recent study (Mubagwa *et al.* 1998) suggests that the decrease in Ca^{2+} uptake is not homogeneous in the failing human heart with previous myocardial infarction. It was shown that Ca^{2+} uptake was reduced in the region close to the infarcted area as compared to regions remote from the infarct.

In this Chapter, the time course and regional characteristics of intracellular Ca^{2+} transients measured with indo-1 from the left ventricular epicardial surface of isolated hearts from rabbits with heart failure are investigated.

Methods

Isolated hearts from the heart failure (n = 17) and sham-operated groups (n = 13) were loaded with indo-1 as described in Chapters 3 and 7. Ca^{2+} transients were measured at the 15 left ventricular epicardial sites according to a map illustrated in Figure 3.5. The durations of the Ca^{2+} transients were measured and compared between 2 groups. Variation of the Ca^{2+} transient durations at different sites within each heart was analysed and this variation was also compared between the 2 groups.

Effect of altered extracellular [Ca^{2+}] on intracellular Ca^{2+} transient duration in control hearts

In a separate set of experiments, Ca^{2+} transients were monitored from the same site on the epicardial surface of 4 isolated Langendorff perfused hearts from the sham-operated group while the extracellular [Ca^{2+}] was decreased from 1.8mM to 0.8mM, or increased to 3.6 mM by perfusion with Tyrode's solution containing the different [Ca^{2+}]. The Ca^{2+} transients were recorded and the duration was measured during right atrial pacing at 350 ms cycle length and at 37°C. Intraventricular pressure was monitored throughout the experiments using a latex balloon.

Results

Figure 8.1 illustrates the range of signals measured at 15 epicardial sites from an isolated heart from the sham-operated group (panel A) and from the heart failure group (panel B). It is clear that the duration of the Ca^{2+} transient varies to a limited extent in sham-operated hearts, the shortest duration was observed at site 7, while the longest duration was observed at site 1 for the heart illustrated in Figure 8.1 A. The recordings from a heart with a significant infarct had several unusual features. Firstly, records made from within the infarct

zone showed no transient changes confirming that this region did not contain significant amounts of viable myocardium. Secondly, the remaining sites showed transient signals with a wide range of time courses, the shortest transient being recorded from site 3, while transients with a particularly long duration were obvious at sites 2 and 8 for the heart illustrated in Figure 8.1 B.

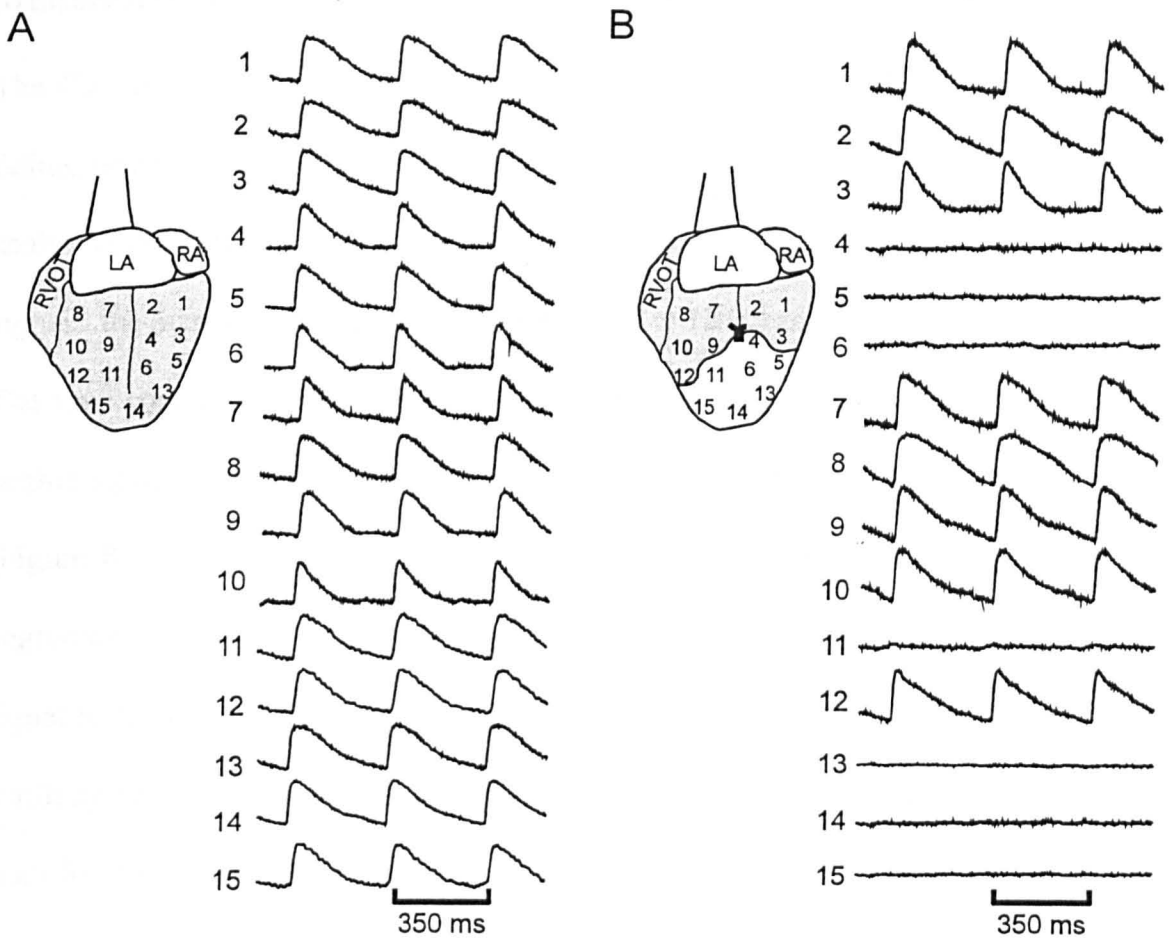

Figure 8.1 **Panel A shows a schematic diagram of an isolated rabbit heart with right ventricle outflow tract (RVOT), left atrium (LA) and right atrium (RA) marked as shown. The marginal branch of the left circumflex artery is represented by a vertical line on the left ventricle. The numbers on the left ventricle are the standard set of 15 sites from which epicardial fluorescence measurements were made. The Ca^{2+} transients recorded at each site from a sham-operated heart are shown beside the appropriate site number. Traces are the average of 30 recordings. Panel B shows parallel recordings made from a heart from the heart failure group with an apical infarct shown as a non-shaded area at the apex of the left ventricle (with the approximate position of the ligature indicated). The Ca^{2+} transients recorded at each site are shown beside the appropriate site number. Traces are the average of 30 recordings.**

Measurement of the time course of Ca^{2+} transients

The Ca^{2+} transients were analysed in all 15 sites obtained from sham-operated hearts. In failing hearts, since recordings from sites within the infarct zone gave no transient signal, analysis only included recordings from the remaining surviving myocardium with transient signals, the number of viable sites ranging from 7 to 12 (mean of 9).

The time course of the Ca^{2+} transients recorded from both groups were analysed from the beginning of the transient signals at each measured site to the various points of the signals (Figure 8.2). The upstroke of the Ca^{2+} transient was measured as the time between the beginning of the signal to 50 % of the peak. The time intervals between the beginning of the signal to the peak, to 25 % decay, to 50 % decay, to 75 % decay and to 90 % decay were similarly measured for each of the epicardial sites. A mean value was obtained from each heart for the upstroke, time to peak (CaD-Peak), time to 25 % decay (CaD-25), time to 50 % decay (CaD-50), time to 75 % decay (CaD-75) and time to 90 % decay (CaD-90). The values obtained from failing hearts were compared with those from controls and are summarised in Table 8.1 and illustrated in Figure 8.3 A. It was shown that there was no difference between the initial upstroke of the Ca^{2+} transients (time to 50 % peak) observed in heart failure and in controls (10.0 ± 0.5 ms vs. 9.5 ± 0.3 ms, p = NS). There was a significant delay in the time to peak Ca^{2+} transient in the heart failure group compared to controls with a difference of 18.9 ms between the mean values in the 2 groups. This difference increased progressively at subsequent points of the time course of the Ca^{2+} transient to 31.7 ms between the mean values in the 2 groups at time to 75 % decay. The difference at time to 90 % decay narrowed slightly to 29.6 ms between the mean values in the 2 groups, but the mean Ca^{2+} transient duration was significantly longer in failing hearts than in controls throughout the whole decay phase of the transient.

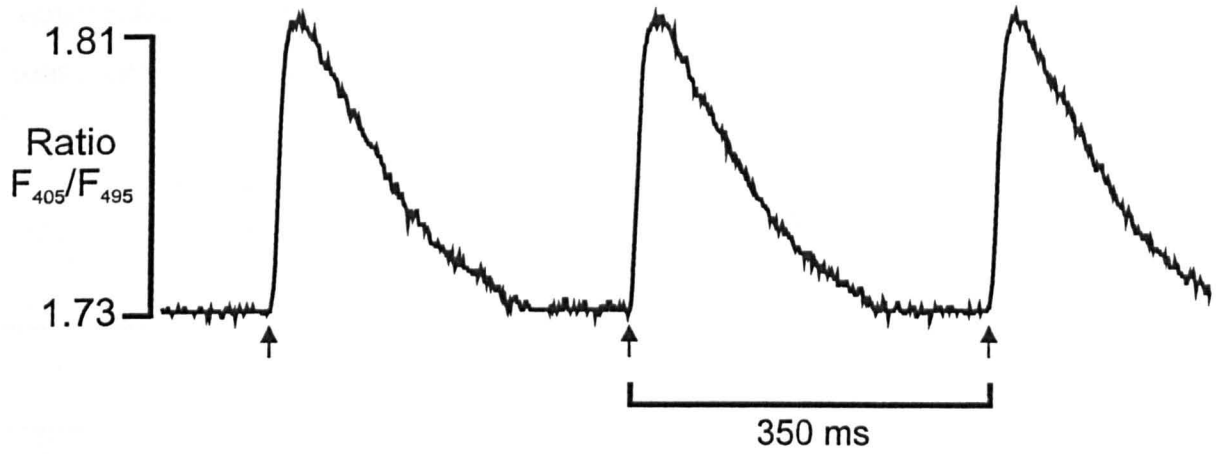

Figure 8.2 **Representative tracing of Ca^{2+} transients recorded from the left ventricular epicardial surface of an isolated Langendorff perfused heart, paced via the right atrium at 350 ms cycle length. Arrows mark the beginning of the transients, the point from where the duration of each signal was measured (see text). The trace represents an average of 30 recordings.**

Table 8.1 Comparison of the time course of Ca^{2+} transients over the left ventricular epicardial surface of isolated hearts from rabbits with heart failure (HF) and controls (Sham).

Measurements were made from the beginning of the Ca^{2+} transient signal at each measured site to the various points of the signal, at a pacing cycle length of 350 ms. The differences between the mean values obtained for the 2 groups at the various points of the Ca^{2+} transient are also shown.

	HF	Sham	p value	Difference (ms)
Time to 50 % Peak (ms) - Upstroke	10.0 ± 0.5	9.5 ± 0.3	NS	0.5
Time to Peak (ms) - CaD-Peak	50.4 ± 3.8	31.5 ± 1.2	< 0.001	18.9
Time to 25 % decay (ms) - CaD-25	107.2 ± 3.7	81.7 ± 1.8	< 0.001	25.5
Time to 50 % decay (ms) - CaD-50	156.2 ± 3.2	124.9 ± 2.6	< 0.001	31.3
Time to 75 % decay (ms) - CaD-75	213.2 ± 3.5	181.5 ± 4.4	< 0.001	31.7
Time to 90 % decay (ms) - CaD-90	268.5 ± 3.3	238.9 ± 7.0	< 0.001	29.6

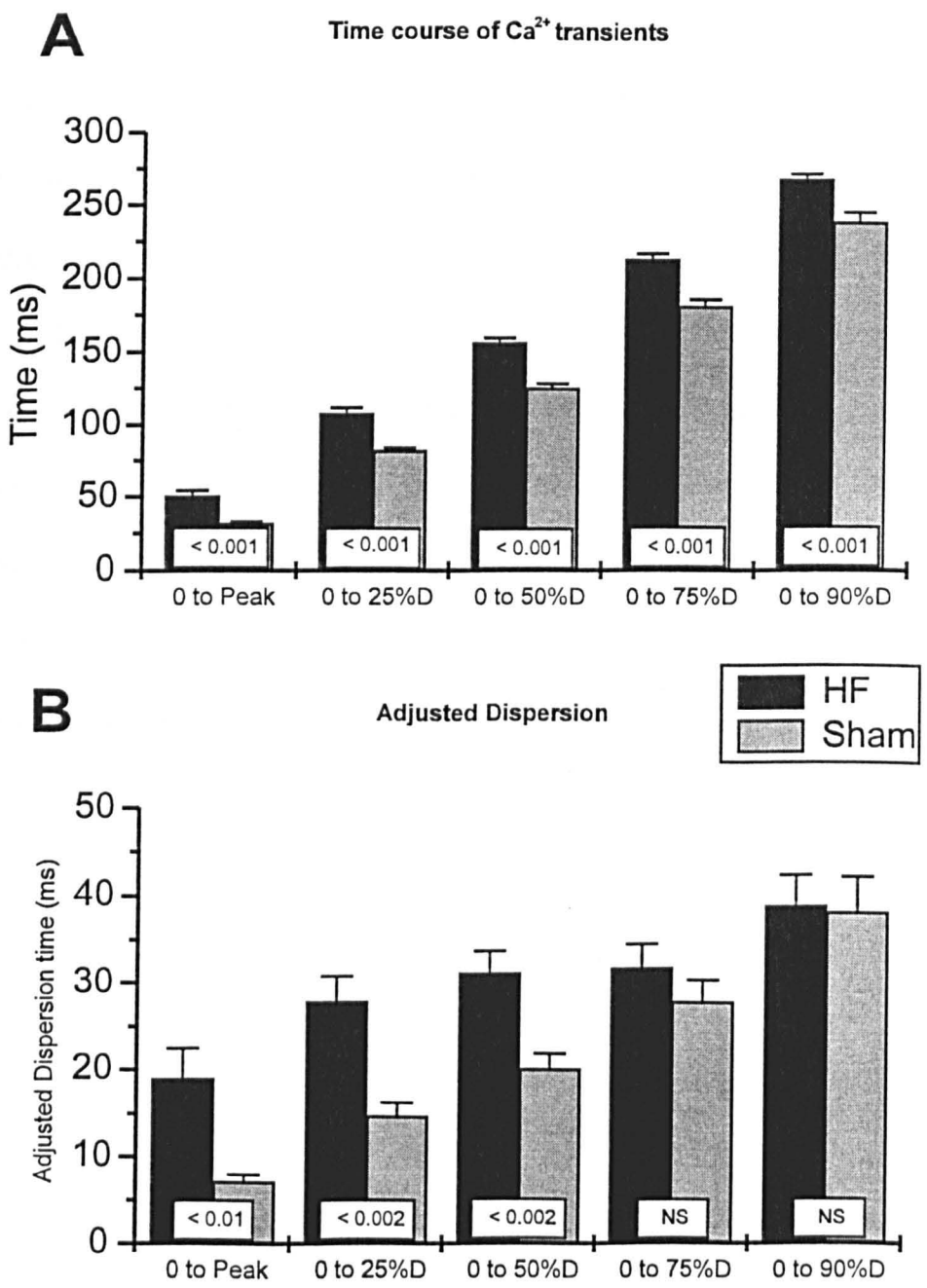

Figure 8.3 **Comparison of (A) the time course of Ca^{2+} transients and (B) adjusted dispersion time (see text) at the various points of the Ca^{2+} transient time course, over the left ventricular epicardial surface of isolated hearts from rabbits with heart failure (HF) and controls (Sham) at a cycle length of 350 ms during right atrial pacing.**

Correlation between Ca^{2+} transient duration and site location

Several methods of analysis were carried out to correlate the Ca^{2+} transient duration with the location of the site measured to see if any particular epicardial sites had consistently long or consistently short Ca^{2+} transient durations in either of the experimental groups. Ca^{2+} transient duration was measured from the beginning of the signal to 50 % decay at each measured site. The mean Ca^{2+} transient duration at each measured site for both experimental groups are shown in Table 8.2. The difference between the 2 experimental groups at each measured site in relation to the variation in Ca^{2+} transient duration will be discussed in a later section *"Dispersion of Ca^{2+} transient duration"*. The analyses described here were carried out to examine the relationship between the epicardial site and Ca^{2+} transient duration measured within each of the experimental groups.

Table 8.2 Comparison of mean Ca^{2+} transient durations (as measured by the beginning of the transient to 50 % decay) at the individual left ventricular epicardial sites in isolated hearts from rabbits with heart failure (HF) and controls (Sham).

Numbers in brackets represent the number of hearts in each group where Ca^{2+} transients were measurable at each site.

Site No.	Ca^{2+} transient duration (ms)		p value
	HF (n = 17)	Sham (n = 13)	
1	158.5 ± 8.5 (17)	134.4 ± 5.6 (13)	< 0.05
2	140.6 ± 6.4 (17)	123.1 ± 9.1 (13)	0.12
3	160.1 ± 10.7 (17)	141.3 ± 8.1 (13)	0.25
4	154.3 ± 6.6 (17)	126.9 ± 5.0 (13)	< 0.005
5	150.6 ± 14.1 (7)	125.3 ± 9.0 (13)	0.13
6	153.7 ± 7.9 (3)	128.6 ± 6.7 (13)	0.09
7	149.2 ± 9.1 (17)	119.8 ± 8.2 (13)	< 0.05
8	163.8 ± 9.9 (17)	136.3 ± 5.8 (13)	< 0.05
9	141.5 ± 8.7 (15)	114.6 ± 8.1 (13)	< 0.05
10	151.1 ± 7.3 (16)	120.3 ± 7.9 (13)	< 0.01
11	184.5 ± 9.3 (4)	125.7 ± 8.4 (13)	< 0.005
12	144.7 ± 10.1 (9)	123.2 ± 8.0 (13)	0.12
13	-	132.8 ± 11.9 (13)	N / A
14	-	129.2 ± 10.5 (13)	N / A
15	-	136.4 ± 5.2 (13)	N / A

Analysis of Variance

Single-factor Analysis of Variance (ANOVA) was carried out with the data in the sham-operated and heart failure groups. In the sham-operated group, an F statistic value of 0.81 was obtained with a non-significant p-value of 0.65 (F - critical value = 1.77 for $p < 0.05$). In the heart failure group, the F statistic value was 1.01, again giving a non-significant p-value of 0.44 (F - critical value = 1.87 for $p < 0.05$). These data suggest that there was no significant trend where a particular epicardial site had a consistently prolonged or brief Ca^{2+} transient duration in either of the experimental groups.

Multiple comparison test (Tukey test)

Single-factor ANOVA is helpful in identifying whether one particular epicardial site had Ca^{2+} transient duration different from the rest of the sites within each experimental group. In order to study the difference between pairs of measured sites, a different method has to be used. Two-sample t-tests are not appropriate as the calculated test statistic, t, and the critical values are designed to test whether the 2 samples are likely to have come from the same population and are therefore not applicable to multiple samples (measured sites). Multiple comparison tests are used for tackling such problems (Zar, 1996). A commonly-used Tukey test was employed to study the relationship between the Ca^{2+} transient duration measured at the different epicardial sites within each experimental group. It was found that the calculated statistic (q value) was below the critical value for significance in both the sham-operated and heart failure groups. This shows that, within each experimental group, there was no correlation between the epicardial site and the Ca^{2+} transient duration measured.

Layer analysis

Further regional analysis of Ca^{2+} transient variation was carried out by dividing the heart into layers according to the geographic locations of the measure sites (see Figure 3.5). Four layers were thus allocated with sites 1, 2, 7 and 8 belonging to the basal layer; sites 3, 4, 9 and 10 to the upper cavity layer; sites 5, 6, 11 and 12 to the lower cavity layer and sites 13, 14 and 15 to the apical layer. The mean Ca^{2+} transient durations for each layer in the 2 experimental groups are summarised in Table 8.3. It is shown that the mean Ca^{2+} transient duration at the basal, upper cavity and lower cavity layers were significantly longer in the heart failure group than controls. The apical layer was where there was a consistent infarct in the heart failure group and thus no measurable Ca^{2+} transients were obtained. The individual layers were compared with each other within experimental groups using the above mentioned methods for individual epicardial sites. Neither single-factor ANOVA nor multiple comparison Tukey test identified any correlation between left ventricular layer and Ca^{2+} transient duration in either of the experimental groups.

Table 8.3 Comparison of mean Ca^{2+} transient durations (as measured by the beginning of the transient to 50 % decay) at the individual left ventricular layers in isolated hearts from rabbits with heart failure (HF) and controls (Sham).

Layer	Ca^{2+} transient duration (ms)		p value
	HF (n = 17)	Sham (n = 13)	
Basal (sites 1, 2, 7, 8)	153.9 ± 4.5	128.1 ± 3.8	< 0.001
Upper cavity (sites 3, 4, 9, 10)	155.5 ± 4.3	125.0 ± 3.8	< 0.001
Lower cavity (sites 5, 6, 11, 12)	153.6 ± 7.0	125.8 ± 3.9	< 0.001
Apical (sites 13, 14, 15)	-	132.8 ± 5.3	N / A

Dispersion of Ca^{2+} transient duration

As mentioned above, there appeared to be a variation in the time course of Ca^{2+} transients obtained at the various sites within the same heart in both experimental groups and this variation appeared to be greater in failing hearts than in controls. This "dispersion" of Ca^{2+} transient duration was studied in greater detail within each experimental group and the results from the 2 groups were compared. Again, the Ca^{2+} transient duration was measured from the beginning of the signal to 50 % decay.

Site by site analysis

The mean Ca^{2+} transient duration at each measured epicardial site for the 2 experimental groups are summarised in Table 8.2. Firstly, these data showed that there was variation in the Ca^{2+} transient duration measured at different sites within the heart failure group and within the sham-operated hearts. Sites 13, 14 and 15 were within the region where there was a consistent infarct in the heart failure group and hence there was no measurable Ca^{2+} transient. When the 2 experimental groups were compared at each individual epicardial site, it was found that the Ca^{2+} transient duration was significantly prolonged at most of the left ventricular epicardial sites (1, 4, 7, 8, 9, 10 and 11) in failing hearts when compared to controls. Ca^{2+} transient duration was also more prolonged in the remaining sites in failing hearts (apart from the infarct zone) than in controls although the difference did not reach statistical significance. This suggests that in these remaining sites (2, 3, 5, 6 and 12), there were Ca^{2+} transients recorded in failing hearts which were of a similar duration as that observed in sham-operated hearts for those particular sites. If we consider the range of Ca^{2+} transient durations obtained in sham-operated hearts to be "physiological", there were some epicardial sites in the failing hearts which had Ca^{2+} transient durations within this "normal"

range and other sites that had much more prolonged Ca^{2+} transient durations. The significance of this increased variation in heart failure was studied by analysing the variation of Ca^{2+} transient duration within each heart in both experimental groups.

Heart by heart analysis - range of values, standard deviation, dispersion

The Ca^{2+} transient durations at all the measured sites within each heart were analysed. The maximum value, minimum value and standard deviation of the Ca^{2+} transient durations for each heart were obtained in the 2 experimental groups. Dispersion was measured as the difference between the maximum and minimum value in each heart. The mean value of these parameters in the heart failure and sham-operated groups are summarised in Table 8.4 and illustrated in Figure 8.4.

Figure 8.4 A uses a box and whiskers plot to compare the average standard deviation and range of the Ca^{2+} transient duration in each experimental group. This figure shows that the range of Ca^{2+} transient durations was increased in the heart failure group and this was mainly due to the higher maximum value, with a smaller increase in the minimum value when compared with the control group. The standard deviation of the Ca^{2+} transient duration in each heart was significantly increased in the heart failure group when compared to controls (29.0 ± 2.0 ms vs. 21.9 ± 1.8 ms, $p < 0.02$).

An alternative method of analysis is to measure the dispersion of the Ca^{2+} transient duration in each heart by the difference between the longest and the shortest duration. Figure 8.4 B shows that dispersion of the Ca^{2+} transient duration was significantly greater in the heart failure group.

Table 8.4 Comparison of variation in Ca^{2+} transient durations (as measured by the beginning of the transient to 50 % decay) within each heart in the heart failure group (HF) and controls (Sham). (See text for discussion)

	HF (n = 17)	Sham (n = 13)	p value
Maximum value (ms)	201.2 ± 4.0	155.0 ± 5.0	< 0.001
Minimum value (ms)	115.1 ± 5.0	90.6 ± 4.3	< 0.002
Standard deviation (ms)	29.0 ± 2.0	21.9 ± 1.8	< 0.02
Dispersion (ms)	86.1 ± 6.6	64.4 ± 5.3	< 0.05
Adjusted dispersion (ms)	31.2 ± 2.4	20.1 ± 1.8	< 0.002

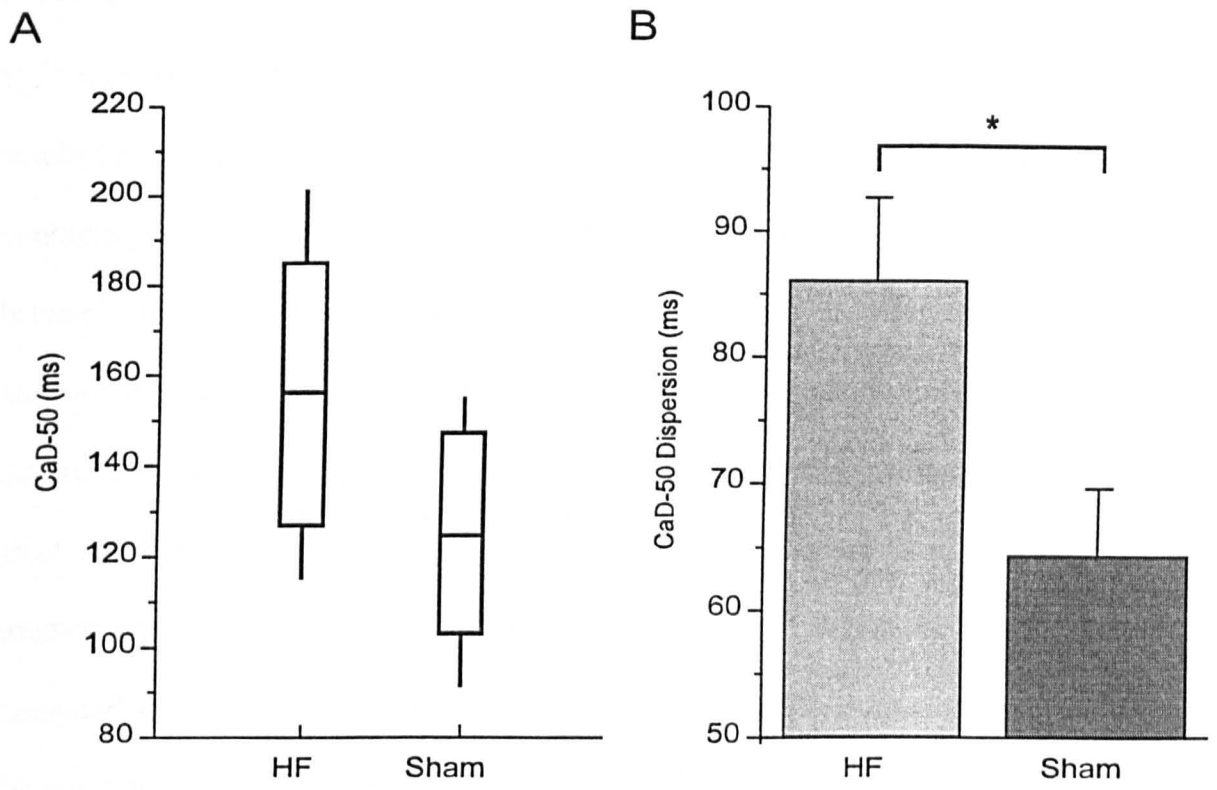

Figure 8.4 **Panel A shows a box and whiskers plot illustrating the range of Ca^{2+} transient duration values (CaD-50) measured from control (Sham) and heart failure (HF) groups. Lines denote the range of CaD-50 values, the upper and lower edges of the box denote the standard deviation, and the middle line denotes the mean value of the CaD-50. Panel B shows a histogram of the mean dispersion of Ca^{2+} transient duration (maximum CaD-50 value - minimum CaD-50 value in each heart) in both control (Sham) and heart failure (HF) groups. Error bars denote standard error. (* indicates a significant difference, $p < 0.05$)**

Adjusted dispersion of Ca^{2+} transient duration

Ca^{2+} transients could be measured from all 15 sites in the control hearts but were not available in the infarcted areas in the failing hearts. The infarcted areas could have contained a particularly long or short Ca^{2+} transient duration. Simply taking the difference between the longest and shortest measured durations in each heart could have underestimated the variation in the failing hearts although this did show a significant difference between the 2 groups. The variation of the Ca^{2+} transient duration appeared to be greater in the heart failure group despite the fact that there were fewer sites sampled. An attempt was made therefore to correct the Ca^{2+} transient dispersion for the number of measured sites in the each heart. This was done using a simple method employed clinically for correcting QT dispersion for the number of ECG leads where the QT interval can be confidently measured (Statters *et al.* 1994). In a study by Day *et al.* (1991), it was found that QT dispersion increased in proportion to the square root of the number of leads measurable and could be "adjusted" by dividing the dispersion by the square root of the number of leads measured. Using this method, adjusted dispersion of the Ca^{2+} transient duration was obtained by dividing the difference between the longest and shortest duration by the square root of the number of measured sites in each heart. It was found that the adjusted dispersion of Ca^{2+} transient duration (measured at 50 % decay) was significantly increased in the heart failure group when compared to controls (31.2 ± 2.4 ms vs. 20.1 ± 1.8 ms, $p < 0.002$, Table 8.4).

As mentioned above, Ca^{2+} transient duration was measured at other points of the time course of the Ca^{2+} transients. The mean duration at the various points during the time course of the Ca^{2+} transients are summarised in Table 8.1 and Figure 8.3 illustrates the comparison between the 2 groups with regard to the mean duration and the adjusted dispersion of the

duration at the various points during the time course of the transients. It shows that the mean Ca^{2+} transient duration in the heart failure group was significantly prolonged at all points during the decay phase of the time course of the Ca^{2+} transient when compared to controls. Adjusted dispersion of the Ca^{2+} transient duration was also increased in the heart failure group when the Ca^{2+} transients were compared at the peak, 25 % - and 50 % - decay of the transients (see Figure 8.3 B). This difference became non-significant during the later part of the cardiac cycle at 75 % - and 90 % - decay of the Ca^{2+} transient signal. This may be due to the fact that the hearts were paced at a near-physiological cycle length of 350 ms; any difference in the terminal part of the Ca^{2+} transient would be difficult to resolve when the transients from different parts of the heart would have decayed to near-diastolic levels. The significant differences in adjusted dispersion of the Ca^{2+} transient duration at the peak, 25 % - and 50 % - decay of the transients between the 2 groups suggest that there was increased variation in the Ca^{2+} transient duration in the heart failure group.

Effect of altered extracellular [Ca^{2+}] on intracellular Ca^{2+} transient duration in control hearts

The effects of altered extracellular [Ca^{2+}] on intracellular Ca^{2+} transient and intraventricular pressure were studied in 4 sham-operated hearts. Extracellular [Ca^{2+}] was decreased from 1.8mM to 0.8mM, and increased to 3.6 mM with the hearts being paced at 350 ms cycle length from the right atrium. The steady state Ca^{2+} transients are shown in Figure 8.5 for one of the experiments. Lowering the extracellular [Ca^{2+}] reduced both the peak systolic and end-diastolic fluorescence ratio. However the duration of the Ca^{2+} transient was prolonged when compared to that measured in normal extracellular [Ca^{2+}]. Conversely, raising extracellular [Ca^{2+}] increased the peak systolic and end-diastolic fluorescence ratio, while the duration of the Ca^{2+} transient was shorter than normal. The results are summarised in

Table 8.5 accompanied by the mean peak systolic pressure and maximum rate of pressure decay. The intraventricular pressure profile of the isolated Langendorff perfused hearts from the heart failure group and the sham-operated group are summarised again in Table 8.6 together with the mean Ca^{2+} transient durations in the 2 groups as measured by the CaD-50 for comparison.

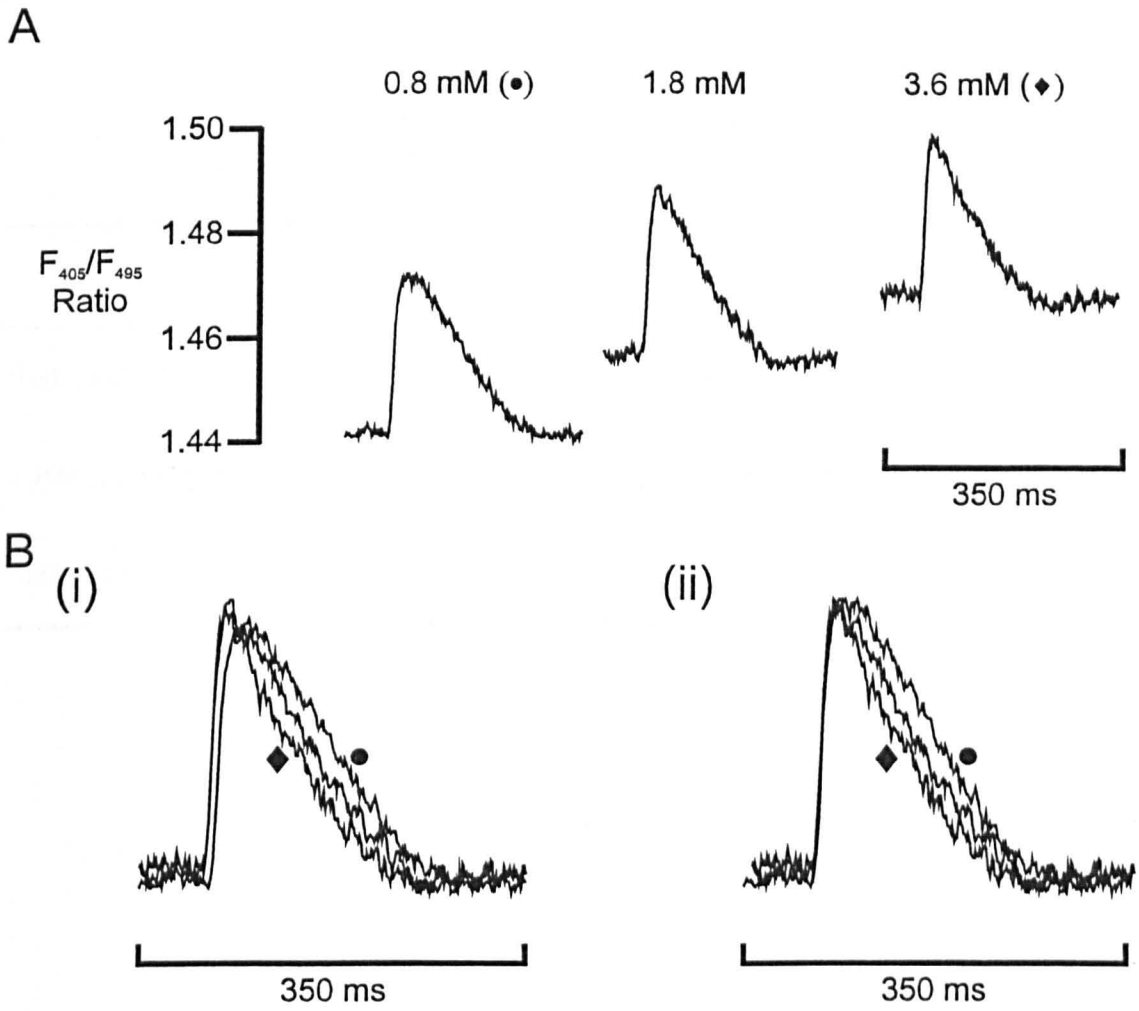

Figure 8.5 **Panel A shows records of fluorescence ratio (F_{405}/F_{495}) from one site on the epicardial surface of an isolated Langendorff perfused rabbit heart from the control group during right atrial pacing at a cycle length of 350 ms. Traces represent the average of 30 records sampled in the presence of 0.8 mM (●), 1.8 mM (normal) and 3.6 mM (◆) extracellular [Ca^{2+}]. Panel B shows (i) the traces superimposed on a common baseline and (ii) normalised traces superimposed and aligned at the upstroke.**

Table 8.5 Effect of altered extracellular [Ca^{2+}] on peak systolic pressure, maximum rate of pressure decay and Ca^{2+} transient duration in 4 isolated sham-operated hearts.

(SysP = left ventricular peak systolic pressure, $-dP.dt^{-1}_{(max)}$ = maximum rate of pressure decay, CaD-50 = mean Ca^{2+} transient duration measured from the beginning of the transient to 50 % decay)

	0.8 mM [Ca^{2+}]	1.8 mM [Ca^{2+}]	3.6 mM [Ca^{2+}]
SysP (mmHg)	28.3 ± 2.1	42.6 ± 2.2	54.5 ± 1.3
$-dP.dt^{-1}_{(max)}$ ($mmHg.ms^{-1}$)	0.32 ± 0.04	0.55 ± 0.05	0.64 ± 0.04
CaD-50 (ms)	139.5 ± 8.8	126.0 ± 9.5	109.0 ± 9.6

Table 8.6 Comparison of left ventricular pressure profile and mean Ca^{2+} transient duration in the isolated Langendorff perfused heart between rabbits with heart failure (HF) and controls (Sham).

(SysP = left ventricular peak systolic pressure, $dP.dt^{-1}_{(max)}$ = maximum rate of pressure change, CaD-50 = mean Ca^{2+} transient duration as measured by the beginning of the transient to 50 % decay)

	HF (n = 17)	Sham (n = 13)	p value
SysP (mmHg)	26.2 ± 3.7	49.0 ± 2.6	< 0.001
$-dP.dt^{-1}_{(max)}$ ($mmHg.ms^{-1}$)	0.32 ± 0.04	0.66 ± 0.05	< 0.001
CaD-50 (ms)	156.2 ± 3.2	124.9 ± 2.6	< 0.001

Discussion

Prolonged Ca^{2+} transient duration in failing hearts

It was shown in this Chapter that Ca^{2+} transients recorded from the left ventricular epicardial surface of hearts from rabbits with heart failure had a significantly more prolonged time course than those obtained from the sham-operated group. There was no significant difference in the initial upstroke of the Ca^{2+} transient (time to 50 % peak) between the 2 groups. However, the mean value of the time to peak Ca^{2+} transient was more prolonged in the failing hearts than in controls. There is therefore a longer delay for the Ca^{2+} transient to rise from 50 % peak to its peak level in the failing hearts. This can result either from a decrease in sarcoplasmic reticulum (SR) Ca^{2+} release in the failing hearts (with a slow rise to peak [Ca^{2+}]) or from an increase in SR Ca^{2+}-reuptake (attempting to restore cytosolic [Ca^{2+}] to baseline before the Ca^{2+} transient has reached its peak). An increase in SR Ca^{2+}-reuptake in the failing hearts is unlikely when the rest of the Ca^{2+} transient time course was analysed in the 2 groups. In fact, a *decrease* in SR Ca^{2+}-reuptake is suggested by the fact that there was a progressive delay in the Ca^{2+} transient duration throughout the decay phase of the Ca^{2+} transient (up to 90 % decay) in the heart failure group when compared to controls (Table 8.1). If there was no difference in SR Ca^{2+} reuptake between the 2 groups, one would expect that the difference in the time to peak Ca^{2+} transient between the 2 groups be maintained throughout the decay phase of the transient. The progressive increase in the difference in the mean values between the 2 groups at the various time points throughout the decay phase (up to 90 % decay) suggests that SR Ca^{2+} reuptake is reduced in the failing hearts compared to controls. The slightly smaller difference between the 2 groups at 90 % decay may be due to the fact that the hearts were paced rather fast at a cycle length

of 350 ms and the Ca^{2+} transients were returning to diastolic levels at that point before the next cardiac cycle. These results suggest that possibly both SR Ca^{2+}-release and SR Ca^{2+}-reuptake are reduced in the heart failure group when compared to controls.

Regional variation in the time course of Ca^{2+} transients

In addition to a prolongation in Ca^{2+} transient durations in the failing hearts, it was also shown in this Chapter that there was increased variation of the Ca^{2+} transient durations within each heart in the heart failure group when compared to controls.

Individual hearts from the sham-operated control group exhibited Ca^{2+} transients with a limited range of durations. The cause of this variation is unknown, regional differences in excitation pattern are not thought to be a factor since Ca^{2+} transients of identical time course were obtained on atrial or ventricular stimulation at the same site recorded with the single light guide. A physiological dispersion of repolarisation is recognised (Brutsaert, 1987) and this may be related to the regional variation in Ca^{2+} transient duration observed in the control hearts. Variation in Ca^{2+} transient durations was also observed within failing hearts but this variation was greater in magnitude than in controls.

There was no consistent relationship between site position and the Ca^{2+} transient duration in either of the experimental groups. No difference was observed when the Ca^{2+} transients obtained from the basal portion of the left ventricle were compared with those from the apex. Some studies have suggested an apex to base difference in cardiac action potential duration (Cohen *et al.* 1976; Watanabe *et al.* 1983). Action potential duration can be affected by mechanical load as a result of mechano-electric feedback (Lab, 1982). It is conceivable that difference in action potential duration between different regions of the heart may be the result of differences in wall tension although it may also be due to differences in intrinsic properties of the myocytes in those regions. Regional differences in

Ca^{2+} handling in the heart have not been fully investigated although one early study (Saari and Johnson, 1980) reported differences in the Ca^{2+} content and uptake rate for different heart segments. Muscle length changes have been shown to affect Ca^{2+} transient duration (Allen and Kurihara, 1982; Allen *et al.* 1988). Differences in regional wall tension in the whole heart can result in different resting sarcomere lengths and different muscle length changes during the cardiac cycle, giving rise to different Ca^{2+} transient durations at various regions of the heart even if the different regions have similar intrinsic properties. In addition, electrical heterogeneity would directly affect Ca^{2+} homeostasis and hence Ca^{2+} transient durations. Mechanical changes which affect the action potential may also cause similar effects on Ca^{2+} handling (Lab *et al.* 1984).

Regional wall tension was not assessed in the experiments described. Another reservation of this study is that the hearts were perfused in the Langendorff mode. The performance of the beating heart is quite different when it is perfused in the Langendorff mode from during anterograde perfusion in the working heart configuration or *in vivo*. Thus the regional wall tension in the Langendorff perfused heart may not represent the conditions *in vivo*. An effort was made to compare the 2 experimental groups at similar loading conditions, i.e. similar sarcomere lengths by inflating the intraventricular balloons to give zero end-diastolic pressure in each heart. Although this cannot ensure that the regional wall tension is similar to the situation *in vivo* or when the heart is ejecting isotonically, the difference in Ca^{2+} transients observed between the heart failure group and the sham-operated group is not due to different loading conditions.

Dispersion of Ca^{2+} transient duration

Further scrutiny of Ca^{2+} signals from the heart failure group reveals that the longer mean duration was a result of abnormally prolonged Ca^{2+} transients in a number of sites in each

heart. Despite recordings being available from fewer sites due to the presence of an apical infarct when compared to controls, the variation of Ca^{2+} transient duration was greater in each heart from the heart failure group. This is obvious from measurements of the range of values (Figure 8.4 A) or from the measure of the dispersion of Ca^{2+} transient duration (Figure 8.4 B). This was also true when the dispersion of Ca^{2+} transient duration was adjusted for the number of sites measured (Table 8.4). Therefore, changes in the myocardium in this model of heart failure in the rabbit appear heterogeneous. Some regions showed pronounced prolongation of the Ca^{2+} transient while the duration of the transients in others were close to normal. As with the normal myocardium in control hearts, there appeared to be no consistent relationship between site position and the duration of the Ca^{2+} transient. In particular, prolonged Ca^{2+} transients were not specifically located at the border between normal and infarcted myocardium suggesting that the remodelling process in heart failure may be a heterogeneous one. A recent study (Mubagwa *et al.* 1998) also suggests that the abnormality in Ca^{2+} handling is not homogeneous in the failing heart with previous myocardial infarct, but it was reported that Ca^{2+} uptake was reduced in the surviving myocardium close to the infarcted area as compared to regions remote from the infarct.

Systolic dysfunction and Ca^{2+} handling

The smaller systolic pressures observed in failing hearts were naturally associated with slower maximum rates of relaxation (see Table 8.6). The limitations of the optical techniques used to measure Ca^{2+} transients prevented the systolic and diastolic intracellular $[Ca^{2+}]$ being measured as discussed in Chapter 7 but it would not be unreasonable to assume that the slower rates of decay of the Ca^{2+} transients in failure hearts were accompanied by a reduced peak systolic $[Ca^{2+}]$. A number of investigators have demonstrated a reduced peak systolic $[Ca^{2+}]$ in isolated myocardial preparations or myocytes from failing hearts

(Beuckelmann *et al.* 1992; Capasso *et al.* 1993). These studies also demonstrated a marked prolongation of the Ca^{2+} transient. Changes in Ca^{2+} transient duration as a result of inotropic changes have been extensively studied in multicellular (Allen and Kurihara, 1980; Endoh and Blinks, 1988) and single cell preparations (Frampton *et al.* 1991; Bers and Berlin, 1995). It was found that the rate of $[Ca^{2+}]$ decline during diastole in cardiac myocytes depends on peak systolic $[Ca^{2+}]$ with a low systolic $[Ca^{2+}]$ being associated with a slowed diastolic $[Ca^{2+}]$ decline. The basis for the effect on time course is thought to be a slowed rate of Ca^{2+} uptake by the sarcoplasmic reticulum.

The possibility that prolongation of Ca^{2+} transient duration observed in failing hearts was a result of reduced peak systolic $[Ca^{2+}]$ was studied by examining the effect of altering the extracellular $[Ca^{2+}]$ on the Ca^{2+} transient duration in the control hearts. When the reduced peak systolic force was mimicked in control hearts by reducing the extracellular $[Ca^{2+}]$ to 0.8 mM, this was accompanied by a prolongation of the Ca^{2+} transient measured at one site on the epicardial surface. In contrast to this, increasing extracellular $[Ca^{2+}]$ to 3.6 mM caused an increased peak systolic pressure and a shortening of the duration of the Ca^{2+} transient. The contractile performance of control hearts perfused with 0.8 mM extracellular Ca^{2+} appeared to be very similar to the average contractile performance of the heart failure group in terms of peak systolic pressure and maximum rate of pressure decay. However, the Ca^{2+} transient duration under conditions of low extracellular $[Ca^{2+}]$ in control hearts was not prolonged to the same extent as that seen in heart failure (see Tables 8.5 & 8.6). The fact that the measurement of Ca^{2+} transient was performed at only one site, weakens this comparison but it would be expected that the effects of lowering extracellular $[Ca^{2+}]$ would have uniform effects on the intracellular $[Ca^{2+}]$ across the ventricle. These results suggest

that the abnormally long Ca^{2+} transients observed in heart failure may be partly explained by a reduced peak systolic intracellular [Ca^{2+}].

The trigger for sarcoplasmic reticulum Ca^{2+} release, namely Ca^{2+} entry via the voltage-sensitive L-type channels is believed to be unchanged in heart failure by many investigators (Beuckelmann *et al.* 1991; Mewes and Ravens, 1994; Kaab *et al.* 1996; Qiu *et al.* 1996; Rozanski *et al.* 1997) although there are reports to the contrary (Rossner, 1991; Hatem *et al.* 1994; Ming *et al.* 1994). In the absence of altered Ca^{2+} trigger influx, a reduced systolic [Ca^{2+}] would result from abnormality of the sarcoplasmic reticulum Ca^{2+} release mechanism. There are reports that the expression, level and function of the sarcoplasmic reticulum Ca^{2+}-release channel are decreased in heart failure (Brillantes *et al.* 1992; D'Agnolo *et al.* 1992; Arai *et al.* 1993; Lachnit *et al.* 1994; Go *et al.* 1995) although these results are not universal (Finkel *et al.* 1992; Sapp and Howlett, 1994; Meyer *et al.* 1995). There is also recent evidence (Gomez *et al.* 1997) that the architectural coupling of the sarcolemmal L-type channel and the sarcoplasmic reticulum Ca^{2+}-release channel is altered so that Ca^{2+} influx is not as effective in evoking Ca^{2+} release. However, the effect that such a decrease in the sensitivity of Ca^{2+}-induced Ca^{2+} release may have on steady state systolic [Ca^{2+}] is debatable. It has been shown that tetracaine (an agent which inhibits Ca^{2+}-induced Ca^{2+} release) only transiently inhibits contraction (and Ca^{2+} transients) in cardiac myocytes and contraction returns to normal when the myocyte gains Ca^{2+} by reducing efflux (via a reduced Na^{+} / Ca^{2+} exchanger tail current) until a balance is reached with influx again (Overend *et al.* 1997a; Overend *et al.* 1997b).

Depressed sarcoplasmic reticulum function is consistent with the results described in this Chapter since the abnormally long Ca^{2+} transients recorded are probably the result of

reduced sarcoplasmic reticulum Ca^{2+} release and / or reuptake in heart failure. The increased variation in Ca^{2+} transient duration over the epicardial surface in failing hearts suggests that the alteration in excitation-contraction coupling may be a heterogeneous process in the whole heart.

CHAPTER 9

LEFT VENTRICULAR EPICARDIAL MONOPHASIC ACTION POTENTIALS IN HEART FAILURE

Introduction

As mentioned in Chapter 1, action potential prolongation is a consistent finding in studies on the failing myocardium and delayed repolarisation is associated with changes in ion channel activity. A prolonged action potential has been shown in myocytes (Beuckelmann *et al.* 1993; Kaab *et al.* 1996; Qiu *et al.* 1996) and muscle preparations (Rossner and Sachs, 1978; Gwathmey *et al.* 1987) isolated from failing hearts but has not been demonstrated under more physiological conditions. Recent studies (Barr *et al.* 1994; Fu *et al.* 1997) have shown an increased dispersion of repolarisation, as suggested by increased QT dispersion on ECG, in patients with heart failure and they also showed that this was a prognostic marker for sudden cardiac death in these patients. Monophasic Action Potential (MAP) is an extracellularly recorded signal that reflects changes in the intracellular action potential (Franz, 1991). MAPs have been used in the whole heart to study repolarisation and the effects of drugs, ischaemia, heart mechanics, etc. in normal and diseased myocardium (Franz *et al.* 1984; Lab, 1991; Yuan *et al.* 1994) and have also been used to examine dispersion of repolarisation in the isolated heart as a result of volume / load changes (Reiter *et al.* 1988; Zabel *et al.* 1996).

This Chapter describes the measurements of MAP signals from the left ventricular epicardial surface of isolated hearts from rabbits with heart failure and the time course and regional characteristics of the signals are analysed.

Methods

MAPs were measured using suction electrodes, as described in Chapter 3, from the epicardial surface of 9 isolated hearts from the heart failure and 5 from the sham-operated group after the Ca^{2+} measurement experiments described in Chapter 8. MAPs were

measured from the same 15 left ventricular epicardial sites where the Ca^{2+} transients were measured, according to the arbitrary map illustrated in Figure 3.5. The isolated hearts were paced at a cycle length of 350 ms via the right atrium and recordings were made at 37 °C. The duration of the MAP signals were measured and compared between 2 groups. Variation of the MAP duration at different sites within each heart was analysed and this variation was also compared between the 2 groups.

Results

A representative tracing of the MAP signals is shown in Figure 9.1. The MAP signals showed a "spike and dome" appearance. There was an initial sharp upstroke ending in a spike followed by a small downward deflection before the dome-shaped repolarisation phase. The small spikes between the MAP signals shown in Figure 9.1 are pacing artefacts as the recordings were made with right atrial pacing at a cycle length of 350 ms.

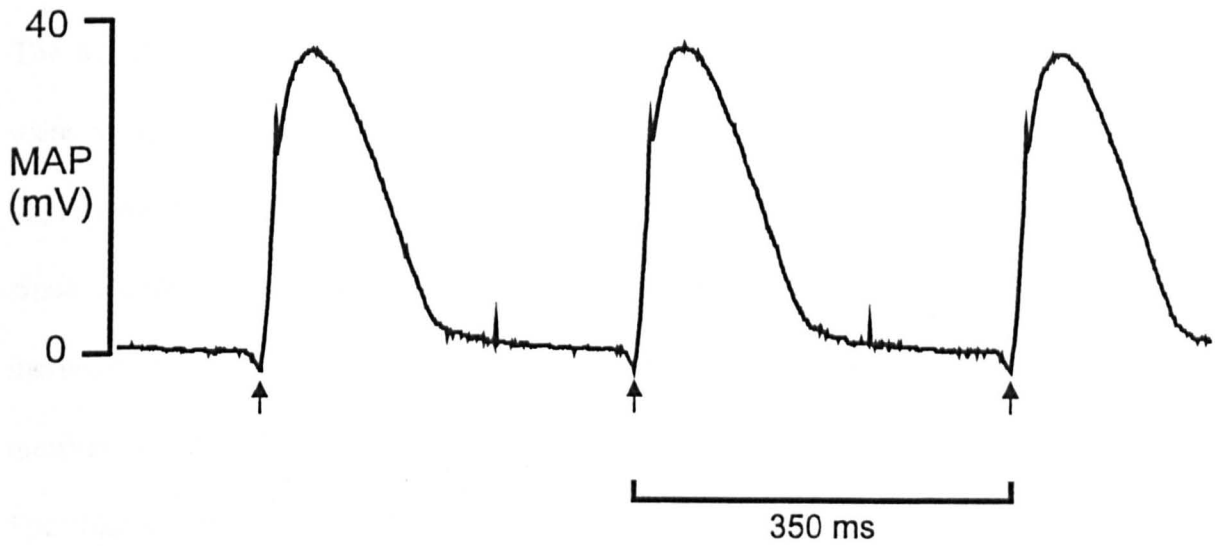

Figure 9.1 **Representative tracing of Monophasic Action Potential (MAP) signals recorded from the left ventricular epicardial surface of an isolated Langendorff perfused heart, paced via the right atrium at 350 ms cycle length. The MAP signals are composed of a spike and dome appearance. Arrows mark the beginning of the upstroke of the signal, the point from where the duration of each signal was measured. The small spikes between the MAP signals are pacing artefacts. The trace represents an average of 10 recordings.**

Measurement of the time course of MAP signals

The MAP signals were recorded from the same epicardial sites where the Ca^{2+} transients were measured in the 9 failing hearts and 5 controls. As with Ca^{2+} transients, the MAP signals were analysed in all 15 sites obtained from sham-operated hearts. In failing hearts, since recordings from sites within the infarct zone gave no MAP signal, analysis only included recordings from the remaining surviving myocardium with transient signals, the number of viable sites ranging from 7 to 12 (mean of 9).

The time course of the MAP signals measured at each left ventricular epicardial site was analysed in a similar way as that described for Ca^{2+} transient duration in Chapter 8. The MAP signals were analysed from the beginning of the sharp upstroke to the various points of the signals. The time intervals between the beginning of the upstroke to the peak, to 25 % decay, to 50 % decay, to 75 % decay and to 90 % decay were measured for each of the epicardial sites. The peak of the signal referred to here represents the peak of the dome component of the signal. In some MAP signals, the spike of the upstroke was of a greater amplitude than the following dome component. The time intervals were all measured from the beginning of the upstroke to the various points with reference to the amplitude of the peak of the dome component (and not the peak of the upstroke). A mean value was obtained for each heart of the time to peak (MAPD-Peak), time to 25 % decay (MAPD-25), time to 50 % decay (MAPD-50), time to 75 % decay (MAPD-75) and time to 90 % decay (MAPD-90). The values obtained from failing hearts were compared with those from controls and are summarised in Table 9.1 and illustrated in Figure 9.2. There was a significant delay in the time to peak (MAPD-Peak) in the failing hearts compared to controls with a difference of 21.4 ms between the mean values in the 2 groups. This difference remained about the same with some variation (18.7 to 23.9 ms) for the rest of the decay phase of the MAP

signal. The mean MAP duration was significantly longer in failing hearts than in controls throughout the MAP signal.

Table 9.1 Comparison of the time course of Monophasic Action Potentials (MAPs) over the left ventricular epicardial surface of isolated hearts from rabbits with heart failure (HF, n = 9) and controls (Sham, n = 5).

Measurements were made from the beginning of the upstroke at each measured site to the various points of the signal at a pacing cycle length of 350 ms. The differences between the mean values obtained for the 2 groups at the various points of the MAP signal are also shown.

	HF	Sham	p value	Difference (ms)
Time to Peak (ms) - MAPD-Peak	56.3 ± 4.1	34.9 ± 1.8	< 0.005	21.4
Time to 25 % decay (ms) - MAPD-25	106.7 ± 3.3	82.8 ± 2.1	< 0.001	23.9
Time to 50 % decay (ms) - MAPD-50	132.4 ± 2.8	110.2 ± 3.3	< 0.001	22.2
Time to 75 % decay (ms) - MAPD-75	152.3 ± 2.4	133.6 ± 4.0	< 0.002	18.7
Time to 90 % decay (ms) - MAPD-90	179.1 ± 4.0	157.2 ± 5.2	< 0.01	21.9

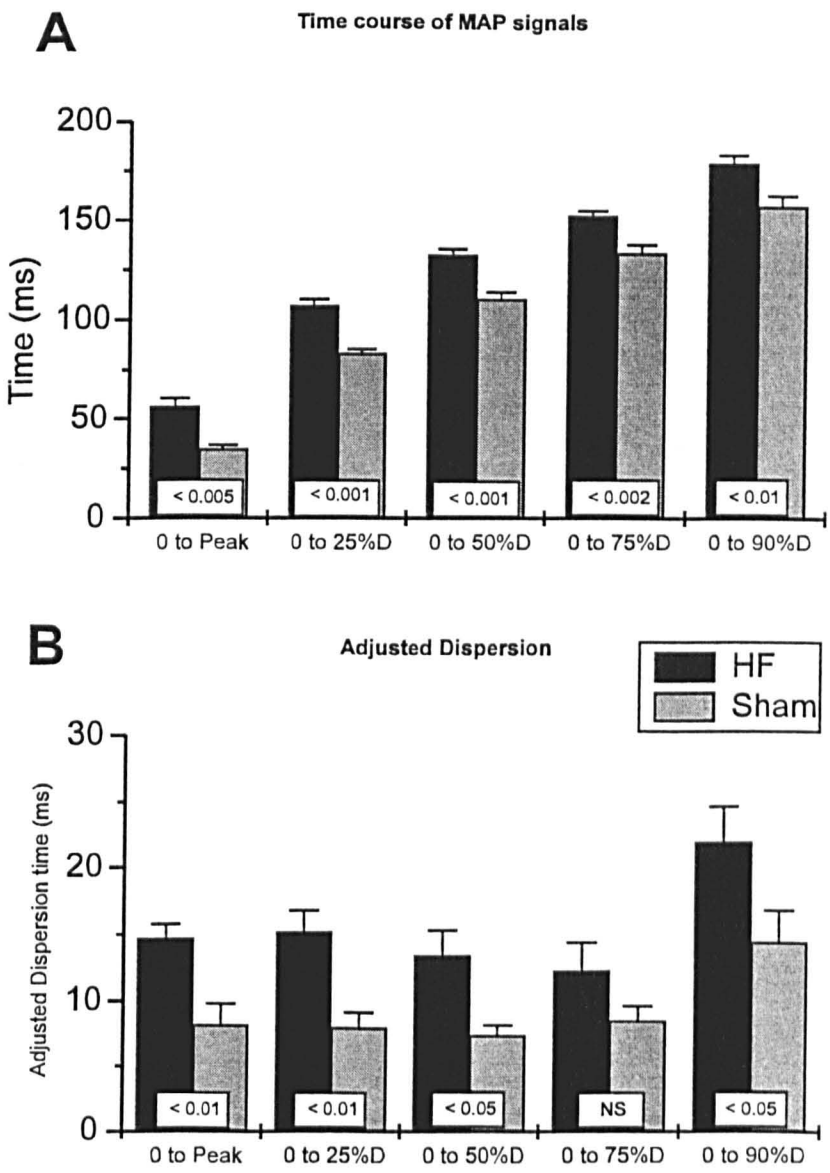

Figure 9.2 **Comparison of (A) the time course of Monophasic Action Potential (MAP) signals and (B) adjusted dispersion time (see text) at the various points of the MAP signal time course, over the left ventricular epicardial surface of isolated hearts from rabbits with heart failure (HF) and controls (Sham) at a cycle length of 350 ms during right atrial pacing.**

Correlation between MAP duration and site location

As with the Ca^{2+} transient duration described in Chapter 8, several methods of analysis were carried out to correlate the MAP duration with the location of the site measured to see if any particular epicardial sites had consistently long or consistently short MAP durations in either of the experimental groups. MAP duration was measured from the beginning of the signal to 50 % decay at each measured site. The mean MAP duration at each measured site for both experimental groups are shown in Table 9.2. The difference between the 2 experimental groups at each measured site in relation to the variation in MAP duration will be discussed in a later section *"Dispersion of MAP duration"*. The analyses described here were carried out to examine the relationship between the epicardial site and MAP duration measured within each of the experimental groups.

Table 9.2 Comparison of mean Monophasic Action Potential (MAP) duration (as measured by the beginning of the upstroke to 50 % decay) at the individual left ventricular epicardial sites in isolated hearts from rabbits with heart failure (HF) and controls (Sham).

Numbers in brackets represent the number of hearts in each group where MAPs were measurable at each site.

Site No.	MAP duration (ms)		p value
	HF (n = 9)	Sham (n = 5)	
1	140.4 ± 6.1 (9)	109.0 ± 2.9 (5)	< 0.01
2	128.5 ± 3.5 (9)	109.8 ± 6.3 (5)	< 0.05
3	142.2 ± 6.0 (9)	112.3 ± 3.8 (5)	< 0.02
4	131.6 ± 5.1 (9)	112.8 ± 5.3 (5)	< 0.05
5	140.3 ± 10.3 (4)	119.0 ± 4.5 (5)	0.08
6	127.0 ± 18.0 (2)	110.0 ± 4.3 (5)	0.28
7	137.6 ± 4.0 (9)	101.0 ± 3.9 (5)	< 0.001
8	124.6 ± 9.9 (9)	106.4 ± 6.6 (5)	< 0.20
9	127.7 ± 6.1 (9)	102.0 ± 5.3 (5)	< 0.02
10	133.3 ± 4.4 (9)	113.8 ± 5.4 (5)	< 0.02
11	124.5 ± 6.5 (4)	109.0 ± 7.8 (5)	0.28
12	138.7 ± 3.9 (9)	119.4 ± 4.4 (5)	< 0.05
13	-	103.6 ± 3.4 (5)	N / A
14	-	116.4 ± 4.6 (5)	N / A
15	-	106.0 ± 2.5 (5)	N / A

Analysis of Variance

Single-factor Analysis of Variance (ANOVA) was carried out with the data in the sham-operated and heart failure groups. In the sham-operated group, an F statistic value of 1.39 was obtained with a non-significant p-value of 0.19 (F - critical value = 1.88 for $p < 0.05$). In the heart failure group, the F statistic value was 0.84, again giving a non-significant p-value of 0.60 (F - critical value = 1.95 for $p < 0.05$). These data suggest that there was no significant trend where a particular epicardial site had consistently prolonged or brief MAP duration within either of the experimental groups.

Multiple comparison test (Tukey test)

Single-factor ANOVA is helpful in identifying whether one particular epicardial site had MAP duration different from the rest of the sites within each experimental group. In order to study the difference between pairs of measured sites, a multiple comparison test, the Tukey test, was employed to study the relationship between the MAP duration measured at the different epicardial sites within each experimental group. It was found that the calculated statistic (q value) was below the critical value for significance in both the sham-operated and heart failure groups. This shows that, within each experimental group, there was no correlation between the epicardial site and the MAP duration measured.

Layer analysis

Further regional analysis of MAP variation was carried out by dividing the heart into layers according to the geographic locations of the measure sites (see Figure 3.5). Four layers were thus allocated with sites 1, 2, 7 and 8 belonging to the basal layer; sites 3, 4, 9 and 10 to the upper cavity layer; sites 5, 6, 11 and 12 to the lower cavity layer and sites 13, 14 and 15 to the apical layer. The mean MAP durations for each layer in the 2 experimental groups are

summarised in Table 9.3. It is shown that the mean MAP duration at the basal, upper cavity and lower cavity layers were significantly longer in the heart failure group than controls. The apical layer was where there was a consistent infarct in the heart failure group and thus no measurable MAP signals were obtained. The individual layers were compared with each other within experimental groups using the above mentioned methods for individual epicardial sites. Neither single-factor ANOVA nor multiple comparison Tukey test identified any correlation between left ventricular layer and MAP duration in either of the experimental groups.

Table 9.3 Comparison of mean Monophasic Action Potential (MAP) duration (as measured by the beginning of the upstroke to 50 % decay) at the individual left ventricular layers in isolated hearts from rabbits with heart failure (HF) and controls (Sham).

Layer	MAP duration (ms)		p value
	HF (n = 9)	Sham (n = 5)	
Basal (sites 1, 2, 7, 8)	131.9 ± 3.1	106.2 ± 2.5	< 0.001
Upper cavity (sites 3, 4, 9, 10)	132.4 ± 2.5	109.8 ± 2.7	< 0.001
Lower cavity (sites 5, 6, 11, 12)	134.0 ± 5.0	114.6 ± 2.6	< 0.001
Apical (sites 13, 14, 15)	-	108.9 ± 2.6	N / A

Dispersion of MAP duration

As mentioned above, there appeared to be a variation in the time course of the MAP signals obtained at the various sites within the same heart in both experimental groups and this variation appeared to be greater in failing hearts than in controls. This "dispersion" of MAP duration was studied in greater detail within each experimental group and the results from the 2 groups were compared. Again, the MAP duration was measured from the beginning of the upstroke to 50 % decay.

Site by site analysis

The mean MAP duration at each measured epicardial site for the 2 experimental groups are summarised in Table 9.2. Firstly, these data showed that there was variation in MAP duration measured at different sites within the heart failure group and within the sham-operated hearts. Sites 13, 14 and 15 were within the region where there was a consistent infarct in the heart failure group and hence there was no measurable MAP signal. When the 2 experimental groups were compared at each of the remaining individual epicardial sites, it was found that the MAP duration was significantly prolonged at all but 3 of the left ventricular epicardial sites in failing hearts when compared to controls. The MAP duration at sites 5, 6 and 11 were longer in the heart failure group than controls but this difference did not reach statistical significance. These 3 sites were frequently involved in the myocardial infarct depending on the level of coronary ligation and the size of the infarct. Thus, viable tissue was only present and MAP signals were only recordable in 4 of the 9 failing hearts at site 5, 2 at site 6 and 4 at site 11. The lack of statistical significance in the MAP duration at these sites between failing hearts and controls may be attributable to the smaller sample at these sites. Another possibility is that these sites contained myocardium

with MAP durations that were close to the normal range. The data obtained from the other epicardial sites suggested that MAP signals obtained from most of the left ventricular epicardial surface were prolonged compared to controls. The variations in MAP duration within each heart in both experimental groups were analysed using methods similar to those described in Chapter 8 for Ca^{2+} transient duration.

Heart by heart analysis - range of values, standard deviation, dispersion

The MAP durations at all the measured sites within each heart were analysed. The maximum value, minimum value and standard deviation of the Ca^{2+} transient durations for each heart were obtained in the 2 experimental groups. Dispersion was measured as the difference between the maximum and minimum value in each heart. The mean value of these parameters in the heart failure and sham-operated groups are summarised in Table 9.4 and illustrated in Figure 9.3.

Figure 9.3 A uses a box and whiskers plot to compare the average standard deviation and range of the MAP duration in each experimental group. This figure shows that the range of MAP durations was increased in the heart failure group and this was mainly due to a significantly higher maximum value. The minimum value was also slightly increased in the heart failure group but this difference did not reach statistical significance ($p = 0.07$) when compared with the control group. The standard deviation of the MAP duration in each heart was significantly increased in the heart failure group when compared to controls (13.6 ± 1.8 ms vs. 9.1 ± 1.0 ms, $p < 0.05$).

Dispersion of MAP duration in each heart was analysed by calculating the difference between the longest and the shortest duration. Figure 9.3 B shows that dispersion of the MAP duration was greater in the heart failure group than controls but this difference did not reach statistical significance (38.6 ± 5.3 ms vs. 27.6 ± 2.5 ms, $p = 0.08$).

Table 9.4 Comparison of variation in Monophasic Action Potential (MAP) durations (as measured by the beginning of the upstroke to 50 % decay) within each heart in the heart failure group (HF) and controls (Sham). (See text for discussion)

	HF (n = 9)	Sham (n = 5)	p value
Maximum value (ms)	147.4 ± 3.2	124.8 ± 2.9	< 0.001
Minimum value (ms)	108.9 ± 4.8	97.6 ± 3.7	0.07
Standard deviation (ms)	13.6 ± 1.8	9.1 ± 1.0	< 0.05
Dispersion (ms)	38.6 ± 5.3	27.6 ± 2.5	0.08
Adjusted dispersion (ms)	13.5 ± 1.9	7.4 ± 0.7	< 0.02

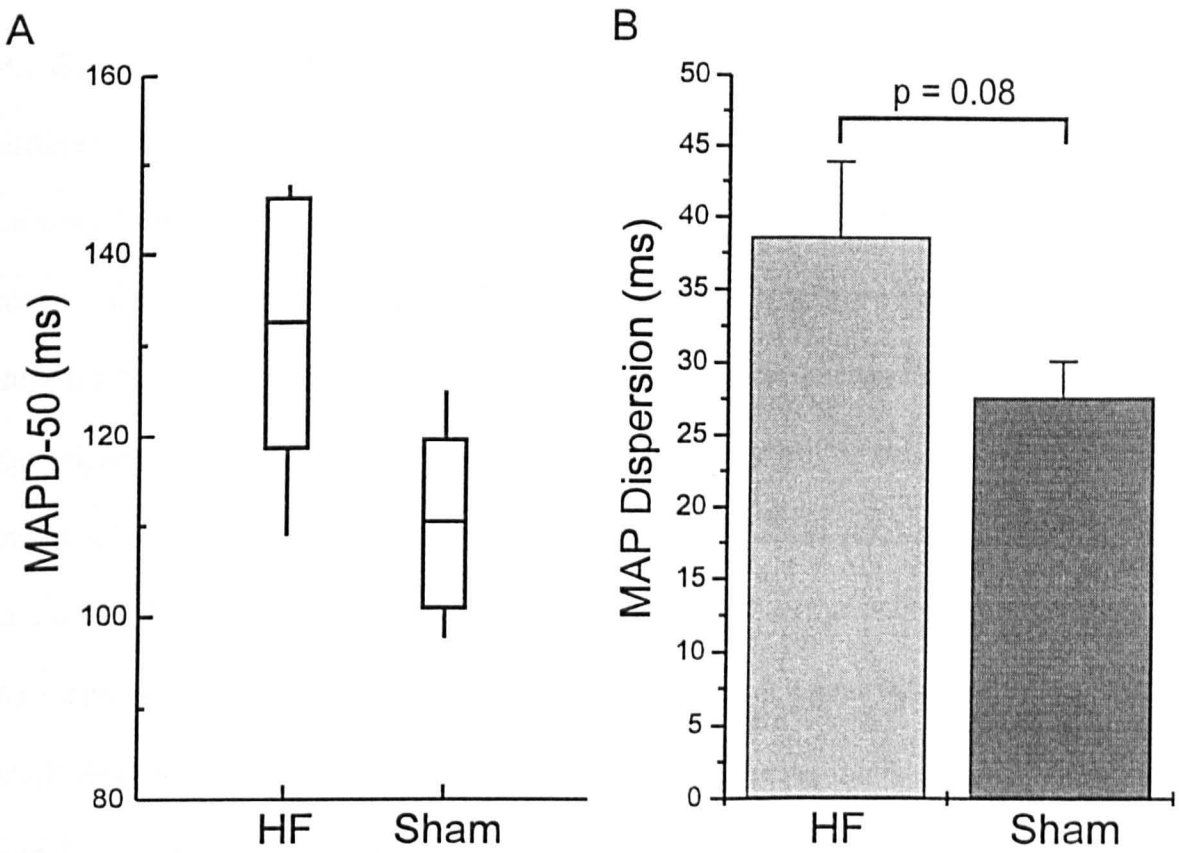

Figure 9.3 **Panel A shows a box and whiskers plot illustrating the range of Monophasic Action Potential duration values (MAPD-50) measured from control (Sham) and heart failure (HF) groups. Lines denote the range of MAPD-50 values, the upper and lower edges of the box denote the standard deviation, and the middle line denotes the mean value of the MAPD-50. Panel B shows a histogram of the mean dispersion of MAP duration (maximum MAPD-50 value - minimum MAPD-50 value in each heart) in both control (Sham) and heart failure (HF) groups. Error bars denote standard error.**

Adjusted dispersion of MAP duration

As discussed in Chapter 8 with dispersion of Ca^{2+} transient duration, simply taking the difference between the longest and shortest durations as a measure of dispersion is probably an over-simplification. The dispersion of MAP duration was corrected for the number of measured sites in the each heart by dividing the difference between the longest and shortest duration by the square root of the number of measured sites in each heart. It was found that the adjusted dispersion of MAP duration (measured at 50 % decay) was significantly increased in the heart failure group when compared to controls (13.5 ± 1.9 ms vs. 7.4 ± 0.7 ms, $p < 0.02$, Table 9.4).

As mentioned above, MAP duration was measured at other points of the time course of the MAP signals. The mean duration at the various points during the time course of the MAP signals are summarised in Table 9.1 and Figure 9.2 illustrates the comparison between the 2 groups with regard to the mean duration and the adjusted dispersion of the duration at the various points during the time course of the signals. It shows that the mean MAP duration in the heart failure group was significantly prolonged at all points during the decay phase of the time course of the MAP signals when compared to controls. Adjusted dispersion of MAP duration was also significantly increased in the heart failure group at the various points during the decay phase of the MAP signals except at 75 % - decay where the difference was not statistically different.

Discussion

It was shown in this Chapter that the MAP signals obtained from the left ventricular epicardial surface of Langendorff perfused hearts isolated from rabbits with heart failure followed a similar trend of abnormality as that seen in Ca^{2+} transients. The MAP duration

was prolonged in the failing hearts when compared to sham-operated controls and there was increased variation of the durations with each heart in the heart failure group than in controls.

Prolonged MAP duration in failing hearts

The time to peak of the dome component of the MAP signal (MAPD-Peak) was significantly delayed in the failing hearts when compared to controls, with a difference of about 20 ms in the mean values in the 2 groups (Table 9.1). This difference was maintained at around the same magnitude throughout the rest of the decay phase of the MAP signal. This shows that the prolongation of MAP duration in the failing heart occurs predominantly during the early part of the MAP signal. It is difficult to infer which ionic currents are responsible for this observation as the MAP signal is only an indirect assessment of the transmembrane action potential. However, these results suggest that ionic currents active during the early repolarisation phase of the action potential may be involved and the prolongation of MAP duration in the failing hearts could have resulted from a reduced outward current, increased inward current, or both.

Regional variation in the time course of MAP signals

Individual hearts from the sham-operated control group exhibited MAP signals with a limited range of durations. Non-uniform recovery of excitability with a physiological dispersion of repolarisation is well-recognised (Han and Moe, 1963; Brutsaert, 1987) and this may be related to the regional variation in MAP duration observed in the control hearts. Variation in MAP durations was also observed within failing hearts but this variation was greater in magnitude than in controls.

There was no consistent relationship between the site position and the MAP duration in either of the experimental groups. No difference was observed when the MAP signals obtained from the basal portion of the left ventricle were compared with those from the apex. Some studies have suggested an apex to base difference in action potential duration (Cohen *et al.* 1976; Watanabe *et al.* 1983). Action potential duration is affected by mechanical load as a result of mechano-electric feedback (Lab, 1982). It is conceivable that difference in action potential duration between different regions of the heart may be the result of difference in wall tension although it may be due to differences in intrinsic properties of the myocytes in those regions. Regional wall tension was not assessed in the experiments described. Another reservation of this study is that the hearts were perfused in the Langendorff mode. The contractile performance of the beating heart is quite different when it is perfused in the Langendorff mode than when it is anterogradely perfused in the working heart configuration, not to mention when *in vivo*. Thus the regional wall tension in the Langendorff perfused heart may not represent the conditions *in vivo*. An effort was made to compare the 2 experimental groups at similar loading conditions by inflating the intraventricular balloons to give zero end-diastolic pressure in each heart. Although this cannot ensure that the regional wall tension is similar to the situation *in vivo* or when the heart is ejecting isotonically, the difference in MAP signals observed between the heart failure group and the sham-operated group should not be due to different loading conditions.

Dispersion of MAP duration

Further scrutiny of MAP signals from the heart failure group reveals that the longer mean duration was a result of abnormally prolonged MAP durations in a majority of sites in each heart. The variation of MAP duration was greater in each heart from the heart failure group

as measured by the standard deviation and adjusted dispersion of the MAP durations. The fact that there was only a small non-significant increase in the shortest MAP duration in each heart in the heart failure group when compared to controls suggests that there were regions in the failing hearts that had MAP durations close to the normal range. Indeed when the MAP durations were compared between the 2 experimental groups at each measured site, there were 3 sites (5, 6 and 11) in the heart failure group which contained MAP signals with prolonged durations that were not statistically different from controls. There may be several reasons for this observation:- (1) As already discussed, the apparent lack of difference could be the result of a smaller sample of measurements at these sites in the heart failure group due to the fact that these sites were frequently involved in the infarct. (2) These regions could have contained myocardium with MAP durations that were close to the normal range. This possibility has been discussed in Chapter 8 as Ca^{2+} transients were found to be significantly prolonged in some of the epicardial sites in the failing hearts whilst in others (sites 2, 3, 5, 6, 12), there was a non-significant prolongation when compared to controls. (3) The fact that these regions were close to the infarct zone (where the ventricular wall was thin) could have made these sites more prone to the effect of stretch or increased wall tension. MAP durations at these sites could be affected by mechano-electric feedback to a greater extent as a result.

The increased variation of the MAP signals with an overall increase in the MAP durations in the heart failure group suggests that changes in the myocardium in this model of heart failure in the rabbit are non-uniform as seen in the results of Ca^{2+} transients described in Chapter 8. The electrical remodelling process in heart failure may well be a heterogeneous one.

CHAPTER 10

CORRELATION BETWEEN MECHANICAL FUNCTION, CA^{2+} HANDLING AND VENTRICULAR REPOLARISATION IN HEART FAILURE

Introduction

In this Chapter, the mechanical function, Ca^{2+} handling and ventricular repolarisation data in the isolated Langendorff perfused hearts from both heart failure and sham-operated groups are correlated.

Methods

Mechanical function and Ca^{2+} handling in heart failure

The pressure profiles of the isolated hearts were compared with the mean duration of Ca^{2+} transients obtained in each heart in the 2 experimental groups.

Cardiac remodelling and Ca^{2+} handling in heart failure

As described in Chapter 4, it was shown that there was significant cardiac remodelling produced by the heart failure model as demonstrated by the increased chamber dimensions on echocardiography and increased tissue weight in the failing hearts. Left ventricular dry weight was correlated with the mean duration of Ca^{2+} transients obtained in the corresponding heart.

Ventricular repolarisation and Ca^{2+} handling in heart failure

In 9 hearts from the heart failure group and 5 from the sham-operated group, Monophasic Action Potentials (MAPs) were measured at the same left ventricular epicardial sites where Ca^{2+} transients were measured. The Ca^{2+} transient and MAP data were compared and correlated in the 2 experimental groups.

Results

Mechanical function and Ca^{2+} handling in heart failure

It was shown in Chapter 6 that the rabbit coronary artery ligation model produced heart failure with significant systolic and diastolic dysfunction. This was demonstrated in the haemodynamic parameters in the working heart configuration and also in the left ventricular pressure profile in the Langendorff perfused hearts where Ca^{2+} measurements were made. The intraventricular pressure profile of the isolated Langendorff perfused hearts from the 17 hearts from the heart failure group and 13 from the sham-operated group are summarised again in Table 10.1 together with the mean Ca^{2+} transient durations in the 2 groups as measured by the CaD-50 (from the beginning of the transient to 50 % - decay, see Chapter 8). The peak systolic pressure in the heart failure group was decreased compared to controls. The maximum rate of pressure decay during diastole was also decreased in the failing hearts (0.32 ± 0.04 mmHg.ms^{-1} vs. 0.66 ± 0.05 mmHg.ms^{-1} in controls, $p < 0.001$) whilst the mean Ca^{2+} transient duration was prolonged (156.2 ± 3.2 ms vs. 124.9 ± 2.6 ms in controls, $p < 0.001$). These 2 latter parameters were considered together in both experimental groups and Figure 10.1 shows that there was a significant correlation between the mean Ca^{2+} transient duration in each heart and the corresponding maximum rate of pressure decay ($r = - 0.63$, $p < 0.001$). This suggests that impaired relaxation in the failing heart was associated with a prolonged Ca^{2+} transient duration.

Table 10.1 Comparison of left ventricular pressure profile and mean Ca^{2+} transient duration in the isolated Langendorff perfused heart between rabbits with heart failure (HF) and controls (Sham).

(SysP = left ventricular peak systolic pressure, $dP.dt^{-1}_{(max)}$ = maximum rate of pressure change, CaD-50 = mean Ca^{2+} transient duration as measured by the beginning of the transient to 50 % decay)

	HF (n = 17)	Sham (n = 13)	p value
SysP (mmHg)	26.2 ± 3.7	49.0 ± 2.6	< 0.001
$-dP.dt^{-1}_{(max)}$ ($mmHg.ms^{-1}$)	0.32 ± 0.04	0.66 ± 0.05	< 0.001
CaD-50 (ms)	156.2 ± 3.2	124.9 ± 2.6	< 0.001

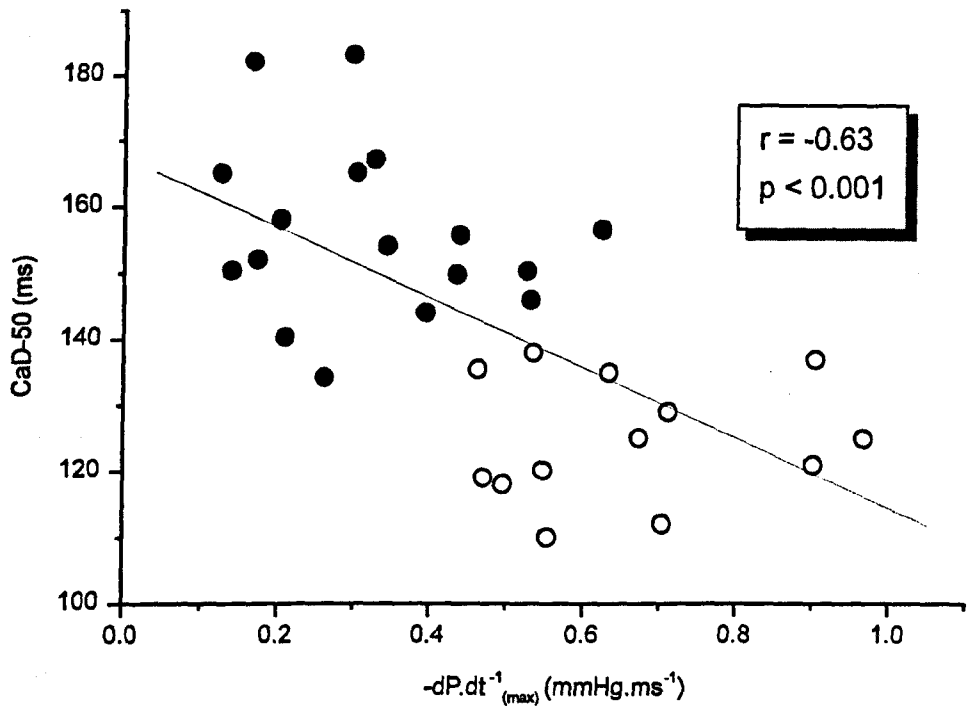

Figure 10.1 **Plot of the mean Ca^{2+} transient duration (CaD-50) in each heart against the corresponding maximum rate of pressure decay [$-dP.dt^{-1}_{(max)}$] for both control (○) and heart failure (●) groups. The solid line is the linear regression of the two variables with the correlation coefficient (r) and significance value (p) shown in the shaded box.**

Cardiac remodelling and Ca^{2+} handling in heart failure

Structural changes in the heart as a result of the coronary artery ligation procedure were described in Chapter 4. Significant cardiac remodelling and compensatory hypertrophy were demonstrated in the remaining surviving myocardium in the failing hearts as a result of the myocardial infarct. Left ventricular dry weight in the 17 hearts from the heart failure group where Ca^{2+} transients were measured, corrected for body weight, was 0.38 ± 0.02 $g.kg^{-1}$. This was significantly greater than the corrected left ventricular dry weight in the 13 hearts from the sham-operated group (0.31 ± 0.01 $g.kg^{-1}$, $p < 0.02$). When the corrected left ventricular dry weight was considered together with the corresponding mean Ca^{2+} transient duration in each heart from the 2 experimental groups, it was found that there was a significant correlation between these 2 parameters ($r = 0.41$, $p < 0.05$, see Figure 10.2). This suggests that compensatory hypertrophy in the failing heart was associated with a prolonged Ca^{2+} transient duration.

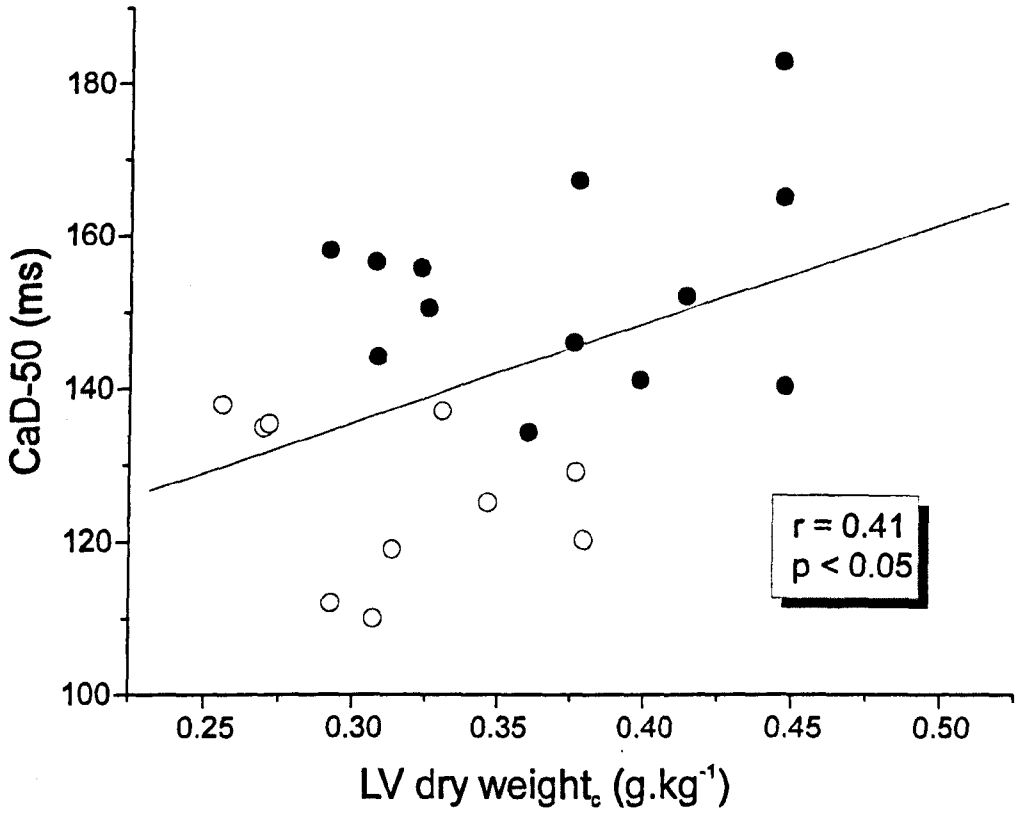

Figure 10.2 Plot of the mean Ca^{2+} transient duration (CaD-50) in each heart against the corresponding corrected left ventricular dry weight (LV dry weightc) for both control (○) and heart failure (●) groups. The solid line is the linear regression of the two variables with the correlation coefficient (r) and significance value (p) shown in the shaded box.

Ventricular repolarisation and Ca^{2+} handling in heart failure

In 9 hearts from the heart failure group and 5 from the sham-operated group, data were available for the Ca^{2+} transient durations measured at the various left ventricular epicardial sites together with the Monophasic Action Potential (MAP) durations at the corresponding sites. It was shown in Chapter 8 that the mean Ca^{2+} transient duration was significantly prolonged in failing hearts when compared to controls and likewise the mean MAP duration was shown in Chapter 9 to be significantly prolonged in failing hearts. Ca^{2+} transient and MAP durations were considered together and the Hotelling's 2-sample t^2-test was employed to compare the 2 experimental groups. Equal covariance matrices were verified in the 2 parameters with the Box's m-test and the Hotelling's test showed that the 2 experimental groups were significantly different with the heart failure group having significantly prolonged Ca^{2+} transient *and* MAP durations (F statistic = 40.6, critical value = 3.07 for $p < 0.05$).

A relationship between Ca^{2+} transient duration and MAP duration was then sought by correlating the Ca^{2+} transient at each measured site in both experimental groups with the corresponding MAP duration at that site. The results are plotted in Figure 10.3. It was evident that the mean durations of both Ca^{2+} transients and MAP signals were prolonged in the heart failure group with greater variation in the 2 parameters in the heart failure group than controls. There was a weak but significant association between the Ca^{2+} transient duration obtained at each left ventricular epicardial site and the corresponding MAP duration recorded at the site in the 2 experimental groups ($r = 0.32$, $p < 0.001$). These data suggest that epicardial sites in failing hearts which had prolonged Ca^{2+} transient durations also tended to have prolonged MAP durations.

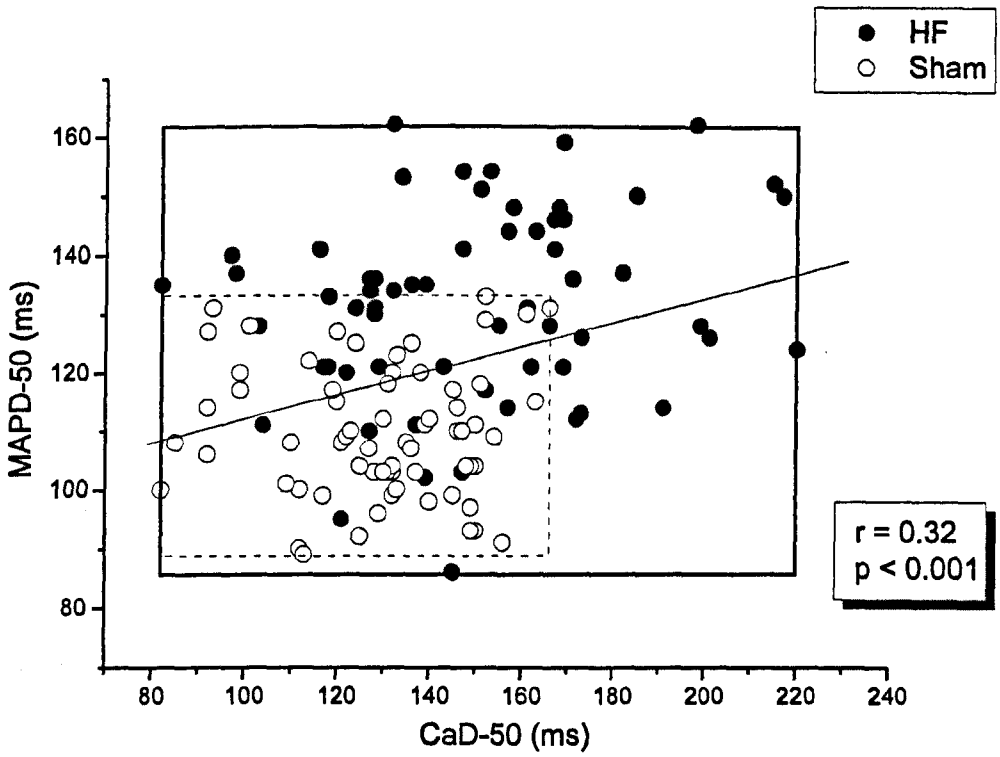

Figure 10.3 Plot of the mean Ca^{2+} transient duration (CaD-50) at each measured epicardial site against the corresponding Monophasic Action Potential duration (MAPD-50) for both control (○) and heart failure (●) groups. Rectangular boxes denote limits of the measured parameters in the heart failure group (solid line) and controls (broken lines). The oblique solid line is the linear regression of the two variables with the correlation coefficient (r) and significance value (p) shown in the shaded box.

Discussion

In the study by Gwathmey *et al.* (1987), ventricular trabeculae isolated from patients with heart failure showed a significant prolongation in tension development with a marked delay in relaxation. Corresponding Ca^{2+} transients were prolonged and action potentials recorded from these trabeculae were also reported to be prolonged. Beuckelmann *et al.* (1992) showed similar findings in ventricular myocytes isolated from patients with heart failure with significant prolongation in both action potentials and Ca^{2+} transients in the failing myocytes. These experiments were, however, carried out under low pacing rates and temperatures. There are no data on such changes under more physiological conditions in the literature.

As discussed in Chapter 1, it would not be unreasonable to suggest that the mechanical abnormalities seen in the failing myocardium are related to changes in Ca^{2+} handling since Ca^{2+} is central in the excitation-contraction coupling process. The data on action potentials and Ca^{2+} transients in heart failure tend to suggest that the abnormalities in Ca^{2+} handling may be associated with electrophysiological abnormalities in the failing myocardium. These abnormalities may have a causal relationship i.e. with abnormal Ca^{2+} handling causing abnormal electrophysiological changes and vice versa. Or, these abnormalities may have been caused by a common stimulus that underlies the whole remodelling process in the failing heart.

An attempt was made in this Chapter to relate the different abnormalities demonstrated in the rabbit coronary artery ligation model of heart failure with each other. Since measurements of mechanical function, Ca^{2+} handling and ventricular repolarisation were made in the same hearts, abnormalities in these parameters could be compared and correlated.

Diastolic dysfunction, hypertrophy and Ca^{2+} handling

It has been shown in earlier Chapters that the rabbit heart failure model described produced significant mechanical abnormalities in the heart demonstrated both *in vivo* and *in vitro*. There was significant systolic and diastolic dysfunction. In the isolated Langendorff perfused heart, a causal link between the duration of the Ca^{2+} transient and mechanical function was suggested by the significant correlation between the CaD-50 value and the maximum rate of left ventricular pressure decay (Figure 10.1). It was shown that pressure decay during diastole was slowed in heart failure and this was associated with a prolongation in the Ca^{2+} transient duration. In addition, failing hearts with prolonged Ca^{2+} transient durations were also found to have increased left ventricular dry weights indicative of significant compensatory hypertrophy. Hypertrophy *per se* is associated with abnormal mechanical profile and Ca^{2+} handling (Gwathmey *et al.* 1993). It is conceivable that hypertrophied myocardium would have an abnormal relaxation profile and that reduced sarcoplasmic reticulum Ca^{2+} uptake during diastole with higher cytosolic $[Ca^{2+}]$ would lead to slowed relaxation. However, the sequence of events that lead to the consequent pathological state in heart failure is unknown. It may be possible that the initial mechanical dysfunction with impaired systolic function increases the stress within the myocardium which then starts off a cascade of changes including those mediated by trophic factors leading to compensatory hypertrophy and structural remodelling and those leading to sarcoplasmic reticulum abnormalities.

Ca^{2+} handling and ventricular repolarisation

Data from the isolated Langendorff perfused hearts where both Ca^{2+} transients and MAP signals were measured suggested an association between the 2 parameters. It was shown that both the Ca^{2+} transient and MAP durations were significantly prolonged in the heart

failure group and there was increased dispersion in both parameters in failing hearts. The significant correlation between the 2 parameters at each measured site in the 2 experimental groups suggest that regions with prolonged Ca^{2+} transients also tended to have prolonged MAP durations. These data demonstrated that there was nonuniform prolongation of both Ca^{2+} transient and MAP durations in the failing hearts.

The results in this Chapter suggest that there are regions in hearts from the heart failure group with compensatory hypertrophy associated with abnormal mechanical profile, altered Ca^{2+} handling and prolonged ventricular repolarisation. This suggests that there is significant remodelling in the failing heart of structural architecture, sarcoplasmic reticulum function and electrical events and that the remodelling process is a patchy and heterogeneous one. These changes can produce not only the reduced pump efficiency seen in heart failure but also an ideal milieu for the induction and propagation of malignant ventricular arrhythmias which are so often seen in heart failure.

CHAPTER 11

EFFECT OF ALTERED CONDUCTION ON MECHANICAL PERFORMANCE IN HEART FAILURE

Introduction

The efficiency of the heart as a pump is dependent on its ability to propel effectively. A brisk contraction from the three-dimensional structure demands co-ordinated movement in the various regions. Since contraction is intimately linked with excitation, the electrical activation pattern of the heart should direct this co-ordinated movement. Thus, any alteration or abnormality in the activation pattern of the heart may directly affect the overall mechanical function of the pump. This Chapter investigates the potential contribution of altered electrical activity and uncoordinated contraction to the overall contractile dysfunction in heart failure.

Normal ventricular activation

The sino-atrial node is the normal electrical pacemaker of the heart and is the seat of the origin of the electrical impulse which propagates through the rest of the heart causing contraction. The fibrous mitral and tricuspid valve rings are devoid of myocardial tissue and act as electrical barrier to the propagation of electrical activity from the atria to the ventricles. The atrioventricular node acts as the flag-station which allows such propagation after a short delay. Investigators in the 19th century like Purkinje, Tawara, Keith, James and His (Acierno, 1994) discovered the presence of a specialised system of tissues in the ventricles using light microscopy. The anatomy of the His-Purkinje system was defined. But it was not until the next century that the experiments of Sir Thomas Lewis demonstrated the importance of this system in the rapid conduction of electrical impulses through the ventricles. In his landmark paper published in 1915 (Lewis and Rothschild, 1915), the wave of excitation in the dog's heart was shown to follow the pathway of the conduction system rather than the muscle fibres. These findings were later confirmed and

expanded by other studies. One elegant study by Durrer *et al.* (1970) demonstrated the normal excitation pattern of the isolated human heart using up to 870 intramural electrodes. By studying the activation times at the various electrode locations, isochronal maps were drawn and the pattern of spread of the excitation wavefronts was obtained. It was shown that the ventricles are excited first from the endocardial surface via the His-Purkinje system near the paraseptal region. The activation wavefronts then spread apically with the posterobasal parts of the ventricles being activated late. Epicardial activation of the ventricles reflects the movements of the intramural excitation wave with early epicardial "breakthroughs" at the paraseptal areas and late epicardial activation near the posterobasal regions.

Abnormal ventricular activation and cardiac performance

It has been the belief of many that the different regions of the ventricle would have to contract almost synchronously in order to generate a sufficiently powerful impulse to propel blood out of its cavity (Rushmer, 1964). Indeed, the total ventricular activation time is normally short (Durrer *et al.* 1970). There is, however, a sequential pattern of excitation and hence activation. This pattern is thought to improve ejection of blood out of the chamber and any alteration to this pattern would lead to suboptimal mechanical function. Furthermore, if the total activation time is prolonged, due to either defects in the specialised conducting system or in the myocardial intercellular coupling, cardiac performance would also be jeopardised.

Studies have shown that conducting system disturbances like left bundle branch block can lead to impaired ventricular performance (Baragan *et al.* 1968). The effect of abnormal ventricular activation on cardiac performance has been investigated especially in patients with implanted permanent pacemakers (Rosenqvist *et al.* 1991; Chirife, 1994). Patients who

require ventricular pacing for conducting system disease usually have the ventricular pacing wire positioned at the right ventricular apex. Right ventricular pacing causes delayed intraventricular conduction and produces an altered ventricular activation pattern similar to that in intrinsic left bundle branch block (Vassallo *et al.* 1986). Rosenqvist *et al.* (1991) demonstrated in patients with intact atrioventricular conduction who were implanted with dual chamber pacemaker system that cardiac performance was impaired when the right atrium and right ventricle were sequentially paced as compared with right atrial pacing only. Normal ventricular activation pattern can be mimicked by pacing from the proximal septum in the right ventricle and it has been shown in dogs that the ventricular activation time can be shortened and cardiac performance improved by proximal septal pacing as opposed to apical pacing (Rosenqvist *et al.* 1996). This further emphasises the importance of normal intraventricular conduction and ventricular activation for optimal cardiac performance. Other studies have also shown that ventricular diastolic function is also dependent on the activation pattern during systole (Xiao *et al.* 1991; Xiao and Gibson, 1994; Stojnic *et al.* 1996). There is a physiological non-uniformity in recovery of excitability (Han and Moe, 1963; Brutsaert, 1987; Stevenson, 1995). The distribution of local recovery properties has been shown to be related to the normal excitation sequence (Burgess *et al.* 1972). Thus, abnormal excitation of the ventricles could lead to alterations in regional repolarisation patterns which could directly affect relaxation and diastolic performance.

The mechanisms underlying the contractile abnormality in heart failure are not fully understood. Asynchronous ventricular contraction as a result of impaired ventricular conduction and non-uniform ventricular activation could potentially play a part in causing systolic and diastolic dysfunction in the failing heart. Vassallo *et al.* (1986) showed that left ventricular activation time during right ventricular pacing was prolonged in patients with

previous anterior myocardial infarcts when compared to those with inferior infarcts although neither group had conducting system disease demonstrable during sinus rhythm. This suggests that delayed intraventricular conduction occurred within the post-infarct myocardium. Intercellular coupling within the myocardium may be impaired in the failing heart and cardiac remodelling and hypertrophy can provide changes which can further impair intraventricular conduction and ventricular activation.

In this Chapter, the effect of abnormal intraventricular conduction on cardiac performance was studied in normal hearts and in hearts from the rabbit heart failure model. The potential contribution of altered ventricular activation in the mechanical dysfunction seen in the failing heart was investigated.

Methods

The effect of altered intraventricular conduction pattern on cardiac mechanical performance was studied in 7 hearts from the heart failure group and 5 from the sham-operated controls. Ca^{2+} transient and MAP signal measurements were made from the various left ventricular epicardial sites in the Langendorff perfused hearts as described in Chapters 3, 8 and 9 using the arbitrary 15-site map (Figure 3.5). At each measured site, the Ca^{2+} and MAP recordings were made during atrial pacing and ventricular pacing at the same cycle length of 350 ms. Pacing was carried out using pairs of platinum electrodes inserted into the right atrial appendage and the posterior aspect of the right ventricular apex for atrial and ventricular pacing respectively. The beginning of the MAP signal at each site represented the local electrical activation time and the beginning of the Ca^{2+} transient represented the timing of the local detectable Ca^{2+} event at that site for both atrial and ventricular pacing. As the recordings were triggered at the upstroke of the pacing stimulus, the local Ca^{2+} transient and MAP activation times at each measured site could be calculated relative to the timing of the

pacing stimulus. The dispersion of activation times with respect to Ca^{2+} transients and MAP signals at the different epicardial sites were used as an index of intraventricular conduction delay i.e. the time taken for the whole left ventricle to be activated during right atrial and right ventricular pacing. Adjusted dispersion was taken as the difference between the earliest and latest activation time in each heart divided by the square root of the number of measured sites - a method used for correcting the dispersion for the number of measured sites as described in Chapter 8. The intraventricular conduction delay was compared in the 2 experimental groups during atrial and ventricular pacing.

Mechanical function of the isolated heart was assessed by intraventricular pressure recorded using a latex balloon inserted into the left ventricle with the volume of the balloon adjusted to give zero end-diastolic pressure. At a constant pacing cycle length of 350 ms, the effect of transition from atrial to ventricular pacing on the pressure profile of the isolated heart was studied in both experimental groups.

Results

The intraventricular conduction pattern was studied first by examining the local activation times for Ca^{2+} transient and MAP signals in both the heart failure and sham-operated groups during atrial and ventricular pacing. The effects of atrial and ventricular pacing on the conduction delay through the left ventricle were analysed. Finally, the effect of different conduction patterns as a result of atrial or ventricular pacing on the mechanical performance of the heart was studied and compared between the 2 experimental groups.

Activation pattern in the left ventricle

Ca^{2+} transient and MAP signal recordings were made at the 15 left ventricular epicardial sites using the pacing stimulus as the trigger. The local activation time for both Ca^{2+} and

MAP signals at each measured site could be easily calculated relative to the pacing stimulus. Analysis of the timing of the beginning of Ca^{2+} and MAP signals at the various epicardial sites was done to assess the pattern of activation of the left ventricle during atrial and ventricular pacing. This was carried out using similar methods as those described in Chapters 8 and 9 for analysing the variation of the time course of Ca^{2+} transient and MAP signals and for assessing the relationship between the epicardial site location and the time course of the signals measured at the site. As opposed to studying the time course of the signals, times between the stimulus and the upstroke of the MAP signals and Ca^{2+} transients were analysed here and the results are described below.

Heart by heart analysis

Firstly, the activation times for Ca^{2+} transients and MAP signals at all the measured sites in each heart were averaged to give a mean Ca^{2+} activation time (Ca-AT) and a mean MAP activation time (MAP-AT) for each heart during atrial and ventricular pacing. As mentioned in previous Chapters, there was no recordable Ca^{2+} transient or MAP signal in the infarcted area in failing hearts. Thus, measurements were available from between 7 to 12 sites (mean 10) in the failing hearts and analysed whilst data were available for all 15 epicardial sites in controls.

The mean MAP-AT during atrial pacing is the time interval between the atrial pacing stimulus to the mean ventricular electrical activation time. This represents the atrio-ventricular conduction delay and is analogous to the PR interval on normal surface electrocardiogram. The mean MAP-AT during ventricular pacing is the time interval between the ventricular pacing stimulus to the mean ventricular electrical activation time. This represents the latency in mean ventricular electrical activation. Similarly for the Ca^{2+} transients, the mean Ca-AT during atrial pacing and during ventricular pacing are the mean

time intervals to Ca^{2+} events in the left ventricle from the atrial and ventricular pacing stimulus respectively.

The mean Ca-AT and MAP-AT during atrial and ventricular pacing for both the heart failure and sham-operated groups are summarised in Table 11.1. The mean MAP-AT during atrial pacing was 107.5 ± 7.3 ms for the heart failure group and 102.1 ± 6.5 ms for controls. Although there was a small numerical difference, this did not reach statistical significance and suggests that atrioventricular conduction was not significantly impaired in the failing hearts. Latency to mean ventricular electrical activation by ventricular pacing was also slightly increased in failing hearts (39.3 ± 2.7 ms vs. 35.6 ± 2.1 ms in controls) but again this difference did not reach statistical significance. Mean Ca-AT during atrial and ventricular pacing were also slightly increased in the heart failure group but the differences were not statistically significant.

From these mean data, it would appear that the difference between the MAP-AT and Ca-AT (i.e. the time delay between electrical and Ca^{2+} events) during atrial pacing or ventricular pacing was greater in the heart failure group than in the sham-operated group. The time intervals between the Ca-AT and MAP-AT were analysed at each epicardial site and these results and the relationship between the Ca-AT and MAP-AT in both experimental groups are described below.

Table 11.1 Comparison of mean Monophasic Action Potential activation time (MAP-AT) and mean Ca^{2+} transient activation time (Ca-AT) (see text) in isolated hearts from rabbits with heart failure (HF) and controls (Sham) during atrial and ventricular pacing.

	HF (n = 7)	Sham (n = 5)	p value
Atrial pacing			
MAP-AT (ms)	107.5 ± 7.3	102.1 ± 6.5	NS
Ca-AT (ms)	116.7 ± 8.4	109.1 ± 6.1	NS
Ventricular pacing			
MAP-AT (ms)	39.3 ± 2.7	35.6 ± 2.1	NS
Ca-AT (ms)	47.5 ± 2.6	40.5 ± 2.6	0.08

Site analysis

(1) Atrial pacing

In order to study the pattern of activation during atrial pacing and to investigate if there was any one epicardial site that was activated consistently early or late with respect to the Ca^{2+} transient or MAP signals, the MAP-AT and Ca-AT were averaged in the 2 experimental groups at each epicardial site. The results are summarised in Table 11.2.

Activation pattern

During atrial pacing, site 5 had the earliest MAP-AT in the heart failure group followed by site 6 and site 3. Ca^{2+} transient activation followed a similar pattern with the earliest Ca-AT at site 5 but followed by site 3 and then site 2. These suggest that early electrical activation and Ca^{2+} transients were recorded from the posterior area of the left ventricle in failing hearts.

Data in the sham-operated group were different with the earliest MAP-AT at site 12 followed by sites 10 and 15. Again the Ca^{2+} transient activation followed closely with the earliest Ca-AT at site 10 followed by sites 11 and 15. These suggest that early electrical activation and Ca^{2+} transients were recorded from the antero-septal portion of the left ventricle in control hearts.

Table 11.2 Comparison of Monophasic Action Potential and Ca^{2+} transient activation times (MAP-AT, Ca-AT) at the individual left ventricular epicardial sites in isolated hearts from rabbits with heart failure (HF) and controls (Sham) during atrial pacing.

Numbers in brackets represent the number of hearts in each group where Ca^{2+} transients and MAPs were measurable at each site.

Site	HF (n = 7)		Sham (n = 5)		p value	
	MAP-AT (ms)	Ca-AT (ms)	MAP-AT (ms)	Ca-AT (ms)	MAP-AT	Ca-AT
1	101.4 ± 9.4 (7)	123.9 ± 9.6 (7)	103.4 ± 3.4 (5)	116.8 ± 10.8 (5)	NS	NS
2	106.3 ± 5.2 (7)	116.3 ± 7.2 (7)	102.8 ± 5.7 (5)	118.6 ± 7.2 (5)	NS	NS
3	99.0 ± 11.9 (7)	112.1 ± 8.7 (7)	100.3 ± 4.5 (5)	113.3 ± 7.1 (5)	NS	NS
4	105.9 ± 14.1 (7)	117.7 ± 11.6 (7)	102.2 ± 4.1 (5)	113.1 ± 8.5 (5)	NS	NS
5	84.6 ± 12.7 (4)	103.0 ± 5.0 (4)	104.6 ± 6.3 (5)	115.4 ± 8.0 (5)	NS	NS
6	91.3 ± 19.6 (2)	119.3 ± 17.9 (2)	103.0 ± 4.4 (5)	116.8 ± 8.5 (5)	NS	NS
7	104.0 ± 8.2 (7)	121.2 ± 12.1 (7)	107.3 ± 8.6 (5)	113.1 ± 8.5 (5)	NS	NS
8	101.2 ± 9.1 (7)	130.9 ± 11.7 (7)	102.2 ± 7.1 (5)	109.5 ± 6.3 (5)	NS	NS
9	109.5 ± 6.5 (7)	132.5 ± 13.8 (7)	108.4 ± 8.2 (5)	112.4 ± 11.1 (5)	NS	NS
10	103.1 ± 5.6 (7)	125.7 ± 12.9 (7)	97.2 ± 5.4 (5)	101.2 ± 8.1 (5)	NS	NS
11	112.0 ± 29.0 (3)	125.0 ± 17.5 (3)	100.5 ± 6.5 (5)	108.3 ± 7.3 (5)	NS	NS
12	104.6 ± 8.9 (6)	126.7 ± 13.7 (6)	92.7 ± 5.9 (5)	109.4 ± 5.3 (5)	NS	NS
13	-	-	102.0 ± 6.4 (5)	113.6 ± 8.9 (5)	-	-
14	-	-	101.2 ± 6.1 (5)	116.8 ± 8.8 (5)	-	-
15	-	-	98.8 ± 10.7 (5)	108.6 ± 7.7 (5)	-	-

(b) (i) ANOVA and multiple comparison Tukey tests

As shown in Table 11.2, there was no difference in the MAP-AT or the Ca-AT recorded at any of the epicardial sites between the heart failure group and controls. In order to investigate the possibility that one of the epicardial sites may have consistently early or late activation in either of the experimental groups, single-factor ANOVA test was used in a similar way as described in Chapters 8 and 9 for relating the time course of the Ca^{2+} transient or MAP signals recorded at each site with the site location. The MAP-AT was examined in the heart failure group and an F-statistic of 0.37 was obtained (p = NS) whilst an F-statistic of 0.59 (p = NS) was obtained for the Ca-AT indicating that there was no single epicardial site in the failing hearts that was consistently activated early or late. Multiple comparison Tukey tests were also performed on all the pairs of measured sites which confirmed no consistent relationship between the site location and the MAP activation time or Ca^{2+} transient activation time in the failing hearts. Similar analyses were performed in the sham-operated group. Single factor ANOVA test yielded an F-statistics of 0.33 (p = NS) for MAP-AT and 0.34 (p = NS) for Ca-AT in the control hearts again indicating no consistent relationship between the site location and activation times. This was confirmed with Tukey tests.

(ii) ANOVA and multiple comparison Tukey tests - adjusted activation times

It was found that there was a wide variation in activation times between the different hearts during atrial pacing. Since the activation times were measured from the beginning of the atrial pacing stimulus to the beginning of the MAP signal or Ca^{2+} transient at the individual sites, the wide variation between hearts represents mainly the difference between atrio-ventricular delays in the individual hearts. This wide variation in atrio-ventricular delay

would mask the small variation in the true ventricular activation time within each heart and make it difficult to identify a pattern of activation with the above-mentioned ANOVA and Tukey tests. An attempt was made thus to correct the MAP-AT and Ca-AT at each measured site in each heart for the atrio-ventricular delay. Since the electrocardiogram was not measured in the isolated hearts, atrio-ventricular delay was not estimated. Thus, the activation times at the measured sites in each heart were adjusted by subtracting the shortest (earliest) activation time in that heart. The adjusted MAP-AT and adjusted Ca-AT at the measured sites in both experimental groups were analysed using ANOVA and Tukey tests and the results are summarised in Table 11.3.

It was shown by ANOVA and Tukey tests that there was no consistent relationship between the site location and the adjusted MAP-AT or adjusted Ca-AT in the failing hearts. The activation patterns in the individual failing heart may be different and hence produced no consistent trend in the group. However, when the adjusted activation times were analysed in the control group, a pattern was observed. ANOVA and Tukey tests on the adjusted MAP-AT showed that site 12 was earlier than site 9. This suggests a consistent activation pattern in the control hearts during atrial pacing with the anteroseptal region being activated first and the basal portion last. The adjusted Ca-AT followed a similar trend with sites around the anteroseptal region (sites 10, 11, 12, 15) being activated earlier than the posterobasal region (sites 1, 2, 4).

Table 11.3 Results of single-factor analysis of variance (ANOVA) and multiple comparison Tukey test on adjusted Monophasic Action Potential and Ca^{2+} transient activation times (MAP-AT and Ca-AT, see text) recorded during atrial pacing at different epicardial sites in hearts from the heart failure group (HF, n = 7) and controls (Sham, n = 5).

	ANOVA		Tukey test	
	F - statistic	p value	site vs. site	p value
HF				
adjusted MAP-AT	1.03	NS	N/A	NS
adjusted Ca-AT	1.04	NS	N/A	NS
Sham				
adjusted MAP-AT	1.93	< 0.04	12 < 9	< 0.05
adjusted Ca-AT	4.24	< 0.001	10 < 1	< 0.01
			10 < 2	< 0.05
			10 < 4	< 0.05
			11 < 1	< 0.05
			12 < 1	< 0.01
			12 < 2	< 0.01
			12 < 4	< 0.05
			12 < 6	< 0.05
			12 < 7	< 0.05
			15 < 1	< 0.05

(c) relationship between MAP-AT and Ca-AT

It was suggested in the previous section on *"Heart by heart analysis"* that the difference between MAP-AT and Ca-AT (i.e. the time delay between electrical and Ca^{2+} events) was greater in the heart failure group as shown in the mean values of the two parameters. This difference was examined at each of the epicardial sites. It was found that the difference between the local MAP activation time and Ca^{2+} transient activation time was greater in failing hearts than in controls (19.3 ± 1.9 ms vs. 10.7 ± 1.1 ms, $p < 0.001$). This suggests that there was greater delay between the electrical and Ca^{2+} events in the failing hearts.

The MAP-AT and corresponding Ca-AT at each epicardial site were then compared and correlated for the 2 experimental groups. The results are illustrated in Figure 11.1 Linear regression lines were drawn and these showed that there was a strong association between the Ca-AT and MAP-AT in both experimental groups. The Ca-AT at each site followed the MAP-AT closely. It was also shown that there was a greater variation in MAP-AT and Ca-AT values at the various epicardial sites in the heart failure group when compared to the sham-operated controls although the mean value appeared to be similar. The variation or dispersion of activation time as a measure of intraventricular conduction delay will be discussed later.

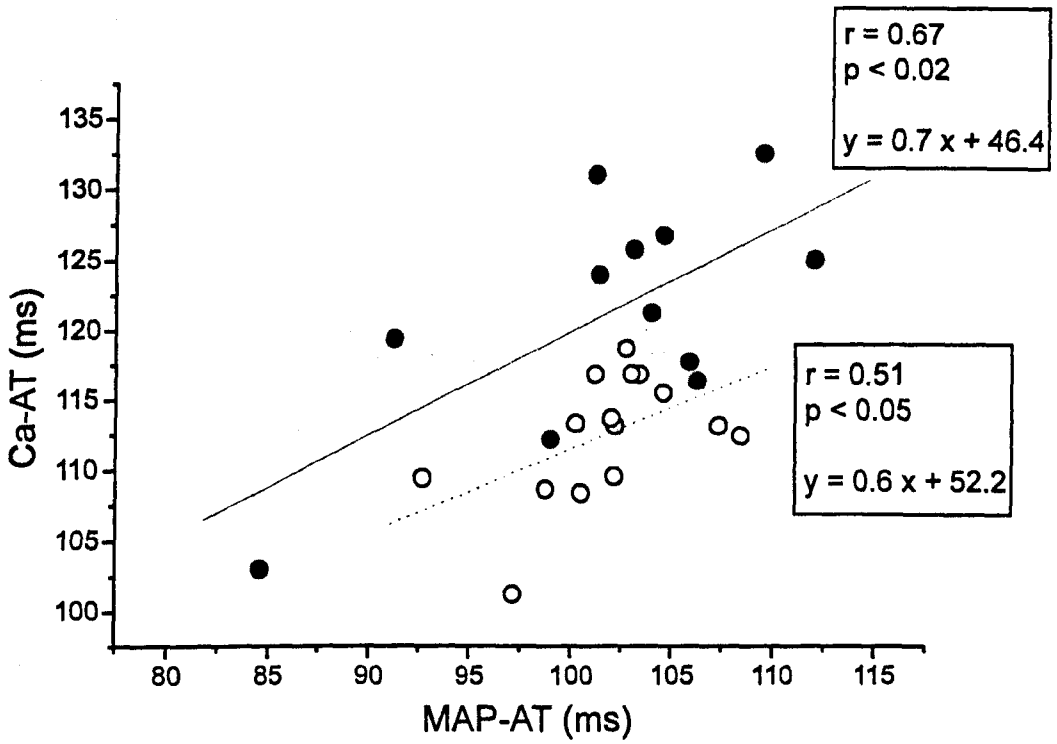

Figure 11.1 Plot of the mean Ca^{2+} transient activation time (Ca-AT) at each epicardial site against the corresponding mean Monophasic Action Potential activation time (MAP-AT) during right atrial pacing at a cycle length of 350 ms for both control (O) and heart failure (●) groups. Linear regression lines of the two variables are shown for the heart failure group (solid line) and controls (broken line) with the correlation coefficient (r), significance value (p) and regression equation shown in boxes.

(2) Ventricular pacing

Similar analyses as those performed for studying the activation pattern during atrial pacing were also carried out for ventricular pacing. The averaged MAP-AT and Ca-AT in the 2 experimental groups at each epicardial site are summarised in Table 11.4.

Activation pattern

During ventricular pacing, site 5 had the earliest MAP-AT in the heart failure group followed by site 3 and site 6. Ca^{2+} transient activation followed a similar pattern with the earliest Ca-AT at site 5, followed by site 3 and then site 1. These suggest that early electrical activation and Ca^{2+} transients were recorded from the posterior area of the left ventricle in failing hearts. Sites 7 and 8 recorded late Ca^{2+} and MAP signals indicating late activation at the anterior and basal portions of the left ventricle. Ventricular pacing electrodes were placed at the posterior aspect of the right ventricular apex. This would be consistent with early activation at site 5 during ventricular pacing and late activation in sites 7 and 8. The pattern of activation in the failing hearts during ventricular pacing was similar to that during atrial pacing with the earliest activation at the posterior area and late activation at the antero-basal area of the left ventricle.

Data in the sham-operated group during ventricular pacing were similar to the heart failure group with the earliest MAP-AT at site 5 followed by sites 13 and 3. Again the Ca^{2+} transient activation followed closely. Late MAP-AT and Ca-AT were recorded at sites 7 and 8. The pattern of activation during ventricular pacing was similar in controls to that in failing hearts with early activation at the postero-apical portion of the left ventricle, next to the pacing site, and late activation at the antero-basal portion of the left ventricle. This was distinctly different from the pattern of activation in the control hearts during atrial pacing.

The patterns of activation during atrial and ventricular pacing in the 2 experimental groups are illustrated in Figure 11.2 using colour coding for the mean MAP-AT at the measured sites.

Table 11.4 Comparison of Monophasic Action Potential and Ca^{2+} transient activation times (MAP-AT, Ca-AT) at the individual left ventricular epicardial sites in isolated hearts from rabbits with heart failure (HF) and controls (Sham) during ventricular pacing.

Numbers in brackets represent the number of hearts in each group where Ca^{2+} transients and MAPs were measurable at each site.

Site	HF (n = 7)		Sham (n = 5)		p value	
	MAP-AT (ms)	Ca-AT (ms)	MAP-AT (ms)	Ca-AT (ms)	MAP-AT	Ca-AT
1	32.8 ± 5.0 (7)	36.0 ± 3.5 (7)	34.5 ± 4.3 (5)	35.3 ± 2.4 (5)	NS	NS
2	36.7 ± 5.3 (7)	42.4 ± 4.7 (7)	38.0 ± 4.4 (5)	38.6 ± 3.4 (5)	NS	NS
3	23.0 ± 5.3 (7)	34.0 ± 5.1 (7)	28.0 ± 4.5 (5)	29.4 ± 2.8 (5)	NS	NS
4	34.0 ± 7.1 (7)	42.3 ± 5.5 (7)	30.3 ± 4.6 (5)	35.5 ± 3.7 (5)	NS	NS
5	20.0 ± 6.1 (4)	29.3 ± 8.1 (4)	22.0 ± 2.9 (5)	26.9 ± 6.1 (5)	NS	NS
6	28.0 ± 7.9 (2)	59.0 ± 9.2 (2)	35.6 ± 4.9 (5)	36.7 ± 5.0 (5)	NS	NS
7	43.0 ± 3.7 (7)	64.0 ± 5.8 (7)	46 ± 4.0 (5)	59.7 ± 2.8 (5)	NS	NS
8	45.7 ± 3.3 (7)	61.0 ± 4.2 (7)	46.6 ± 1.7 (5)	52.5 ± 4.8 (5)	NS	NS
9	45.3 ± 1.1 (7)	53.0 ± 3.5 (7)	44.3 ± 3.5 (5)	56.4 ± 8.2 (5)	NS	NS
10	38.8 ± 3.4 (7)	56.3 ± 7.1 (7)	43.0 ± 1.4 (5)	51.2 ± 5.5 (5)	NS	NS
11	34.0 ± 8.2 (3)	38.0 ± 8.5 (3)	37.4 ± 2.0 (5)	44.1 ± 2.4 (5)	NS	NS
12	34.3 ± 1.2 (6)	45.2 ± 3.0 (6)	34.2 ± 5.1 (5)	47.8 ± 1.8 (5)	NS	NS
13	-	-	26.6 ± 4.7 (5)	28.5 ± 5.2 (5)	-	-
14	-	-	30.3 ± 6.5 (5)	33.9 ± 5.5 (5)	-	-
15	-	-	29.8 ± 1.3 (5)	39.0 ± 4.7 (5)	-	-

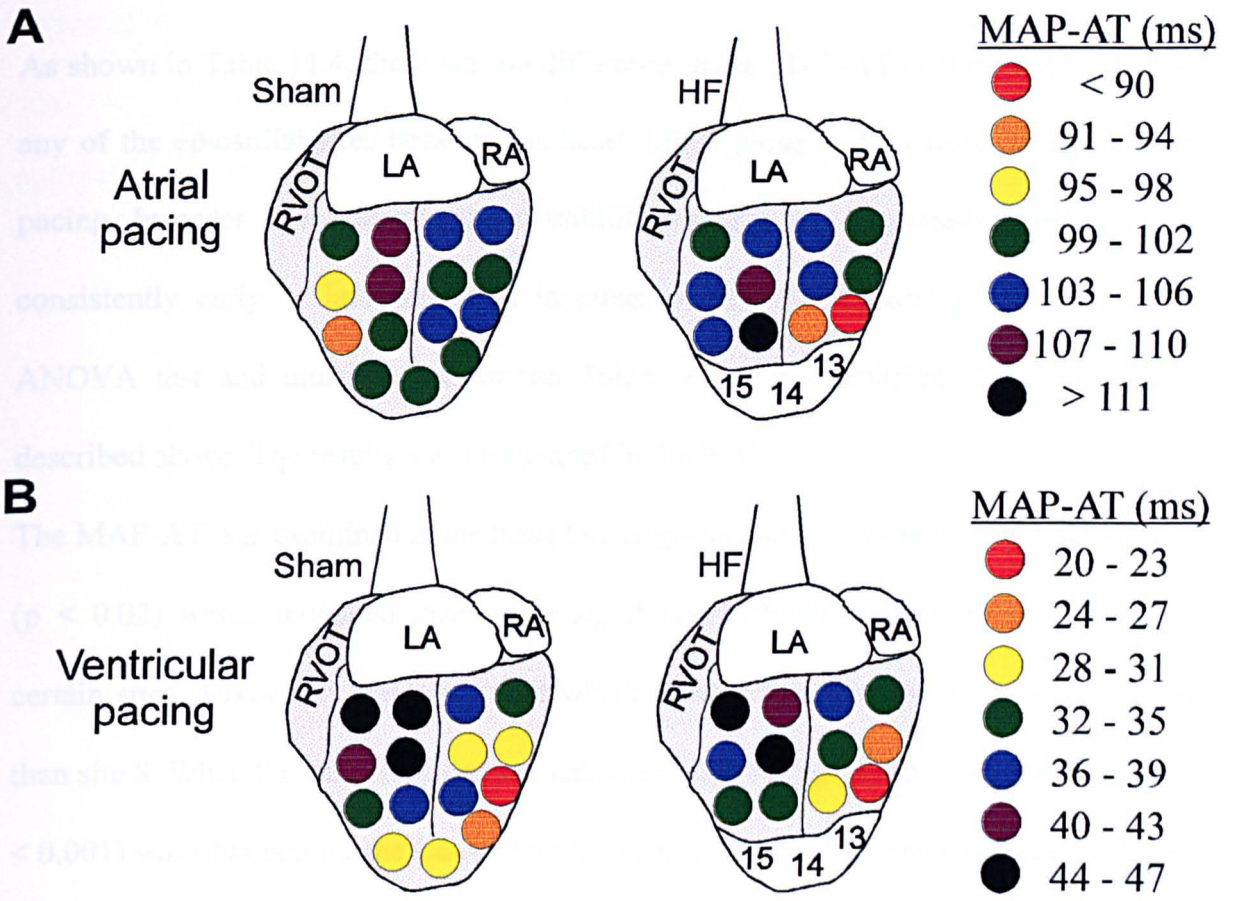

Figure 11.2 Panel A shows schematic diagrams of two rabbit hearts with right ventricle outflow tract (RVOT), left atrium (LA) and right atrium (RA) marked as shown - the heart on the right represents one from the heart failure group (HF) and the one on the left from the control group (Sham). The marginal branch of the left circumflex artery is represented by a vertical line on the left ventricle and the infarct in the HF heart is marked by the non-shaded area with site numbers 13, 14 and 15 representing the sites with a consistent infarct. The mean Monophasic Action Potential activation time (MAP-AT) at all of the measured sites, during right atrial pacing at a cycle length of 350 ms, are coded according to the colour scale shown on the right and illustrated for the 2 groups. Panel B shows parallel data for MAP-AT during pacing near the right ventricular apex.

(b) ANOVA and multiple comparison Tukey tests

As shown in Table 11.4, there was no difference in the MAP-AT or the Ca-AT recorded at any of the epicardial sites between the heart failure group and controls during ventricular pacing. In order to investigate the possibility that one of the epicardial sites may have consistently early or late activation in either of the experimental groups, single-factor ANOVA test and multiple comparison Tukey test were employed as for atrial pacing described above. The results are summarised in Table 11.5.

The MAP-AT was examined in the heart failure group and an F-statistic of 2.6 was obtained ($p < 0.02$) which indicated there were significant differences between the MAP-AT at certain sites. Tukey test was performed which showed that site 5 was significantly earlier than site 8. When the Ca-AT was examined in the heart failure group, an F-statistic of 5.6 ($p < 0.001$) was obtained for the Ca-AT indicating again that there were significant differences between the Ca-AT at certain sites. Tukey test showed that site 1 was significantly earlier than sites 7, 8 and 10; site 3 was significantly earlier than sites 7 and 8; and site 5 was significantly earlier than sites 7, 8 and 10. These results confirm the initial impression from the mean data above that the posterior portion of the left ventricle was activated early and the antero-basal portion activated late during ventricular pacing in the heart failure group.

Similar analyses were performed in the sham-operated group. Single factor ANOVA test yielded an F-statistic of 3.6 ($p < 0.001$) for MAP-AT and 5.0 ($p < 0.001$) for Ca-AT in the control hearts which indicated there were significant differences between the activation times at certain sites. Tukey tests were then performed to examine pairs of sites. For MAP-AT, site 5 was significantly earlier than sites 7, 8, 9 and 10 and site 13 was significantly earlier than sites 7 and 8. For Ca-AT, both sites 3 and 5 were significantly earlier than sites 7, 8, 9, and 10; sites 6, 13 and 14 were significantly earlier than site 7; and in addition, site

13 was also significantly earlier than site 9. Again, these data supported the initial impression from the mean values of MAP-AT and Ca-AT at the different activation sites that early activation occurred at the postero-apical portion of the left ventricle with late activation at the antero-basal portion in control hearts during ventricular pacing.

Table 11.5 Results of single-factor analysis of variance (ANOVA) and multiple comparison Tukey test on Monophasic Action Potential and Ca^{2+} transient activation times (MAP-AT and Ca-AT) recorded during ventricular pacing at different epicardial sites in hearts from the heart failure group (HF, n = 7) and controls (Sham, n = 5).

	ANOVA		Tukey test	
	F - statistic	p value	site vs. site	p value
HF				
MAP-AT	2.6	< 0.02	5 < 8	< 0.05
Ca-AT	5.6	< 0.001	1 < 7	< 0.01
			1 < 8	< 0.01
			1 < 10	< 0.05
			3 < 7	< 0.01
			3 < 8	< 0.05
			5 < 7	< 0.01
			5 < 8	< 0.01
			5 < 10	< 0.05
Sham				
MAP-AT	3.6	< 0.001	5 < 7	< 0.01
			5 < 8	< 0.01
			5 < 9	< 0.05
			5 < 10	< 0.05
			13 < 7	< 0.05
			13 < 8	< 0.05
Ca-AT	5.0	< 0.001	3 < 7	< 0.01
			3 < 8	< 0.05
			3 < 9	< 0.01
			3 < 10	< 0.05
			5 < 7	< 0.001
			5 < 8	< 0.05
			5 < 9	< 0.01
			5 < 10	< 0.05
			6 < 7	< 0.05
			13 < 7	< 0.01
			13 < 9	< 0.01
			14 < 7	< 0.05

(c) relationship between MAP-AT and Ca-AT

As with the data during atrial pacing, the difference between MAP-AT and Ca-AT was examined at each of the epicardial sites during ventricular pacing in the 2 experimental groups. It was found that the difference between the local MAP activation time and Ca^{2+} transient activation time was greater in failing hearts than in controls (12.1 ± 2.3 ms vs. 5.9 ± 1.2 ms, $p < 0.02$). This suggests again that there was greater delay between the electrical and Ca^{2+} events in the failing hearts during ventricular pacing as well as during atrial pacing.

The MAP-AT and corresponding Ca-AT at each epicardial site were then compared and correlated for the 2 experimental groups. The results are illustrated in Figure 11.3. Linear regression lines were drawn and these showed that there was a strong association between the Ca-AT and MAP-AT in both experimental groups. The Ca-AT at each sites followed the MAP-AT closely as with atrial pacing. The data from the 2 experimental groups were very similar with similar mean values as demonstrated earlier. The variation in MAP-AT and Ca-AT values at the various epicardial sites were not so different between the 2 groups as seen in the data during atrial pacing. This would appear that the pattern of ventricular activation and possibility conduction delay were similar in the 2 groups during ventricular pacing but different during atrial pacing. This will be discussed below especially examining the variation or dispersion of activation time as a measure of intraventricular conduction delay.

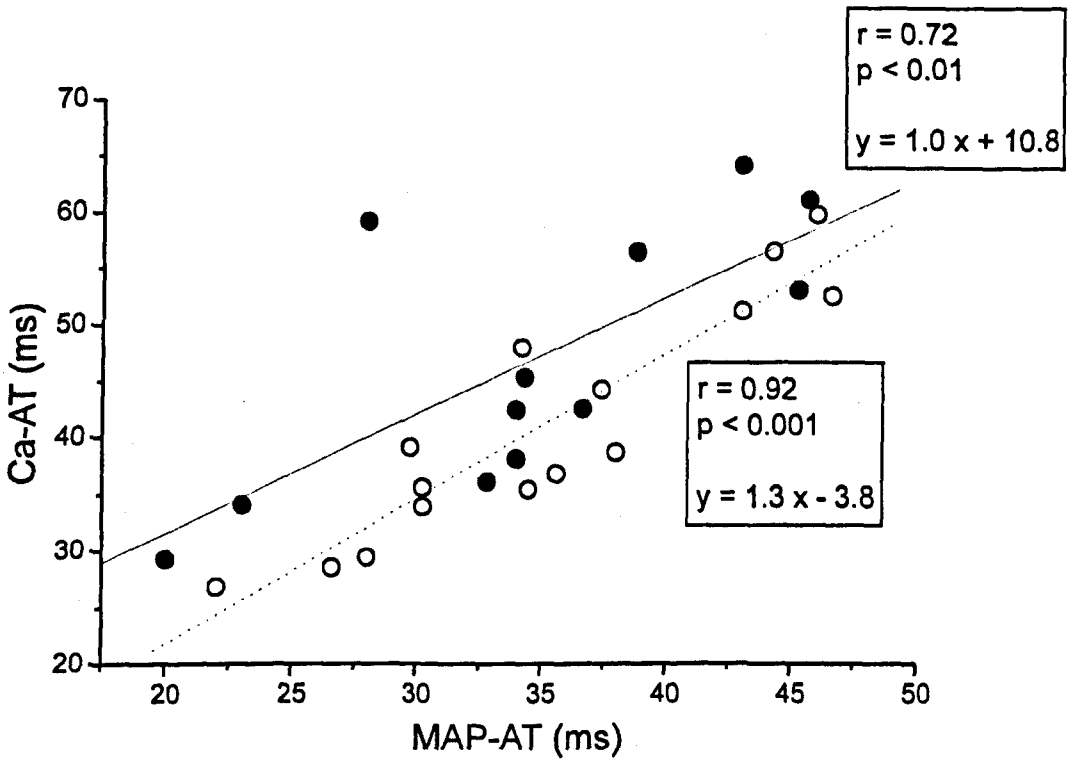

Figure 11.3 Plot of the mean Ca^{2+} transient activation time (Ca-AT) at each epicardial site against the corresponding mean Monophasic Action Potential activation time (MAP-AT) during right ventricular pacing at a cycle length of 350 ms for both control (○) and heart failure (●) groups. Linear regression lines of the two variables are shown for the heart failure group (solid line) and controls (broken line) with the correlation coefficient (r), significance value (p) and regression equation shown in boxes.

Intraventricular conduction delay

As shown in the above sections on MAP and Ca^{2+} transient activation times, the pattern of activation was different during atrial pacing between the heart failure group and controls whilst the pattern of activation was similar on ventricular pacing. It was shown that the pattern of activation was different between atrial and ventricular pacing in the control group whilst it was quite similar between atrial and ventricular pacing in the heart failure group. This implies that there may be some abnormality in ventricular activation in failing hearts during atrial pacing. Normally, atrial pacing leads to ventricular activation via the specialised conducting tissues with almost synchronous activation of the whole ventricle whilst ventricular pacing usually leads to delayed ventricular conduction with the ventricle being activated sequentially from myocyte to myocyte not involving the specialised conducting system. Right ventricular pacing typically leads to a left bundle branch block pattern on the surface electrocardiogram. Thus, there may be abnormality in intraventricular conduction in the failing hearts during atrial pacing. This was investigated by examining the variation or dispersion of the activation times in both experimental groups.

Intraventricular conduction delay could be estimated by studying the earliest and latest activation times in each heart. The adjusted dispersion of MAP activation times and Ca^{2+} transient activation times were calculated in each heart by taking the difference between the earliest and latest activation time divided by the square root of the number of measured sites. This was used as a measure of intraventricular conduction delay and the results are shown in Table 11.6.

Firstly, it was shown that adjusted dispersion for MAP-AT was increased in the heart failure group during atrial pacing when compared to controls (6.6 ± 0.9 ms vs. 4.3 ± 0.2 ms, $p < 0.05$). The increased adjusted MAP-AT dispersion suggests that there was a wider range of

electrical activation times in the failing hearts leading to increased intraventricular conduction delay. In the control hearts, the adjusted MAP-AT dispersion increased significantly from 4.3 ± 0.2 ms to 9.0 ± 0.8 ms on transition from atrial to ventricular pacing ($p < 0.01$). This was consistent with increased intraventricular conduction delay with right ventricular pacing which is known to produce altered intraventricular conduction similar to that seen in left bundle branch block. The adjusted MAP-AT dispersion was 6.6 ± 0.9 ms in the failing hearts during atrial pacing indicating that there was delayed intraventricular conduction compared to controls but the magnitude of the delay was smaller than that seen in control hearts during ventricular pacing. This suggests that the intraventricular conduction delay observed in failing hearts during atrial pacing was less than that during left bundle branch block. Unfortunately, this could not be confirmed with electrocardiogram as this was not measured but the coronary ligation procedure could not have directly caused damage to the conducting system as the infarct produced was typically at the left ventricular apex. In the failing hearts, ventricular pacing led to a non-significant rise in the adjusted MAP-AT dispersion to 8.4 ± 0.8 ms indicating some further intraventricular conduction delay with ventricular pacing compared to atrial pacing.

The adjusted Ca-AT dispersion followed a similar trend as the adjusted dispersion for MAP-AT. However, the significance of an increased adjusted Ca-AT dispersion in the failing hearts during atrial and ventricular pacing with a wider range of Ca-AT in failing hearts is more difficult to appreciate. It was shown in earlier sections that the delay between MAP-AT and Ca-AT was increased in failing hearts. Even in the absence of delayed intraventricular conduction, there could have been a wider range of Ca-AT depending on the MAP-AT to Ca-AT delay at the various epicardial sites. Increased intraventricular

conduction delay in the failing hearts as shown by the increased MAP-AT dispersion would lead to even greater Ca-AT dispersion.

Table 11.6 Comparison of adjusted dispersion in Monophasic Action Potential activation time (MAP-AT) and Ca^{2+} transient activation time (Ca-AT) (see text) in isolated hearts from rabbits with heart failure (HF) and controls (Sham) during atrial and ventricular pacing.

	HF (n = 7)	Sham (n = 5)	p value
Adjusted dispersion in MAP-AT (ms)			
Atrial pacing	6.6 ± 0.9	4.3 ± 0.2	< 0.05
Ventricular pacing	8.4 ± 0.8	9.0 ± 0.8	NS
p value	NS	< 0.01	
Adjusted dispersion in Ca-AT (ms)			
Atrial pacing	19.9 ± 3.9	6.8 ± 0.7	< 0.02
Ventricular pacing	16.4 ± 1.5	9.7 ± 0.7	< 0.01
p value	NS	< 0.05	

Effect of atrial and ventricular pacing on intraventricular conduction delay

As shown above, the adjusted dispersions for MAP-AT and Ca-AT were increased in the failing hearts during atrial pacing and there appeared to be different changes to these parameters on switching from atrial to ventricular pacing. A relationship was sought between the adjusted MAP-AT and Ca-AT dispersions during atrial pacing and the effect of switching to ventricular pacing. The adjusted dispersions in each heart during atrial pacing were correlated with the change (increase or decrease) in these parameters on switching from atrial to ventricular pacing. The results are illustrated in Figures 11.4 and 11.5.

Figure 11.4 shows that there was a significant association between the adjusted MAP-AT dispersion, i.e. intraventricular conduction delay, during atrial pacing and the effect of ventricular pacing on dispersion. It shows that hearts which had little intraventricular conduction delay during atrial pacing , i.e. all of the control hearts and some of the failing hearts, had increased conduction delay on ventricular pacing whilst the remainder of the failing hearts which started with significant conduction delay during atrial pacing had little change or a small decrease in the intraventricular conduction delay on ventricular pacing.

Again, a similar trend emerged with the data on adjusted Ca-AT dispersion during atrial pacing and the effect of ventricular pacing with Figure 11.5 showing a significant association between them. Hearts which had a small adjusted Ca-AT dispersion during atrial pacing, i.e. again all the control hearts and some failing hearts, had increased Ca-AT dispersion on ventricular pacing whilst the remainder of the failing hearts which had increased Ca-AT dispersion during atrial pacing had a decrease in Ca-AT dispersion on ventricular pacing. As mentioned above, it is difficult to appreciate the significance of increased Ca-AT dispersion in the failing hearts as the relationship between Ca^{2+} transient activation time and MAP activation time could be a complex one. With increased MAP-AT

dispersion in the failing hearts and the heterogeneous behaviour of MAP-AT dispersion on ventricular pacing, it is even more difficult to understand the true significance of the events that occur with Ca-AT dispersion.

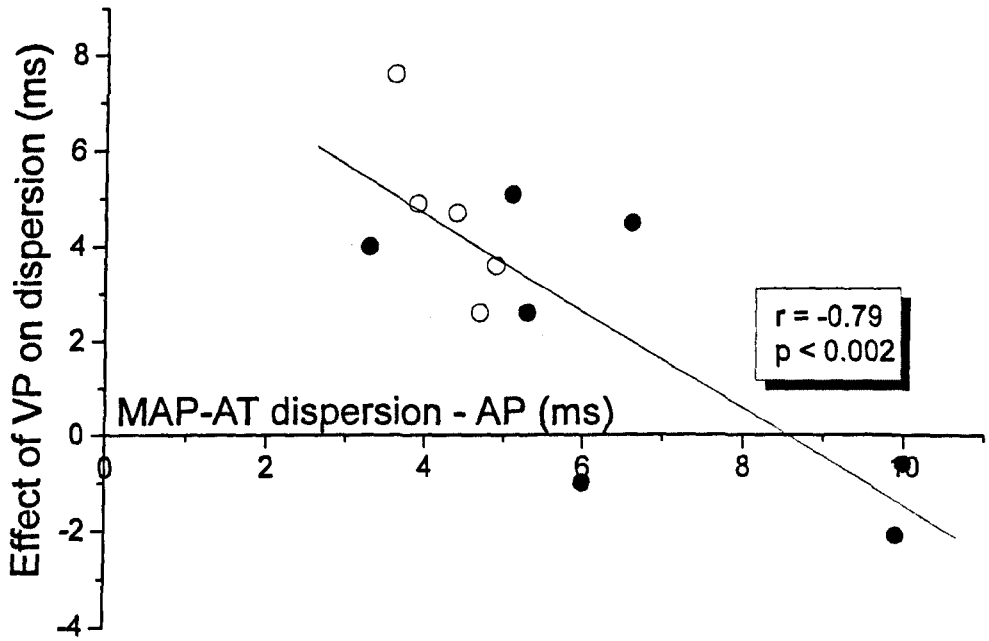

Figure 11.4 Plot of the change in adjusted dispersion of Monophasic Action Potential activation time (MAP-AT dispersion) in each heart on switching from atrial to ventricular pacing (VP) against the MAP-AT dispersion during atrial pacing (AP) at a cycle length of 350 ms for both control (○) and heart failure (●) groups. The solid line represents linear regression of the two variables with the correlation coefficient (r) and significance value (p) shown in the shaded box.

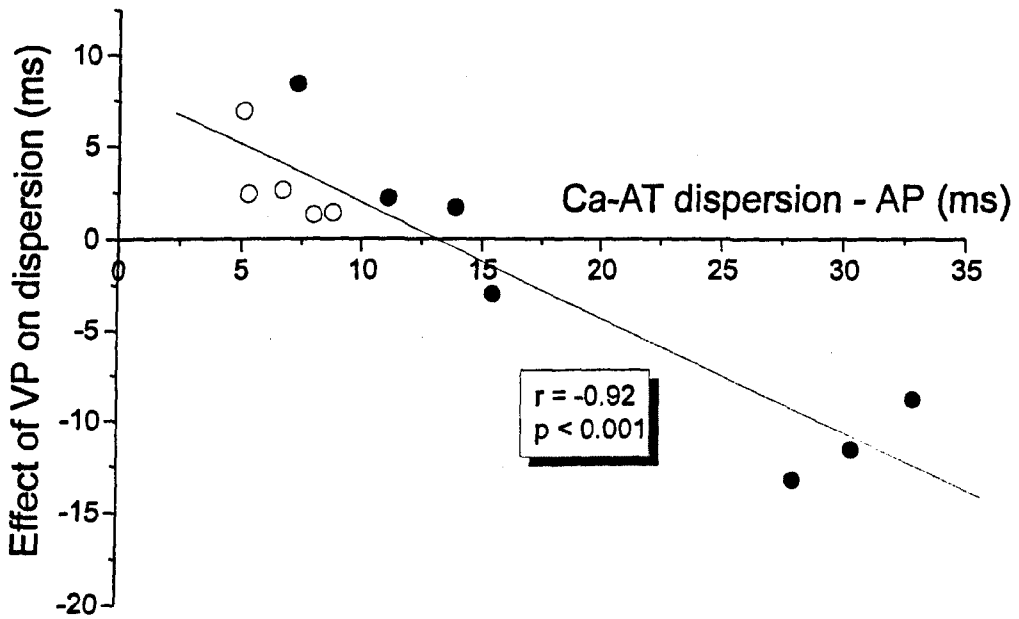

Figure 11.5 Plot of the change in adjusted dispersion of Ca^{2+} transient activation time (Ca-AT dispersion) in each heart on switching from atrial to ventricular pacing (VP) against the Ca-AT dispersion during atrial pacing (AP) at a cycle length of 350 ms for both control (○) and heart failure (●) groups. The solid line represents linear regression of the two variables with the correlation coefficient (r) and significance value (p) shown in the shaded box.

Effect of altered conduction pattern on cardiac performance

The above sections showed that the ventricular activation pattern was different during atrial and ventricular pacing in normal hearts and intraventricular conduction delay was increased during ventricular pacing when compared to atrial pacing. In failing hearts, the ventricular activation pattern was different from that in controls during atrial pacing with increased intraventricular conduction delay and the response to ventricular pacing was different from that in controls. Previous Chapters have demonstrated significant mechanical dysfunction in the hearts isolated from rabbits with coronary artery ligation induced heart failure. This section investigates the relationship between the altered ventricular activation pattern with delayed intraventricular conduction and the impaired mechanical performance in the failing hearts. The pressure profile of the 2 experimental groups during atrial and ventricular pacing were analysed and the results are shown in Table 11.7.

Peak systolic pressure

During atrial pacing, peak systolic pressure was significantly lower in failing hearts as compared to controls (36.9 ± 6.3 mmHg vs. 49.6 ± 3.0 mmHg, $p < 0.05$) indicating significant left ventricular dysfunction. The effects of changing from atrial to ventricular pacing in typical experiments in a failing heart and a sham-operated heart are shown in Figure 11.6. There was a significant decrease in peak systolic pressure in sham-operated hearts on changing from atrial to ventricular pacing but not in failing hearts. The difference in peak systolic pressure between the 2 groups became marginal on ventricular pacing (36.1 ± 6.4 mmHg in failing hearts vs. 46.7 ± 2.8 mmHg in controls, $p = 0.08$).

Table 11.7 Comparison of pressure profile in isolated Langendorff perfused hearts from rabbits with heart failure (HF) and controls (Sham) during atrial and ventricular pacing.

	HF (n = 7)	Sham (n = 5)	p value
Peak Systolic Pressure (mmHg)			
Atrial pacing	36.9 ± 6.3	49.6 ± 3.0	< 0.05
Ventricular pacing	36.1 ± 6.4	46.7 ± 2.8	0.08
p value	NS	< 0.001	
Maximum rate of pressure rise [$+dP.dt^{-1}_{(max)}$ - $mmHg.ms^{-1}$]			
Atrial pacing	0.67 ± 0.08	0.99 ± 0.09	< 0.02
Ventricular pacing	0.63 ± 0.08	0.89 ± 0.07	< 0.05
p value	0.08	< 0.05	
Maximum rate of pressure decay [$-dP.dt^{-1}_{(max)}$ - $mmHg.ms^{-1}$]			
Atrial pacing	0.43 ± 0.06	0.64 ± 0.05	< 0.05
Ventricular pacing	0.41 ± 0.05	0.58 ± 0.05	< 0.05
p value	NS	< 0.05	

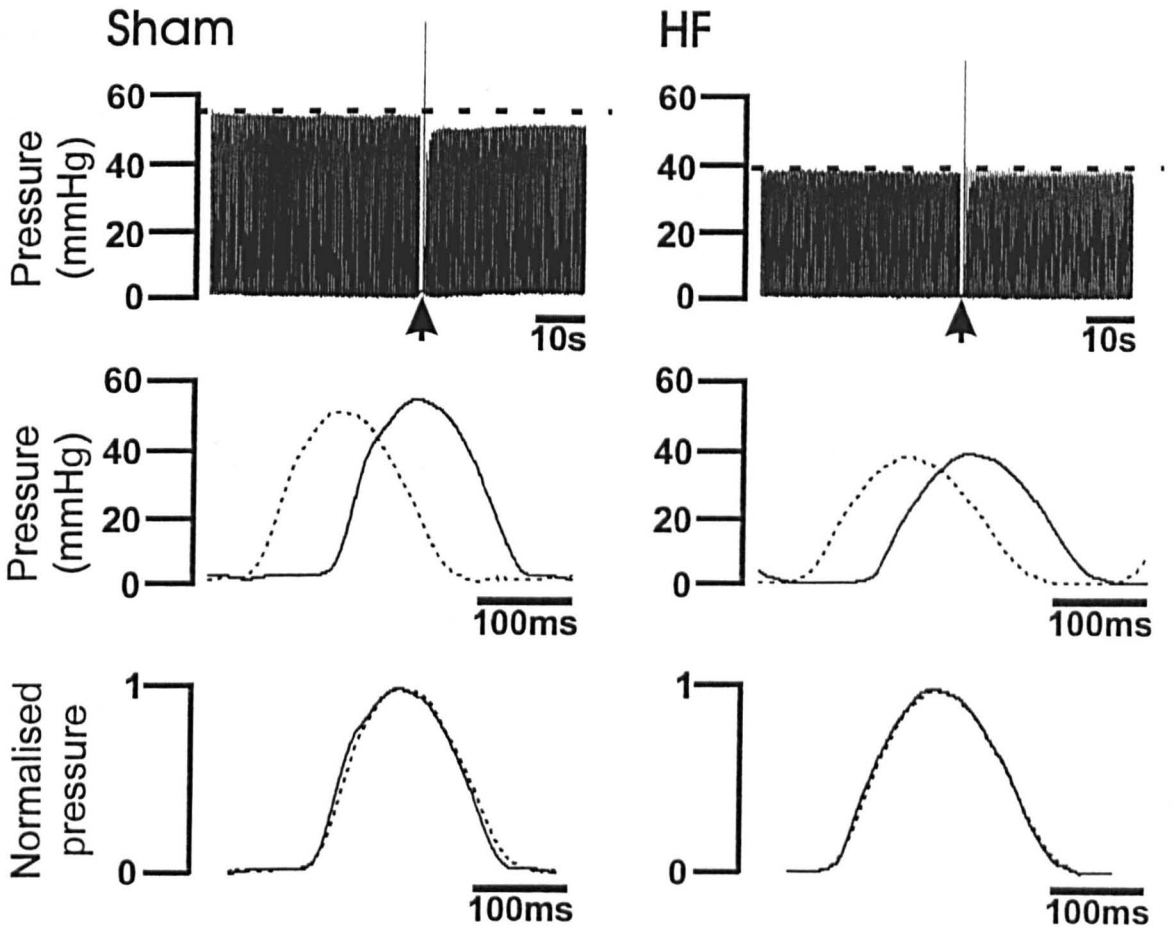

Figure 11.6 Top Panel Left ventricular pressure in a control heart (Sham) and a failing heart (HF) shown as continuous tracing with arrows marking the change from right atrial to right ventricular pacing at a constant cycle length of 350 ms. Middle Panel Left ventricular pressure shown in expanded scale for one cardiac cycle at steady state during atrial pacing (solid line) and ventricular pacing (broken line), aligned at the stimulus impulse. Bottom Panel Expanded pressure tracings for one cardiac cycle as in (Middle Panel) normalised and superimposed.

Maximum rates of pressure rise and decay

The results of the maximum rate of pressure rise and of pressure decay followed a similar trend as that seen in peak systolic pressure (Table 11.7). These values were lower in the heart failure group when compared to controls during atrial and ventricular pacing. On changing from atrial to ventricular pacing, there was a significant decrease in both parameters in the control hearts but not in the failing hearts. This again illustrated the presence of systolic and diastolic dysfunction in the failing hearts.

Pressure profile vs. Conduction delay

The changes in peak systolic pressure in both experimental groups with atrial and ventricular pacing paralleled those seen in conduction delay as measured by adjusted MAP-AT dispersion with atrial and ventricular pacing (Tables 11.6 and 11.7). There was a significant increase in conduction delay with a significant decrease in systolic pressure in the control hearts on changing from atrial to ventricular pacing. There was a slight increase in conduction delay and slight decrease in pressure in failing hearts on transition from atrial to ventricular pacing but these changes were not significant. It would appear that the decrease in systolic pressure on ventricular pacing could be related to the increase in conduction delay. Changes in systolic pressure were thus correlated with changes in adjusted MAP-AT dispersion on changing from atrial to ventricular pacing and Figure 11.7 shows that there was a significant association between the 2 parameters ($r = -0.75$, $p < 0.005$).

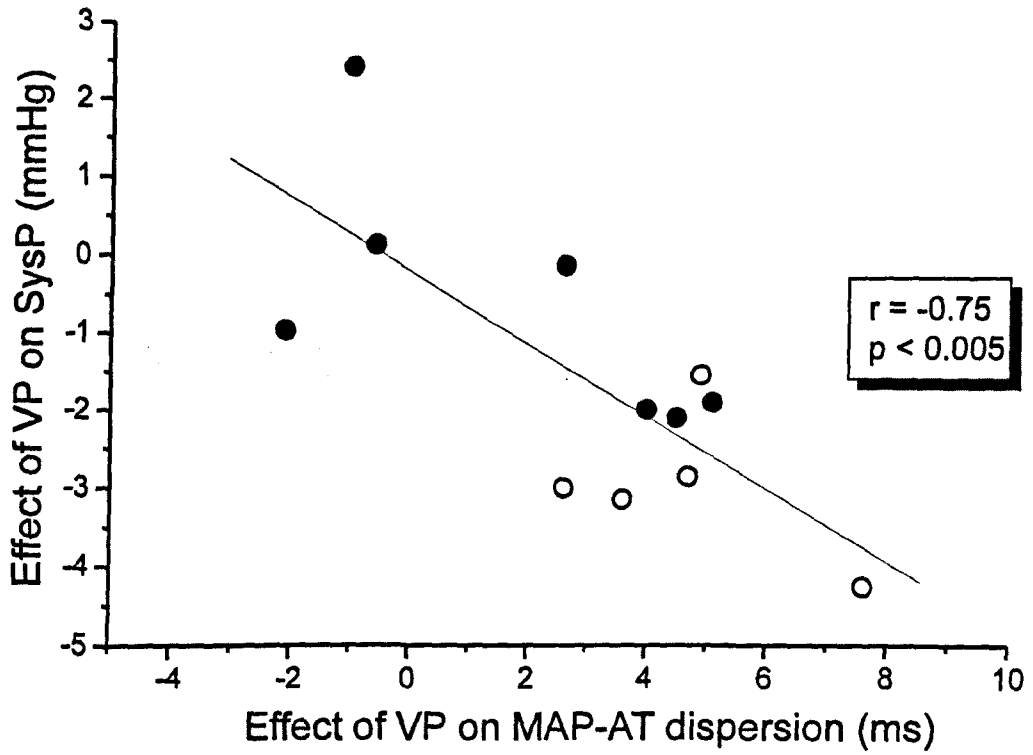

Figure 11.7 **Plot of the change in peak left ventricular systolic pressure (SysP) on switching from atrial to ventricular pacing (VP) in each heart against the corresponding change in the adjusted dispersion of Monophasic Action Potential activation time for both control (O) and heart failure (●) groups. The solid line is the linear regression of the two variables with the correlation coefficient (r) and significance value (p) shown in the shaded box.**

Contribution of conduction delay to mechanical dysfunction in heart failure

During atrial pacing, adjusted MAP-AT dispersion in failing hearts and hence conduction delay was increased when compared to controls (6.6 ± 0.9 ms vs. 4.3 ± 0.2 ms, $p < 0.05$) but this conduction delay in the failing hearts during atrial pacing was smaller in magnitude when compared to the conduction delay in control hearts during ventricular pacing (9.0 ± 0.8 ms). This implies that although there was conduction delay in the failing hearts during atrial pacing, the delay was not to the extent of left bundle branch block as would be expected from right ventricular pacing in the control hearts. The mean decrease in systolic pressure in the control hearts from atrial to ventricular pacing was 2.9 ± 0.4 mmHg and this is small when compared to the difference in systolic pressure between failing hearts and controls during atrial pacing (36.9 ± 6.3 mmHg vs. 49.6 ± 3.0 mmHg).

Similarly, the maximum rate of pressure rise and of pressure decay during atrial pacing were much lower in the failing hearts, when compared to controls, than would be expected simply due to delayed intraventricular conduction in controls hearts on right ventricular pacing. Although delayed intraventricular conduction could contribute to systolic and diastolic dysfunction, there had to be additional factors leading to the impaired cardiac performance in failing hearts.

Discussion

The results described in this Chapter showed that ventricular activation pattern was altered with delayed intraventricular conduction in hearts from rabbits with heart failure and this could explain at least part of the mechanical dysfunction seen in heart failure.

During atrial pacing, the ventricles should be activated via the specialised conducting His-Purkinje system in normal hearts. The left ventricular activation pattern in the control hearts

during atrial pacing followed a similar pattern as that described by Durrer *et al.* (1970) with early activation near the paraseptal region and late activation near the basal portion of the left ventricle. Intraventricular conduction delay was small with a brief total ventricular activation time. Right ventricular pacing altered the ventricular activation pattern with delayed intraventricular conduction / excitation. Systolic and diastolic performance were impaired on ventricular pacing. The better mechanical performance during atrial pacing (when compared to ventricular pacing) could not be attributed to improved left ventricular filling with atrial pacing as there was an intraventricular balloon in the left ventricle with cardiac contraction being isovolumetric in the Langendorff mode. In addition, the pulmonary veins leading to the left atrium were not tied off in these experiments and thus atrial contraction would have no haemodynamic consequences on left ventricular filling.

In the failing hearts, the ventricular activation pattern during atrial pacing was different from that in controls. There was early ventricular activation at the posterior part of the left ventricle, similar to the pattern seen during right ventricular pacing in either control or failing hearts. Intraventricular conduction was delayed during atrial pacing when compared to controls. The presence of left bundle branch block in the failing hearts could not be ruled out but this was thought not to be the case for several reasons:- (a) the myocardial infarct produced in these hearts was consistently at the apical region of the left ventricle and should not directly involve the left bundle branch and (b) conduction delay, as measured by adjusted MAP-AT dispersion, in the failing heart during atrial pacing was smaller than the conduction delay produced by right ventricular pacing in control hearts, which should produce ventricular activation similar to left bundle branch block pattern. Electrocardiography was not performed in these experiments which should otherwise produce extra information on intraventricular conduction and identify any potential

conducting system disturbance. One other criticism of this study may be the fact that the MAP signals and Ca^{2+} transients were sequentially measured. Simultaneous measurements at the various epicardial sites would have given more accurate activation data but this would require much more sophisticated equipment arrangements and more advanced technology. The delayed intraventricular conduction seen in failing hearts during atrial pacing could be due to intercellular uncoupling within the remodelled myocardium. On ventricular pacing, there was further increase in intraventricular conduction delay with ventricular activation possibly resembling that of frank left bundle branch block as with control hearts during ventricular pacing.

Increased intraventricular conduction delay appeared to be associated with decrease in mechanical performance in control hearts on changing from atrial to ventricular pacing. Intraventricular conduction delay and impaired cardiac performance were both observed in failing hearts during atrial pacing. However, the degree of intraventricular conduction delay was smaller and the degree of mechanical dysfunction greater than what would be expected in control hearts during ventricular pacing. The impaired cardiac performance seen in the failing hearts could not be completely but could be partly explained by the delayed intraventricular conduction seen.

These data show that increased intraventricular conduction delay resulting from non-uniform ventricular activation with ventricular pacing decreased cardiac mechanical performance in control hearts and suggest that part of the impaired cardiac performance seen in heart failure may be explained by delayed intraventricular conduction and non-uniform ventricular activation possibly as a result of secondary changes in the failing ventricular myocardium.

CHAPTER 12

SYNOPSIS

In this thesis, a rabbit coronary artery ligation model was used to study the mechanical performance, Ca^{2+} handling and ventricular activation / repolarisation in heart failure. An attempt was made to examine these aspects under conditions as close to those *in vivo* as possible. Mechanical performance was firstly examined *in vivo* using echocardiography and this was also examined *in vitro* together with the Ca^{2+} handling and electrical aspects in the isolated whole heart paced at a rate close to the physiological heart rate of the rabbit.

Heart failure in the rabbit coronary artery ligation model

Cardiac mechanical performance was assessed in the heart failure model *in vivo* with echocardiography (Chapter 4). By 7 weeks after the ligation of the marginal branch of the circumflex coronary artery with the production of an apical infarct, significant abnormalities were found in the heart on ultrasound. Ejection fraction was lower and cardiac dimensions (left atrial dimension and left ventricular end-diastolic dimension) were increased in the rabbits which had coronary artery ligation. Significant organ congestion was also present, similar to the human clinical syndrome of heart failure, with increased lung and liver weights in the rabbits with heart failure. The degree of congestion appeared to correlate with the degree of cardiac dysfunction present, which was presumed to relate to the degree of the insult on the heart caused by the initial infarct. Cardiac remodelling and hypertrophy were also suggested in the heart failure group by the increased left and right ventricular dry weights. These cardiac and systemic changes seen in the rabbit model parallel those commonly observed in human heart failure as a result of previous myocardial damage from ischaemic heart disease (Parmley, 1989).

Mechanical performance of the failing heart *in vitro*

Cardiac mechanical performance was also assessed in the heart failure model *in vitro* in isolated hearts both in the working heart configuration and during Langendorff perfusion (Chapter 6). At baseline working heart conditions [with a pre-load of 10 cmH_2O (8 mmHg) and after-load of 75 cmH_2O (55 mmHg)], the failing hearts were found to have low cardiac output, decreased peak systolic pressure with slowed rate of pressure rise and a high end-diastolic pressure with slowed rate of relaxation, when compared to controls. Similar systolic and diastolic abnormalities were observed with the Langendorff-perfused failing hearts. The contractile dysfunction observed *in vitro* correlated well with that observed *in vivo* on echocardiography. The failing hearts were also found to have reduced passive compliance compared to controls which could be the result of cardiac remodelling with hypertrophy and fibrosis in the failing hearts.

The Frank-Starling relationship was examined in the working heart mode to assess the ability of the failing heart to respond to the positive inotropic stimulus of an increase in muscle length and improve cardiac performance with stepwise increases in pre-load. It was found that the Frank-Starling relationship was attenuated in the failing hearts when compared to controls. There is debate in the literature as to whether the failing myocardium is able to use the Frank-Starling mechanism (Schwinger *et al.* 1994; Holubarsch *et al.* 1996). The results of the current study suggest that the failing hearts were operating at different Frank-Starling curves from controls and that the Frank-Starling mechanism was altered in the failing hearts but might not be completely absent. These findings would be in agreement with a shift of the pressure-volume curve to the right and upwards, which has been shown in chronic heart failure with left ventricular dilatation and hypertrophy (LeJemtel and Sonnenblick, 1993).

The slow response, which is a slow increase in inotropy over time after a step increase in muscle length, was also found to be attenuated in the failing hearts when this was studied with the increase in pre-load from 10 to 15 cm H_2O (i.e. 8 to 11 mmHg). There is evidence that the slow response may be mediated via cyclic AMP (Kentish *et al.* 1992). Down-regulation of β-adrenoceptors is a well-recognised feature in heart failure (Bristow *et al.* 1982) and reduced basal cyclic AMP level has also been shown in heart failure (Bohm *et al.* 1994) which can potentially lead to an attenuated slow response. The slow response has not been examined in heart failure and the current study appears to be the first to try and address this issue. The attenuated slow response observed suggests that this mechanism, which can potentially improve mechanical performance in response to increase in pre-load, was impaired in the failing hearts and this could have contributed towards the attenuated Frank-Starling relationship seen in the failing hearts.

Ca^{2+} handling in the failing heart

Ca^{2+} transients were measured in the isolated Langendorff perfused hearts using an indo-1 fluorescence system developed to examine the beat-to-beat variation of $[Ca^{2+}]$ at different regions over the left ventricular epicardial surface with a single-core light guide. When the time course of the Ca^{2+} transients were analysed, it was found that failing hearts had more prolonged Ca^{2+} transients with a delay in time to peak amplitude and further delay during the decay phase of the transients (Chapter 8). The prolongation of Ca^{2+} transient duration was not uniform over the left ventricular epicardial surface in failing hearts with some areas having Ca^{2+} transient durations that were close to the range of values observed in controls whilst the Ca^{2+} transient durations at other areas were markedly prolonged. As a result, there was wider variation or increased dispersion of Ca^{2+} transient duration in the failing hearts

compared to controls. However, there was no consistent relationship between the prolonged Ca^{2+} transient duration and the left ventricular epicardial location.

The finding of prolonged Ca^{2+} transient durations in the failing heart concurs with published reports on prolonged Ca^{2+} transients in failing myocardial tissues (Gwathmey *et al.* 1987; Perreault *et al.* 1992) and myocytes (Beuckelmann *et al.* 1992; Capasso *et al.* 1993). The current study appears to be the first to show prolonged Ca^{2+} transient durations in the whole heart at a near-physiological heart rate. It was also shown in this study that the prolongation of the Ca^{2+} transient was associated with delayed relaxation in the failing hearts. Abnormal sarcoplasmic reticulum (SR) function is believed to be the main cause of abnormal Ca^{2+} transients in heart failure (Phillips *et al.* 1998). The prolonged Ca^{2+} transients observed in the current study suggest abnormal Ca^{2+} handling in the failing hearts which is consistent with abnormal SR Ca^{2+}-release and / or Ca^{2+}-reuptake. The increased dispersion of Ca^{2+} transient duration and lack of association between the prolonged Ca^{2+} transient duration and left ventricular epicardial location suggest that there is a regional heterogeneity to the abnormal Ca^{2+} handling in heart failure.

Ventricular repolarisation in heart failure

Electrical events were examined in heart failure by measuring Monophasic Action Potentials (MAPs) at the same sites over the left ventricular epicardial surface of the Langendorff perfused hearts from where the Ca^{2+} transients were measured. A similar pattern as that of the Ca^{2+} transients emerged when the time course of the MAP signals were analysed and their durations measured (Chapter 9). Failing hearts were shown to have prolonged MAP durations and there was an increased dispersion of MAP durations when compared to controls. Again, there was no consistent relationship between the prolonged MAP duration and left ventricular epicardial location.

Action potential prolongation is the most consistent electrophysiological abnormality in heart failure and it has been shown in failing myocytes (Rossner and Sachs, 1978; Beuckelmann *et al.* 1993; Ming *et al.* 1994; Kaab *et al.* 1996; Qiu *et al.* 1996; Rozanski *et al.* 1997) and myocardial tissues (Gwathmey *et al.* 1987; Beuckelmann *et al.* 1993). The finding of prolonged MAP durations in the failing heart in the current study is in agreement with such findings. Similar results have been shown in isolated hearts from a pacing-induced heart failure model in the dog (Wang *et al.* 1994). The prolonged action potential in heart failure is believed to be the result of changes in ion channel activity, a process termed electrical remodelling; and it appears that alterations in the activities of certain K^+ channels are involved in this process (Näbauer and Kaab, 1998).

Increased QT dispersion has been shown in patients in heart failure (Barr *et al.* 1994; Fu *et al.* 1997) and was associated with an increased risk of sudden death (presumed to be arrhythmic in origin). The QT interval is the electrocardiographic representation of the ventricular repolarisation phase. Increased dispersion of repolarisation or refractoriness has also been shown in patients with dilated cardiomyopathy (Dinerman *et al.* 1997) and in the surviving, remodelled myocardium in patients with previous myocardial infarction (Vassallo *et al.* 1988; Ramdat-Misier *et al.* 1995). The findings of prolonged MAP duration together with an increased dispersion of MAP duration in the current study suggest that the electrical remodelling process in heart failure may well be a heterogeneous one.

It was also shown in this study that there was an association between the prolonged Ca^{2+} transient and MAP durations in the failing hearts (Chapter 10). In other words, the results suggest that the abnormal SR Ca^{2+}-release and / or Ca^{2+}-reuptake activity may be associated with the electrical remodelling process in heart failure. The two pathophysiological

processes may be interrelated with a mutual, causal relationship or they may have arisen from a common stimulus.

Altered ventricular activation and mechanical performance in the failing heart

In addition to ventricular repolarisation data, the MAP signals measured also gave information on ventricular activation over the left ventricular epicardial surface of the Langendorff-perfused heart. It was shown that there was greater dispersion of the MAP activation times in the failing hearts during atrial pacing when the ventricles were activated via the His-Purkinje system as in sinus rhythm. This suggested that there was delayed ventricular activation over the epicardial surface or delayed intraventricular conduction in the failing hearts (Chapter 11). Right ventricular pacing increased this delay in ventricular activation in both failing hearts and controls so that the intraventricular conduction delay was similar in both groups - presumably by creating an activation pattern similar to left bundle branch block.

It was also shown that the ventricular activation pattern during atrial pacing was altered in the failing hearts. The activation pattern in controls during atrial pacing followed what would be expected with normal intraventricular conduction whilst that in failing hearts followed a pattern similar to that during right ventricular pacing. The lesser degree of intraventricular delay during atrial pacing in the failing hearts than during ventricular pacing suggested against frank left bundle branch block during atrial pacing although this could not be excluded.

Increased dispersion of ventricular activation has been shown in patients with dilated cardiomyopathy (Dinerman *et al.* 1997), similar to the findings in the current study. This may be the result of disease in the specialised conducting system or could be due to cellular

uncoupling which has been suggested by alterations in gap junctions in the remodelled myocardium (Peters *et al.* 1993).

The possibility that mechanical performance in failing hearts could be affected by altered conduction pattern was investigated by observing the isovolumic pressure profile of the isolated hearts during atrial and ventricular pacing. It was found that mechanical performance was impaired, with lower peak systolic pressure and slowed rate of contraction and relaxation, in controls when changing from atrial to ventricular pacing indicating that increased intraventricular conduction delay resulted in a deterioration in mechanical performance. On the other hand, the failing hearts were not significantly affected by such a manoeuvre whilst their mechanical performance was significantly reduced when compared to controls during atrial pacing. The interpretation of these results would be that ventricular activation was abnormal in the failing hearts during atrial pacing which contributed to impaired mechanical performance and further intraventricular conduction delay induced with ventricular pacing did not cause further deterioration in mechanical performance.

What next?

The experiments included in this thesis have shown that there were abnormalities in intracellular Ca^{2+} handling and in ventricular electrical events in isolated hearts from rabbits with heart failure. These abnormalities can contribute towards the mechanical dysfunction and arrhythmogenic tendency seen in heart failure. One major limitation of the study was that the Ca^{2+} transient and Monophasic Action Potential (MAP) measurements were made sequentially at the various left ventricular epicardial sites with MAP measurements being made after the Ca^{2+} transient measurements. The relationship between these measurements and their variations over the ventricular epicardial surface could be better elucidated with simultaneous, multi-site measurements of both Ca^{2+} transients and MAPs. This would

require the development of alternative experimental set-up and possibly more advanced technology.

Another potential area of future research based on the Ca^{2+} measurement techniques developed could be the study of Ca^{2+} transients during ventricular arrhythmias in heart failure. As mentioned in Chapter 1, there appears to be an association between abnormal intracellular [Ca^{2+}] and the induction and maintenance of ventricular fibrillation (Merillat *et al.* 1990; Kihara and Morgan, 1991). The possibility that abnormal Ca^{2+} handling may have a role to play in the arrhythmogenic tendency in heart failure could be investigated in the isolated heart with Ca^{2+} and MAP measurements (as described in this thesis) during arrhythmias e.g. ventricular fibrillation and the characteristics during arrhythmia induction can also be studied.

There is growing interest in the prospect of improving sarcoplasmic reticulum (SR) function via adenovirus gene transfer techniques (Hajjar *et al.* 1997). Such transgenic techniques may be used to try and restore SR function in heart failure. For example, the effects of upregulation of SR Ca^{2+}-ATPase on mechanical performance, intracellular Ca^{2+} handling and possibly electrical events in heart failure may be investigated in the whole heart using an animal model like the rabbit coronary artery ligation model and techniques outlined in this thesis.

The subject of *"Dispersion"* is an interesting one and an increased dispersion or variation in many parameters appear to be the feature in heart failure. The results in this thesis have shown increased dispersion in the time course of Ca^{2+} transients, time course of MAP signals and in ventricular activation in heart failure with increased *spatial* variation of such parameters over the epicardial surface of the left ventricles. There is recent evidence that there may be increased *temporal* variation in some phenomena in heart failure as well

(Berger *et al.* 1997). Berger *et al.* (1997) showed that there were increased beat-to-beat fluctuations in QT interval in patients with dilated cardiomyopathy suggesting temporal lability in ventricular repolarisation. This adds a further dimension to the subject of *"Dispersion"* which already carries a rather unpredictable notion. Increased dispersion implies heterogeneity, disorder and a non-uniform or chaotic pattern and increased dispersion of recovery of excitability has been known to predispose to ventricular fibrillation (Han and Moe, 1963), which has been regarded as a chaotic rhythm (Billman, 1992). However, there is recent evidence that even this most disorderly of cardiac rhythms, ventricular fibrillation, appears to have some periodicity and spatio-temporal order (Gray *et al.* 1998; Witkowski *et al.* 1998). These may have important implications in further studies in the cellular basis for the arrhythmogenic tendency and mechanical dysfunction in heart failure.

REFERENCES

Acierno, L.J. (1994) The electrophysiologic control of the heart. In: Acierno, L.J. (Ed.) *History of Cardiology*, 1st edn. pp. 239-264. Carnforth: The Parthenon Publishing Group Limited.

Allen, D.G. and Kurihara, S. (1980) Calcium transients in mammalian ventricular muscle. *European Heart Journal* **1**, 5-15.

Allen, D.G. and Kurihara, S. (1982) The effects of muscle length on intracellular calcium transients in mammalian cardiac muscle. *Journal Of Physiology-London* **327**, 79-94.

Allen, D.G. and Kentish, J.C. (1985) The cellular basis of the length tension relation in cardiac muscle. *Journal Of Molecular And Cellular Cardiology* **17**, 821-840.

Allen, D.G., Nichols, C.G. and Smith, G.L. (1988) The effects of changes in muscle length during diastole on the calcium transient in ferret ventricular muscle. *Journal Of Physiology-London* **406**, 359-370.

Allen, D.G., Lee, J.A. and Smith, G.L. (1989) The consequences of simulated ischaemia on intracellular Ca^{2+} and tension in isolated ferret ventricular muscle. *Journal Of Physiology-London* **410**, 297-323.

Allessie, M.A., Bonke, F.I.M. and Schopman, F.J.G. (1976) Circus movement in rabbit atrial muscle as a mechanism of tachycardia. II. The role of nonuniform recovery of excitability in the occurence of unidiretional block, as studied with multiple microelectrodes. *Circulation Research* **39**, 168-177.

Allessie, M.A., Bonke, F.I.M. and Schopman, F.J.G. (1977) Circus movement in rabbit atrial muscle as a mechanism of tachycardia. III. The "leading circle" concept: a new model of circus movement in cardiac tissue without the involvement of an anatomical obstacle. *Circulation Research* **41**, 9-18.

Allessie, M.A., Schalij, M.J., Kirchhof, C.J.H.J., Boersma, L., Huybers, M. and Hollen, J. (1989) Experimental electrophysiology and arrhythmogenicity - anisotropy and ventricular tachycardia. *European Heart Journal* **10**, 2-8.

Antzelevitch, C., Sicouri, S., Litovsky, S.H., Lukas, A., Krishnan, S.C., Didiego, J.M., Gintant, G.A. and Liu, D.W. (1991) Heterogeneity within the ventricular wall: Electrophysiology and pharmacology of epicardial, endocardial, and M cells. *Circulation Research* **69**, 1427-1449.

Anversa, P., Kajstura, J. and Olivetti, G. (1996) Myocyte death in heart failure. *Current Opinion In Cardiology* **11**, 245-251.

Arai, M., Alpert, N.R., MacLennan, D.H., Barton, P. and Periasamy, M. (1993) Alterations in sarcoplasmic reticulum gene expression in human heart failure - a possible mechanism for alterations in systolic and diastolic properties of the failing myocardium. *Circulation Research* **72**, 463-469.

Aronson, R.S. and Ming, Z. (1993) Cellular mechanisms of arrhythmias in hypertrophied and failing myocardium. *Circulation* **87**, 76-83.

Assayag, P., Carre, F., Chevalier, B., Delcayre, C., Mansier, P. and Swynghedauw, B. (1997) Compensated cardiac hypertrophy: arrhythmogenicity and the new myocardial phenotype. I. Fibrosis. *Cardiovascular Research* **34**, 439-444.

Backx, P.H. and ter Keurs, H.E.D.J. (1993) Fluorescent properties of rat cardiac trabeculae microinjected with fura-2 salt. *American Journal Of Physiology* **264**, H1098-H1110.

Baragan, J., Fernandez-Caamano, F., Sozutek, Y., Coblence, B. and Lenegre, J. (1968) Chronic left complete bundle branch block: phonocardiographic and mechanocardiographic study of 30 cases. *British Heart Journal* **30**, 196-202.

Barr, C.S., Naas, A., Freeman, M., Lang, C.C. and Struthers, A.D. (1994) QT dispersion and sudden unexpected death in chronic heart failure. *Lancet* **343**, 327-329.

Bartel, S., Stein, B., Eschenhagen, T., Mende, U., Neumann, J., Schmitz, W., Krause, E.G., Karczewski, P. and Scholz, H. (1996) Protein-phosphorylation in isolated trabeculae from nonfailing and failing human hearts. *Molecular And Cellular Biochemistry* **157**, 171-179.

Bassani, J.W.M., Bassani, R.A. and Bers, D.M. (1995) Calibration of Indo-1 and resting intracellular $[Ca]_{(i)}$ in intact rabbit cardiac myocytes. *Biophysical Journal* **68**, 1453-1460.

Bazan, E., Sole, M.J., Schwartz, A. and Johnson, C.L. (1991) Dihydropyridine receptor binding sites in the cardiomyopathic hamster heart are unchanged from control. *Journal Of Molecular And Cellular Cardiology* **23**, 111-117.

Bentivegna, L.A., Kihara, Y. and Morgan, J.P. (1991) Techniques for measuring intracellular Ca^{2+} concentrations in the isolated perfused heart. *Methods in Molecular and Cellular Biology* **2**, 103-111.

Berger, R.D., Kasper, E.K., Baughman, K.L., Marban, E., Calkins, H. and Tomaselli, G.F. (1997) Beat-to-beat QT interval variability: novel evidence for repolarisation lability in ischemic and nonischemic dilated cardiomyopathy. *Circulation* **96**, 1557-1565.

Berlin, J.R., Cannell, M.B. and Lederer, W.J. (1989) Cellular origins of the transient inward current in cardiac myocytes - role of fluctuations and waves of elevated intracellular calcium. *Circulation Research* **65**, 115-126.

Bers, D.M. (1991) *Excitation-contraction coupling and cardiac contractile force*, 1st edn. Dordrecht: Kluwer Academic Publishers.

Bers, D.M. and Berlin, J.R. (1995) Kinetics of $[Ca]_{(i)}$ decline in cardiac myocytes depend on peak $[Ca]_{(i)}$. *American Journal Of Physiology-Cell Physiology* **37**, C 271-C 277.

Beuckelmann, D.J., Näbauer, M. and Erdmann, E. (1991) Characteristics of calcium-current in isolated human ventricular myocytes from patients with terminal heart failure. *Journal Of Molecular And Cellular Cardiology* **23**, 929-937.

Beuckelmann, D.J., Näbauer, M. and Erdmann, E. (1992) Intracellular calcium handling in isolated ventricular myocytes from patients with terminal heart failure. *Circulation* **85**, 1046-1055.

Beuckelmann, D.J., Näbauer, M. and Erdmann, E. (1993) Alterations of K^+ currents in isolated human ventricular myocytes from patients with terminal heart failure. *Circulation Research* **73**, 379-385.

Beuckelmann, D.J., Jansen, E. and Erdmann, E. (1995) A pacemaker current is expressed in isolated ventricular myocytes from patients with heart failure. *Circulation* **92**, 2411

Billman, G.E., Mcilroy, B. and Johnson, J.D. (1991) Elevated myocardial calcium and its role in sudden cardiac death. *Faseb Journal* **5**, 2586-2592.

Billman, G.E. (1992) Cellular mechanisms for ventricular fibrillation. *News In Physiological Sciences* **7**, 254-259.

Bing, O.H.L., Brooks, W.W., Conrad, C.H., Sen, S., Perreault, C.L. and Morgan, J.P. (1991) Intracellular calcium transients in myocardium from spontaneously hypertensive rats during the transition to heart failure. *Circulation Research* **68**, 1390-1400.

Bohm, M., Reiger, B., Schwinger, R.H.G. and Erdmann, E. (1994) cAMP concentrations, cAMP-dependent protein kinase activity, and phospholamban in nonfailing and failing myocardium. *Cardiovascular Research* **28**, 1713-1719.

Bouanani, N.E., Perennec, J., Ezzaher, A., Jdaiaa, H. and Crozatier, B. (1994) Sarcoplasmic reticulum function abnormalities in rabbit failing hearts. *Comptes Rendus De L Academie Des Sciences Serie III-Sciences De La Vie-Life Sciences* **317**, 825-831.

Brandes, R., Figueredo, V.M., Camacho, S.A., Massie, B.M. and Weiner, M.W. (1992) Suppression of motion artifacts in fluorescence spectroscopy of perfused hearts. *American Journal Of Physiology* **263**, 972-980.

Brandes, R., Figueredo, V.M., Camacho, S.A., Baker, A.J. and Weiner, M.W. (1993a) Quantitation of cytosolic [Ca^{2+}] in whole perfused rat hearts using Indo-1 fluorometry .1. *Biophysical Journal* **65**, 1973-1982.

Brandes, R., Figueredo, V.M., Camacho, S.A., Baker, A.J. and Weiner, M.W. (1993b) Investigation of factors affecting fluorometric quantitation of cytosolic [Ca^{2+}] in perfused hearts .2. *Biophysical Journal* **65**, 1983-1993.

Braunwald, E. and Ross, J.J. (1963) The ventricular end-diastolic pressure. *Circulation* **34**, 147-150.

Braunwald, E. and Kloner, R.A. (1982) The stunned myocardium: prolonged, postischemic ventricular dysfunction. *Circulation* **66**, 1146-1149.

Braunwald, E. and Pfeffer, M.A. (1991) Ventricular enlargement and remodelling following acute myocardial infarction: mechanisms and management. *American Journal Of Cardiology* **68**, 1D-6D.

Braunwald, E. and Grossman, W. (1992) Clinical aspects of heart failure. In: Braunwald, E. (Ed.) *Heart Disease*, 4th edn. pp. 444-463. Philadelphia: WB Saunders.

Brillantes, A.M., Allen, P., Takahashi, T., Izumo, S. and Marks, A.R. (1992) Differences in cardiac calcium release channel (ryanodine receptor) expression in myocardium from patients with end stage heart failure caused by ischemic versus dilated cardiomyopathy. *Circulation Research* **71**, 18-26.

Bristow, M.R., Ginsburg, R., Minobe, W.A., Cubicciotti, R.S., Sageman, W.S., Lurie, K., Billingham, M.E., Harrison, D.C. and Stinson, E.B. (1982) Decreased catecholamine sensitivity and b-adrenergic density in failing human hearts. *New England Journal Of Medicine* **307**, 205-211.

Bristow, M.R., Gilbert, E.M., Abraham, W.T., Adams, K.F., Fowler, M.B., Hershberger, R.E., Kubo, S.H., Narahara, K.A., Ingersoll, H., Krueger, S., Young, S. and Shusterman, N. (1996) Carvedilol produces dose-related improvements in left ventricular function and survival in subjects with chronic heart failure. *Circulation* **94**, 2807-2816.

Brooks, W.W., Bing, O.H.L., Litwin, S.E., Conrad, C.H. and Morgan, J.P. (1994) Effects of treppe and calcium on intracellular calcium and function in the failing heart from the spontaneously hypertensive rat. *Hypertension* **24**, 347-356.

Brooks, W.W., Conrad, C.H. and Morgan, J.P. (1995) Reperfusion-induced arrhythmias following ischemia in intact rat heart - role of intracellular calcium. *Cardiovascular Research* **29**, 536-542.

Brutsaert, D.L. (1987) Nonuniformity - a physiologic modulator of contraction and relaxation of the normal heart. *Journal Of The American College Of Cardiology* **9**, 341-348.

Buda, A.J. and Zotz, R.J. (1986) Serial assessment of circumferential regional left ventricular function following complete cornary occlusion. *American Heart Journal* **112**, 447-452.

Burgess, M.J., Green, L.S., Millar, K., Wyatt, R. and Abildskov, J.A. (1972) The sequence of normal ventricular recovery. *American Heart Journal* **84**, 660-669.

Califf, R.M., McKinnis, R.A., Burke, J., Lee, K.L., Harrell, F.E., Behar, V.S., Pryor, D.B., Wagner, G.S. and Rosati, R.A. (1982) Prognostic implications of ventricular arrhythmias during 24 hour ambulatory monitoring in patients undergoing cardiac catheterisation for coronary artery disease. *American Journal Of Cardiology* **50**, 23-31.

Campbell, A.K. and Sala-Newby, G. (1993) Bioluminescent and chemiluminescent indicators for molecular signalling and function in living cells. In: Mason, W.T. (Ed.) *Fluorescent and luminescent probes for biological activity*, 1st edn. pp. 58-82. London: Academic Press.

Cannell, M.B. and Thomas, M.V. (1994) Intracellular ion measurement with fluorescent indicators. In: Ogden, D. (Ed.) *Microelectrode Technique - The Plymouth Workshop Handbook*, 2nd edn. pp. 317-345. Cambridges: The Company of Biologists Limited.

Capasso, J.M., Li, P. and Anversa, P. (1993) Cytosolic calcium transients in myocytes isolated from rats with ischemic heart failure. *American Journal Of Physiology* **265**, H1953-H1964.

Cascio, W.E., Johnson, T.A. and Gettes, L.S. (1995) Electrophysiologic changes in ischemic ventricular myocardium .1. influence of ionic, metabolic, and energetic changes. *Journal Of Cardiovascular Electrophysiology* **6**, 1039-1062.

Casolo, G., Bali, E., Taddei, T., Amuhasi, J. and Gori, C. (1989) Decreased spontaneous heart rate variability in congestive heart failure. *American Journal Of Cardiology* **64**, 1162-1167.

CAST Investigators, (1989) Effect of encainide and flecainide on mortality in a randomised trial of arrhythmia suppression after myocardial infarction: The Cardiac Arrhythmia Suppression Trial (CAST). *New England Journal Of Medicine* **321**, 406-412.

Cerbai, E., Pino, R., Porciatti, F., Sani, G., Toscano, M., Maccherini, M., Giunti, G. and Mugelli, A. (1997) Characterization of the hyperpolarization-activated current, I_f, in ventricular myocytes from human failing heart. *Circulation* **95**, 568-571.

Chakko, C.S. and Gheorghiade, M. (1985) Ventricular arrhythmias in severe heart failure - incidence, significance, and effectiveness of antiarrhythmic therapy. *American Heart Journal* **109**, 497-504.

Cheng, W., Li, B.S., Kajstura, J., Li, P., Wolin, M.S., Sonnenblick, E.H., Hintze, T.H., Olivetti, G. and Anversa, P. (1995) Stretch-induced programmed myocyte cell death. *Journal Of Clinical Investigation* **96**, 2247-2259.

Chien, K.R., Knowlton, K.U., Zhu, H. and Chien, S. (1991) Regulation of cardiac gene expression during myocardial growth and hypertrophy: Molecular studies of an adaptive physiologic response. *Faseb Journal* **5**, 3037-3046.

Chirife, R. (1994) Left heart function during right heart pacing. *PACE-Pacing And Clinical Electrophysiology* **17**, 1451-1455.

Cohen, I., Giles, W.R. and Noble, D. (1976) Cellular basis for the T-wave of the electrocardiogram. *Nature* **262**, 657-661.

Cohn, J.N., Levine, T.B., Olivari, M.T., Garberg, V., Lura, D., Francis, G.S., Simon, A.B. and Rector, T. (1984) Plasma norepinephrine as a guide to prognosis in patients with chronic congestive heart failure. *New England Journal Of Medicine* **311**, 819-823.

Cohn, J.N., Archibald, D.G., Ziesche, S., Franciosa, J.A., Harston, W.E., Tristani, F.E., Dunkman, W.B., Jacobs, W., Francis, G.S., Flohr, K.H., Goldman, S., Cobb, F.R., Shah, P.M., Saunders, R., Fletcher, R.D., Loeb, H.S., Hughes, V.C. and Baker, B. (1986) Effect of vasodilator therapy on mortality in chronic congestive heart failure - results of a Veterans Administration Cooperative Study. *New England Journal Of Medicine* **314**, 1547-1552.

Cohn, J.N., Johnson, G., Ziesche, S., Cobb, F., Francis, G., Tristani, F., Smith, R., Dunkman, W.B., Loeb, H., Wong, M.L., Bhat, G., Goldman, S., Fletcher, R.D., Doherty, J., Hughes, C.V., Carson, P., Cintron, G., Shabetai, R. and Haakenson, C. (1991) A comparison of enalapril with hydralazine isosorbide dinitrate in the treatment of chronic congestive-heart-failure. *New England Journal Of Medicine* **325**, 303-310.

Colucci, W.S. (1996) Apoptosis in the heart. *New England Journal Of Medicine* **335**, 1224-1226.

Cory, C.R., Mccutcheon, L.J., O'Grady, M., Pang, A.W., Geiger, J.D. and Obrien, P.J. (1993) Compensatory down-regulation of myocardial Ca channel in SR from dogs with heart failure. *American Journal Of Physiology* **264**, H 926-H 937.

Coulshed, D.S. and Cowan, J.C. (1991) Contraction-excitation feedback in an ejecting whole heart model - dependence of action potential duration on left ventricular diastolic and systolic pressures. *Cardiovascular Research* **25**, 343-352.

Cowie, M.R., Mosterd, A., Wood, D.A., Deckers, J.W., Poole-Wilson, P.A., Sutton, G.C. and Grobbee, D.E. (1997) The epidemiology of heart failure. *European Heart Journal* **18**, 208-225.

Currie, S. and Smith, G.L. (1996) Phosphorylation of phospholamban is altered after myocardial infarction. *Journal Of Molecular And Cellular Cardiology* **28**, A144

D'Agnolo, A., Luciani, G.B., Mazzucco, A., Gallucci, V. and Salviati, G. (1992) Contractile properties and Ca^{2+} release activity of the sarcoplasmic reticulum in dilated cardiomyopathy. *Circulation* **85**, 518-525.

Davey, P., Bateman, J., Mulligan, I.P., Forfar, C., Barlow, C. and Hart, G. (1994) QT interval dispersion in chronic heart failure and left ventricular hypertrophy - relation to autonomic nervous system and Holter tape abnormalities. *British Heart Journal* **71**, 268-273.

Davies, C.H., Davia, K., Bennett, J.G., Pepper, J.R., Poole-Wilson, P.A. and Harding, S.E. (1995) Reduced contraction and altered frequency response of isolated ventricular myocytes from patients with heart failure. *Circulation* **92**, 2540-2549.

Davies, C.H., Harding, S.E. and Poole-Wilson, P.A. (1996) Cellular mechanisms of contractile dysfunction in human heart failure. *European Heart Journal* **17**, 189-198.

Day, C.P., Mccomb, J.M. and Campbell, R.W.F. (1990) QT dispersion - an indication of arrhythmia risk in patients with long QT intervals. *British Heart Journal* **63**, 342-344.

Day, C.P., Mccomb, J.M., Matthews, J. and Campbell, R.W.F. (1991) Reduction in QT dispersion by sotalol following myocardial infarction. *European Heart Journal* **12**, 423-427.

De Bakker, J.M.T., Van Capelle, F.J.L., Janse, M.J., Wilde, A.A.M., Coronel, R., Becker, A.E., Dirigemans, K.P., Van Hemel, N.M. and Haver, R.N.W. (1988) Re-entry as a cause of ventricular tachycardia in patients with chronic ischemic heart disease - electrophysiological and anatomic correlation. *Circulation* **77**, 589-606.

Deferrari, G.M., Viola, M.C., Damato, E., Antolini, R. and Forti, S. (1995) Distinct patterns of calcium transients during early and delayed afterdepolarizations induced by isoproterenol in ventricular myocytes. *Circulation* **91**, 2510-2515.

Denvir, M.A., MacFarlane, N.G., Cobbe, S.M. and Miller, D.J. (1995) Sarcoplasmic reticulum and myofilament function in chemically treated ventricular trabeculae from patients with heart failure. *Cardiovascular Research* **30**, 377-385.

Denvir, M.A., MacFarlane, N.G., Miller, D.J. and Cobbe, S.M. (1996) Enhanced SR function in saponin-treated ventricular trabeculae from rabbits with heart failure. *American Journal Of Physiology-Heart And Circulatory Physiology* **40**, H 850-H 859.

Di Virgilio, F., Steinberg, T.H. and Silverstien, S.C. (1990) Inhibition of Fura-2 sequestration and secretion with organic anion transport blockers. *Cell Calcium* **11**, 57-62.

Didiego, J.M. and Antzelevitch, C. (1994) High $[Ca^{2+}]_{(o)}$-induced electrical heterogeneity and extrasystolic activity in isolated canine ventricular epicardium - phase-2 reentry. *Circulation* **89**, 1839-1850.

Dinerman, J.L., Berger, R., Haigney, M.C.P., Lawrence, J.H., Tomaselli, G.F. and Calkins, H. (1997) Dispersion of ventricular activation and refractoriness in patients with idiopathic dilated cardiomyopathy. *American Journal Of Cardiology* **79**, 970

Dougherty, A.H., Naccarelli, G.V., Gray, E.L., Hicks, C.H. and Goldstein, R.A. (1984) Congestive heart failure with normal systolic function. *American Journal Of Cardiology* **54**, 778-782.

Dougherty, C.M. and Burr, R.L. (1992) Comparison of heart rate variability in survivors and nonsurvivors of cardiac arrest. *American Journal Of Cardiology* **70**, 441-448.

Doval, H.C., Nul, D.R., Grancelli, H.O., Varini, S.D., Soifer, S., Corrado, G., Dubner, S., Scapin, O. and Perrone, S.V. (1996) Nonsustained ventricular tachycardia in severe heart failure - independent marker of increased mortality due to sudden death. *Circulation* **94**, 3198-3203.

Durrer, D., van Dam, R.T., Freud, G.E., Janse, M.J., Meijler, F.L. and Arzbaecher, R.C. (1970) Total excitation of the isolated human heart. *Circulation* **41**, 899-912.

Dzau, V.J. (1993) Tissue renin-angiotensin system in myocardial hypertrophy and failure. *Archives of Internal Medicine* **153**, 937-942.

Edler, I. and Hertz, C.H. (1954) The use of ultrasonic reflectoscope for the continuous recording of the movements of heart walls. *Kungliga Fysiografiska Sallskapets i Lund forhandlingar* **24**, 1-19.

Elsner, D. and Riegger, G.A.J. (1995) Characteristics and clinical relevance of animal models of heart failure. *Current Opinion In Cardiology* **10**, 253-259.

Endoh, M. and Blinks, J.R. (1988) Actions of sympathomimetic amines on the Ca^{2+} transients and contractions of rabbit myocardium: reciprocal changes in myofibrillar responsiveness to Ca^{2+} mediated through alpha- and beta-adrenoceptors. *Circulation Research* **62**, 247-265.

Eriksson, H. (1995) Heart failure: a growing public health problem. *Journal of Internal Medicine* **237**, 135-141.

Evans, S.J., Levi, A.J. and Jones, J.V. (1995) Wall stress induced arrhythmia is enhanced by low potassium and early left ventricular hypertrophy in the working rat heart. *Cardiovascular Research* **29**, 555-562.

Fabiato, A. and Fabiato, F. (1975) Contractions induced by a calcium-triggered release of calcium from the sarcoplasmic reticulum of single skinned cardiac cells. *Journal Of Physiology-London* **249**, 469-495.

Fabiato, A. (1983) Calcium-induced release of calcium from the cardiac sarcoplasmic reticulum. *American Journal Of Physiology* **245**, C 1-C 14.

Fedida, D. and Giles, W.R. (1991) Regional variations in action potentials and transient outward current in myocytes isolated from rabbit left ventricle. *Journal Of Physiology-London* **442**, 191-209.

Feigenbaum, H., Waldhaussen, J.A. and Hyde, L.P. (1965) Ultrasound diagnosis of pericardial effusion. *JAMA-Journal Of The American Medical Association* **191**, 711-714.

Feldman, A.M., Ray, P.E., Silan, C.M., Mercer, J.A., Minobe, W. and Bristow, M.R. (1991) Selective gene expression in failing human heart - quantification of steady state levels of messenger-RNA in endomyocardial biopsies using the polymerase chain reaction. *Circulation* **83**, 1866-1872.

Ferguson, D.W., Abboud, F.M. and Mark, A.L. (1984) Selective impairment of baroreflex-mediated vasoconstrictor responses in patients with ventricular dysfunction. *Circulation* **69**, 451-460.

Field, M.L., Azzawi, A., Styles, P., Henderson, C., Seymour, A.M.L. and Radda, G.K. (1994) Intracellular Ca^{2+} transients in isolated perfused rat heart - measurement using the fluorescent indicator Fura-2/AM. *Cell Calcium* **16**, 87-100.

Figueredo, V.M., Brandes, R., Weiner, M.W., Massie, B.M. and Camacho, S.A. (1993) Endocardial versus epicardial differences of intracellular free calcium under normal and ischemic conditions in perfused rat hearts. *Circulation Research* **72**, 1082-1090.

Figueredo, V.M. and Camacho, S.A. (1995) Basic mechanisms of myocardial dysfunction - cellular pathophysiology of heart failure. *Current Opinion In Cardiology* **10**, 246-252.

Finkel, M.S., Marks, E.S., Patterson, R.E., Speir, E.H., Steadman, K. and Keiser, H.R. (1986) Increased cardiac calcium channels in hamster cardiomyopathy. *American Journal Of Cardiology* **57**, 1205-1206.

Finkel, M.S., Marks, E.S., Patterson, R.E., Speir, E.H., Steadman, K.A. and Keiser, H.R. (1987) Correlation of changes in cardiac calcium channels with hemodynamics in syrian hamster cardiomyopathy and heart failure. *Life Sciences* **41**, 153-159.

Finkel, M.S., Li, S., Romeo, R.C., Oddis, C.V. and Salama, G. (1992) Radioligand binding and inotropic effects of ryanodine in the cardiomyopathic syrian hamster. *Journal Of Cardiovascular Pharmacology* **19**, 610-617.

Flesch, M., Schwinger, R.H.G., Schiffer, F., Frank, K., Sudkamp, M., Kuhnregnier, F., Arnold, G. and Bohm, M. (1996) Evidence for functional relevance of an enhanced expression of the Na^{+}-Ca^{2+} exchanger in failing human myocardium. *Circulation* **94**, 992-1002.

Fralix, T.A., Heineman, F.W. and Balaban, R.S. (1990) Effects of tissue absorbency on NAD(P)H and Indo-1 fluorescence from perfused rabbit hearts. *Febs Letters* **262**, 287-292.

Frampton, J.E., Orchard, C.H. and Boyett, M.R. (1991) Diastolic, systolic and sarcoplasmic reticulum [Ca^{2+}] during inotropic interventions in isolated rat myocytes. *Journal of Physiology* **437**, 351-375.

Franciosa, J.A., Wilen, M., Ziesche, S. and Cohn, J.N. (1983) Survival in men with severe chronic left ventricular failure due to either coronary heart disease or idiopathic dilated cardiomyopathy. *American Journal Of Cardiology* **51**, 831-836.

Francis, G.S. (1986) Development of arrhythmias in the patient with congestive heart-failure - patho-physiology, prevalence and prognosis. *American Journal Of Cardiology* **57**, B 3-B 7.

Francis, G.S. and Chu, C. (1994) Compensatory and maladaptive responses to cardiac dysfunction. *Current Opinion In Cardiology* **9**, 280-288.

Frank, O. (1895) Zur dynamik des herzmuskels. *Zeitschrift fur Biologie* **32**, 370-447.

Franklin, K.J. (1933) *A short history of physiology*, London: Bale.

Franz, M.R., Flaherty, J.T., Platia, E.V., Bulkley, B.H. and Weisfeldt, M.L. (1984) Localization of regional myocardial ischemia by recording of monophasic action-potentials. *Circulation* **69**, 593-604.

Franz, M.R., Burkhoff, D., Yue, D.T. and Sagawa, K. (1989) Mechanically induced action potential changes and arrhythmia in isolated and *in situ* canine hearts. *Cardiovascular Research* **23**, 213-223.

Franz, M.R. (1991) Method and theory of monophasic action potential recording. *Progress In Cardiovascular Diseases* **33**, 347-368.

Franz, M.R., Cima, R., Wang, D., Profitt, D. and Kurz, R. (1992) Electrophysiological effects of myocardial stretch and mechanical determinants of stretch-activated arrhythmias. *Circulation* **86**, 968-978.

Fu, G.S., Meissner, A. and Simon, R. (1997) Repolarization dispersion and sudden cardiac death in patients with impaired left ventricular function. *European Heart Journal* **18**, 281-289.

Furukawa, T., Kimura, S., Furukawa, N., Bassett, A.L. and Myerburg, R.J. (1992) Potassium rectifier currents differ in myocytes of endocardial and epicardial origin. *Circulation Research* **70**, 91-103.

Gaasch, W.H., Levine, H.J., Quinones, M.A. and Alexander, J.K. (1976) Left ventricular compliance: mechanisms and clinical implications. *American Journal Of Cardiology* **38**, 645-653.

Garg, R., Packer, M., Pitt, B. and Yusuf, S. (1993) Heart failure in the 1990s - evolution of a major public health problem in cardiovascular medicine. *Journal Of The American College Of Cardiology* **22**, A 3-A 5.

Go, L.O., Moschella, M.C., Watras, J., Handa, K.K., Fyfe, B.S. and Marks, A.R. (1995) Differential regulation of 2 types of intracellular calcium release channels during end-stage heart failure. *Journal Of Clinical Investigation* **95**, 888-894.

Goldsmith, S.R. and Dick, C. (1993) Differentiating systolic from diastolic heart failure - pathophysiologic and therapeutic considerations. *American Journal Of Medicine* **95**, 645-655.

Gomez, A.M., Valdivia, H.H., Cheng, H., Lederer, M.R., Santana, L.F., Cannell, M.B., McCune, S.A., Altschuld, R.A. and Lederer, W.J. (1997) Defective excitation-contraction coupling in experimental cardiac hypertrophy and heart failure. *Science* **276**, 800-806.

Gray, R.A., Pertsov, A.M. and Jalife, J. (1998) Spatial and temporal organisation during cardiac fibrillation. *Nature* **392**, 75-78.

Grossman, W., McLaurin, L.P. and Rolett, E.L. (1979) Alterations in left ventricular relaxation and diastolic compliance in congestive cardiomyopathy. *Cardiovascular Research* **13**, 514-522.

Grossman, W. (1990) Diastolic dysfunction and congestive heart failure. *Circulation* **81**, 1-7.

Grynkiewicz, G., Poenie, M. and Tsien, R.Y. (1985) A new generation of Ca^{2+} indicators with greatly improved fluorescence properties. *Journal Of Biological Chemistry* **260**, 3440-3450.

Gupta, R.C., Shimoyama, H., Tanimura, M., Nair, R., Lesch, M. and Sabbah, H.N. (1997) SR Ca^{2+}-ATPase activity and expression in ventricular myocardium of dogs with heart failure. *American Journal Of Physiology-Heart And Circulatory Physiology* **42**, H12-H18.

Gwathmey, J.K., Copelas, L., MacKinnon, R., Schoen, F.J., Feldman, M.D., Grossman, W. and Morgan, J.P. (1987) Abnormal intracellular calcium handling in myocardium from patients with end-stage heart failure. *Circulation Research* **61**, 70-76.

Gwathmey, J.K., Slawsky, M.T., Hajjar, R.J., Briggs, G.M. and Morgan, J.P. (1990) Role of intracellular calcium handling in force interval relationships of human ventricular myocardium. *Journal Of Clinical Investigation* **85**, 1599-1613.

Gwathmey, J.K., Bentivegna, L.A., Ransil, B.J., Grossman, W. and Morgan, J.P. (1993) Relationship of abnormal intracellular calcium mobilization to myocyte hypertrophy in human ventricular myocardium. *Cardiovascular Research* **27**, 199-203.

Gwathmey, J.K. and Ingwall, J.S. (1995) Basic pathophysiology of congestive heart failure. *Cardiology in Review* **3**, 282-291.

Hajjar, R.J. and Gwathmey, J.K. (1992) Cross-bridge dynamics in human ventricular myocardium - regulation of contractility in the failing heart. *Circulation* **86**, 1819-1826.

Hajjar, R.J., Kang, J.X., Gwathmey, J.K. and Rosenzweig, A. (1997) Physiological effects of adenoviral gene transfer of sarcoplasmic reticulum calcium ATPase in isolated rat myocytes. *Circulation* **95**, 423-429.

Halperin, B.D., Adler, S.W., Mann, D.E. and Reiter, M.J. (1993) Mechanical correlates of contraction-excitation feedback during acute ventricular dilatation. *Cardiovascular Research* **27**, 1084-1087.

Han, J. and Moe, G.K. (1963) Nonuniform recovery of excitability in ventricular muscle. *Circulation Research* **14**, 44-60.

Hanley, P.J. and Loiselle, D.S. (1998) Mechanisms of force inhibition by halothane and isoflurane in intact rat cardiac muscle. *Journal Of Physiology-London* **506**, 231-244.

Hansen, D.E., Borganelli, M., Stacy, G.P. and Taylor, L.K. (1991) Dose-dependent inhibition of stretch-induced arrhythmias by gadolinium in isolated canine ventricles - evidence for a unique mode of antiarrhythmic action. *Circulation Research* **69**, 820-831.

Hart, G. (1994) Cellular electrophysiology in cardiac hypertrophy and failure. *Cardiovascular Research* **28**, 933-946.

Hasenfuss, G., Mulieri, L.A., Leavitt, B.J., Allen, P.D., Haeberle, J.R. and Alpert, N.R. (1992) Alteration of contractile function and excitation contraction coupling in dilated cardiomyopathy. *Circulation Research* **70**, 1225-1232.

Hasenfuss, G., Reinecke, H., Studer, R., Meyer, M., Pieske, B., Holtz, J., Holubarsch, C., Posival, H., Just, H. and Drexler, H. (1994) Relation between myocardial-function and expression of sarcoplasmic- reticulum Ca^{2+}-ATPase in failing and nonfailing human myocardium. *Circulation Research* **75**, 434-442.

Hasenfuss, G., Reinecke, H., Studer, R., Pieske, B., Meyer, M., Drexler, H. and Just, H. (1996) Calcium cycling proteins and force-frequency relationship in heart failure. *Basic Research In Cardiology* **91**, 17-22.

Hatem, S.N., Sham, J.S.K. and Morad, M. (1994) Enhanced Na^{+}-Ca^{2+} exchange activity in cardiomyopathic Syrian hamster. *Circulation Research* **74**, 253-261.

Hefti, M.A., Harder, B.A., Eppenberger, H.M. and Schaub, M.C. (1997) Signaling pathways in cardiac myocyte hypertrophy. *Journal Of Molecular And Cellular Cardiology* **29**, 2873-2892.

Hicks, M.N., McIntosh, M.A., Kane, K.A., Rankin, A.C. and Cobbe, S.M. (1995) The electrophysiology of rabbit hearts with left ventricular hypertrophy under normal and ischemic conditions. *Cardiovascular Research* **30**, 181-186.

Higham, P.D., Furniss, S.S. and Campbell, R.W.F. (1995) QT dispersion and components of the QT interval in ischemia and infarction. *British Heart Journal* **73**, 32-36.

Hii, J.T.Y., Wyse, D.G., Gillis, A.M., Duff, H.J., Solylo, M.A. and Mitchell, B. (1992) Precordial qt interval dispersion as a marker of torsade-de-pointes - disparate effects of class ia antiarrhythmic drugs and amiodarone. *Circulation* **86**, 1376-1382.

Ho, K.K.L., Anderson, K.M., Kannel, W.B., Grossman, W. and Levy, D. (1993) Survival after the onset of congestive heart failure in Framingham Heart Study subjects. *Circulation* **88**, 107-115.

Ho, K.K.L., Pinsky, J.L., Kannel, W.B. and Levy, D. (1993) The epidemiology of heart failure - the Framingham study. *Journal Of The American College Of Cardiology* **22**, A 6-A 13.

Hoffman, B.F., Cranefield, P.F., Lepeschkin, E., Surawicz, B. and Herrlich, H.C. (1959) Comparison of cardiac monophasic action potentials recorded by intracellular and suction electrodes. *American Journal Of Physiology* **196**, 1297-1301.

Holubarsch, C., Ruf, T., Goldstein, D.J., Ashton, R.C., Nickl, W., Pieske, B., Pioch, K., Ludemann, J., Wiesner, S., Hasenfuss, G., Posival, H., Just, H. and Burkhoff, D. (1996) Existence of the Frank-Starling mechanism in the failing human heart - investigations on the organ, tissue, and sarcomere levels. *Circulation* **94**, 683-689.

Hope, J.A. (1832) *Treatise on the Diseases of the Heart and Great Vessels*, London: William-Kidd.

Hove-Madsen, L. and Bers, D.M. (1992) Indo-1 binding to protein in permeabilised ventricular myocytes alters its spectral and Ca binding properties. *Biophysical Journal* **63**, 89-97.

Howlett, S.E. and Gordon, T. (1987) Calcium channels in normal and dystrophic hamster cardiac muscle: [^{3}H] nitrendipine binding studies. *Biochemical Pharmacology* **36**, 2653-2659.

Jalal, S., Williams, G.R., Mann, D.E. and Reiter, M.J. (1992) Effect of acute ventricular dilation on fibrillation thresholds in the isolated rabbit heart. *American Journal Of Physiology* **263**, H1306-H1310.

James, T.N. (1996) Long reflections on the QT interval - the 6th annual Gordon K Moe lecture. *Journal Of Cardiovascular Electrophysiology* **7**, 738-759.

Jauch, W., Hicks, H.N. and Cobbe, S.M. (1994) Effects of contraction-excitation feedback on electrophysiology and arrhythmogenesis in rabbits with experimental left ventricular hypertrophy. *Cardiovascular Research* **28**, 1390-1396.

Josephson, M.E. (1993) Recurrent ventricular tachycardia. In: Josephson, M.E. (Ed.) *Clinical cardiac electrophysiology - techniques and interpretation*, 2nd edn. pp. 417-615. Philadelphia: Lea & Febiger.

Kaab, S., Nuss, H.B., Chiamvimonvat, N., Orourke, B., Pak, P.H., Kass, D.A., Marban, E. and Tomaselli, G.F. (1996) Ionic mechanism of action potential prolongation in ventricular myocytes from dogs with pacing-induced heart failure. *Circulation Research* **78**, 262-273.

Kannel, W.B. and Belanger, A.J. (1991) Epidemiology of heart failure. *American Heart Journal* **121**, 951

Katz, L.N., Feinberg, H. and Shaffer, A.B. (1960) Hemodynamic aspects of congestive heart failure. *Circulation* **21**, 95-111.

Kentish, J.C., Davey, R. and Largen, P. (1992) Isoprenaline reverses the slow force responses to a length change in isolated rabbit papillary muscle. *Pflugers Archiv-European Journal Of Physiology* **421**, 519-521.

Kienzle, M.G., Ferguson, D.W., Birkett, C.L., Myers, G.A., Berg, W.J. and Mariano, J. (1992) Clinical hemodynamic and sympathetic neural correlates of heart rate variability in congestive heart failure. *American Journal Of Cardiology* **69**, 761-767.

Kihara, Y., Grossman, W. and Morgan, J.P. (1989) Direct measurement of changes in intracellular calcium transients during hypoxia, ischemia and reperfusion of the intact mammalian heart. *Circulation Research* **65**, 1029-1044.

Kihara, Y. and Morgan, J.P. (1991) Intracellular calcium and ventricular fibrillation - studies in the aequorin-loaded isovolumic ferret heart. *Circulation Research* **68**, 1378-1389.

Kirchhefer, U., Neumann, J. and Schmitz, W. (1997) Calcium/calmodulin-dependent phosphorylation of phospholamban in human heart failure. *Faseb Journal* **11**, A109.

Kiss, E., Ball, N.A., Kranias, E.G. and Walsh, R.A. (1995) Differential changes in cardiac phospholamban and sarcoplasmic reticular Ca-ATPase protein levels. *Circulation Research* **77**, 759-764.

Kleiger, R.E., Miller, J.P., Bigger, J.T., Moss, A.J. and Multicenter Post-Infarction Research Group, (1987) Decreased heart rate variability and its association with increased mortality after acute myocardial infarction. *American Journal Of Cardiology* **59**, 256-262.

Kleiman, R.B. and Houser, S.R. (1989) Outward currents in normal and hypertrophied feline ventricular myocytes. *American Journal Of Physiology* **256**, H1450-H1461.

Kobayashi, A., Yamashita, T., Kaneko, M., Nishiyama, T., Hayashi, H. and Yamazaki, N. (1987) Effects of verapamil on experimental cardiomyopathy in the Bio 14.6 syrian hamster. *Journal Of The American College Of Cardiology* **10**, 1128-1134.

Kottkamp, H., Hindricks, G., Chen, X., Brunn, J., Willems, S., Haverkamp, W., Block, M., Breithardt, G. and Borggrefe, M. (1995) Radiofrequency catheter ablation of sustained ventricular tachycardia in idiopathic dilated cardiomyopathy. *Circulation* **92**, 1159-1168.

Kuo, C.S., Amlie, J.P., Munakata, K., Reddy, C.P. and Surawicz, B. (1983a) Dispersion of monophasic action potential durations and activation times during atrial pacing, ventricular pacing, and ventricular premature stimulation in canine ventricles. *Cardiovascular Research* **17**, 152-161.

Kuo, K.S., Munakata, K., Reddy, P. and Surawica, B. (1983b) Characteristics and possible mechanism of ventricular arrhythmia dependent on the dispersion of action potential durations. *Circulation* **67**, 1356-1367.

Kuo, T.H., Johnson, D.F., Tsang, W. and Wiener, J. (1987) Photoaffinity-labeling of the calcium-channel antagonist receptor in the heart of the cardiomyopathic hamster. *Biochemical And Biophysical Research Communications* **148**, 926-933.

Kuo, T.H., Tsang, W., Wang, K.K.W. and Carlock, L. (1992) Simultaneous reduction of the sarcolemmal and SR calcium ATPase activities and gene expression in cardiomyopathic hamster. *Biochimica Et Biophysica Acta* **1138**, 343-349.

La Rovere, M.T., Bigger, J.T., Marcus, F.I., Mortara, A. and Schwartz, P.J. (1998) Baroreflex sensitivity and heart rate variability in prediction of total cardiac mortality after myocardial infarction. *Lancet* **351**, 478-484.

Lab, M.J. (1982) Contraction-excitation feedback in myocardium - physiological basis and clinical relevance. *Circulation Research* **50**, 757-766.

Lab, M.J., Allen, D.G. and Orchard, C.H. (1984) The effects of shortening on myoplasmic calcium-concentration and on the action-potential in mammalian ventricular muscle. *Circulation Research* **55**, 825-829.

Lab, M.J. (1991) Monophasic action potentials and the detection and significance of mechanoelectric feedback *in vivo*. *Progress In Cardiovascular Diseases* **34**, 29-35.

Lachnit, W.G., Phillips, M., Gayman, K.J. and Pessah, I.N. (1994) Ryanodine and dihydropyridine binding patterns and ryanodine receptor messenger-RNA levels in myopathic hamster heart. *American Journal Of Physiology* **267**, H1205-H1214.

Laflamme, M.A. and Becker, P.L. (1996) Ca^{2+}-induced current oscillations in rabbit ventricular myocytes. *Circulation Research* **78**, 707-716.

Lakatta, E.G. and Jewell, B.R. (1977) Length-dependent activation. *Circulation Research* **40**, 251-257.

Langendorff, O. (1895) Untersuchungen am uberlebenden Saugethierherzen. *Pflugers Archive ges Physiol.* **61**, 291-332.

Lederer, W.J., Berlin, J.R., Cohen, N.M., Hadley, R.W., Bers, D.M. and Cannell, M.B. (1990) Excitation-contraction coupling in heart cells - roles of the sodium calcium exchange, the calcium current, and the sarcoplasmic reticulum. *Annals Of The New York Academy Of Sciences* **588**, 190-206.

Lee, H.C., Smith, N., Mohabir, R. and Clusin, W.T. (1987) Cytosolic calcium transients from the beating mammalian heart. *Proceedings Of The National Academy Of Sciences Of The United States Of America* **84**, 7793-7797.

Lee, H.C., Mohabir, R., Smith, N., Franz, M.R. and Clusin, W.T. (1988) Effect of ischemia on calcium-dependent fluorescence transients in rabbit hearts containing Indo-1 - correlation with monophasic action potentials and contraction. *Circulation* **78**, 1047-1059.

LeJemtel, T.H. and Sonnenblick, E.H. (1993) Heart failure - adaptive and maladaptive processes - introduction. *Circulation* **87**, 1-4.

Lerman, B.B. (1996) Mechanoelectrical feedback - maturation of a concept. *Journal Of Cardiovascular Electrophysiology* **7**, 17-19.

Lew, W.Y.W. (1988) Time-dependent increase in left ventricular contractility following acute volume loading in the dog. *Circulation Research* **63**, 635-647.

Lewis, T. and Rothschild, M.A. (1915) The excitatory process in the dog's heart. Part 2. The ventricles. *Philosoplical Transactions of the Royal Society of London* **B206**, 181-226.

Limas, C.J., Olivari, M.T., Goldenberg, T.B., Benditt, D.G. and Simon, A. (1987) Calcium uptake by cardiac sarcoplasmic reticulum in human dilated cardiomyopathy. *Cardiovascular Research* **21**, 601-605.

Linck, B., Boknik, P., Eschenhagen, T., Muller, F.U., Neumann, J., Nose, M., Jones, L.R., Schmitz, W. and Scholz, H. (1996) Messenger-RNA expression and immunological quantification of phospholamban and SR Ca^{2+}-ATPase in failing and nonfailing human hearts. *Cardiovascular Research* **31**, 625-632.

Ling, G. and Gerard, R.W. (1949) The normal membrane potential of frog sartorius fibres. *Journal of Cellular and Comparative Physiology* **34**, 383-396.

Litovsky, S.H. and Antzelevitch, C. (1988) Transient outward current prominent in canine ventricular epicardium but not endocardium. *Circulation Research* **62**, 116-126.

Liu, D.W., Gintant, G.A. and Antzelevitch, C. (1993) Ionic bases for electrophysiological distinctions among epicardial, mid-myocardial, and endocardial myocytes from the free wall of the canine left ventricle. *Circulation Research* **72**, 671-687.

Lorell, B.H., Apstein, C.S., Cunningham, M.J., Schoen, F.J., Weinberg, E.O., Peeters, G.A. and Barry, W.H. (1990) Contribution of endothelial cells to calcium dependent fluorescence transients in rabbit hearts loaded with Indo-1. *Circulation Research* **67**, 415-425.

Luckhoff, A. (1986) Measuring cytosolic free calcium concentration in endothelial cells with Indo-1 - the pitfall of using the ratio of 2 fluorescence intensities recorded at different wavelengths. *Cell Calcium* **7**, 233-248.

Luo, W.S., Wolska, B.M., Grupp, I.L., Harrer, J.M., Haghighi, K., Ferguson, D.G., Slack, J.P., Grupp, G., Doetschman, T., Solaro, R.J. and Kranias, E.G. (1996) Phospholamban gene dosage effects in the mammalian heart. *Circulation Research* **78**, 839-847.

Luu, M., Stevenson, W.G., Stevenson, L.W., Baron, K. and Walder, J. (1989) Diverse mechanisms of unexpected cardiac arrest in advanced heart failure. *Circulation* **80**, 1675-1680.

Mackenzie, J. (1913) *Diseases of the heart*, 3rd edn. Oxford: Oxford Medical Publications.

Marban, E., Kitakaze, M., Koretsune, Y., Yue, D.T., Chacko, V.P. and Pike, M.M. (1990) Quantification of $[Ca^{2+}]_i$ in perfused hearts - critical evaluation of the 5F-BAPTA and nuclear magnetic resonance method as applied to the study of ischemia and reperfusion. *Circulation Research* **66**, 1255-1267.

Massie, B.M. and Shah, N.B. (1996) The heart failure epidemic - magnitude of the problem and potential mitigating approaches. *Current Opinion In Cardiology* **11**, 221-226.

Maurice, J.P., Kypson, A.P., Skaer, C.A. and Koch, W.J. (1997) b-adrenergic signalling characteristics in an infarct heart failure model. *Circulation* **96**, I-362

Maxwell, M.P., Hearse, D.J. and Yellon, D.M. (1987) Species variation in the coronary collateral circulation during regional ischaemia: a critical determination on the rate of evolution and extent of myocardial infarction. *Cardiovascular Research* **21**, 737-746.

McIntosh, M.A., Cobbe, S.M., Kane, K.A. and Rankin, A.C. (1998) Action potential prolongation and potassium currents in left ventricular myocytes isolated from hypertrophied rabbit hearts. *Journal Of Molecular And Cellular Cardiology* **30**, 43-53.

McKay, R.G., Pfeffer, M.A., Pasternak, R.C., Markis, J.E., Come, P.C., Nakao, S., Alderman, J.D., Ferguson, J.J., Safian, R.D. and Grossman, W. (1986) Left ventricular remodelling after myocardial infarction: a corollary to infarct expansion. *Circulation* **74**, 693-702.

McKee, P.A., Castelli, W.P., McNamara, P.M. and Kannel, W.B. (1971) The natural history of congestive heart failure: the Framingham study. *New England Journal Of Medicine* **285**, 1442-1446.

McMurray, J., McDonagh, T., Morrison, C.E. and Dargie, H.J. (1993a) Trends in hospitalisation for heart failure in Scotland 1980-1990. *European Heart Journal* **14**, 1158-1162.

McMurray, J., Hart, W. and Rhodes, G. (1993b) An evaluation of the cost of heart failure to the National Health Services in the UK. *British Journal of Medical Economics* **6**, 99-110.

Mercadier, J.J., Lompre, A.M., Duc, P., Boheler, K.R., Fraysse, J.B., Wisnewsky, C., Allen, P.D., Komajda, M. and Schwartz, K. (1990) Altered sarcoplasmic reticulum Ca^{2+}-ATPase gene-expression in the human ventricle during end stage heart failure. *Journal Of Clinical Investigation* **85**, 305-309.

Merillat, J.C., Lakatta, E.G., Hano, O. and Guarnieri, T. (1990) Role of calcium and the calcium channel in the initiation and maintenance of ventricular fibrillation. *Circulation Research* **67**, 1115-1123.

Mewes, T. and Ravens, U. (1994) L-type calcium currents of human myocytes from ventricle of nonfailing and failing hearts and from atrium. *Journal Of Molecular And Cellular Cardiology* **26**, 1307-1320.

Meyer, M., Schillinger, W., Pieske, B., Holubarsch, C., Heilmann, C., Posival, H., Kuwajima, G., Mikoshiba, K., Just, H. and Hasenfuss, G. (1995) Alterations of sarcoplasmic reticulum proteins in failing human dilated cardiomyopathy. *Circulation* **92**, 778-784.

Ming, Z., Nordin, C., Siri, F. and Aronson, R.S. (1994) Reduced calcium current density in single myocytes isolated from hypertrophied failing guinea-pig hearts. *Journal Of Molecular And Cellular Cardiology* **26**, 1133-1143.

Mirsky, I. (1984) Assessment of diastolic function - suggested methods and future considerations. *Circulation* **69**, 836-841.

Miyata, H., Silverman, H.S., Sollott, S.J., Lakatta, E.G., Stern, M.D. and Hansford, R.G. (1991) Measurement of mitochondrial free Ca^{2+} concentration in living single rat cardiac myocytes. *American Journal Of Physiology* **261**, H1123-H1134.

Mohabir, R., Lee, H.C., Kurz, R.W. and Clusin, W.T. (1991) Effects of ischemia and hypercarbic acidosis on myocyte calcium transients, contraction, and pH_i in perfused rabbit hearts. *Circulation Research* **69**, 1525-1537.

Movsesian, M.A., Bristow, M.R. and Krall, J. (1989) Ca^{2+} uptake by cardiac sarcoplasmic reticulum from patients with idiopathic dilated cardiomyopathy. *Circulation Research* **65**, 1141-1144.

Movsesian, M.A., Colyer, J., Wang, J.H. and Krall, J. (1990) Phospholamban-mediated stimulation of Ca^{2+} uptake in sarcoplasmic reticulum from normal and failing hearts. *Journal Of Clinical Investigation* **85**, 1698-1702.

Movsesian, M.A., Karimi, M., Green, K. and Jones, L.R. (1994) Ca^{2+}-transporting ATPase, phospholamban, and calsequestrin levels in nonfailing and failing human myocardium. *Circulation* **90**, 653-657.

Mubagwa, K., Kaplan, P., Shivalkar, B., Miserez, M., Leunens, V., Morgers, M. and Flameng, W. (1998) Calcium uptake by the sarcoplasmic reticulum, high energy content and histological changes in ischemic cardiomyopathy. *Cardiovascular Research* **37**, 515-523.

Mulieri, L.A., Hasenfuss, G., Leavitt, B., Allen, P.D. and Alpert, N.R. (1992) Altered myocardial force-frequency relation in human heart failure. *Circulation* **85**, 1743-1750.

Naqvi, R.U. and MacLeod, K.T. (1994) Effect of hypertrophy on mechanisms of relaxation in isolated cardiac myocytes from guinea-pig. *American Journal Of Physiology-Heart And Circulatory Physiology* **36**, H1851-H1861.

Narang, R., Cleland, J.G.F., Erhardt, L., Ball, S.G., Coats, A.J.S., Cowley, A.J., Dargie, H.J., Hall, A.S., Hampton, J.R. and Poole-Wilson, P.A. (1996) Mode of death in chronic heart failure - a request and proposition for more accurate classification. *European Heart Journal* **17**, 1390-1403.

Narula, J., Haider, N., Virmani, R., Disalvo, T.G., Kolodgie, F.D., Hajjar, R.J., Schmidt, U., Semigran, M.J., Dec, G.W. and Khaw, B.A. (1996) Apoptosis in myocytes in end-stage heart failure. *New England Journal Of Medicine* **335**, 1182-1189.

Näbauer, M., Beuckelmann, D.J. and Erdmann, E. (1993) Characteristics of transient outward current in human ventricular myocytes from patients with terminal heart failure. *Circulation Research* **73**, 386-394.

Näbauer, M., Beuckelmann, D.J., Uberfuhr, P. and Steinbeck, G. (1996) Regional differences in current density and rate-dependent properties of the transient outward current in subepicardial and subendocardial myocytes of human left ventricle. *Circulation* **93**, 168-177.

Näbauer, M. and Kaab, S. (1998) Potassium channel down-regulation in heart failure. *Cardiovascular Research* **37**, 324-334.

Neely, J.R., Liebermeister, H., Battersby, E.J. and Morgan, H.E. (1966) Effect of pressure development on oxygen consumption by isolated rat heart. *American Journal Of Physiology* **212**, 804-814.

Nelson, G.R., Cohn, P.F. and Gorlin, R. (1975) Prognosis in medically treated coronary disease - influence of ejection fraction compared to other parameters. *Circulation* **52**, 408-412.

Noble, M.I.M. and Drakeholland, A.J. (1994) Lack of importance in humans of the slow component of the response of force to an increase in cardiac-muscle length. *Clinical Science* **87**, 547-551.

Orchard, C.H., Eisner, D.A. and Allen, D.G. (1983) Oscillations of intracellular Ca^{2+} in mammalian cardiac muscle. *Nature* **304**, 735-738.

Overend, C.L., Eisner, D.A. and O'Neill, S.C. (1997a) The effect of tetracaine on spontaneous Ca^{2+} release and sarcoplasmic reticulum calcium content in rat ventricular myocytes. *Journal Of Physiology-London* **502**, 471-479.

Overend, C.L., O'Neill, S.C. and Eisner, D.A. (1997b) Tetracaine only transiently inhibits contractions of rat isolated ventricular myocytes. *Journal Of Physiology-London* **504P**, P82

Packer, M. and Lee, W.H. (1986) Provocation of hyper- and hypokalemia sudden death during treatment with and withdrawal of converting-enzyme inhibition in severe chronic congestive heart failure. *American Journal Of Cardiology* **57**, 347-348.

Packer, M. (1988) Survival in patients with chronic heart failure and its potential modification by drug therapy. In: Cohn, J.N. (Ed.) *Drug treatment of heart failure*, 2nd edn. pp. 273 Secaucus: ATC International.

Packer, M., Carver, J.R., Rodeheffer, R.J., Ivanhoe, R.J., Dibianco, R., Zeldis, S.M., Hendrix, G.H., Bommer, W.J., Elkayam, U., Kukin, M.L., Mallis, G.I., Sollano, J.A., Shannon, J., Tandon, P.K. and Demets, D.L. (1991) Effect of oral milrinone on mortality in severe chronic heart-failure. *New England Journal Of Medicine* **325**, 1468-1475.

Packer, M. (1992) Lack of relation between ventricular arrhythmias and sudden death in patients with chronic heart failure. *Circulation* **85**, 50-56.

Packer, M., Bristow, M.R., Cohn, J.N., Colucci, W.S., Fowler, M.B., Gilbert, E.M. and Shusterman, N.H. (1996) The effect of carvedilol on morbidity and mortality in patients with chronic heart failure. *New England Journal Of Medicine* **334**, 1349-1355.

Pagani, E.D., Alousi, A.A., Grant, A.M., Older, T.M., Dziuban, S.W. and Allen, P.D. (1988) Changes in myofibrillar content and Mg-ATPase activity in ventricular tissues from patients with heart failure caused by coronary artery disease, cardiomyopathy, or mitral valve insufficiency. *Circulation Research* **63**, 380-385.

Parmley, W.W. and Chuck, L. (1973) Length-dependent changes in myocardial contractile state. *American Journal Of Physiology* **224**, 1195-1199.

Parmley, W.W. (1989) Pathophysiology and current therapy of congestive heart failure. *Journal Of The American College Of Cardiology* **13**, 771-785.

Patterson, S.W., Piper, H. and Starling, E.H. (1914) The regulation of the heart beat. *Journal of Physiology* **48**, 465-513.

Perreault, C.L., Shannon, R.P., Komamura, K. and Morgan, J.P. (1992) Abnormalities in intracellular calcium regulation and contractile function in myocardium from dogs with pacing-induced heart failure. *Journal Of Clinical Investigation* **89**, 932-938.

Peters, N.S., Green, C.R., Poole-Wilson, P.A. and Severs, N.J. (1993) Reduced content of connexin43 gap-junctions in ventricular myocardium from hypertrophied and ischaemic human hearts. *Circulation* **88**, 864-875.

Pfeffer, J.M. (1991) Progressive ventricular dilation in experimental myocardial infarction and its attenuation by angiotensin converting enzyme inhibition. *American Journal Of Cardiology* **68**, D 17-D 25.

Pfeffer, M.A., Braunwald, E., Moye, L.A., Basta, L., Brown, E.J., Cuddy, T.E., Davis, B.R., Geltman, E.M., Goldman, S., Flaker, G.C., Klein, M., Lamas, G.A., Packer, M., Rouleau, J., Rouleau, J.L., Rutherford, J., Wertheimer, J.H. and Hawkins, C.M. (1992) Effect of captopril on mortality and morbidity in patients with left ventricular dysfunction after myocardial infarction - results of the survival and ventricular enlargement trial. *New England Journal Of Medicine* **327**, 669-677.

Phillips, R.M., Narayan, P., Gomez, A.M., Dilly, K., Jones, L.R., Lederer, W.J. and Altschuld, R.A. (1998) Sarcoplasmic reticulum in heart failure: central player or bystander? *Cardiovascular Research* **37**, 346-351.

Pieske, B., Kretschmann, B., Meyer, M., Holubarsch, C., Weirich, J., Posival, H., Minami, K., Just, H. and Hasenfuss, G. (1995) Alterations in intracellular calcium handling associated with the inverse force-frequency relation in human dilated cardiomyopathy. *Circulation* **92**, 1169-1178.

Podrid, P.J., Fogel, R.I. and Fuchs, T.T. (1992) Ventricular arrhythmia in congestive heart failure. *American Journal Of Cardiology* **69**, G 82-G 96.

Pogwizd, S.M., Hoyt, R.H., Saffitz, J.E., Corr, P.B., Cox, J.L. and Cain, M.E. (1992) Reentrant and focal mechanisms underlying ventricular tachycardia in the human heart. *Circulation* **86**, 1872-1887.

Poole-Wilson, P.A. (1993) Relation of pathophysiologic mechanisms to outcome in heart failure. *Journal Of The American College Of Cardiology* **22**, A 22-A 29.

Priori, S.G., Napolitano, C., Diehl, L. and Schwartz, P.J. (1994) Dispersion of the QT interval - a marker of therapeutic efficacy in the idiopathic long QT syndrome. *Circulation* **89**, 1681-1689.

Pye, M.P. and Cobbe, S.M. (1992) Mechanisms of ventricular arrhythmias in cardiac failure and hypertrophy. *Cardiovascular Research* **26**, 740-750.

Pye, M.P. (1992) Mechanisms of ventricular arrhythmias in heart failure: the role of contraction-excitation feedback. University of Wales. M.D.

Pye, M., Quinn, A.C. and Cobbe, S.M. (1994) QT interval dispersion - a noninvasive marker of susceptibility to arrhythmia in patients with sustained ventricular arrhythmias. *British Heart Journal* **71**, 511-514.

Pye, M.P., Black, M. and Cobbe, S.M. (1996) Comparison of *in vivo* and *in vitro* hemodynamic function in experimental heart failure -use of echocardiography. *Cardiovascular Research* **31**, 873-881.

Pye, M.P. and Cobbe, S.M. (1996) Arrhythmogenesis in experimental models of heart failure: the role of increased load. *Cardiovascular Research* **32**, 248-257.

Qiu, D.Y., Zhang, Z.H., Caref, E.B., Boutjdir, M., Jain, P. and Elsherif, N. (1996) Cellular and ionic basis of arrhythmias in postinfarction remodeled ventricular myocardium. *Circulation Research* **79**, 461-473.

Rahimtoola, S.H. (1989) The hibernating myocardium. *American Heart Journal* **117**, 211-221.

Ramdat-Misier, A.R., Opthof, T., Van Hemel, N.M., Vermeulen, J.T., De Bakker, J.M.T., Defauw, J.J.A.M., Van Capelle, F.J.L. and Janse, M.J. (1995) Dispersion of refractoriness in noninfarcted myocardium of patients with ventricular tachycardia or ventricular fibrillation after myocardial infarction. *Circulation* **91**, 2566-2572.

Rasmussen, R.P., Minobe, W. and Bristow, M.R. (1990) Calcium-antagonist binding-sites in failing and nonfailing human ventricular myocardium. *Biochemical Pharmacology* **39**, 691-696.

Reinecke, H., Studer, R., Vetter, R., Holtz, J. and Drexler, H. (1996) Cardiac Na^+/Ca^{2+} exchange activity in patients with end-stage heart failure. *Cardiovascular Research* **31**, 48-54.

Reiter, M.J., Synhorst, D.P. and Mann, D.E. (1988) Electrophysiological effects of acute ventricular dilatation in the isolated rabbit heart. *Circulation Research* **62**, 554-562.

Reiter, M.J., Mann, D.E. and Williams, G.R. (1993) Interaction of hypokalemia and ventricular dilatation in isolated rabbit hearts. *American Journal Of Physiology* **265**, H1544-H1550.

Rensma, P.L., Allessie, M.A., Lammers, W.J.E.P., Bonke, F.I.M. and Schalij, M.J. (1988) The length of the excitation wave as an index for susceptibility to reentrant atrial arrhythmias. *Circulation Research* **62**, 395-410.

Rials, S.J., Wu, Y., Ford, N., Pauletto, F.J., Abramson, S.V., Rubin, A.M., Marinchak, R.A. and Kowey, P.R. (1995) Effect of left ventricular hypertrophy and its regression on ventricular electrophysiology and vulnerability to inducible arrhythmia in the feline heart. *Circulation* **91**, 426-430.

Roden, D.M. (1996) Ionic mechanisms for prolongation of refractoriness and their proarrhythmic and antiarrhythmic correlates. *American Journal Of Cardiology* **78**, 12-16.

Roden, D.M., Lazzara, R., Rosen, M., Schwartz, P.J., Towbin, J. and Vincent, G.M. (1996) Multiple mechanisms in the Long-QT syndrome: current knowledge, gaps and future directions. *Circulation* **94**, 1996-2012.

Rosenqvist, M., Isaaz, K., Botvinick, E.H., Dae, M.W., Cockrell, J., Abbott, J.A., Schiller, N.B. and Griffin, J.C. (1991) Relative importance of activation sequence compared to atrioventricular synchrony in left-ventricular function. *American Journal Of Cardiology* **67**, 148-156.

Rosenqvist, M., Bergfeldt, L., Haga, Y., Ryden, J., Ryden, L. and Owall, A. (1996) The effect of ventricular activation sequence on cardiac performance during pacing. *PACE-Pacing And Clinical Electrophysiology* **19**, 1279-1286.

Rossner, K.L. and Sachs, H.G. (1978) Electrophysiological study of Syrian hamster hereditary cardiomyopathy. *Cardiovascular Research* **12**, 436-443.

Rossner, K.L. (1991) Calcium current in congestive heart failure of hamster cardiomyopathy. *American Journal Of Physiology* **260**, H1179-H1186.

Rouetbenzineb, P., Mohammadi, K., Perennec, J., Poyard, M., Bouanani, N.E. and Crozatier, B. (1996) Protein kinase C isoform expression in normal and failing rabbit hearts. *Circulation Research* **79**, 153-161.

Rozanski, G.J., Xu, Z., Whitney, R.T., Murakami, H. and Zucker, I.H. (1997) Electrophysiology of rabbit ventricular myocytes following sustained rapid ventricular pacing. *Journal Of Molecular And Cellular Cardiology* **29**, 721-732.

Rushmer, R.F., Franklin, D.L. and Ellis, R.M. (1956) Left ventricular dimensions recorded by sonocardiometry. *Circulation Research* **4**, 684-688.

Rushmer, R.F. (1964) Initial ventricular impulse: a potential key to cardiac evaluation. *Circulation* **29**, 268-283.

Ryder, K.O., Bryant, S.M. and Hart, G. (1993) Membrane current changes in left ventricular myocytes isolated from guinea-pigs after abdominal aortic coarctation. *Cardiovascular Research* **27**, 1278-1287.

Saari, J.T. and Johnson, J.A. (1980) Calcium kinetic in individual heart segments. *Cardiovascular Research* **14**, 731-4.

Sapp, J.L. and Howlett, S.E. (1994) Density of ryanodine receptors is increased in sarcoplasmic reticulum from prehypertrophic cardiomyopathic hamster heart. *Journal Of Molecular And Cellular Cardiology* **26**, 325-334.

Sasaki, T., Incis, M., Kimura, Y., Kuzuya, T. and Tada, M. (1992) Molecular mechanism of regulation of Ca^{2+} pump ATPase by phospholamban in cardiac sarcoplasmic reticulum. *Journal Of Biological Chemistry* **267**, 1674-1677.

Scheuermann, D.W. (1993) The ultrastructure of cardiac muscle in health and disease. *Micron* **24**, 47-73.

Schmidt, U., Hajjar, R.J., Carles, M. and Gwathmey, J.K. (1996) Reduced phosphorylation level of phospholamban in human heart failure. *Circulation* **94**, 1479

Schultz, E. (1936) Elektrophysiologie des Herzens bei einphasischer Ableitung. *Ergebn Physiol Exper Pharmakol* **38**, 493-620.

Schwartz, P.J., LaRovere, T. and Vanoli, E. (1992) Autonomic nervous system and sudden cardiac death: experimental basis and clinical observations for post-myocardial infarction risk stratification. *Circulation* **85**, I 77-I 91.

Schwinger, R.H.G., Bohm, M., Koch, A., Schmidt, U., Morano, I., Eissner, H.J., Uberfuhr, P., Reichart, B. and Erdmann, E. (1994) The failing human heart is unable to use the Frank-Starling mechanism. *Circulation Research* **74**, 959-969.

Schwinger, R.H.G., Bohm, M., Schmidt, U., Karcsewski, P., Bavendiek, U., Flesch, M., Krause, H. and Erdmann, E. (1995) Unchanged protein levels of SERCA II and phospholamban but reduced Ca^{2+} uptake and Ca^{2+}-ATPase activity from dilated cardiomyopathy patients compared with patients with nonfailing hearts. *Circulation* **92**, 3220-3228.

Sipido, K.R. and Callewaert, G. (1995) How to measure intracellular [Ca^{2+}] in single cardiac-cells with Fura-2 or Indo-1. *Cardiovascular Research* **29**, 717-726.

Siri, F.M., Krueger, J., Nordin, C., Ming, Z. and Aronson, R.S. (1991) Depressed intracellular calcium transients and contraction in myocytes from hypertrophied and failing guinea-pig hearts. *American Journal Of Physiology* **261**, H 514-H 530.

Skolnick, R.L., Litwin, S.E. and Spitzer, K.W. (1996) Reduced sensitivity of Na/H exchange to ATII in surviving myocytes from infarcted hearts. *Journal Of Molecular And Cellular Cardiology* **28**, A166

Smith, H.J. and Nuttall, A. (1985) Experimental models of heart failure. *Cardiovascular Research* **19**, 181-186.

Spann, J.F., Covell, J.W., Eckberg, D.L., Sonnenblick, E.H., Ross, J.J. and Braunwald, E. (1972) Contractile performance of the hypertrophied and chronically failing cat ventricle. *American Journal Of Physiology* **223**, 1150-1157.

Stamm, R.B., Carabello, B.A., Mayers, D.L. and Martin, R.P. (1982) Two-dimensional echocardiographic measurement of left ventricular ejection fraction: prospective analysis of what constitutes an adequate determination. *American Heart Journal* **104**, 136-144.

Starling, E.H. (1918) *The Linacre lecture on the law of the heart given at Cambridge, 1915*, London: Longmans, Green.

Statters, D.J., Malik, M., Ward, D.E. and Camm, A.J. (1994) QT dispersion - problems of methodology and clinical significance. *Journal Of Cardiovascular Electrophysiology* **5**, 672-685.

Stevenson, W.G., Stevenson, L.W., Weiss, J. and Tillisch, J.H. (1988) Inducible ventricular arrhythmias and sudden death during vasodilator therapy of severe heart failure. *American Heart Journal* **116**, 1447-1454.

Stevenson, W.G., Stevenson, L.W., Middlekauff, H.R. and Saxon, L.A. (1993) Sudden death prevention in patients with advanced ventricular dysfunction. *Circulation* **88**, 2953-2961.

Stevenson, W.G. (1995) Mechanisms and management of arrhythmias in heart failure. *Current Opinion In Cardiology* **10**, 274-281.

Stewart, A.W. (1985) Muscle fluorometry - a determination of the depth of penetration. *Experientia* **41**, 456-458.

Stojnic, B.B., Stojanov, P.L., Angelkov, L., Pavlovic, S.U., Radjen, G.S. and Velimirovic, D.B. (1996) Evaluation of asynchronous left ventricular relaxation by doppler echocardiography during ventricular pacing with AV synchrony (VDD): comparison with atrial pacing (AAI). *PACE-Pacing And Clinical Electrophysiology* **19**, 940-944.

Studer, R., Reinecke, H., Bilger, J., Eschenhagen, T., Bohm, M., Hasenfuss, G., Just, H., Holtz, J. and Drexler, H. (1994) Gene expression of the cardiac Na^{+}-Ca^{2+} exchanger in end stage human heart failure. *Circulation Research* **75**, 443-453.

Surawicz, B. (1996) Will QT dispersion play a role in clinical decision-making? *Journal Of Cardiovascular Electrophysiology* **7**, 777-784.

Swedberg, K. (1987) Effects of enalapril on mortality in severe congestive heart failure - results of the Cooperative North Scandinavian Enalapril Survival Study (CONSENSUS). *New England Journal Of Medicine* **316**, 1429-1435.

Sytkowski, P.A., Kannel, W.B. and D'Agostino, R.B. (1990) Changes in risk factors and the decline in mortality from cardiovascular disease. *New England Journal Of Medicine* **322**, 1635-1641.

Szabo, B., Sweidan, R., Rajagopalan, C.V. and Lazzara, R. (1994) Role of Na^{+} Ca^{2+} exchange current in Cs^{+}-induced early afterdepolarizations in purkinje fibers. *Journal Of Cardiovascular Electrophysiology* **5**, 933-944.

Taggart, P., Sutton, P. and Lab, M. (1992a) Interaction between ventricular loading and repolarization - relevance to arrhythmogenesis. *British Heart Journal* **67**, 213-215.

Taggart, P., Sutton, P., Lab, M., Runnalls, M., Obrien, W. and Treasure, T. (1992b) Effect of abrupt changes in ventricular loading on repolarization induced by transient aortic occlusion in humans. *American Journal Of Physiology* **263**, H 816-H 823.

Takahashi, T., Allen, P.D., Lacro, R.V., Marks, A.R., Dennis, A.R., Schoen, F.J., Grossman, W., Marsh, J.D. and Izumo, S. (1992a) Expression of dihydropyridine receptor (Ca^{2+} channel) and calsequestrin genes in the myocardium of patients with end stage heart failure. *Journal Of Clinical Investigation* **90**, 927-935.

Takahashi, T., Allen, P.D. and Izumo, S. (1992b) Expression of A-type, B-type, and C-type natriuretic peptide genes in failing and developing human ventricles - correlation with expression of the Ca^{2+}-ATPase gene. *Circulation Research* **71**, 9-17.

Tan, L.B. (1987) Clinical and research implications of new concepts in the assessment of cardiac pumping performance in heart failure. *Cardiovascular Research* **21**, 615-622.

Teerlink, J.R., Goldhaber, S.Z. and Pfeffer, M.A. (1991) An overview of contemporary aetiologies of congestive heart failure. *American Heart Journal* **121**, 1852-1853.

Tennant, R. and Wiggers, C.J. (1935) The effect of coronary occlusion on myocardial contraction. *American Journal Of Physiology* **112**, 351-361.

Thandroyen, F.T., Morris, A.C., Hagler, H.K., Ziman, B., Pai, L., Willerson, J.T. and Buja, L.M. (1991) Intracellular calcium transients and arrhythmia in isolated heart cells. *Circulation Research* **69**, 810-819.

The SOLVD investigators, (1991) Effect of enalapril on survival in patients with reduced left ventricular ejection fractions and congestive heart failure. *New England Journal Of Medicine* **325**, 293-302.

Thuringer, D., Coulombe, A., Deroubaix, E., Coraboeuf, E. and Mercadier, J.J. (1996) Depressed transient outward current density in ventricular myocytes from cardiomyopathic syrian hamsters of different ages. *Journal Of Molecular And Cellular Cardiology* **28**, 387-401.

Tomaselli, G.F., Beuckelmann, D.J., Calkins, H.G., Berger, R.D., Kessler, P.D., Lawrence, J.H., Kass, D., Feldman, A.M. and Marban, E. (1994) Sudden cardiac death in heart failure - the role of abnormal repolarization. *Circulation* **90**, 2534-2539.

Tsien, R.Y. (1981) A non-disruptive technique for loading calcium buffers and indicators into cells. *Nature* **290**, 527-528.

Tucci, P.J.F., Bregagnollo, E.A., Spadaro, J., Cicogna, A.C. and Ribeiro, M.C.L. (1984) Length dependence of activation studied in the isovolumic blood-perfused dog heart. *Circulation Research* **55**, 59-66.

Turvey, S.E. and Allen, D.G. (1994) Changes in myoplasmic sodium concentration during exposure to lactate in perfused rat heart. *Cardiovascular Research* **28**, 987-993.

Vahl, C.F., Bonz, A., Timek, T. and Hagl, S. (1994) Intracellular calcium transient of working human myocardium of 7 patients transplanted for congestive heart failure. *Circulation Research* **74**, 952-958.

Vassallo, J.A., Cassidy, D.M., Miller, J.M., Buxton, A.E., Marchlinski, F.E. and Josephson, M.E. (1986) Left ventricular endocardial activation during right ventricular pacing - effect of underlying heart disease. *Journal Of The American College Of Cardiology* **7**, 1228-1233.

Vassallo, J.A., Cassidy, D.M., Kindwall, K.E., Marchlinski, F.E. and Josephson, M.E. (1988) Nonuniform recovery of excitability in the left ventricle. *Circulation* **78**, 1365-1372.

Vatner, D.E., Sate, N., Kiuchi, K., Shannon, R.P. and Vatner, S.F. (1994) Decrease in myocardial ryanodine receptors and altered excitation contraction coupling early in the development of heart failure. *Circulation* **90**, 1423-1430.

Vermeulen, J.T., Mcguire, M.A., Opthof, T., Coronel, R., De Bakker, J.M.T., Klopping, C. and Janse, M.J. (1994) Triggered activity and automaticity in ventricular trabeculae of failing human and rabbit hearts. *Cardiovascular Research* **28**, 1547-1554.

Wagner, J.A., Reynolds, I.J., Weisman, H.F., Dudeck, P., Weisfeldt, M.L. and Snyder, S.H. (1986) Calcium antagonist receptors in cardiomyopathic hamster: selective increases in heart, muscle, brain. *Science* **232**, 515-518.

Wagoner, L.E. and Walsh, R.A. (1996) The cellular pathophysiology of progression to heart failure. *Current Opinion In Cardiology* **11**, 237-244.

Wang, Z.F., Taylor, L.K., Denney, W.D. and Hansen, D.E. (1994) Initiation of ventricular extrasystoles by myocardial stretch in chronically dilated and failing canine left ventricle. *Circulation* **90**, 2022-2031.

Wankerl, M., Bohm, M., Morano, I., Ruegg, J.C., Eichhorn, M. and Erdmann, E. (1990) Calcium sensitivity and myosin light chain pattern of atrial and ventricular skinned cardiac fibers from patients with various kinds of cardiac disease. *Journal Of Molecular And Cellular Cardiology* **22**, 1425-1438.

Watanabe, T., Delbridge, L.M., Bustamante, J.O. and McDonald, T.F. (1983) Heterogeneity of the action potential in isolated rat ventricular myocytes. *Circulation Research* **52**, 280-290.

Weber, K.T. and Brilla, C.G. (1991) Pathological hypertrophy and cardiac interstitium - fibrosis and renin-angiotensin-aldosterone system. *Circulation* **83**, 1849-1865.

White, E., Boyett, M.R. and Orchard, C.H. (1995) The effects of mechanical loading and changes of length on single guinea-pig ventricular myocytes. *Journal Of Physiology-London* **482**, 93-107.

Whitmer, J.T., Kumar, P. and Solaro, R.J. (1988) Calcium-transport properties of cardiac sarcoplasmic reticulum from cardiomyopathic syrian hamsters (Bio 53.58 and 14.6) - evidence for a quantitative defect in dilated myopathic hearts not evident in hypertrophic hearts. *Circulation Research* **62**, 81-85.

Wiggers, C.J. (1952) *Circulatory Dynamics*, New York: Grune & Stratton Inc.

Wikman-Coffelt, J., Stefenelli, T., Wu, S.T., Parmley, W.W. and Jasmin, G. (1991a) $[Ca^{2+}]_i$ transients in the cardiomyopathic hamster heart. *Circulation Research* **68**, 45-51.

Wikman-Coffelt, J., Wu, S.T. and Parmley, W.W. (1991b) Intracellular endocardial calcium and myocardial function in rat hearts. *Cell Calcium* **12**, 39-50.

Wit, A.L., Allessie, M.A., Bonke, F.I.M., Lammers, W., Smeets, J. and Fenoglio, J.J. (1982) Electrophysiological mapping to determine the mechanism of experimental ventricular tachycardia initiated by premature impulses: experimental approach and initial results demonstrating re-entrant excitation. *American Journal Of Cardiology* **49**, 166-185.

Witkowski, F.X., Leon, L.J., Penkoske, P.A., Giles, W.R., Spano, M.L., Ditto, W.L. and Winfree, A.T. (1998) Spatiotemporal evolution of ventricular fibrillation. *Nature* **392**, 78-82.

Wolff, M.R., Whitesell, L.F. and Moss, R.L. (1995) Calcium sensitivity of isometric tension is increased in canine experimental heart failure. *Circulation Research* **76**, 781-789.

Wollert, K.C., Taga, T., Saito, M., Narazaki, M., Kishimoto, T., Glembotski, C.C., Vernallis, A.B., Heath, J.K., Pennica, D., Wood, W.I. and Chien, K.R. (1996) Cardiotrophin-1 activates a distinct form of cardiac-muscle cell hypertrophy - assembly of sarcomeric units in series via gp130 leukemia inhibitory factor receptor-dependent pathways. *Journal Of Biological Chemistry* **271**, 9535-9545.

Wong, A.Y.K. and Rautaharju, P.M. (1968) Stress distribution within the left ventricular wall approximated as a thick ellipsoidal shell. *American Heart Journal* **75**, 649-662.

Xiao, H.B., Lee, C.H. and Gibson, D.G. (1991) Effect of left bundle branch block on diastolic function in dilated cardiomyopathy. *British Heart Journal* **66**, 443-447.

Xiao, H.B. and Gibson, D.G. (1994) Absent septal Q wave: a marker of the effects of abnormal activation pattern on left ventricular diastolic function. *British Heart Journal* **72**, 45-51.

Yuan, S.W., Blomstromlundqvist, C. and Olsson, S.B. (1994) Monophasic action potentials - concepts to practical applications. *Journal Of Cardiovascular Electrophysiology* **5**, 287-308.

Zabel, M., Portnoy, S. and Franz, M.R. (1995) Electrocardiographic indexes of dispersion of ventricular repolarization - an isolated heart validation study. *Journal Of The American College Of Cardiology* **25**, 746-752.

Zabel, M., Portnoy, S. and Franz, M.R. (1996) Effect of sustained load on dispersion of ventricular repolarization and conduction time in the isolated intact rabbit heart. *Journal Of Cardiovascular Electrophysiology* **7**, 9-16.

Zar, J.H. (1996) Multiple comparisons. In: Zar, J.H. (Ed.) *Biostatistical analysis*, 3rd edn. pp. 211-234. New Jersey: Prentice-Hall International Inc.

Zhang, X., Tillotson, D.L., Moore, R.L., Zelis, R. and Cheung, J.Y. (1996) Na/Ca exchange currents and SR Ca contents in postinfarction myocytes. *American Journal Of Physiology* **271**, C1800-C1807.